Superoxide Dismutases and Superoxide Reductases

Yuewei Sheng,[†] Isabel A. Abreu,*,[‡,§] Diane E. Cabelli,*,[‖] Michael J. Maroney,*,[⊥] Anne-Frances Miller,*,[#] Miguel Teixeira,*,[‡] and Joan Selverstone Valentine*,[†,∇]

[†]Department of Chemistry and Biochemistry, University of California Los Angeles, Los Angeles, California 90095, United States

[‡]Instituto de Tecnologia Química e Biológica António Xavier, Universidade Nova de Lisboa, Av. da República, 2780-157, Oeiras, Portugal
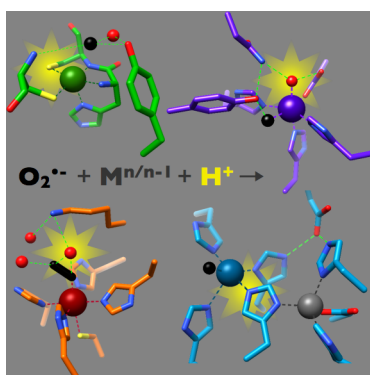
[§]Instituto de Biologia Experimental e Tecnológica, Av. da República, Qta. do Marquês, Estação Agronómica Nacional, Edifício IBET/ITQB, 2780-157, Oeiras, Portugal

[‖]Chemistry Department, Brookhaven National Laboratory, Upton, New York 11973, United States

[⊥]Department of Chemistry, University of Massachusetts Amherst, Amherst, Massachusetts 01003, United States

[#]Department of Chemistry, University of Kentucky, Lexington, Kentucky 40506-0055, United States

[∇]Department of Bioinspired Sciences, Ewha Womans University, Seoul 120-750, Republic of Korea

CONTENTS

1. INTRODUCTION

Superoxide, $O_2^{\bullet-}$, is formed in all living organisms that come in contact with air, and, depending upon its biological context, it may act as a signaling agent, a toxic species, or a harmless intermediate that decomposes spontaneously. Its levels are limited in vivo by two different types of enzymes, superoxide reductase (SOR) and superoxide dismutase (SOD). Although superoxide has long been an important factor in evolution, it was not so when life first emerged on Earth at least 3.5 billion years ago. At that time, the early biosphere was highly reducing and lacking in any significant concentrations of dioxygen (O_2), very different from what it is today. Consequently, there was little or no $O_2^{\bullet-}$ and therefore no reason for SOR or SOD enzymes to evolve. Instead, the history of biological $O_2^{\bullet-}$ probably commences somewhere around 2.4 billion years ago, when the biosphere started to experience what has been termed the "Great Oxidation Event", a transformation driven by the increase in O_2 levels, formed by cyanobacteria as a product of oxygenic photosynthesis.[1] The rise of O_2 on Earth caused a reshaping of existing metabolic pathways, and it triggered the development of new ones.[2] Its appearance led to the formation of the so-called "reactive oxygen species" (ROS), for example, superoxide, hydrogen peroxide, and hydroxyl radical, and to a need for antioxidant enzymes and other antioxidant systems to protect against the growing levels of oxidative damage to living systems.

Dioxygen is a powerful four-electron oxidizing agent, and the product of this reduction is water.

$$O_2 + 4H^+ + 4e^- \rightarrow 2H_2O \tag{1}$$

When O_2 is reduced in four sequential one-electron steps, the intermediates formed are the three major ROS, that is, $O_2^{\bullet-}$, H_2O_2, and $HO^{\bullet}$.

$$O_2 + e^- \rightarrow O_2^{\bullet-} \tag{2}$$

$$O_2^{\bullet-} + 2H^+ + e^- \rightarrow H_2O_2 \tag{3}$$

$$H_2O_2 + H^+ + e^- \rightarrow H_2O + HO^{\bullet} \tag{4}$$

$$HO^{\bullet} + H^+ + e^- \rightarrow H_2O \tag{5}$$
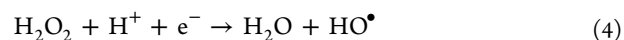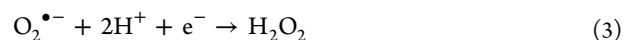
Each of these intermediates is a potent oxidizing agent. The consequences of their presence to early life must have been an enormous evolutionary challenge. In the case of superoxide, we find the SOD and SOR enzymes to be widely distributed throughout current living organisms, both aerobic and anaerobic, suggesting that, from the start of the rise of O_2 on Earth, the chemistry of superoxide has been an important factor during evolution.

The SORs and three very different types of SOD enzymes are redox-active metalloenzymes that have evolved entirely independently from one another for the purpose of lowering superoxide concentrations. SORs catalyze the one-electron reduction of $O_2^{\bullet-}$ to give H_2O_2, a reaction requiring two protons per superoxide reacted as well as an external reductant to provide the electron (eq 6). SODs catalyze the disproportionation of superoxide to give O_2 and H_2O_2, a reaction requiring one proton per superoxide reacted, but no external reductant (eq 7).

$$O_2^{\bullet-} + 2H^+ + e^- \xrightarrow{\text{SOR}} H_2O_2 \tag{6}$$

$$2O_2^{\bullet-} + 2H^+ \xrightarrow{SOD} O_2 + H_2O_2 \qquad (7)$$
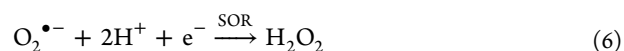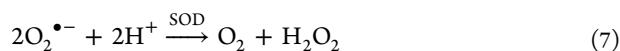
All of the SOR enzymes contain only iron, while the three types of SODs are the nickel-containing SODs (NiSOD), the iron- or manganese-containing SODs (FeSOD and MnSOD), and the copper- and zinc-containing SODs (CuZnSOD). Although the structures and other properties of these four types of metalloenzymes are quite different, they all share several characteristics, including the ability to react rapidly and selectively with the small anionic substrate $O_2^{\bullet-}$. Consequently, there are some striking similarities between these otherwise dissimilar enzymes, many of which can be explained by considering the nature of the chemical reactivity of $O_2^{\bullet-}$ (see below).

Numerous valuable reviews describing the SOD and SOR enzymes have appeared over the years, but few have covered and compared all four classes of these enzymes, as we attempt to do here. Thus, the purpose of this Review is to describe, compare, and contrast the properties of the SOR and the four SOD enzymes; to summarize what is known about their evolutionary pathways; and to analyze the properties of these enzymes in light of what is known of the inherent chemical reactivity of superoxide.

2. SUPEROXIDE AND THE ENZYMES THAT CONTROL IT

2.1. Superoxide and Hydroperoxyl

Dioxygen is a powerful four-electron oxidant, but most of its oxidizing capability is released only after the third electron is added, that is, when the O—O bond breaks and hydroxyl radical is formed, as can be seen from the reduction potentials in Table 1.

Table 1. Standard Reduction Potential of Dioxygen Species in Water, pH 7, 25 °C[3]

reaction	$E°$ (V) vs NHE[a]
$O_2 + e^- \rightarrow O_2^{\bullet-}$	-0.18^b
$O_2^{\bullet-} + e^- + 2H^+ \rightarrow H_2O_2$	$+0.91$
$H_2O_2 + e^- + H^+ \rightarrow H_2O + OH^{\bullet}$	$+0.39$
$OH^{\bullet} + e^- + H^+ \rightarrow H_2O$	$+2.31$
$O_2 + 2e^- + 2H^+ \rightarrow H_2O_2$	$+0.28^b$
$H_2O_2 + 2e^- + 2H^+ \rightarrow 2H_2O$	$+1.35$
$O_2 + 4e^- + 4H^+ \rightarrow 2H_2O$	$+0.81^b$

[a]Normal hydrogen electrode = NHE. [b]The standard state used here is unit pressure.

Superoxide, $O_2^{\bullet-}$, is a relatively small anion, highly soluble in water, where it is strongly solvated by four tightly hydrogen-bonded water molecules.[4] Hydroperoxyl, HO_2, the protonated form of superoxide, is a weak acid with a pK_a of 4.8, similar to that of acetic acid. Therefore, the predominant species present in aqueous solutions of superoxide at pH 7 is the small $O_2^{\bullet-}$ anion itself along with its strongly associated four water molecules. This species is the substrate for the SOD and SOR enzymes. Superoxide absorbs light in the ultraviolet range with a maximum at 245 nm and extinction coefficient of 2350 M^{-1} cm^{-1}, while hydroperoxyl absorbs at 225 nm with an extinction coefficient of 1400 M^{-1} cm^{-1}.[5]

$O_2^{\bullet-}$ and HO_2 are both kinetically competent one-electron reductants in a wide variety of reactions, but for most reactions only HO_2, and not $O_2^{\bullet-}$, is a kinetically competent one-electron oxidant because of the need for either a proton or a coordinated metal ion to stabilize the peroxide dianion, O_2^{2-}, as it is formed. These principles are illustrated quite clearly by the pH-dependence for the spontaneous disproportionation of superoxide (Figure 1). At very low pH, the predominant
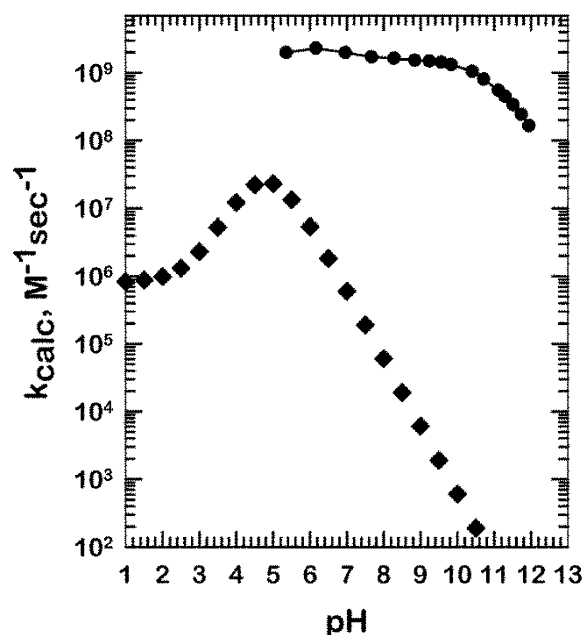
Figure 1. The rate constants of superoxide self-disproportionation (◆) and disproportionation catalyzed by human CuZnSOD as a function of pH (●) are shown for comparison.

species is HO_2, an uncharged species, which acts both as a reductant and as an oxidant:

$$HO_2 + HO_2 \rightarrow H_2O_2 + O_2$$

$$k = 8.3 \times 10^5 \text{ M}^{-1} \text{ s}^{-1} \qquad (8)$$
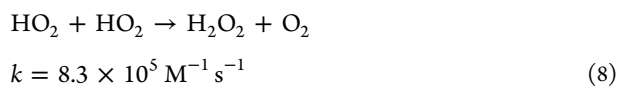
At very high pH, the predominant species is $O_2^{\bullet-}$ itself, and it is quite stable under these conditions. The two superoxide anions repel each other and naked O_2^{2-} is unstable, so the disproportionation reaction does not proceed at all:

$$O_2^{\bullet-} + O_2^{\bullet-} \rightarrow \text{no reaction} \qquad (9)$$
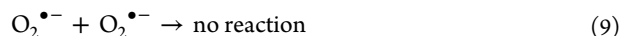
The disproportionation reaction is fastest at pH = pK_a = 4.8, where the concentrations of HO_2 and $O_2^{\bullet-}$ are equal, the former acting as oxidant and the latter as a reductant:

$$HO_2 + O_2^{\bullet-} \xrightarrow{H^+} H_2O_2 + O_2$$

$$k = 9.7 \times 10^7 \text{ M}^{-1} \text{ s}^{-1} \qquad (10)$$
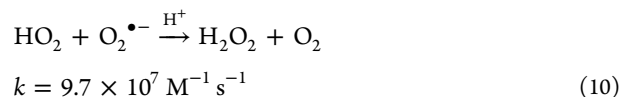
The requirement for a proton to stabilize the O_2^{2-} as it is formed is clearly seen in the failure of $O_2^{\bullet-}$ to oxidize most organic substrates, including peptides, nucleic acids, lipids, and carbohydrates, at rates competitive with superoxide disproportionation in aqueous solution.[5] The exceptions are substrates such as ascorbate[6] or hydroquinone,[7] which have hydrogen atoms available for proton-coupled electron transfer reactions, thus providing a kinetic pathway for fast oxidation of the substrate:

$$\text{substrate–H} + O_2^{\bullet-} \rightarrow \text{substrate}\bullet + HO_2^{-} \qquad (11)$$
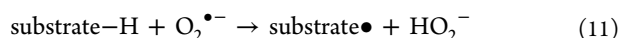
In addition to protons, metal ions can also be used to stabilize O_2^{2-} as it is formed, and there are several examples of rapid oxidative addition reactions in which $O_2^{\bullet-}$ enters the first coordination sphere of a reduced metal ion such as Fe^{2+} or Mn^{2+} and oxidizes it to form a peroxo complex of the oxidized metal ion (eq 12).[8] This inner-sphere oxidative addition

$$L_nM^{2+} + O_2^{\bullet-} \longrightarrow L_nM^{3+}(O_2^{2-}) \xrightarrow[\text{OH}^-]{\text{H}_2\text{O}} L_nM^{3+} + H_2O_2 \qquad (12)$$
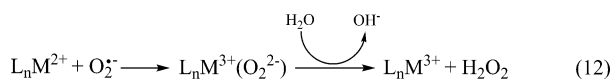
reaction has been observed in SORs (section 7) and in MnSOD (section 4), and it may also be occurring in some of the other SODs (sections 3−6). In aqueous solution, the peroxo ligand may subsequently be protonated and dissociate, and the final product will be the oxidized metal complex plus H_2O_2 (eq 12). In this case, the reduction to peroxide can occur in a separate step from protonation, thus providing a two-step kinetic pathway enabling fast oxidation of metal ions and complexes by $O_2^{\bullet-}$.

2.2. Rise of Dioxygen, Superoxide, and Oxidative Stress on Earth

When life first arose on Earth, the oceans and the land were highly reducing. Thus, the redox metals that were present within minerals existed almost entirely in their reduced states, and sulfur existed predominantly as sulfides.[9] The atmosphere was anoxic, consisting largely of CO_2 and water vapor, with smaller amounts of N_2, H_2, and CH_4, and with O_2 concentrations estimated to be about 10^{-5} of what they are now.[10] In such an environment, oxidative stress due to O_2 and ROS was irrelevant to early life. Even when early organisms acquired the ability to harness the energy of light in photosynthesis, the earliest biological photosynthetic reactions were nonoxygenic, using sources of reducing equivalents other than water, and the atmosphere continued to be anoxic.

The atmosphere and the surface composition of the Earth were transformed dramatically about 2.4−2.0 billion years ago in the Great Oxidation Event as a direct consequence of oxygenic photosynthesis in cyanobacteria.[11] Oxygenic photosynthesis makes use of water molecules as a source of the reducing equivalents needed to reduce carbon dioxide, and O_2 is produced as a byproduct that is highly toxic even to the cyanobacteria that form it. O_2 concentrations from oxygenic photosynthesis rose slowly and unevenly during the Great Oxidation Event, first generating small "oxygen oases" in the oceans[12] and only much later accumulating in the atmosphere. The surface of the Earth and minerals dissolved in the oceans contained many highly reduced inorganic minerals, and oxidation of these, for example, oxidation of Fe^{2+} to Fe^{3+} and sulfide to sulfate, consumed much of the O_2 produced early on, but ultimately O_2 gas began to accumulate in the atmosphere.

Living organisms need sources of energy, and the first forms of energy available to early anaerobic life were derived from chemical and photochemical reactions of the wide variety of electron donors and electron acceptors on the surface of the Earth; one of the most abundant electron donors available was Fe^{2+}.[11,13] Thus, early anaerobic iron-oxidizing bacteria may have produced significant amounts of Fe^{3+} prior to the buildup of O_2 in the atmosphere.[14] Abiotic photochemistry also expanded the range of reduction potentials that would have been encountered by early life. For example, photochemically driven oxidation of Fe^{2+}-containing minerals such as siderite,

$FeCO_3$, may have caused production of Fe^{3+}-containing minerals and H_2, without any involvement from living organisms.[15] Conversion of Fe^{2+} to Fe^{3+} on the Earth's surface prior to the Great Oxidation Event[16] may be responsible for one of the earliest forms of biological oxidative stress. Not only would readily soluble forms of Fe^{2+} have been converted to insoluble ferric oxyhydroxides, from which microbes would not be able to obtain the iron they needed, but an additional threat would be posed by the fact that the ferric ion, even in a relatively insoluble form, is an inherently strong oxidant and, in the wrong place in an electron-rich, highly reducing world, would have presented an oxidative threat to living organisms.

There is good reason to believe that early organisms may have begun to adapt to intermittent low levels or "whiffs" of O_2, generated either biologically or abiologically prior to the Great Oxidation Event, even though the atmosphere remained largely anoxic.[12,17] One possible abiotic source of early O_2 is H_2O_2 formed by the action of ultraviolet radiation on the surface of ice. Photolysis of H_2O by high-energy ultraviolet radiation causes homolysis to $HO^{\bullet}$ and $H^{\bullet}$, which recombine to give H_2O, H_2O_2, and H_2. When this occurs on the surface of ice, at temperatures below the freezing point of water, H_2 escapes leaving the H_2O_2 to accumulate and freeze with the ice. Evidence that this phenomenon has occurred in modern times comes from seasonal variations in H_2O_2 content in ice cores from Antarctica consistent with formation of H_2O_2 in the ice at the times when the ozone hole allows high-energy ultraviolet radiation from the sun to shine on the Antarctic ice fields.[18]

Possible further evidence for the early presence of H_2O_2 and O_2 comes from analysis of the evolutionary history of two enzymes. Manganese catalase, whose substrate is H_2O_2, is a particularly ancient enzyme, which is known to have evolved well before the atmosphere of Earth contained significant amounts of O_2.[19] Catalase-catalyzed decomposition of such H_2O_2 thus seems a likely source for the O_2 that appeared prior to oxygenic photosynthesis. Additional support comes from the proposal that dioxygen reductases related to cytochrome c oxidase, which catalyzes the four-electron reduction of O_2 to water, also appeared before the Great Oxidation Event.[20]

We can infer the types of challenges faced by the earliest anaerobic organisms by studying reactions of O_2 and ROS in modern anaerobic bacteria, but this model should be applied with caution. Many anaerobes (if not all) have been found to contain antioxidant enzymes,[21] and even membrane-associated O_2 reductases, suggesting that some of these anaerobes may have evolved from aerobes and that the presence of significant concentrations of O_2 in the atmosphere of modern Earth has played a role in the evolution of modern organisms, even those that cannot now survive in its presence. It is thus likely that early life was even more susceptible to damage by O_2 and ROS than modern strict anaerobes. The organisms that survived the rise of O_2 must have hidden in niches where O_2 was low or found the means to defend themselves against it. Early forms of life that we cannot even imagine may have become extinct.

Discussions of biological oxidative stress tend to focus primarily on the ROS that are formed by reduction of O_2, but it is important to appreciate that direct reactions of O_2 itself can be very damaging in vivo. For example, a striking feature of anaerobic bacteria is the widespread use of radical enzymes to catalyze key metabolic steps.[22] Such enzymes occur much less frequently in aerobic organisms, and it is easy to see why when we consider the stabilities of the radical intermediates. The glycyl radical is relatively stable in the absence of O_2 due to the

delocalization of the unpaired electron over the peptide bond. However, in the presence of O_2, such intermediates are rapidly and irreversibly inactivated by reaction of the carbon radical center with O_2 (Scheme 1).

Scheme 1. Reaction of a Glycyl Radical Enzyme Intermediate with O_2
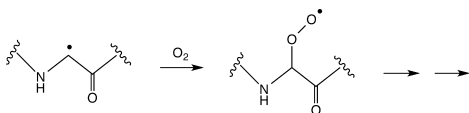
Another class of sites that is particularly vulnerable to irreversible reactions with O_2 is solvent-exposed low-potential metal sites in metalloenzymes.[21b] Solvent-exposed iron−sulfur clusters, for example, are particularly labile, reacting irreversibly not only with superoxide (see below) but also with hydrogen peroxide[23] and with O_2 itself.[24]

The membranes of early organisms may also have been highly susceptible to direct reactions with O_2, particularly if they contained unsaturated fatty acids and no lipid-soluble antioxidant molecules to protect them. This vulnerability is heightened by the fact that O_2 is more soluble in the nonpolar environment of the membrane interior than in the aqueous environment of the cell.[25] Unsaturated lipids are extremely susceptible to free radical autoxidation via a radical chain mechanism unless a chain-breaking antioxidant molecule, such as α-tocopherol, is present to trap the peroxy radical intermediates.[26]

Even if an early anaerobic organism were somehow able to survive damage due to direct reactions of intracellular O_2 with vulnerable components, it would still have to contend with intracellular superoxide. All living cells, whether aerobic or anaerobic, contain components such as reduced flavins[27] that are both highly reducing and capable of reacting rapidly with O_2 to produce superoxide. Although its reactivity pattern is entirely different from that of O_2, superoxide can also react with and damage vulnerable components of the cell.

Superoxide has the thermodynamic capacity to be a strong oxidant, but it is generally not reactive with common components of cells such as peptides, carbohydrates, nucleic acids, or lipids and thus is not an indiscriminant "super" oxidant.[28] Discovery of the chemical reactions responsible for its toxicity was due in large part to the observation by Touati and co-workers[29] that *Escherichia coli* (*E. coli*) bacteria engineered to contain no SOD genes were incapable of synthesizing adequate amounts of branched-chain, aromatic, and sulfur-containing amino acids due to inactivation of biosynthetic enzymes containing labile iron−sulfur clusters at their active sites. These same enzymes had earlier been observed by Brown and co-workers to be inactivated by hyperbaric O_2 in wild-type *E. coli*[30] (reviewed in ref 27). Further work demonstrated many examples of labile iron−sulfur clusters in their reduced states that were oxidized rapidly and irreversibly by reaction with superoxide.[31] Labile iron−sulfur containing species are widespread among organisms, and they appear to be major targets of superoxide. Other superoxide-sensitive entities have also been proposed, and it is likely that other targets remain to be discovered.[27] Thus, superoxide is a selective oxidant, relatively unreactive with most components of cells, but highly reactive with some essential sites and therefore highly toxic.

It is interesting to speculate about what characteristics of ancient cells would make them more or less likely to survive initial exposures to O_2. One possibility is that some early cells acquired the ability to carry out reduction of extracellular substrates such as insoluble ferric oxyhydroxides, analogous to modern iron-reducing bacteria, and there is considerable evidence suggesting that the ability to reduce extracellular Fe^{3+} appeared very early and was widespread in ancient organisms.[32] The systems that carried out extracellular one-electron reduction of Fe^{3+} to Fe^{2+} are highly likely to have been able to reduce O_2 efficiently to superoxide. A common example of such a system in modern organisms is the NADPH oxidase family of enzymes, many of which are known to reside in cellular membranes and function either to produce extracellular superoxide or to reduce extracellular Fe^{3+} to Fe^{2+} or Cu^{2+} to Cu^{1+}.[33] The ability to reduce extracellular O_2 to $O_2^{\bullet-}$ seems to be widespread among living cells,[34] and this extracellular reaction may have provided significant protection to some of the earliest forms of life because the hydrophilic $O_2^{\bullet-}$ anion, unlike the hydrophobic O_2 molecule, would not pass readily through membranes to the interior of the cell. Thus, reducing O_2 to $O_2^{\bullet-}$ outside of the cell would exclude O_2 from entering and reacting directly with intracellular components of the cell and also prevent intracellular generation of $O_2^{\bullet-}$.

As O_2 concentrations rose in the atmosphere, this mechanism to exclude it from the interior of cells would no longer have been sufficient, and antioxidant systems would have been required within cells to protect them from O_2 and $O_2^{\bullet-}$. The earliest of such intracellular antioxidant systems were probably reductive in nature: SOR enzymes, for example, which reduce $O_2^{\bullet-}$ to H_2O_2, and peroxidases, which reduce H_2O_2 to water at the expense of other reduced substrates.[35] Thus, O_2 may have been excluded from cells by reduction to extracellular $O_2^{\bullet-}$ or, when it did enter cells, detoxified by sequential reduction of O_2 to $O_2^{\bullet-}$ and then to H_2O_2 and finally to water. An advantage to anaerobic organisms of these reductive antioxidant enzymes is that, unlike SOD and catalase, O_2 is not a product of their reactions. Moreover, electrons, which readily react with O_2 and form $O_2^{\bullet-}$, are consumed by SOR reactions, limiting the production of superoxide in cells.

To deal with rising levels of O_2, a direct strategy is to reduce it by four electrons all the way to water; this process may have been catalyzed early on by the widespread cytoplasmic flavodiiron proteins,[36] which perform this reaction with turnovers almost identical to those of the "canonical" membrane attached heme−copper or cytochrome *bd* oxygen reductases. Interestingly, cyanobacteria, the first organisms to have oxygenic photosystems and for which O_2 is a toxic byproduct, are particularly rich in those enzymes.[36b,37]

Another strategy to control levels of $O_2^{\bullet-}$ and H_2O_2 is to catalyze their disproportionation using SOD and catalase enzymes. No external sources of reducing equivalents are needed for the reactions catalyzed by these enzymes, and $O_2^{\bullet-}$ and H_2O_2 are converted rapidly to O_2 and water. The advantage of the disproportionation strategy is that no input of energy is required, and, probably for this reason, SOD enzymes overwhelmingly dominate the superoxide defense systems in aerobic organisms, as well as being found in many anaerobes, despite the fact that they generate toxic O_2.

The rise of O_2 on Earth was a major factor in the evolutionary history of SORs and SODs, not only because of increasing levels of biological oxidative stress but also because of changes in the availability of redox-active transition metal

Table 2. Distribution, Location, and Quaternary Structure of SODs and SORs

	Archaea	Bacteria	Eukarya
NiSOD	none	cytosol (hexamer)	cytosol[a] (unknown)
FeSOD	cytosol (tetramer)	cytosol (dimer or tetramer)	cytosol, glycosomes, mitochondria[b] (tetramer[b])
			chloroplasts (dimer or tetramer)
MnSOD	cytosol (tetramer)	cytosol (dimer or tetramer)	mitochondrial matrix (tetramer)
			cytosol[c] (dimer)
			peroxisomes (tetramer)
			chloroplasts (unknown)
CuZnSOD	genes identified in Methanobacteria[d]	periplasm (monomer or dimer)	cytosol[c] (dimer)
			mitochondrial IMS, nucleus (dimer)
			chloroplasts, peroxisomes (dimer)
			extracellular space[e] (tetramer)
SOR	cytosol[f] (tetramer or dimer[g])	cytosol[f] (tetramer or dimer[g])	unknown (tetramer)

[a]Eukaryotic NiSOD is found in the cytosol of some green algae. [b]FeSOD is found in protist *Tetrahymena pyriformis*. [c]Cytosolic MnSOD is found in *C. albicans* and many crustaceans, which also express a mitochondrial MnSOD. [d]The gene of CuZnSOD has been identified in two Methanobacteria, *Methanosarcina acetivorans* (Gene Access Number: NP_617328.1) and *Methanocella arvoryzae* (Gene Access Number: YP_684494.1). [e]Extracellular CuZnSOD is found in mammals and many plants. [f]The proposed cytosolic location of prokaryotic SORs comes from the absence of detectable translocation signal peptides in the translated amino acid sequences; there are, however (see section 7), a few sequences with putative twin-arginine signatures. [g]1Fe-SORs with a single catalytic domain are tetramers; SORs with an extra desulforedoxin-like domain, with or without the FeCys$_4$ metal center, are homodimers.

ions.[38] Prior to the Great Oxidation Event, Fe, Mn, and Ni ions were soluble and relatively abundant in the early reducing oceans, whereas Zn and Cu were tied up in insoluble sulfide-containing minerals in the crust.[39] As the oceans became more oxidizing, Fe was transformed into insoluble ferric oxy-hydroxides, and Cu and Zn into much more soluble aquated ions.[39] Consistent with these changes in the bioavailability of metal ions and as described below in section 4, FeSOD is the most ancient of the SODs and probably first appeared when Fe was relatively abundant. MnSOD and NiSOD appeared later as iron-sparing strategies developed in response to diminishing availability of Fe. CuZnSOD, similar to other copper-containing enzymes,[40] arose later than the other SODs, after copper became bioavailable in the more oxidizing environment of Earth in the Cu^{2+} form. Even before FeSOD appeared, it is possible that inorganic Mn^{2+}, which was soluble and relatively abundant in the early oceans, acted as a primordial SOD and/or catalase, providing some early protection against $O_2^{\bullet-}$ and H_2O_2 toxicity by catalyzing the disproportionation of these ROS.[41]

2.3. Enzymes That Catalyze Reactions of Superoxide

The distribution, subcellular location, and quarternary structures of SODs and SORs are summarized in Table 2, and are quite diverse. NiSOD was discovered in the cytosol of *Streptomyces* and cyanobacteria,[42] as well as in a few green algae.[43] Although FeSOD was originally considered a cytosolic bacterial enzyme,[44] it is also present in archaea[45] and in the chloroplasts of plants,[46] as well as in the cytosol, glycosomes, and mitochondria of protists.[47] MnSOD was identified in the cytosol of archaea[48] and bacteria,[44] and eukaryotic cells typically contain MnSOD in the mitochondrial matrix. In many eukaryotic organisms, such as humans and *Saccharomyces cerevisiae*, MnSOD is located exclusively in the mitochondrial matrix, while in *Candida albicans*[49] and many crustaceans,[50] an additional isoform of MnSOD is present in the cytosol. Similarly, plant cells express additional MnSODs in their peroxisomes[51] and chloroplasts.[46a] Bacterial CuZnSOD is located in the periplasm.[52] In eukaryotic cells, CuZnSOD is primarily cytosolic but is also present in the mitochondrial

intermembrane space and nucleus.[53] Plants also contain additional CuZnSODs in their chloroplasts[51] and peroxisomes,[51,54] and mammals[55] and many plants[51] secrete an extracellular isoform of CuZnSOD. SORs are present in all three domains of life, especially in anaerobic archaea and bacteria.[56] It was also identified in unicellular eukaryotes.[57] In general, it is assumed that they are cytoplasmic due to the absence of identified translocation signal peptides in their amino acid sequences. Nevertheless, there are already a few examples with putative twin arginine translocation motifs, which may indicate a periplasmic localization, but this must wait experimental confirmation.[58]

The protein folds of the SODs and SORs have been elucidated and are correlated with the different roles and locations the enzymes serve (Table 2). Crystal structures of NiSOD have been reported for two enzymes from *Streptomyces*, and they are both homohexamers.[42,59] Fe- and MnSOD exist in both the dimeric and the tetrameric forms: Bacterial Fe- and MnSOD are predominantly dimeric, although FeSOD from *Mycobacterium tuberculosis*[51] and MnSOD from *Thermus thermophilus*[60] have a tetrameric structure. Archaeal Fe- and MnSOD,[48,51,61] as well as an FeSOD isolated from a eukaryote, *Tetrahymena pyriformis*,[62] are reported to be tetrameric. Both homodimeric and homotetrameric FeSODs have been identified in plant species.[51] MnSOD located in the mitochondrial matrix[63] and peroxisomes[64] of eukaryotes is tetrameric, and the cytosolic forms were found to be dimeric.[50,65] In eukaryotic organisms, intracellular CuZnSOD is almost exclusively dimeric with the only exception thus far found in the monomeric isozyme IV from *Oryza sativa* (rice),[54] and the extracellular isoform is homologous to intracellular CuZnSOD but is tetrameric.[54] Bacterial periplasmic CuZnSOD has either a monomeric or a dimeric structure;[66] *E. coli* CuZnSOD is known to be monomeric,[67] while the enzymes from *Photobacterium leiognathi*,[68] *Actinobacillus pleuropneumoniae*,[69] and *Salmonella typhimurium*[70] are dimers, albeit with distinct dimer interfaces and electrostatic recognition residues as compared to eukaryotic CuZnSOD.[68a]

The quaternary structures of SORs appear to be related to their domain composition. So far, there are only experimental

data on 1Fe- and 2Fe-SORs: if the N-terminal desulforedoxin-like domain is present, whether having the FeCys$_4$ center or not, the enzymes are homodimeric; 1Fe-SORs with no extra domain besides the catalytic one are tetrameric[71] (see Figure 2, section 7).
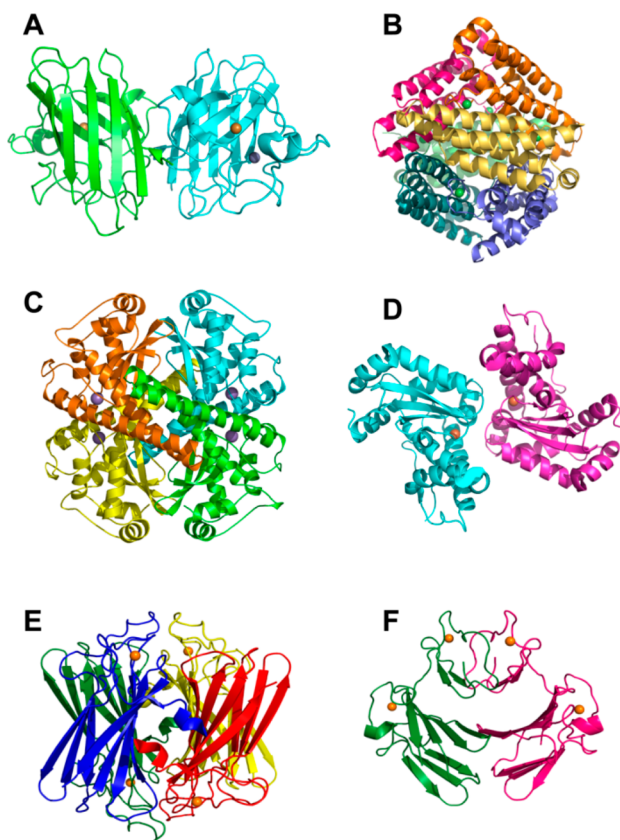

Figure 2. Stereo ribbon diagrams of SODs and SORs: (A) CuZnSOD (PDB code: 1PU0); (B) NiSOD (PDB code: 1T6U); (C) MnSOD (PDB code: 3LSU); (D) FeSOD (PDB code: 3JS4); (E) *P. furiosus* 1Fe-SOR (PDB code: 1DO6); and (F) *D. desulfuricans* 2Fe-SOR (PDB code: 1DFX). The diagrams are colored by chains, and the metal ions are shown as spheres. The diagrams were generated using the PyMOL Molecular Graphics System.[396]

With the exception of FeSOD and MnSOD, which are closely related, the overall structures of the SODs and SORs as well as their active site configurations (Figure 2) are diverse and entirely unrelated to one another, consistent with the conclusion that these enzymes represent examples of convergent evolution. Nevertheless, despite their structural differences, there are many striking mechanistic similarities.

2.3.1. Mechanism. The first and most obvious of the similarities between these enzymes is that they all contain redox-active metal ions at their active sites: $Ni^{2+/3+}$ in NiSOD, $Fe^{2+/3+}$ in FeSOD and SOR, $Mn^{2+/3+}$ in MnSOD, and $Cu^{1+/2+}$ in CuZnSOD. The SOD enzymes all catalyze $O_2^{\bullet-}$ disproportionation by a very similar ping-pong mechanism with $O_2^{\bullet-}$ acting alternately to reduce the oxidized metal ion and then to oxidize the reduced metal ion. The SOR enzymes carry out only the latter of these steps; that is, $O_2^{\bullet-}$ carries out the Fe^{2+} oxidation step but not the Fe^{3+} reduction step.

2.3.2. SOD Activities: pH and Concentration Effects. The enzymatic activities of the four types of SOD enzymes are strikingly similar (Figure 3). The rates of reaction of the enzymes with $O_2^{\bullet-}$ are near the diffusion-controlled limit, and they vary remarkably little over the physiologically relevant pH range (Figure 3).
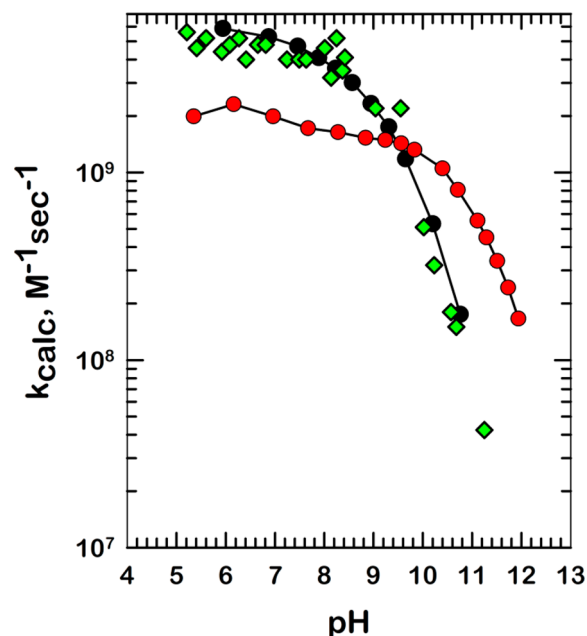
Figure 3. The reactivity of SODs as a function of pH. The enzymes are: human CuZnSOD (red ●), *E. coli* MnSOD (●), and *S. seoulensis* NiSOD (green ◆).

In comparing the rates of the spontaneous versus the SOD-catalyzed rates of disappearance of $O_2^{\bullet-}$, it is important to note the very dramatic effect of the concentration of $O_2^{\bullet-}$ and, in the case of the enzyme-catalyzed reaction, the concentration of the SOD. The spontaneous disproportionation of superoxide is bimolecular and thus proceeds at rates that are proportional to $[O_2^{\bullet-}]$,[2] whereas the rates of the enzyme-catalyzed reaction are first-order in enzyme and in $O_2^{\bullet-}$ concentration and proceed at rates proportional to $[O_2^{\bullet-}]$. Thus, as can be seen in Table 3,

Table 3. Half-Life of Superoxide Decay by Spontaneous Disproportionation or Disproportionation Catalyzed by SOD

$[O_2^{\bullet-}]$ (M)	[SOD] (M)	$t_{1/2}$	acceleration factor
10^{-6}	none	3000 ms	
10^{-6}	10^{-9}	175 ms	20×
10^{-9}	none	hours	
10^{-9}	10^{-9}	175 ms	10 000×
10^{-9}	10^{-6}	0.175 ms	10 000 000×

low concentrations of superoxide can persist for hours, and so the effect of SOD on the rate of $O_2^{\bullet-}$ disappearance is much more dramatic under those conditions. In other words, the presence of a SOD enzyme transforms the disproportionation of $O_2^{\bullet-}$ from being second-order in $[O_2^{\bullet-}]$ to a sequence of two reactions that are each first-order in $[O_2^{\bullet-}]$ and can therefore occur rapidly even at low concentrations of the substrate. Thus, an SOD can maintain low physiological concentrations of superoxide at approximately 2×10^{-10} M.[72]

2.3.3. Reduction Potentials. To be thermodynamically competent to carry out both steps of the reaction, the reduction potentials, $E°$, of the SOD enzymes must fall between −0.18

and +0.91 V, the potentials for one-electron reduction of O_2 and one-electron reduction of $O_2^{\bullet-}$, so that $O_2^{\bullet-}$ can both oxidize the reduced form of the metal ion and reduce the oxidized form (Figure 4). Moreover, for optimal turnover, the
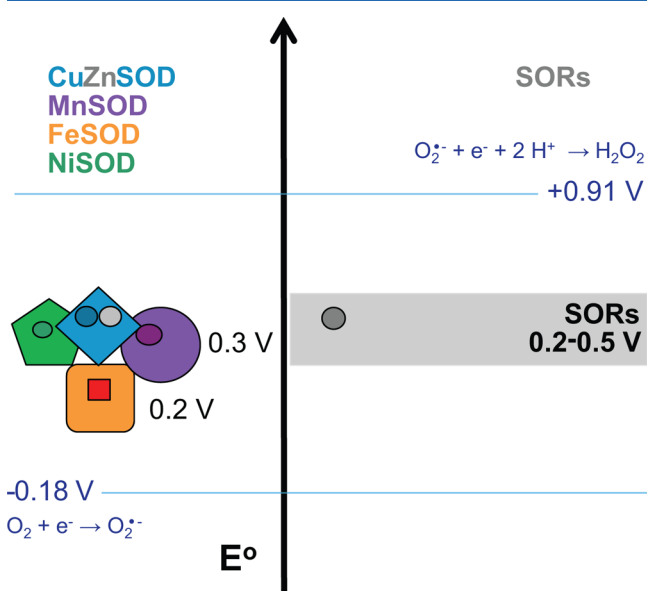
Figure 4. The reduction potentials of the catalytic metal ion in SODs and SORs fall between the potentials for one-electron oxidation and one-electron reduction of superoxide.

$E°$ should be near the average of the $E°$s for the two reactions,[73] and NiSOD (0.29 V),[59] FeSOD (~0.1 V),[74] MnSOD (~0.3 V),[75] and CuZnSOD (0.32 and 0.36 V for human and bovine, respectively)[76] do indeed achieve appropriate intermediate reduction potentials. (It should be noted that the $E°$s of SODs are often difficult to measure with precision due to very slow equilibration between the active site and bulk solution.) As discussed further below, the reduction potential of the metal ion became fine-tuned to an optimum value by each of the SODs in the course of evolution. It is interesting to note that the SOR enzymes have reduction potentials similar to those of the SODs (Figure 4), despite the fact that they do not carry out the oxidation of superoxide (see section 7 for further discussion).

$$O_2^{\bullet-} + \text{enzyme}_{ox} \rightarrow O_2 + \text{enzyme}_{red} \qquad (13)$$

$$O_2^{\bullet-} + 2H^+ + \text{enzyme}_{red} \rightarrow H_2O_2 + \text{enzyme}_{ox} \qquad (14)$$

2.3.4. Inner- versus Outer-Sphere Pathways. In theory, $O_2^{\bullet-}$ can reduce an oxidized metal ion by either an inner-sphere or an outer-sphere pathway. In an inner-sphere mechanism, $O_2^{\bullet-}$ becomes a ligand in the first coordination sph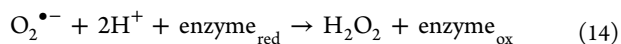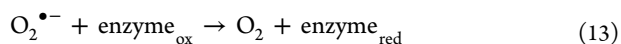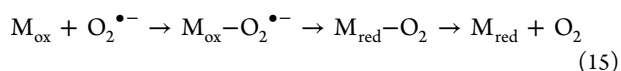ere of the oxidized metal ion at the active site prior to electron transfer and release of O_2. If there is not an open coordination position on the metal ion, a ligand exchange reaction must take place for superoxide to enter the first coordination sphere.

$$M_{ox} + O_2^{\bullet-} \rightarrow M_{ox}{-}O_2^{\bullet-} \rightarrow M_{red}{-}O_2 \rightarrow M_{red} + O_2 \qquad (15)$$

In an outer-sphere mechanism, a prior ligand exchange reaction is not required, but the electron transfer would take

place with $O_2^{\bullet-}$ outside of the first coordination sphere and thus further away from the metal ion.

The reaction in which $O_2^{\bullet-}$ oxidizes the reduced enzyme, which occurs in both the SOR and the SOD enzymes, is more challenging because of the requirement that the peroxide dianion, O_2^{2-}, be stabilized by bonding either to a metal ion or to a proton when superoxide accepts an electron and is reduced to peroxide. An inner-sphere mechanism utilizes the metal ion to stabilize the peroxide, and therefore the reduced enzyme must have either an open coordination site on the reduced metal ion or a rapidly exchangeable ligand so that exchange takes place prior to electron transfer. For SODs, it also requires that the resulting peroxo ligand be able to dissociate rapidly so that the oxidized enzyme is freed to react with another superoxide.

An outer-sphere mechanism utilizes only proton donors to stabilize peroxide (Scheme 2). Thus, $O_2^{\bullet-}$ must be docked at a

Scheme 2. Transfer of Two Protons Is Necessary for the Formation of H_2O_2
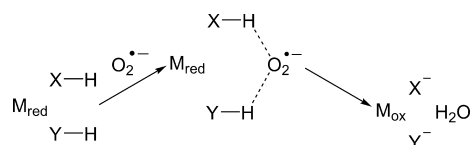
site that contains one or more proton donors capable of hydrogen bonding to $O_2^{\bullet-}$ and of transferring one or two protons to O_2^{2-} as it is formed. The proton donors at the superoxide docking site may include water molecules in the first coordination shell of superoxide as well as amino acid residues.

Because the substrate of the SOR and SOD enzymes is a small anion, it is not surprising to find that these enzymes tend to bind other small anions as well and that these small anions can sometimes act as inhibitors of the enzymatic reactions. This property of the enzymes is discussed in more detail below in sections 3−7. Studies of thermodynamics and kinetics of anion binding to these enzymes have proved quite useful in understanding the nature of their interactions with superoxide.

2.3.5. Selectivity. Another important property of the SOR and SOD enzymes is their ability to react selectively with superoxide in both their oxidized (SODs) and their reduced (SODs and SORs) states. In particular, the reduced enzymes are oxidized rapidly by superoxide but not by O_2, and the oxidized forms of SODs are reduced rapidly by superoxide. In the case of the SOR enzymes, they can be reduced by electrons transferred by rubredoxins or other cellular reductants (ultimately reduced by NAD(P)H oxidoreductases).

2.3.6. Electrostatic Guidance. To achieve fast reactions with $O_2^{\bullet-}$, the Fe, Mn, and CuZn SOD enzymes have evolved so that superoxide is guided into the active site channel using the distribution of electrostatic charges on the surfaces of the enzymes. Consequently, the catalytic rate constants for reactions of these enzymes with superoxide are very dependent on the ionic strength of the medium.[77] In the case of NiSOD, this ionic strength effect is not observed, presumably because the Ni site on NiSOD is much more exposed and thus more available for reactions with superoxide, while the Fe, Mn, and Cu centers of the other SODs are located at the bottom of narrow solvent-accessible channels. The active site in SORs is solvent-exposed, but surrounded by basic residues conferring a positive surface charge possibly favoring superoxide attraction

through an electrostatic antenna, and/or helping to strip the hydrated superoxide anion of its water molecules.

2.3.7. Proton Uptake by SODs upon Reduction.
The Fe, Mn, and CuZn SOD enzymes share another property that is undoubtedly related to their catalytic mechanisms and their remarkable abilities to catalyze rapid $O_2^{\bullet-}$ disproportionation at pH 7. Reduction of the oxidized forms of these enzymes is accompanied by the uptake of a proton. In the case of Fe- or MnSOD, the proton uptake occurs on the solvent ligand, which changes from OH^- to H_2O, while in CuZnSOD the bridging imidazole side chain becomes protonated (see sections 4−6). It is unknown if NiSOD shares this property.

2.3.8. Peroxidative Reaction.
Another property shared by some but not all SODs is irreversible inactivation of the enzyme resulting from reaction of the reduced SOD with H_2O_2. This reaction, generally termed the peroxidative reaction, is the result of a Fenton-type reaction in which the reduced metal ion at the active site reduces H_2O_2 to generate hydroxyl radical, which then reacts with amino acid residues nearby. Interestingly, eukaryotic CuZnSODs and most FeSODs react rapidly in this fashion with H_2O_2, whereas MnSOD and prokaryotic CuZnSODs[78] do not. NiSOD is also inhibited by hydrogen peroxide, but in this case the reaction appears to be reversible because SOD activity is restored when peroxide is removed. The reactions of the SODs with H_2O_2 are discussed further in sections 3−6.

2.3.9. Distinctive Characteristics of Individual Enzyme Types.
The properties of each of the different classes of SOD and SOR enzymes are discussed in detail in sections 3−7, each providing more detail on distinctive characteristics of the enzyme representing areas of active research. In the case of NiSOD, this characteristic is the use of sulfur-containing ligands to adjust the reactivity of the metal center. In the case of FeSOD, it is the redox tuning of the iron center that allows similar-looking proteins to optimize the reactivity of Mn or Fe with superoxide. For MnSOD, it is the diminution of SOD activity at high substrate concentrations. For CuZnSOD, it is how mutations in the human SOD1 gene cause familial amyotrophic lateral sclerosis (FALS). Finally, for SOR, it is the unique properties that make it an SOR rather than an SOD.

3. NICKEL SUPEROXIDE DISMUTASE

3.1. History and Properties

All known SODs utilize a redox metal center that cycles between oxidized and reduced states that differ by one electron during catalysis, the so-called ping-pong mechanism (see above). Furthermore, the optimum reduction potential for SOD catalysis is midway between the potentials associated with the oxidation and reduction of $O_2^{\bullet-}$, ~0.36 V. These are difficult values for Ni^{2+}_{aq} ions to achieve because water will both oxidize and reduce at potentials less extreme than Ni^{2+}_{aq}. In fact, of the redox metal ions found in SODs, only nickel does not catalyze superoxide disproportionation in aqueous solution.[79] This likely stems from the fact that calculations estimate the $Ni^{3+/2+}_{aq}$ reduction potential at +2.26 V.[80] Because this value lies outside the potentials bracketed by $O_2^{\bullet-}$ oxidation and reduction and cannot be supported in aqueous media, it explains both the fact that nickel has only one stable oxidation state in aqueous media, Ni^{2+}, and the lack of $O_2^{\bullet-}$ redox catalysis.[81] Thus, it came as a surprise to the community studying SODs when a nickel-dependent SOD, NiSOD, was discovered by Youn and Kang, et al., ca. 1996 in *Streptomyces*

species.[82] In addition to isolating a protein with SOD activity (using the indirect method involving cytochrome *c* reduction by $O_2^{\bullet-}$ produced by xanthine/xanthine oxidase), these researchers observed an $S = 1/2$ EPR signal ($g = 2.304$, 2.248, 2.012), with resolved superhyperfine splitting arising from one N-donor ($A = 2$ mT) on the high-field feature (Figure 5), in the as-isolated (~50% oxidized) enzyme. This
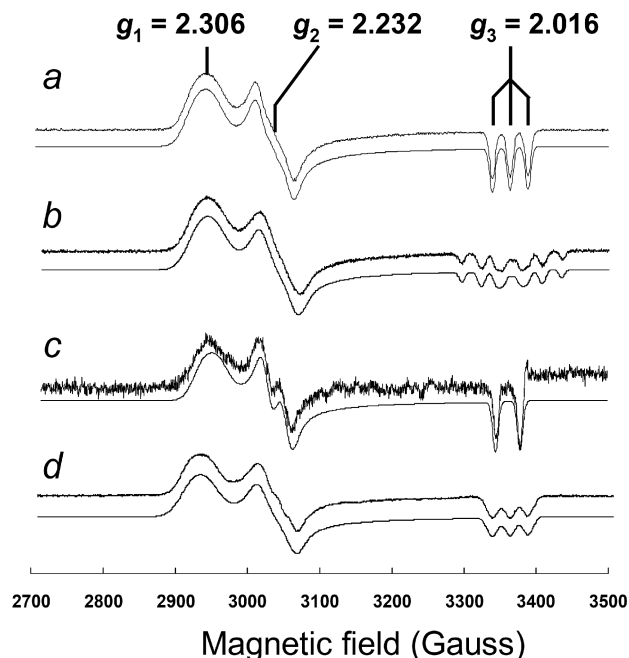
Figure 5. X-band EPR spectra of NiSOD. The experimental spectrum in each panel (upper spectrum) is compared to a simulated spectrum (lower spectrum) (reprinted with permission from ref 89). (a) Native enzyme with naturally abundant isotopes. The simulation uses the following parameters: $g_{xyz} = 2.306$, 2.232, and 2.016; $A_{xyz} = 16.2$, 17.7, and 24.6 G; and $l_{xyz} = 28$, 17, and 7.8 G. (b) NiSOD enriched with ^{61}Ni, giving unambiguous identification of the rhombic EPR signal to Ni. The simulation is based on the assumption that the signal is a composite of 87% of the ^{61}Ni ($I = 3/2$) signal and 13% of the normal Ni ($I = 0$) signal. Hyperfine splitting values used for the nitrogen are as in (a) and for ^{61}Ni are $A_{xyz} = 5$, 5, and 30 G. (c) NiSOD enriched with ^{15}N. The spectrum shows two prominent lines in the g_3 region instead of three as for normal enzyme, indicating that at least one nitrogen ligand is involved in Ni coordination in resting enzyme. Hyperfine splitting values used for ^{15}N are $A_{xyz} = 22.7$, 24.8, and 34.4 G. A clear splitting is observed in the $g = 2.23$ region, which was not resolved in spectra with ^{14}N donors at 100 K. (d) NiSOD enriched with ^{33}S gives direct evidence for sulfur ligands of Ni. The simulation assumes equal hyperfine interaction with two ^{33}S nuclei. Hyperfine splitting values used for ^{33}S are $A_{xyz} = 3.6$, 3.6, and 3.6 G. Microwave frequency, 9.482 GHz; temperature, 100 K.

EPR signal was remarkably similar to those found earlier for nickel-containing hydrogenases,[82a] established the presence of low-spin Ni^{3+} in the native enzyme, and implicated the $Ni^{3+/2+}$ couple in catalysis.

The observation of a Ni^{3+} species places demands on the protein environment of the nickel center to support this oxidation state. Nature uses electron-rich cysteine thiolate ligands to stabilize Ni^{3+} in a number of enzymes that have redox-active nickel centers,[83] as previously proposed for the [NiFe] hydrogenases (refer to the review by Lubitz in this thematic issue[84]). Initially, this seemed an unlikely ligand

environment for a nickel-dependent SOD, given the reactivity of S-donors to oxygen and peroxide,[85] and the absence of any S-donor ligands in the metal sites of any other SOD. As will be discussed in section 7, SORs have also a S-donor (cysteine) as one of the ligands to the catalytic iron site. X-ray absorption spectroscopy (XAS) detected the presence of multiple S-donor ligands in the nickel site, and established that a change in ligation from five-coordinate pyramidal to four-coordinate planar occurred upon reduction of the Ni center.[86] The fact that the protein contains only three S atoms, associated with Cys2, Cys6, and Met28 (*S. coelicolor* numbering), and mutation of Met28 had no effect, implicated the N-terminus as the Ni-binding locus.[87] Despite the presence of potentially oxidation-sensitive S-donors, kinetic studies using pulse-radiolytic generation of $O_2^{\bullet-}$ confirmed that the enzyme was an SOD that features catalytic rates close to the diffusion limit (10^9 M^{-1} s^{-1}), that are pH-independent near physiological pH (pH ≈ 5− 9.5), and virtually indistinguishable from the kinetic character-istics of *E. coli* MnSOD (Figure 6).[86] Thus, like other SODs, NiSOD does not exhibit saturation kinetics at any concen-tration remotely close to physiological.

Figure 6. A comparison of the pH-dependence of k_{cat} for native *S. seoulensis* NiSOD (green), recombinant *S. coelicolor* NiSOD (blue), and *E. coli* MnSOD (magenta).

Each SOD has a distinctive pattern of inhibition by anions and other small molecules, such as hydrogen peroxide. CuZnSOD is sen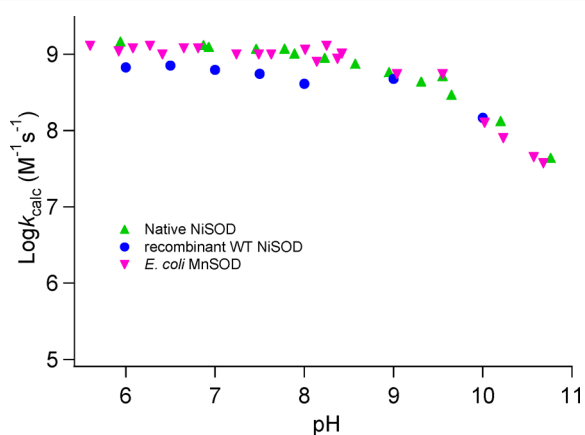sitive to inhibition by H_2O_2 and cyanide, whereas FeSOD is strongly inhibited by H_2O_2, but not cyanide. MnSOD is weakly inhibited by azide, but not by cyanide or H_2O_2. NiSOD is inhibited by cyanide and H_2O_2, but only weakly inhibited by azide, and thus most closely resembles the inhibition pattern of CuZnSOD.[82a] The interaction of these inhibitors with NiSOD was examined in more detail,[88] and it was found that 200 mM azide perturbs the EPR and CD spectra of the resting, oxidized enzyme, but these perturbations are small and identical to those produced by ^{15}N-labeled azide. They are therefore due to unresolved N-superhyperfine interactions and can be attributed to minor structural perturbations of the nickel site rather than ligation of azide by the nickel center. This led to a model wherein azide binds to the protein at an anion binding site that is near to the vacant sixth coordination position of the nickel and involves interaction with the N−H groups of the amides of Asp3 and Cys6, and is near to the OH group of Tyr9,[88] a structure that is in agreement with the crystal structure of the Cl$^-$/Br$^-$ anion complexes of a Y9F mutant enzyme (see below).[59]

3.2. Structure

3.2.1. Molecular Structure.
Eleven crystal structures for NiSODs are available as of 2013 in the PDB, including structures for as-isolated (partially oxidized) (1Q0D), and X-ray radiation (1Q0G)- or dithionite (1Q0K)-reduced *S. seoulensis* NiSOD,[89] and apo (1T6I)- and holo (1T6U)-wild-type NiSOD from *S. coelicolor*.[88a] In addition, there are structures available for Y9F (3G4Z)- and D3A (3G5O)-mutant *S. coelicolor* enzyme.[59] As the structures of the mutants are more relevant to the reaction mechanism, they are discussed in more detail in that section.

The protein structures of the wild-type enzymes from *S. seoulensis* and *S. coelicolor* are virtually identical, which is not surprising considering that their amino acid sequences are 90% identical. The structures reveal that the protein is an 80-kDa homohexamer composed of 13.4 kDa monomers that are antiparallel 4-helix bundles, each containing a nickel active site (Figure 7). The hexameric quaternary structure in solution has been confirmed by ultracentrifugation, ESI−MS under non-denaturing conditions, and by size-exclusion chromatography, and does not depend on N-terminal processing or incorpo-ration of nickel.[59,89,90] Apo-NiSOD protein is virtually identical to holo-enzyme in 3D structure except that the N-terminal Ni-hook motif is disordered in the absence of the metal.[88a] The hexamer is composed of helical subunits that form a roughly 60 Å diameter hollow sphere, with a 20 Å diameter interior void that is filled with water and cocrystallized ions.[88a,89] This structure is unique among SODs, which have a β-barrel structure (CuZnSOD) or both α- and β-structure (Fe/MnSOD) and do not exhibit hexameric quaternary structures (see Figure 2).

The hexamer structure can be viewed as a dimer of trimers, where the three monomers in the trimer resemble the legs of a piano stool, and the hexamer involves putting two trimers together so that the legs interdigitate (Figure 7). It features a 3-fold axis of symmetry (through the seats of both piano stools) that relates the monomers within each trimer, and three perpendicular 2-fold axes of symmetry that relate neighboring monomers from two trimeric units. The hexameric structure is supported by several salt bridges, hydrophobic, and hydrogen-bonding interactions that include an intersubunit hydrogen bond between Glu17 and the N−H group of the apical His1 imidazole ligand of the nickel site,[59,88a,89] the mechanistic role of which is discussed below in more detail.

The nickel sites are located at the N-terminus of each subunit (Figure 7), which places them in a distorted octahedral arrangement in the hexamer, with Ni−Ni distances of ~25 Å. The nickel ligands include the two thiolate S-donors, Cys2 and Cys6, and three different N-donors, including the N-terminal amine and imidazole side chain from His1, and the amidate from Cys2. Thus, four of the five nickel ligands are derived from the first two amino acid residues. These residues are part of what has been termed the "nickel hook" motif, which is characteristic of all NiSODs and is structurally facilitated by Pro5 in a *cis*-conformation that positions Cys6 as the last ligand in the sequence.[43a,88a] Although the nickel site is near the surface of the protein, it is effectively protected from solvent access by the hook motif. In the properly configured nickel hook, Val8 blocks access to the sixth coordination position, opposite the imidazole side chain of His1.

Ligation of the His1 imidazole side chain is a feature of the oxidized, five-coordinate pyramidal Ni^{3+} center, and gives rise to the observed N-hyperfine splitting in the EPR spectrum
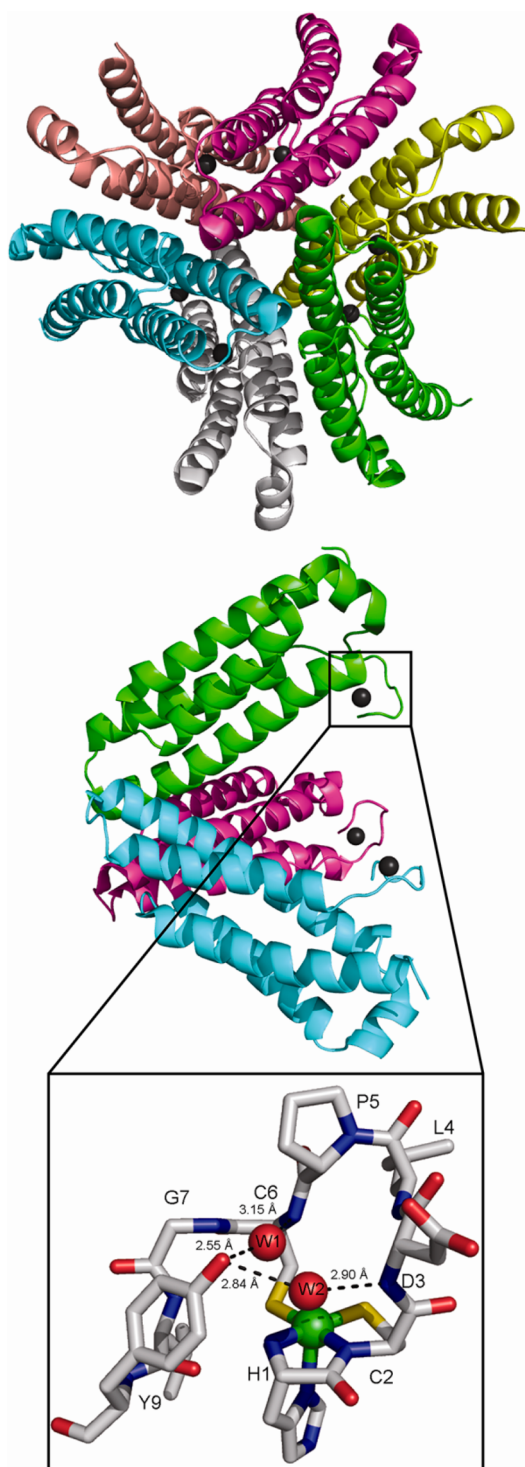
Figure 7. Structure of *S. coelicolor* NiSOD (PDB code: 1T6U) viewed down the 3-fold axis of the hexamer (top); a single trimeric unit (middle) viewed along a 2-fold axis in the hexamer, and the Ni-hook motif (bottom), in the oxidized state and showing the active site water molecules and hydrogen-bonding network. This figure was generated using the PyMOL Molecular Graphics System.[396]

(Figure 7).[88a,89] Upon reduction, the apical imidazole dissociates from the metal, resulting in a four-coordinate planar Ni^{2+} center with an N_2S_2 donor atom set provided by the remaining four active site ligands.[88a,89] This change in coordination number due to loss of a His imidazole ligand is also found in the structures for resting oxidized and reduced

CuZnSOD;[91] similarly, in most SORs the reduction of the iron ion is accompanied by a dissociation of an Fe ligand (in this case, a glutamate, see section 7). The as-isolated protein preparation has been found to be a mixture of oxidized and reduced nickel sites, with His-on or His-off nickel centers, respectively;[88a,89] thus the His1 imidazole occupies multiple positions in the structures. Double integration of the first derivative EPR signal showed that as-isolated protein solution contains approximately 50% Ni^{3+}, and that this value did not change upon addition of oxidants, a feature that might suggest some sort of redox cooperativity between subunits.[59]

3.2.2. Electronic Structure. The electronic structure of the nickel sites has been addressed by spectroscopic probes and calculations using the structure of the active site as a starting point,[88b] and is summarized by the frontier molecular orbital diagram in Figure 8. The rhombic EPR signal characteristic of
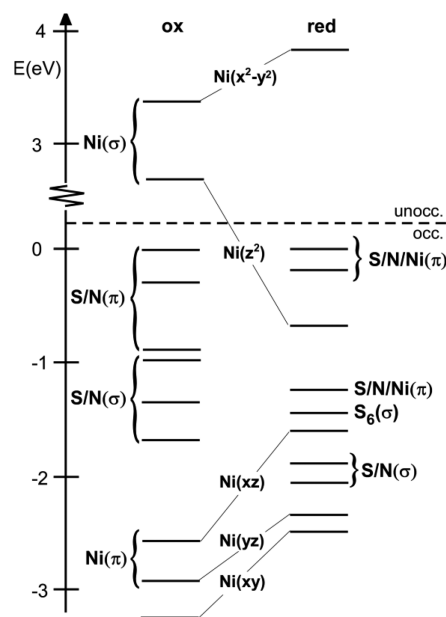
Figure 8. DFT frontier molecular orbital energy diagrams for oxidized (His-on, spin−down orbitals from an unrestricted calculation) and reduced (His-off) NiSOD (adapted from ref 88b).

the oxidized enzyme (Figure 5) is consistent with a low-spin d^7 Ni^{3+} site, giving rise to an $S = 1/2$ center with the single unpaired electron in a d_{z^2} orbital (a single occupied molecular orbital, SOMO), as in the EPR active forms of the nickel center of Ni-hydrogenases. The predominantly nickel character of the $S = 1/2$ species is consistent with the large hyperfine splitting (30 G) observed on the highest field feature upon incorporation of ^{61}Ni ($I = 3/2$).[89] The assignment of ^{14}N-superhyperfine splitting ($I = 1$) on the high-field feature was confirmed by ^{15}N ($I = 1/2$) substitution,[89] which also revealed previously unresolved superhyperfine splitting contributions at the resonances associated with other g-values, and by Q-band ENDOR.[92] The superhyperfine splitting associated with enzyme prepared with ^{33}S is small (3.6 G), isotropic within experimental error, and consistent with the largely nickel-centered radical and the d_{z^2} SOMO that nonetheless has significant covalent interactions with the ligands in the σ-bonding system.[89]

The electronic absorption spectrum of the as-isolated (resting oxidized) NiSOD is dominated by an absorption

maximum at ~380 nm with a high extinction coefficient ($\varepsilon \approx$ 6800 M^{-1} cm^{-1}, calculated per Ni^{3+} center) that has been assigned to a largely S(Cys) $\rightarrow$ Ni^{3+} ligand to metal charge transfer transition (LMCT) based on calculations and resonance Raman data.[88b] Raman spectra obtained by irradiating at 380 nm revealed bands at 349, 365, and 391 cm^{-1} associated with Ni–S vibrations. The MCD spectrum is dominated by *C*-terms, consistent with this electronic structure and providing the ability to separate the spectral features associated with Ni^{3+} in the sample from those of diamagnetic Ni^{2+} centers, where the charge-transfer transitions are shifted into the UV region and the spectrum consists largely of much less intense ligand field transitions that resemble the spectra of planar Ni^{2+} complexes with N$_2$S$_2$ coordination.[88b]

These spectral features buttress the computational models of the electronic structure of the oxidized and reduced sites (Figure 8), which reproduce the EPR *g*-values and hyperfine splittings observed for the oxidized Ni^{3+} center and are consistent with the d$_{z^2}^1$ ground state.[88b] The calculations also point to the importance of interactions with the anionic ligands in the equatorial plane (Cys2, Cys6, and the Cys2 amidate) that lead to filled/filled antibonding π-interactions with Ni that lower the reduction potential of the active site. The loss of the apical His1 imidazole ligand upon reduction strongly stabilizes the d$_{z^2}$ orbital, resulting in HOMOs (highest occupied molecular orbital) for the Ni^{2+} site that are comprised largely of filled π-orbitals from Ni^{2+} and the three anionic equatorial ligands. By increasing the energy and nickel character of the HOMO in the reduced site, the π-interactions make the site easier to oxidize and promote metal versus sulfur oxidation.[88b] A mechanistic implication from computational models is that the redox molecular orbital for the two NiSOD half-reactions is different (d$_{z^2}$ for O$_2^{\bullet-}$ oxidation, Ni d$_{x^2-y^2}$/S/N p for O$_2^{\bullet-}$ reduction).[88b]

3.3. Catalytic Mechanism

SODs achieve catalysis via the ping-pong mechanism, in which the metal center oscillates between oxidized and reduced states that differ by one electron.[93] As such, the general SOD mechanism consists of two half-reactions, where substrate oxidation produces O$_2$ and the reduced metal site, and substrate reduction produces H$_2$O$_2$ and the oxidized metal site. In the case of NiSOD, the study of these half-reactions is complicated by the fact that the solution of the as-isolated enzyme contains a roughly 50–50 mixture of Ni^{3+} sites and Ni^{2+} sites, and that it cannot be oxidized further.[59] As a result, only the overall rate of catalysis and the initial reaction of the fully reduced enzyme can be studied.

The discussion above convincingly identifies the Ni$^{3+/2+}$ couple as the relevant metal redox chemistry for NiSOD. Redox titrations have established that NiSOD, like all SODs, has a reduction potential (0.29 V) that is close to the optimum potential for catalysis.[59] Kinetic analysis of the rate of consumption of pulse radiolytically generated O$_2^{\bullet-}$ in the presence of NiSOD shows that like other SODs, the reaction is essentially diffusion limited ($k_{cat} \approx 10^9$ M^{-1} s^{-1} per nickel site) and independent of pH near physiological values (Figure 6),[59,87,86] indicating that protons for H$_2$O$_2$ production are derived from a protein residue. In fact, the reaction rate and pH dependence of k_{cat} for NiSOD is identical to that of MnSOD,[86] despite the lack of any metal site structural features in common between the enzymes.

3.3.1. Outer- versus Inner-Sphere. Each half-reaction could proceed by either outer-sphere, where no Ni–O$_2^{\bullet-}$ bond forms, or inner-sphere mechanisms that involve formation of a Ni–O$_2^{\bullet-}$ complex, or a mixture of these two mechanisms. For NiSOD there is considerable disagreement regarding even this most basic feature of the reaction mechanism. Theoretical calculations of the reaction mechanism have assumed an inner-sphere mechanism and are thus nearly silent on this issue (see above). The presence of an open coordination position on the Ni^{3+} center might suggest coordination of the substrate, as well as inhibition by other anions, and electrostatic steering. However, unlike other SODs, the apparent lack of an ionic strength effect on k_{cat} indicates that this aspect is not as important for NiSOD catalysis, perhaps because of the more solvent-accessible active site. The open coordination site might reflect the need for a low-spin electronic configuration, while anion inhibition could arise from competition for an anion-binding site other than the metal center. The observation that azide does not bind to the Ni center (see above) argues in favor of an outer-sphere mechanism.[88] Perhaps the most compelling experimental data in this regard are the anion binding site crystallographically characterized for the Cl$^-$ and Br$^-$ complexes of Tyr9Phe-NiSOD (Figure 9).[59] The anions are
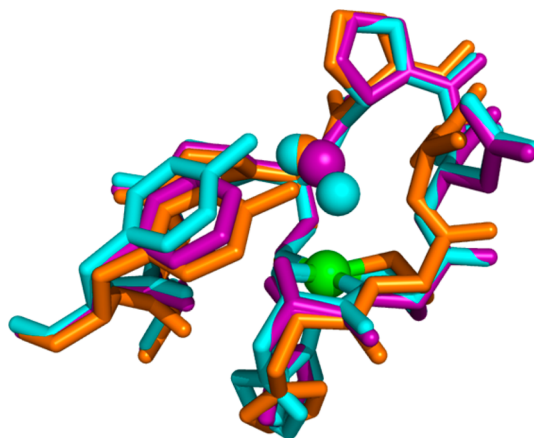
Figure 9. Superposition of the Ni-hook domains of WT (blue), Tyr9Phe (purple), and Asp3Ala (orange) NiSODs showing the position of residue 9 (reproduced from ref 59). The green sphere represents the Ni position in all three structures, and the purple sphere indicates the Cl$^-$ or Br$^-$ position in Tyr9Phe-NiSOD. The blue and orange spheres represent water molecules present in WT and Asp3Ala NiSOD, respectively.

found in the same location that was originally proposed for azide binding to account for the small perturbation of the Ni spectroscopic features.[88a] In WT-NiSOD, Tyr9 lies near the vacant sixth coordination position of the nickel center, with a Ni–O distance of 5.47 Å, and is involved in hydrogen-bonding interactions with two ordered water molecules at 2.56 Å (W1) and at 2.84 Å (W2). It is in a position to control access of anions to the active site and appears to play the same role as the "gateway tyrosine" found in MnSODs[94] and FeSODs.[95] The active site water molecules also accept hydrogen bonds from amides (Cys6 to W1 and Asp3 to W2). In the Tyr9Phe-NiSOD mutant *S. coelicolor* enzyme, W1 is replaced by Cl$^-$ or Br$^-$, with a Ni–Cl distance of 3.5 Å, a nonbonded distance that does not result in the observation of Cl hyperfine splitting in the EPR spectrum.[59] Like WT-NiSOD, the crystals contain mixtures of Ni^{3+} (His-on) and Ni^{2+} (His-off) sites, and there is no

indication of Cl⁻ coordination in either site. Thus, the data support an outer-sphere redox mechanism for both half reactions. Furthermore, another mutant, Asp3Ala-NiSOD, changes the position of Tyr9 such that the phenol group is ~1 Å closer to the nickel site (Figure 9) and alters the chemistry with H_2O_2: WT-NiSOD is reversibly inhibited by H_2O_2, which reduces Ni^{3+}, while Asp3Ala-NiSOD loses activity during turnover and is irreversibly inhibited by H_2O_2.[59] Although Asp3Ala-NiSOD exhibits reduced activity relative to WT-NiSOD, this is not due to a change in the properties of the nickel site. The EPR spectrum observed is essentially that of WT-NiSOD, and redox titrations show that the reduction potential is unchanged.[59] In the Ni-hook configuration adopted by Asp3Ala-NiSOD, Tyr9 is in a position that would be less effective in inhibiting access of H_2O_2 to the nickel site and could even stabilize formation of a Ni–OOH peroxo or superoxo adduct that results in oxidation of Tyr9.[59]

3.3.2. The Roles of the Nickel Ligands.

The ligand and protein environments of the active sites of SODs evolved such that three essential features for catalysis were reached: (1) Adjustment of the metal reduction potential to an optimum level for catalysis (~0.36 V); (2) control of anion ($O_2^{\bullet-}$) access to the active site, as discussed above for Tyr9; and (3) availability of a source of protons for formation of H_2O_2. The role of the nickel ligands in NiSOD in those features has been addressed using a mutagenic approach, which has resulted in a number of mutant proteins with lower catalytic activity.[81,90,96] The activities of mutant NiSODs have been reviewed.[81,97]

Unlike Fe- or Mn-SOD, where the metal has an aqua ligand whose protonation state and hydrogen-bonding interactions can be used to adjust the reduction potential, NiSOD has no aqua ligand and instead employs thiolate ligation from Cys2 and Cys6 as the primary mechanism for adjusting it. Sulfur-donor ligands play a critical role in the redox biochemistry of nickel. Without these electron-rich donors, the $Ni^{3+/2+}$ couple would lie at potentials that are above those that can be accessed by biological oxidants. Indeed, in biology, thiolate (cysteinate) ligation is closely associated with nickel centers that play a redox role.[83] Mutation of the Cys2 and Cys6 residues to Ser, individually or in tandem, gave rise to NiSOD mutant proteins that were catalytically inactive and did not display a Ni^{3+} EPR signal, indicating that they were isolated as Ni^{2+} complexes.[90] All three mutants were essentially spectroscopically identical, and spectral analyses showed that none of the nickel sites involved Cys ligation,[90,96] even if one of the pair of Cys residues was present. Further, the Ni^{2+} centers in the Cys mutants were high-spin ($S = 1$),[96] indicating that in addition to the importance of Cys ligation for the reduction potential, the presence of both Cys ligands is required for the low-spin electronic configuration.

In addition to their role in determining the reduction potential and electronic structure of the active site, the Cys ligands in NiSOD also appear to be the source of protons for the production of H_2O_2. The low sulfur content of the enzyme made it possible to address the role of the Cys ligands using S K-edge XAS (Figure 10).[98] The as-isolated (oxidized) enzyme reveals two pre-edge transitions associated with excitation of sulfur 1s electrons into vacancies in both the $3d_{z^2}$ and the $3d_{x^2-y^2}$ orbitals of low-spin d^7 Ni^{3+}, essentially high-energy LMCT. Upon reduction in the X-ray beam, the lower energy transition is lost, appropriate for the formation of low-spin d^8 Ni^{2+} with vacancies only in the $3d_{x^2-y^2}$ orbital. However, when NiSOD was reduced with H_2O_2, essentially running the reductive half-
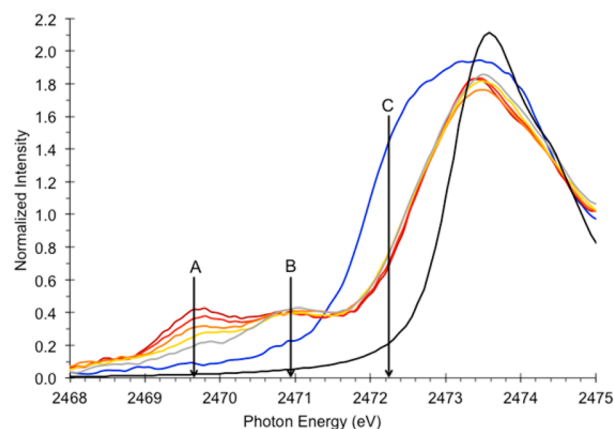
Figure 10. S K-edge spectra for *S. coelicolor* WT NiSOD during photoreduction in the X-ray beam (red-gray spectra) and reduced with H_2O_2 (blue). The NiSOD samples are compared with spectrum obtained from cysteine (black) (adapted from ref 99 with permission). The feature marked A (2469.7 eV) is lost upon X-ray reduction, while B (2470.9) is retained.

reaction in reverse, no pre-edge features were observed.[98] The loss of these features was attributed to protonation of the Cys ligands, which would shift the transition involved up near the S K-edge in energy.[98] The broadened edge for this sample is consistent with this expectation. This result is in agreement with computational models that favor protonations of Cys ligands in the reduced enzyme,[99] although these calculations disagree on which Cys residue is the H⁺ donor to the substrate.

3.3.3. Computational Studies.

Computational studies of the reaction mechanism have identified several features that may be important to the mechanism. Noting that the crystallographic bond distance between Ni and the apical histidine imidazole ligand, Ni–N(His), in NiSOD structures is quite long (2.3–2.6 Å)[88a,89] and involves a hydrogen-bonding interaction with Glu17 from a neighboring subunit that is supported by an intrasubunit hydrogen bond with Arg47 (Figure 11), several DFT computational models were developed to explore the influence of these hydrogen-bond interactions on the Ni–N(His) distance and the energy of the redox active orbital, d_{z^2}.[88b] The results show a trend that increases the Ni–N(His) distance from 2.07 Å without hydrogen bonding to 2.16 Å with both hydrogen-bond interactions intact, but not to the extent suggested by the crystal structure. (Other bond distances are predicted by the DFT models within 0.05 Å of the crystallographically determined values.[88b]) The 2.07 Å distance is typical of Ni–N(His) distances in small molecule structures,[88a] consistent with other calculations,[99a] and more consistent with distances obtained from EXAFS analysis of as-isolated NiSOD (average Ni–N = 1.91 Å),[86] and may suggest that the disorder in His1 due to the presence of more than one conformation in the crystal structures leads to a determination of an apical Ni–N distance that is too long. In any event, lengthening the axial interaction is expected to stabilize the redox active orbital, and thus the apical Ni–N(His) interaction is important to tuning the reduction potential of the active site.

The reaction pathway involved in $O_2^{\bullet-}$ disproportionation has also been addressed using DFT to explore the potential energy surface, in inner-sphere processes.[99a] The preferred mechanism is shown in Figure 12 and features a reduced form of NiSOD that features a protonated Cys ligand and retains
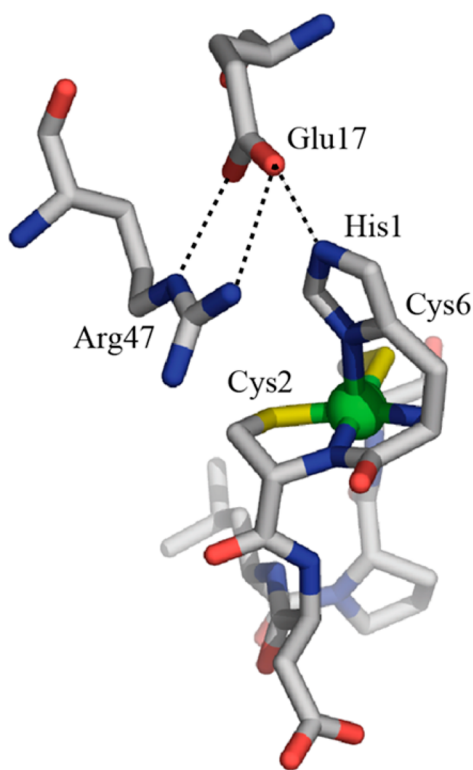
Figure 11. The Ni-hook motif shown with intersubunit His1···Glu17 hydrogen bond and supporting intrasubunit Glu17···Arg47 interaction.

axial His1 imidazole coordination. This results in a five-coordinate square-pyramidal high-spin Ni^{2+} species that has not been detected experimentally. Cys2 was favored for this role over Cys6 because it has a larger electronic density at the solvent-accessible face of the N$_2$S$_2$ plane. The reaction proceeds via two transition states. The transition state for O$_2^{\bullet-}$ oxidation involves the transfer of a proton from coordinated OOH to Cys2. The transition state for substrate reduction features transfer of the Cys2-SH proton to the proximal O-atom in the Ni−OOH complex. Thus, the only transition states involved in the reaction mechanism feature proton transfer between the substrate and a group present in the active site, which is also a characteristic of the reaction pathway for CuZnSOD, where the bridging imidazolate plays this role,[100] or as proposed for the SORs, where a lysine residue close to the metal site may act as a proton-donor or enhance the acidity of a water molecule in the site (see section 7). The investigators noted that for NiSOD, substrate binding is favorable only in the oxidative phase, and this binding is nearly thermoneutral, which could be interpreted as evidence of an outer-sphere mechanism for both half-reactions.[99a]

Other sites for protonation were considered, including the His1 imidazole ligand, resulting in a mechanism that uses the same ligand as the proton donor/acceptor as found for CuZnSOD.[99a] However, in the pyramidal NiSOD active site, the His1 imidazole occupies the apical position and is thus *trans* to the site of OOH binding, whether it binds directly to the nickel center or in the anion binding site (see above), and is thus blocked from direct interaction with the substrate via the ligands in the basal plane. Therefore, a role for the His1 imidazole ligand as the primary proton donor/acceptor seems unlikely and would need to be mediated by other protein residues. Calculations indicate that all pathways involving His1

imidazole protonation are less favorable.[99a] Nonetheless, protonation of His1 by the Cys-SH in intermediate 4 (Figure 12) would lead to formation of the resting Ni^{2+} state of the enzyme, a planar, diamagnetic, *cis*-NiN$_2$S$_2$ complex. Additional calculations systematically investigated the protonation site in NiSOD and reached similar conclusions, although in this case Cys6 was favored over Cys2 as the proton donor/acceptor.[99b]

3.4. Evolution and Genomics

Although the gene encoding NiSOD, *sodN*, has been identified in eukaryotic green algae,[43] it is mainly found in bacteria. The *sodN* gene encodes a protein that includes a variable N-terminal extension that is removed in the mature enzyme by a peptidase (*sodX*),[101] producing an enzyme with His at the N-terminus, a post-translational modification that was first indicated by N-terminal sequencing.[82a] This led to several strategies for producing recombinant enzyme with the properly processed N-terminus.[87−89] In *Streptomyces*, the expression of *sodN* is induced by the presence of Ni^{2+} ions using Nur, a transcriptional regulator of the Fur (ferric uptake regulator) family.[102] The transcription of alternative SODs, such as the FeSOD found in *Streptomyces coelicolor*, is repressed by micromolar levels of Ni^{2+} via Nur.[102b]

NiSOD is the most common SOD in marine organisms. As of 2013, there are over 85 gene sequences identified as *sodN*,[43a,81] each of which codes for proteins that contain the highly conserved (HCXXPCXXY)-N-terminal nickel hook. Phylogenetic trees have been constructed using these sequences and the Sargasso Sea metagenome.[43a] These studies produced dendrograms containing four major clusters: I-actinomycetes; II-cyanobacteria; IIIa-gammaproteobacteria and IIIb-bacteroidetes; and IV-planctomycetes, cyanobacteria, and deltaproteobacteria.[43a] Relative to the nickel hook sequence found in *Streptomyces* species, HCDLPCGVY-, the residues that provide the nickel ligands (His1, Cys2, and Cys6) are invariant, and most other variations involve conservative replacements. Tyr9 is substituted in only one sequence (by Phe), and Pro5 is replaced by Tyr or Phe in two sequences from *Mycobacterium* species.[43a] More variable residues in the nickel hook motif include Asp3, which is substituted by Gln or Glu in proteins from cluster IV, Gly7, which is substituted by Ala or Lys in some cluster III sequences, and Val8, which is replaced by Ile in several sequences in clusters III and IV.[43a] The genetic data also support the hypothesis that NiSOD evolved in response to the decreased availability of iron in marine environments that was a consequence of the evolution of oxygenic photosynthesis.[43a] Other organisms may have acquired NiSOD via lateral gene transfers.[43a]

3.5. Comparisons to Other SODs

NiSOD appears to represent a case of convergent evolution that resulted initially from an evolutionary adaptation to use Ni as the requisite redox metal, and its emergence accompanied the decreased availability of Fe in the ocean that resulted from oxygenic photosynthesis. The use of Ni as the redox center in a superoxide dismutase was made possible by the features of the metal-binding site, which adjust the Ni$^{3+/2+}$ couple reduction potential to the required range. This resulted from the evolution of the Ni-hook, which provides all five of the nickel ligands from the first six amino acid residues (His1, Cys2, and Cys6) and provides an elegant mechanism to stabilize Ni^{3+} and tune the reduction potential for catalysis. Nonetheless, NiSOD evolved many of the features found in other SODs to catalyze a pH-independent reaction at diffusion-limited rates. These
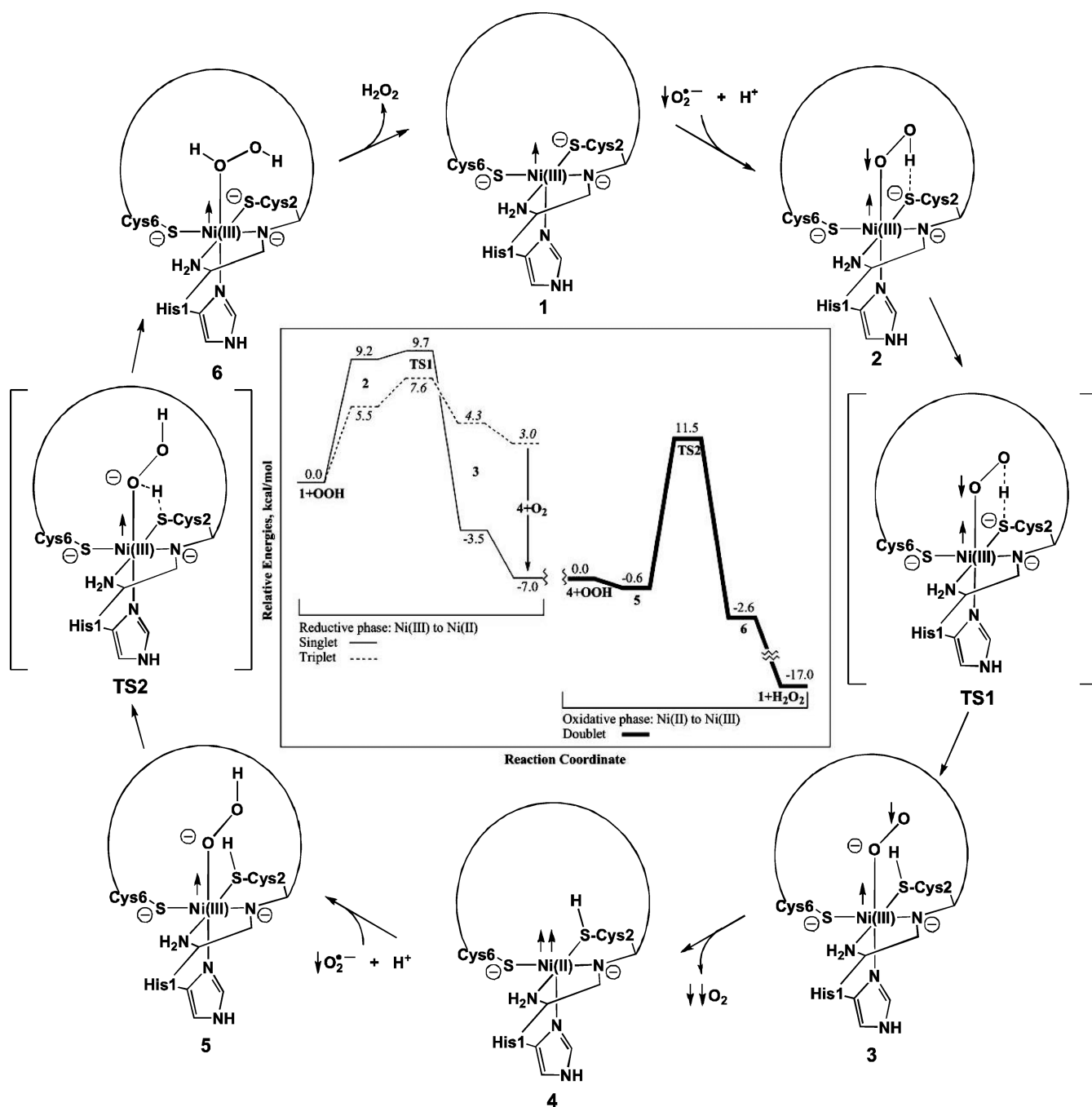
Figure 12. Proposed catalytic cycle for NiSODs from DFT calculations and free energy diagrams (center) for the oxidative and reductive half-reactions (adapted from ref 97).

features include the presence of a "gateway tyrosine", like that found in MnSODs and FeSODs, that controls substrate access to the active site, and the use of a protein residue (cysteine) as a proton donor/acceptor site in analogy with the bridging His imidazolate in CuZnSOD. The result is a distinct structural class of SOD that catalyzes $O_2^{\bullet-}$ disproportionation by a mechanism that bears many similarities with other versions of the enzyme.

4. IRON SUPEROXIDE DISMUTASES

4.1. History and Properties

FeSOD was first discovered in *E. coli* in 1973,[103] shortly after the discovery of CuZnSOD in 1969[104] and MnSOD in 1970,[105]

and soon thereafter it was found in a variety of other bacteria including anaerobes[106] (reviewed in ref 107). The first eukaryotic FeSOD was discovered in a protist in 1977,[47,108] and it was found in a plant soon thereafter.[109] Even archaea possess FeSOD,[110] so FeSOD is represented in all three kingdoms of life. Section 4.5 provides a discussion of phylogenetic insights obtained from comparison of FeSOD and MnSOD amino acid sequences.

Early on it was realized that FeSODs and MnSODs are similar to each other but different from CuZnSOD.[111] This homology was established beyond doubt by demonstration that the crystal structure of a MnSOD was similar to that of an FeSOD with respect to secondary and tertiary structure (Figure

13).[112] In addition, all known FeSODs and MnSODs employ the same amino acids to coordinate the active site Fe or Mn ion. Given that the FeSODs and MnSODs are evidently members of the same protein family, it is not surprising that there are also SODs from this family that can use either metal ion. Early reports showed that a number of organisms that have a single gene encoding an FeSOD or a MnSOD produce the Mn version when exposed to O_2 or when deficient in Fe, but the Fe version otherwise.[113] These SODs display activity under
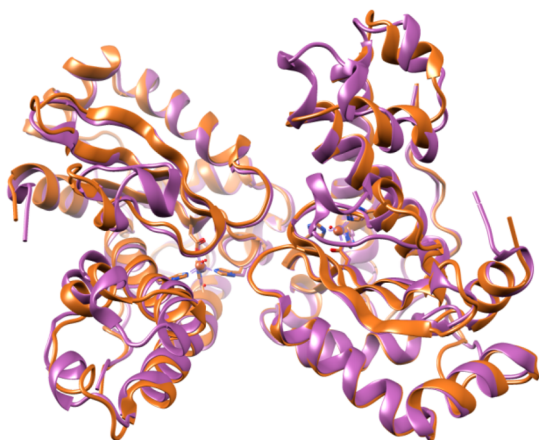
Figure 13. Overlay of the backbones of *E. coli* FeSOD (orange) and MnSOD (magenta) based on the coordinates of Lah et al (PDB code: 1ISB).[126a] and Borgstahl et al (PDB code: 1D5N).[397] This figure and Figures 17, 21, and 22 were generated using Chimera[398] and swissPDBviewer.[399]

Table 4. A Selection of SODs Whose Activity is Metal-Specific, Preferential for One of Fe or Mn, or Cambialistic

SOD protein	Fe-supported activity[a] (units/mg protein)	Mn-supported activity[a] (units/mg protein)
E. coli (Fe)SOD[75a]	7000	10
Sulfolobus sulfataricus[115] (archaeal)	930	5
Propionibacterium freudenreichii (shermanii) (actinobacterial)[116]	810	790
Bacteroides fragilis[114a]	1300	640
Porphyromonas gingivalis[117]	2200	3700
Pyrobaculum aerophilum (pH 7.8)[118] (archaeal)	500	2800
Aerophylum pernix[119] (archaeal)	220	1200
Mycobacterium smegmatis[120] (actinobacterial)	340	4800
Methylomonas-J[121]	170	4600
Rhodobacter capsulatus[122]	1 equiv[b]	42 equiv[b]
Streptococcus mutans[123]	230[c]	4500
E. coli (Mn)SOD[74a,124]	10	7000

[a]Based on the standard assay[104] and corrected for substoichiometric Fe or Mn incorporation. [b]Only relative activities were reported, "equiv" stands for equivalents. [c]This activity can be explained by Mn present.

the same conditions with either Fe or Mn bound (Table 4)[113b,114] and so are called cambialistic (Latin cambium: exchange or change) or Fe/MnSODs hereafter. We use the terms FeSOD and MnSOD for SODs that are believed to be active with Fe or Mn, respectively, but not both. As expected,

the cambialistic Fe/MnSODs also display the canonical structure characteristic of the entire family of FeSODs, Fe/MnSODs, and MnSODs (Fe- and/or MnSODs hereafter).

As described in section 2, the ping-pong mechanism shared by all types of SODs requires that the enzyme's reduction potential ($E°$) fall between those of superoxide oxidation and reduction. This is already a natural feature of the $Fe^{3+/2+}$ couple, so only modest redox tuning is required for the FeSOD protein to bring the $Fe^{3+/2+}$ couple to an optimal $E°$. By contrast, the much higher intrinsic $E°$ of the $Mn^{3+/2+}$ couple posed a challenge that evolution solved by repositioning and replacing just a few key residues with only minor changes to the overall structure. To understand how the metal-binding sites of the FeSODs and MnSODs confer SOD activity on each of their respective metal ions, we first introduce the structure of FeSOD and then review its mechanism. The mechanism of MnSOD incorporates additional complexity, as discussed in section 5.3.

4.2. Structure

As of 2014, the protein data bank contained ~90 structures of FeSODs and MnSODs. Their monomers have been found to share the same two-domain fold (Figure 13).[112,125] The C-terminal domain is comprised of three β-sheets surrounded by α-helices wherein two Fe ligands are located in the third β-strand and the loop that follows it. The N-terminal domain is α-helical with the first and the last helices each providing one ligand to the active site Fe. The loop or middle helix shown in Figure 13 for *E. coli* FeSOD and MnSOD, respectively, is absent among tetrameric Fe- and/or MnSODs where the corresponding amino acids extend the two main helices and participate in the interface between dimers.

Each monomer of FeSOD contains an active site organized around a single Fe ion. Fe is coordinated in trigonal bipyramidal geometry with the side chains of His73, His160, and Asp156 as the equatorial ligands, and the side chain of His26 and H_2O (or OH^-) as its axial ligands (Figure 14, inset). (Numbering of *E. coli* FeSOD will be used throughout this section.) Upon coordination of an azide ligand to oxidized FeSOD, the $N(His73)-Fe^{3+}-N(His160)$ angle opens further to accommodate N_3^- and creates a roughly octahedral geometry.[126]

The OH^-/H_2O ligand, which has a slow exchange rate with bulk water,[127] forms hydrogen bonds with the ligand Asp^- and the conserved active site Gln that tether it in place (Gln 69 in *E. coli* FeSOD).[126a,128] Therefore, this OH^-/H_2O is considered to be an integral part of the active site, in contrast to Fe-bound labile solvent molecules in various other enzymes, which are replaced by substrates during the catalytic cycles.[129] When the FeSOD iron is oxidized (Fe^{3+}), the solvent ligand is believed to be OH^-, whereas when the iron is reduced (Fe^{2+}), the solvent ligand is H_2O.[130] The same applies to MnSOD.[130c,131]

The OH^-/H_2O ligand is linked to a highly conserved hydrogen-bonding network, beginning with Gln69 and including conserved Tyr34 and His30. Tyr34 and His30 connect the OH^-/H_2O ligand to bulk water as well as to the site in which substrate binds (Figure 14).[126a,130a] The active site Gln is hydrogen bonded to the side chains of Asn72 and Trp122. Additional conserved hydrogen bonds link the active site to the interface between FeSOD monomers, which includes a hydrogen bond between active site residues His160 of one monomer and Glu159 of the other, and a hydrogen bond between His30 of one monomer and Tyr163 of the other. As discussed below, this extensive network of interactions tunes
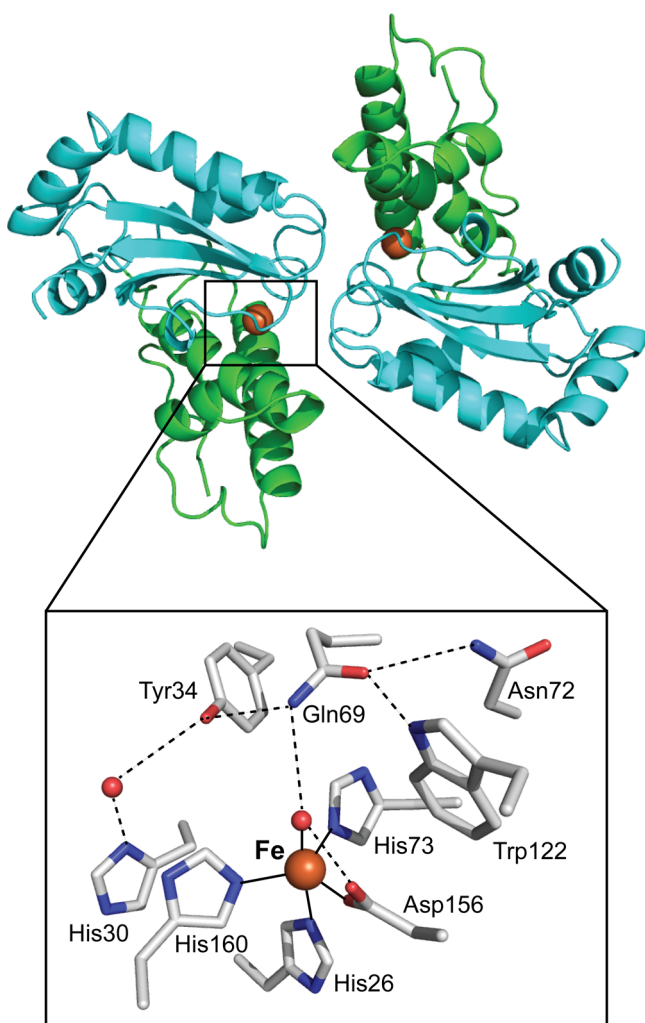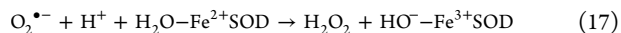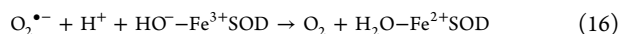
Figure 14. Ribbon structure of *E. coli* FeSOD (top) and close-up view of the active site (bottom) based on the coordinates of Lah et al.[126a] (PDB code: 1ISB). Hydrogen bonds are dashed lines, and coordination bonds are solid lines. Within each monomer, the N-terminal domain is in green and the C-terminal domain is in teal. This figure was generated using the PyMOL Molecular Graphics System.[396]

the properties of active site residues, and distributes the energetic costs over the rest of the FeSOD structure.

4.3. Catalytic Mechanism

FeSOD's ping-pong reaction involves alternating reduction and oxidation of the metal ion but acquisition of a proton in both of the two half-reactions (eq 16–eq 17).

$$O_2^{\bullet -} + H^+ + HO^- - Fe^{3+}SOD \rightarrow O_2 + H_2O - Fe^{2+}SOD \quad (16)$$

$$O_2^{\bullet -} + H^+ + H_2O - Fe^{2+}SOD \rightarrow H_2O_2 + HO^- - Fe^{3+}SOD \quad (17)$$

Proton transfers make critical contributions to the mechanisms of all SODs and SORs because protonation of superoxide is required for it to be readily reduced to peroxide (eq 17).[132] In FeSODs and MnSODs, a proton is acquired by the OH$^-$ ligand in conjunction with Fe reduction (eq 16), and release of a proton from the resulting H$_2$O ligand then makes a proton available to protonate superoxide (eq 17). Thus, the H$_2$O ligand is believed to serve as a local proton donor to nascent peroxide,[132b,133] with the active site hydrogen-bond network providing a proton relay[134] that mediates proton movement, determines the placement of protons,[133a] and enables the active

site to draw upon bulk water for the second proton,[135] which is required for product release (eq 17).[131,136] As is shown in Scheme 3, the catalytic mechanism can be broken down into five steps that will be discussed individually below.

4.3.1. Step 1: Inner-Sphere Binding of O$_2^{\bullet -}$ to Fe^{3+}SOD. O$_2^{\bullet -}$ is considered to coordinate directly to Fe^{3+} in Fe^{3+}SOD (inner-sphere binding, Scheme 3, step 1); as such coordination has been demonstrated for the small anions N$_3^-$, F$^-$, and OH$^-$.[126b,137] Moreover, N$_3^-$ and F$^-$ are competitive inhibitors of FeSOD, with inhibition constants consistent with their binding to the oxidized state of the enzyme.[131] Azide's K_M increases at high pH with a pK_a comparable to that for coordination of OH$^-$ to Fe^{3+}, indicating that OH$^-$ is also a competitive inhibitor.[131] This is consistent with the fact that FeSOD activity diminishes at high pH due to an increase in the K_M but little effect on k_{cat}.[131,138] Thus, in Fe^{3+}SOD, inhibition at high pH does not stem from deprotonation of an active site residue, but from the action of OH$^-$ itself as a competitive inhibitor.

While the crystal structure of N$_3^-$-ligated FeSOD serves as a model for the oxidized enzyme·substrate complex,[126] N$_3^-$ is 50% larger than O$_2^{\bullet -}$ and there is evidence that steric conflict with Tyr34 forces N$_3^-$ to bind at an angle that is different from the orientation adopted by O$_2^{\bullet -}$ (see below). Thus, N$_3^-$ probably does not accurately model the interaction of O$_2^{\bullet -}$ with amino acids of the active site.

O$_2^{\bullet -}$ binding may benefit from a synergy between Fe^{3+} coordination and hydrogen bonding from Tyr34. Fe^{3+}SOD has a 20-fold higher affinity than does Fe^{2+}SOD for F$^-$, suggesting that coordination to Fe^{3+} provides the largest contribution to binding energy.[95b] Hydrogen bonding with Tyr34 also favors substrate binding based on the 2–5-fold lower K_d's displayed by WT-Fe^{3+}SOD as compared to Y34F-Fe^{3+}SOD for small anions.[95b] Tyr34 acts to exclude anions larger than O$_2^{\bullet -}$,[95b] as the K_d for N$_3^-$ binding is 20-fold lower for Y34F-Fe^{3+}SOD than for WT Fe^{3+}SOD.

SCN$^-$, Cl$^-$, HCOO$^-$, and SO$_4^{2-}$ are also competitive inhibitors, although they do not coordinate to Fe.[131,140] It is possible that the noncoordinating anions disrupt substrate binding by sterically blocking part of the binding site and/or by occupying a positively charged region that normally contributes to the electrostatic attraction of superoxide to FeSOD.

4.3.2. Step 2: Reduction of Fe^{3+}SOD and Release of O$_2$. Electron transfer from O$_2^{\bullet -}$ to Fe^{3+} likely occurs rapidly upon binding, and no discrete enzyme·substrate (E·S) intermediate has been observed.[131] Moreover, calculations indicate that O$_2^{\bullet -}$ coordinated to Fe^{3+}SOD(OH$^-$) is unstable relative to O$_2$ + Fe^{2+}SOD(OH$_2$) (Scheme 3, step 2).[133c] A model for the reverse reaction (O$_2$ + Fe^{2+}SOD(OH$_2$) → O$_2^{\bullet -}$ + Fe^{3+}SOD(OH$^-$) + H$^+$) would be NO + Fe^{2+}SOD(OH$_2$) → NO$^-$ + Fe^{3+}SOD(OH$^-$) + H$^+$, as the product formed from this reaction is best described as Fe^{3+}SOD coordinated by NO$^-$,[141] analogous to Fe^{3+}SOD coordinated by O$_2^{\bullet -}$ in the forward reaction. The same study also demonstrated that the H$_2$O ligand of Fe^{2+}SOD released a proton in forming NO$^-$· Fe^{3+}SOD. This indicates that the forward reaction (Scheme 3, step 2) involves uptake of a proton by the OH$^-$ ligand in conjunction with reduction of Fe^{3+}SOD by O$_2^{\bullet -}$,[141,142] consistent with the findings of Bull and Fee in the absence of substrate.[131]

The active site hydrogen-bond network offers several paths for proton uptake from bulk water, and partial redundancy is revealed by mutagenesis studies of FeSOD and

Scheme 3. Mechanism of FeSOD[a]

Step 1 ⟶ (O₂•⁻)

Step 2 ⟶ (O₂)

Step 3

Step 4

Step 5 (H₂O₂, 2H⁺)

Structures labeled with Gln69, Tyr34, Asp156, His, Fe³⁺, Fe²⁺, bulk water throughout.
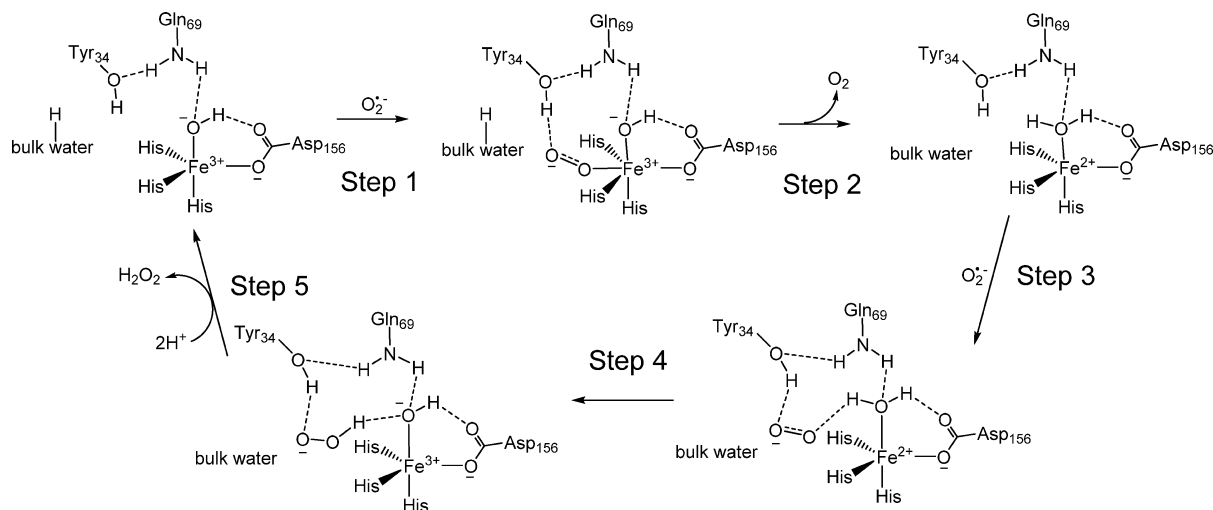
[a]Steps 1 and 2 contribute to eq 16, and steps 3, 4, and 5 contribute to eq 17. The individual second-order rate constants for eqs 16 and 17 are 5.2×10^8 and 5.5×10^8 M^{-1} s^{-1}, respectively,[131,138] for FeSOD from *Photobacterium leiognathi* at pH 8, consistent with steady-state turnover with $k_{cat}/K_M = 5.2 \times 10^8$ M^{-1} s^{-1}.[139]

MnSOD.[135a,c,d,143] Analogous partial redundancies of amino acid residues putatively involved in proton-transfer were observed in SORs (see section 7). Theoretical studies suggest that $O_2^{\bullet-}$ itself may participate in an active site relay during its fleeting presence as a bound species.[133c] Moreover, a Grotthüss-type proton-hopping relay allows that participating high-pK_a residues such as Gln69 need not ever be deprotonated, although the identities of protons associated with them may change. Thus, the active site hydrogen-bond network is envisioned as a molecular bucket brigade involving the OH$^-$/H$_2$O ligand, Gln69, Tyr34, and His30 mediating net acquisition of a proton from bulk water with the specific proton acquired to form the H$_2$O ligand deriving from Gln69 (see Figure 14).

The uncharged O$_2$ formed as a result of electron transfer is expected to depart readily from the active site because Fe^{2+}SOD does not react rapidly with O$_2$ in air-saturated buffer (oxidation occurs on a time scale of minutes to hours). This low reactivity with O$_2$ is reminiscent of that of SORs (see section 7) and contrasts with that of the mononuclear nonheme Fe sites of oxygenase enzymes, in which O$_2$ reacts readily with the Fe^{2+} state of the enzyme once the co-substrate is bound (reviewed in refs 129a,144).

4.3.3. Step 3: Outer-Sphere Binding of $O_2^{\bullet-}$ to Fe^{2+}SOD. Early work on FeSOD found that small anions do not coordinate directly to Fe^{2+} even though they do coordinate directly to Fe^{3+}.[145] Likely explanations are the lower charge of Fe^{2+} and that Asp$^-$ becomes the dominant ligand when protonation of the OH$^-$ ligand converts it to the weaker ligand H$_2$O, and Asp$^-$ discourages ligand binding in the empty site via the *trans* effect. There are good reasons why evolution might favor an active site that does not employ inner-sphere $O_2^{\bullet-}$ binding to Fe^{2+}. If the site favored coordination of anions to Fe^{2+}, then HO$_2^-$ could do so and might engage in Fenton chemistry, generating ROS.[146] FeSOD is inactivated by treatment with H$_2$O$_2$, but only slowly.[147]

Positive evidence for outer-sphere binding of anions to Fe^{2+}SOD was obtained by monitoring the NMR signals of active site residues when the protein was titrated with F$^-$.[95b] Effects on the backbone ^{13}C and ^{15}N resonances were limited to residues near Tyr34,[148] so F$^-$ was proposed to bind Tyr34. ^{1}H NMR chemical shift changes for residues throughout the active site were very similar to those produced by deprotonation of Tyr34 and were therefore attributed to changes in the hydrogen-bonding network.[149] ^{15}N NMR spectra showed that the side chain of Gln69 also responds to F$^-$ binding, consistent with the presence of a hydrogen bond between Gln69 and Tyr34.[150]

Tyr34's phenolic OH interacts favorably with small anions (F$^-$) but restricts access of larger anions to the active site (N$_3^-$), as the K_d for F$^-$ was higher in Y34F-Fe^{2+}SOD than in WT but the K_d for N$_3^-$ was lower.[95b] Thus, Tyr34 provides steric selectivity. In addition, ionization of Tyr34 prevents small anion binding, as Y34F-Fe^{2+}SOD binds F$^-$ independent of pH but WT-Fe^{2+}SOD ceases to bind F$^-$ at high pH.[95b,149] Although no pH equilibrium affecting the Fe^{2+} of Fe^{2+}SOD could be detected by Mössbauer spectroscopy,[145b] a pK_a close to that of the oxidized state was inferred on the basis of elegant work by Bull and Fee.[131] Indeed, ^{1}H NMR as a function of pH revealed an active site pK_a of 8.5 ± 0.1,[149] which was identified with deprotonation of Tyr34-based ^{13}C NMR of Fe^{2+}SOD incorporating ^{13}C in the ζ position of Tyr side chains.[130c,143] Thus, although high pH decreases the efficiency of substrate binding in both oxidation states, this reflects different events in the two cases.[151]

4.3.4. Step 4: Reduction of $O_2^{\bullet-}$ by Fe^{2+}SOD and First Protonation of the Resulting Peroxide Dianion. Liberation of a proton from the H$_2$O ligand as Fe^{2+} becomes oxidized injects a proton into the hydrogen-bonding network at the very time at which protonation of $O_2^{\bullet-}$ will favor its reduction to peroxide.[130c,152] These two events are likely to be very strongly coupled because the labile proton of the H$_2$O ligand is only two bonds away from Fe. In simple complexes, the pK_a of a coordinated water molecule decreases by 7 upon oxidation of Fe^{2+} to Fe^{3+}, corresponding to a coupling of 40 kJ/mol.[153] We hypothesize that proton transfer to nascent peroxide to form HOO$^-$ could compete with formation of an inner-sphere Fe^{3+}−peroxo complex if the proton is transferred to the O closest to Fe (Scheme 3, step 4).

The position at which O_2^{2-} becomes protonated first is a critical question and remains unsolved. Calculations of the reactions of MnSOD found that hydroperoxide would become stably bound to Mn^{3+} if the distal O of superoxide was protonated as it was being reduced to peroxide; however, if the O atom of superoxide closest the Mn^{3+} were protonated first, the hydroperoxide anion would accept a hydrogen bond from Tyr34 rather than coordinating to Mn^{3+}. Tyr34 then donates a proton to HO_2^-, leading to formation of H_2O_2, if the nearby water molecule between Tyr34 and His30 is included in the model.[154] We hypothesize in Scheme 3, step 4 that FeSOD may be analogous to MnSOD in this respect, with formation of hydroperoxide anion hydrogen bonded to Tyr34 favored over formation of a stable Fe^{3+}−hydroperoxide complex, due to protonation of the peroxo oxygen closest to the Fe center before protonation of the distal O. On the basis of a spectroscopically validated computational model for Fe^{3+}SOD coordinated by NO^-,[141] and assuming a similar geometry for peroxide (albeit not directly coordinated to Fe^{3+}), the peroxide O nearer the Fe would be a little over 2.7 Å from the O of the OH^-/H_2O ligand. Thus, rapid and efficient proton transfer should be possible. In this scenario, the distal O of hydroperoxide anion is situated between the phenolic O atom of Tyr34 and the His30 side chain. On the basis of an estimated pK_a near 10, Tyr34 would donate a proton to the hydroperoxide anion (pK_a of 11.6)[155] to form H_2O_2. Alternatively, if the distal O were protonated first, one might expect to observe formation of an inner-sphere peroxo intermediate as observed for MnSOD (see section 5). Although experiments seeking inner-sphere Fe^{3+}−peroxo intermediates have been performed, none has been detected.

4.3.5. Step 5: Protonation of Hydroperoxide and Departure from the Active Site.
Product release is believed to be the rate-limiting step,[131] yet it is still not well understood. Reduction of $O_2^{•-}$ (eq 17) was found to be slower than the oxidation of $O_2^{•-}$ (eq 16) in FeSOD, and the rate-limiting step was considered to be a chemical reaction because the enzyme can be saturated.[131] Moreover, the fact that k_{cat} displays a kinetic solvent isotope effect indicates that a step involving a solvent-exchangeable proton is rate limiting.

Because K_M increases at basic pH values (see above) but k_{cat} does not, the donor of the rate-limiting proton must remain protonated up to pH 11 at least. The H_2O ligand of the reduced enzyme satisfies this criterion, as does Tyr34 when hydrogen bonded to an anion. Moreover, acidic buffers able to donate a proton provided only weak rate acceleration, indicating that the rate-limiting step is substantially internal proton transfer.[136] The sum of the evidence is consistent with transfer of a proton from Tyr34 (and His30) to peroxide as the rate-limiting step, but further experiments are required to resolve this important question and permit comparison of the mechanism of FeSOD with that of MnSOD.[130c,133b] Being neutral, H_2O_2 is not expected to remain in the active site, and abundant small anions present at physiological ionic strengths could aid in its displacement from the anion-binding pocket.

4.3.6. Peroxidative Reaction.
Although H_2O_2 is a product of the reaction catalyzed by SODs, many FeSODs react with sub-millimolar H_2O_2 with the result being enzyme inactivation accompanied by the oxidation of Trp residue(s);[147b,c,156] additional loss of Fe[147b] and oxidation of His and Cys[147a] may also occur. Inactivation has been demonstrated for the FeSODs of *Pseudomonas ovalis*,[147a] *E. coli*,[147c] and *Porphyromonas gingivalis*.[156a] Nevertheless, the peroxidative reaction of

FeSOD is relatively slow, with a second-order rate constant of only 0.4 M^{-1} s^{-1} for *P. gingivalis*[156a] and 0.6 M^{-1} s^{-1} for *E. coli*[147c] FeSODs at pH 7.8, thus allowing FeSODs to provide biologically effective defense against superoxide even in the presence of low levels of H_2O_2.

If a SOD is inactivated by H_2O_2, it is often claimed that the SOD must be an FeSOD or a CuZnSOD and, if it is not inactivated by H_2O_2, that it must be a MnSOD (or NiSOD).[156b,157] However, it should be noted that there are several examples of Fe-supported SOD activity that is not sensitive to H_2O_2.[158] So far, these have corresponded to cambialistic Fe/MnSODs from archaea or actinobacteria and related bacteria.

The first reaction between Fe^{3+}SOD and H_2O_2 is reduction of the Fe^{3+}.[139,147c,158b] After that, the peroxidative reaction of FeSODs likely follows a mechanism similar to that of Fenton chemistry, with Fe^{2+}SOD reducing hydrogen peroxide to produce OH^- and metal-bound hydroxyl radical, $^•OH·$ Fe^{3+}SOD, which may be better described as ferryl oxygen, $O{=}Fe^{4+}$ $(+H^+)$.[146b] The observed outcome is believed to represent the product of ensuing very rapid reactions with the protein such as, for example, oxidation of a Trp side chain. The participation of Fe in this series of reactions has been demonstrated by the fact that apo-FeSOD, unlike holo-FeSOD, does not suffer loss of spectroscopic signatures of Trp side chains in the presence of H_2O_2.[147b,158b]

Optical changes occurring on the same time scale as the loss of activity in the holo-enzyme have been interpreted as loss of the spectral contribution of Trp and gain of spectral contributions from oxidized products of Trp.[147] Trp158 was deduced to be a principal target of modification, and the product was proposed to be *N*-formylkynurenine based on its mass[156a] and the spectral changes.[147c] Trp158 is present in almost all FeSODs and MnSODs, and its side chain lies within 5 Å of the Fe, making it a plausible casualty of Fe-catalyzed Fenton reactions and making it likely that covalent modification of Trp158 would disrupt active site structure and function.

It has also been proposed that Trp71 is modified as part of inactivation by H_2O_2, and Beyer and Fridovich reported that 4.5 Trp per FeSOD monomer were modified in the course of enzyme inactivation by H_2O_2.[147b] It is interesting to note, however, that an FeSOD possessing a Tyr in place of Trp71 is also sensitive to H_2O_2.[159] The ambiguity with respect to the residue(s) modified is possibly a consequence of the high and nonspecific reactivity expected from hydroxyl radicals, in conjunction with the fact that oxidizing equivalents are known to be able to move between aromatic side chains,[160] leading to a distribution of oxidation products.

The reactions of H_2O_2 with Fe-substituted MnSOD (Fe(Mn)SOD) have potential physiological relevance because human Fe(Mn)SOD was found to have H_2O_2-based radical generating ability analogous to that observed for CuZnSOD but absent in the native MnSOD.[161] Thus, human Fe(Mn)SOD in 0.5 mM H_2O_2 mediated oxidation of ABTS (2,2′-azinobis-(3ethylbenzthiazoline-6-sulfonate), with reaction rates roughly 1/10th the rate observed for CuZnSOD.[161] Fe(Mn)SOD is produced in *E. coli* when Fe is abundant but Mn is not,[162] and in yeast under conditions that disrupt Fe homeostasis.[163] Even human mitochondria are known to accumulate anomalously high Fe levels under conditions of X-linked sideroblastic anemia[164] or ferritinopathy,[165] raising the possibility that some Fe(Mn)SOD is formed. Thus, Fe(Mn)SOD's reactivity with

3872

dx.doi.org/10.1021/cr4005296 | *Chem. Rev.* 2014, 114, 3854−3918

H_2O_2, in addition to its lowered SOD activity, could increase the severity of oxidative stress.[166]

4.4. Redox Tuning

4.4.1. Fe and Mn Are Similar But Not Fully Interchangeable.
Fe and Mn are neighbors in the periodic table and have similar ionic radii in both the 3+ and the 2+ states (Table 5), so it is not surprising that *E. coli*'s (Fe)SOD and (Mn)SOD proteins can each bind either Fe or Mn. Indeed, Fe(Mn)SOD (Fe-substituted MnSOD) can be produced in vivo in *E. coli*,[162] especially by overexpressing the (Mn)SOD protein under regulation of a non-native promoter, because its native promoter suppresses expression in the presence of Fe.[167] Whittaker succeeded in measuring stabilities of (Mn)SOD protein and MnSOD as well as Fe(Mn)SOD and determined that $K_d = 0.3-3$ nM for Mn^{2+}, 2×10^{-9} nM for Mn^{3+}, 25 nM for Fe^{2+}, and 5×10^{-10} nM for Fe^{3+}.[168] Thus, (Mn)SOD protein has comparable affinities for the two 3+ metal ions, with the 2+ ions, especially Fe^{2+}, binding much more weakly. Nevertheless, binding is sufficiently tight that this is unlikely to be a basis for selective production of correctly metalated enzymes,[169] considering that the intracellular concentrations of Fe and Mn in *E. coli* are estimated to be on the order of micromolar to tens of micromolar under normal circumstances.[169] The generally greater abundance of Fe in bacteria that do not actively accumulate Mn can explain the formation of some Fe(Mn)SOD when *E. coli* cells are grown in Fe-rich medium.[170]

Despite each protein's ability to bind the other metal ion, many Fe(Mn)SODs and Mn-substituted FeSODs (Mn(Fe)-SODs) are virtually inactive in the standard catalytic assay.[104] As early as 1976, it was shown that the Mn ion in *E. coli* MnSOD protein could be replaced by diverse metal ions, including Co, Ni, Zn, or Fe,[124] and that Fe in *E. coli* FeSOD protein could be replaced by many of the same, as well as Cd, Cr, and Mn.[176] However, in each case, activity was only recovered with the native ion, that is, Mn but not Fe for *E. coli* MnSOD and Fe but not Mn for *E. coli* FeSOD. Indeed, *E. coli* possesses separate FeSOD and MnSOD genes that encode structurally homologous proteins, which nonetheless only share 43% identity at the amino acid sequence level. Evidently

evolution has selected different amino acids to activate different metal ions in SOD, despite retention of the same overall structure.

Experiments on FeSOD and MnSOD have therefore sought to learn what features of the protein and the metal ion are needed for the system to go beyond metal ion binding, to reactivity. Because both metal ions can execute SOD chemistry in their corresponding proteins and both proteins support it, the defect in the metal-swapped SODs must lie in interactions between the metal ion and the protein.[177] Indeed, a mismatch between the redox tuning applied by the protein and the intrinsic $E°$ of the metal ion can explain the inactivity of metal-swapped SODs.

4.4.2. Explaining the Inactivity of Metal-Substituted *E. coli* FeSOD and MnSOD.
SOD reactivity is subject to the thermodynamic requirement that the $E°$ of the bound metal ion be between the potentials of the two superoxide half-reactions, ideally midway between them near 0.36 V.[178] However, for analogous complexes of Mn and Fe, the $E°$ of the high spin 3+/2+ couple is generally 300−500 mV higher for the Mn version (Table 5).

These very different intrinsic $E°$'s would require their SOD proteins to make different adjustments to produce a midpoint potential near 0.36 V as required for the active holoenzyme.[74a] The $E°$ of Fe for the 3+/2+ couple (for the high-spin hexa-aquo complex) is near 0.77 V, but that of Mn is near 1.5 V (Table 5). Thus, both proteins must depress the $E°$ of the bound metal ion (via coordination of the negatively charged Asp^- ligand and electron-rich His ligands), but the MnSOD protein must depress the $E°$ of its bound metal ion by an additional ~0.4 V (Figure 15). This redox-tuning model predicts that Fe(Mn)-SOD, in which the low $E°$ metal ion is bound by the more $E°$-depressing protein, should have a $E°$ much lower than those of the native SODs. Conversely, Mn(Fe)SOD, in which the high-$E°$ metal ion is bound by the less $E°$-depressing active site, should have an $E°$ much higher than either of the native enzymes (Figure 15).[177,179] Experiments showed that the $E°$ of Fe is ~0.3 V higher when Fe is bound in *E. coli* FeSOD protein than when it is bound in the *E. coli* MnSOD protein, and the $E°$ of Mn is ~0.5 V higher when Mn is bound in the FeSOD protein than when it is bound in the MnSOD protein.[74a,75a] Indeed, *E. coli* Mn(Fe)SOD is fully reduced as-isolated, whereas *E. coli* MnSOD is generally substantially oxidized.[75a]

The redox-tuning explanation for metal ion activity predicts that each metal-substituted SOD will lack activity for one half reaction but retain it for the other, with Fe(Mn)SOD predicted to retain the ability to reduce $O_2^{•-}$ (based on its predicted low $E°$) but lacking catalytic activity due to an inability to accept electrons from $O_2^{•-}$ (active in eq 17 but not eq 16). Experiments confirmed that Fe(Mn)SOD could bind substrate and mediate both electron and proton transfer to $O_2^{•-}$, lacking only ability to accept an electron from it.[74a] Conversely, Mn(Fe)SOD could not be oxidized by $O_2^{•-}$ (although, in this instance, binding of F^- and N_3^- and therefore possibly $O_2^{•-}$ too was compromised).[75a] The redox tuning explanation was additionally supported by a study showing that mutation of *Porphyromonas gingivalis* SOD that produces a higher $E°$ for bound metal ion also results in elevation of Fe-supported activity but diminution of Mn-supported activity.[180] Although the optical and EPR spectra of *E. coli* FeSOD and Fe(Mn)SOD display distinctions,[135a,181] the geometric and electronic structures of their active sites are overwhelmingly similar, and the very different $E°$'s must be the consequence of some other

Table 5. Ionic Radii and Midpoint Potentials of 3+/2+ Couples of Analogous Complexes of Fe and Mn[a]

property/metal	Mn	Fe
ionic radius of 3+ state (pm)	78.5 pm	78.5 pm
ionic radius of 2+ state (pm)	97 pm	92 pm
$E°'$ of $(H_2O)_6$ complex[b]	1.51 V	0.77 V
$E°'$ of EDTA complex[c]	0.83 V	0.10 V
$E°$ of $LM(H_2O)(OH^-)$, M = Mn, Fe	0.42 V	0.05 V
L = 2,6-diacetylpyridinebis(semioxamazide) = dapsox, at pH 7.8[d]		
$E°$ of $LM(OH^-)$, M = Mn, Fe	−1.51 V	−1.79 V
L = $N[CH_2CH_2NC(O)NHC(CH_3)_3]_3$ (in DMSO vs $Fc^{+/0}$)[e]		
$E°$ of (Fe)SOD at pH 7.4[f,g]	>0.9	0.1
(Mn)SOD at pH 7.8[g,h]	0.3	−0.25

[a]All midpoint potentials are in water and reported vs NHE unless stated otherwise. [b]Reference 171. [c]Reference 172. [d]Reference 173. [e]Reference 174. [f]Reference 74a. [g]Because of the slow equilibration of SOD with mediators, on the order of hours, the titrations should be considered to be in quasi-equilibrium only, and the obtained midpoint potentials are therefore only ± ~50 mV.[74a,131,175] [h]Reference 75a.
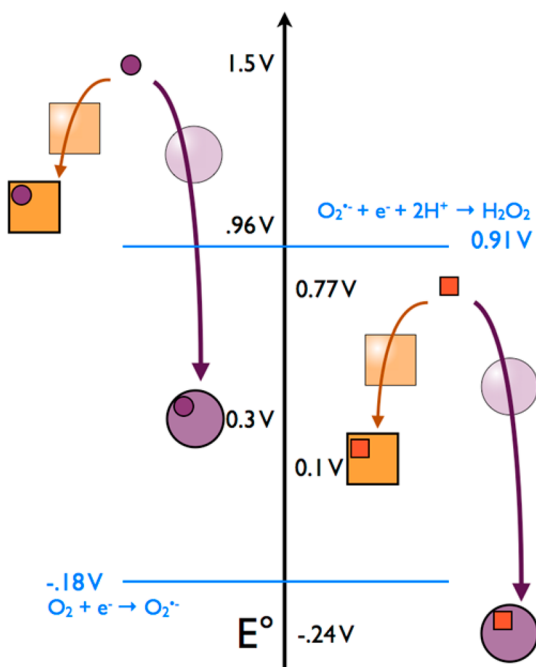
Figure 15. Cartoon of the differential redox tuning by the (Fe)SOD and (Mn)SOD proteins and its effects on the Fe and Mn high-spin 3+/2+ couples (adapted from refs 179,192 with $E°$'s drawn from refs 3,74a,75a). Orange squares depict the (Fe)SOD protein and violet circles represent the (Mn)SOD protein; the corresponding metal ions are shown as red squares or purple circles. Apo-proteins lack the symbol for the metal ion. Reduction potentials vs NHE are marked on the vertical axis, and the protein–metal ion complexes or hexaaquo complexes are positioned vertically in accordance with this scale.

differences.[182] Analogous conclusions were drawn from similar detailed comparisons of *E. coli* MnSOD and Mn(Fe)-SOD.[75a,183]

The inactivity of Fe(Mn)SOD has been attributed to other causes.[135a,184] Diverse Fe^{3+}(Mn)SODs were shown to have elevated affinities for small anions,[135a,185] consistent with replacement of Mn^{3+} by Fe^{3+} and the higher affinity of Fe^{3+} for a sixth ligand.[120,135a,185] However, competitive inhibition by OH^- binding as a sixth ligand does not suffice to explain the lower activity of Fe(Mn)SOD because higher affinity for anions should also extend to $O_2^{•-}$, which would therefore retain ability to compete with OH^- for binding to the Fe^{3+}(Mn)SOD site just as it does for the Fe^{3+}SOD site.

A difference in redox tuning can also explain Fe(Mn)SOD's low but significant activity at low pH, because the $E°$ will rise as pH drops (60 mV/pH unit for a redox reaction in which one proton is acquired per electron). Thus, at pH 6, 1.8 pH units below the pH used in the standard assay, the depressed $E°$ of Fe(Mn)SOD will benefit from a ~110 mV boost for proton-coupled reduction, improving its ability to perform the limiting half reaction, eq 16. This is consistent with the −0.24 V $E°$ measured for Fe(Mn)SOD, which, while much lower than that of FeSOD, is only a little lower than the midpoint of the first half reaction (−0.18 V), so a ~110 mV boost would bring the $E°$ of Fe(Mn)SOD into the range in which it would recover competence for eq 16. Thus, different redox tuning can explain the different metal ion requirements for activity for the FeSODs and MnSODs that have been studied, although quantitative characterizations have so far focused only on the FeSOD and MnSOD of *E. coli*.

4.4.3. Mechanism of Redox Tuning in FeSOD: Gln69.

Fundamentally, tuning the $E°$ corresponds to changing the stability of one participating oxidation state relative to the other. In simple metal ion complexes, this is commonly accomplished by modifying the coordination sphere. However, the origin of the different tuning applied by the *E. coli* (Fe)SOD and (Mn)SOD proteins is not predominantly coordination geometry or other interactions whose energies would depend on the electronic configuration, because the (Mn)SOD protein produces much lower $E°$s for both metal ions, even though Fe goes from d^5 to d^6 configuration upon reduction, whereas Mn goes from d^4 to d^5. Indeed, the two active sites are virtually superimposable.

Enzyme catalytic sites are often buried within proteins to exclude water and the low dielectric magnifies energies associated with charge. Thus, changes in charge can be very destabilizing. Buried metal sites often circumvent this cost by acquiring a proton in conjunction with metal ion reduction. In such cases of proton-coupled electron transfer, the measured $E°$ reflects the energy associated with proton acquisition as well as the ease of reducing the metal ion. This emerged as a proposed basis for the different redox tuning in (Fe)SOD versus (Mn)SOD because the two proteins and coordination spheres are overwhelmingly similar in other respects. Therefore, it was proposed that the ease of protonating the ligand OH^- was different in these two SOD proteins.

Although seemingly small, the protonation state of the OH^-/H_2O ligand has the capacity to affect strongly the reduction potential of the metal site because coordinated OH^- will favor the oxidized state of the metal ion much more than coordinated H_2O, for both Fe and Mn (Figure 16).[130b] Thus, a protein able to stabilize the OH^- state of this ligand will de facto stabilize Mn^{3+} over Mn^{2+} and lower the $E°$. This mechanism is most effective when proton transfer is coupled to electron transfer. Because this is the case for both FeSOD[131] and MnSOD,[130c]
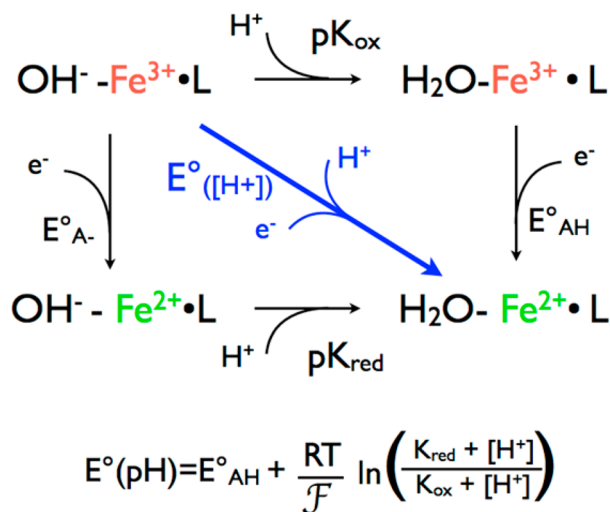
Figure 16. Thermodynamic cycle of metal ion reduction coupled to proton transfer for the example of Fe^{3+}SOD, where L is the SOD protein. The energy associated with reduction of Fe^{3+} coordinated to the protonated form of an acidic ligand is considered in the form of the reduction potential $E°_{AH}$; the corresponding potential for Fe^{3+} coordinated to the deprotonated form of the ligand is $E°_{A^-}$; the energy for protonation of the ligand is considered in the form of pK_a's: pK_a^{ox} for the case where the Fe is oxidized and pK_a^{red} for the case where the metal ion is reduced.

both of these proteins have the possibility of tuning the metal ion's $E°$ via modulation of the energy associated with proton uptake, that is, changing the pK_a's of the OH^-/H_2O ligand in the reduced and oxidized states (Figure 16).[74a,130c] This proposal is supported by recent theoretical studies showing that the energy of electron acquisition for Fe is −0.54 eV in FeSOD but −0.49 eV in Fe(Mn)SOD.[182a] The 0.05 V difference is less than 20% of the observed difference. However, the calculated pK_a's of the two reduced states differ by 7.7 pH units or 0.46 V.[182a] This is more than sufficient to account for the observed ~0.3 V difference between the reduction potentials of FeSOD and Fe(Mn)SOD.

The pK_a of the OH^-/H_2O ligand will depend on the two hydrogen bonds in which this ligand participates (Figure 14). The hydrogen bond to the ligand Asp^- is within the metal ion coordination sphere and therefore does not bring outside influences to bear upon the OH^-/H_2O. However, the OH^-/H_2O ligand is coupled to the protein matrix by the hydrogen bond with Gln69 of FeSOD (or Gln146 of MnSOD, E. coli numbering). This glutamine side chain is itself engaged in three hydrogen bonds, which tie Gln69's position and orientation to other elements of FeSOD's secondary structure (Tyr34) and even the other domain of the monomer (Trp122) (Figure 14). Thus, Gln69 is the focal point of a network of hydrogen bonds that connects the OH^-/H_2O ligand to diverse portions of SOD's structure and allows the protein to modulate the strength of the hydrogen bond with Gln69. In human MnSOD, mutation of the active site Gln to Glu results in a 14 °C increase in the T_m,[135c] demonstrating that Gln does not provide optimal stability. Gln's conservation must therefore stem from a different contribution to the active site that is sufficiently important to be sustained despite a cost to stability. Mutations of the Gln of E. coli MnSOD have shown that this residue has striking consequences for metal ion binding and function[135b] and confirmed the importance of this residue for redox tuning.[186]

Finally, the active site Gln derives from different locations in the structures of E. coli FeSOD and MnSOD,[187] and this distinction is the most consistently conserved difference between FeSODs and MnSODs in general.[188] Specifically, the active site Gln derives from a helix in the N-terminal domain of FeSOD (position 69 in E. coli), but from a loop between β strands in the C-terminal domain of MnSOD (position 146 in E. coli).[187b]

If the Gln is to depress the $E°$ more in MnSOD than it does in FeSOD, by favoring the OH^- state of the OH^-/H_2O ligand, it should donate a stronger hydrogen bond to the OH^-/H_2O ligand in (Mn)SOD protein than in the (Fe)SOD protein. In fact, when the Fe^{2+}-containing versions of these two proteins were compared, the paramagnetic shift of the Gln side chain of Fe^{2+}(Mn)SOD was almost twice as large as that of the Gln of Fe^{2+}SOD, demonstrating that the Gln146 side chain of Fe^{2+}(Mn)SOD is more strongly coupled to Fe^{2+} than is Gln69 of Fe^{2+}SOD, in turn supporting the proposal that the Gln of (Mn)SOD protein forms a stronger hydrogen bond to the OH^-/H_2O ligand than does the Gln of the (Fe)SOD protein. This is consistent with the model that the difference in the $E°$ tuning applied by these proteins derives from different modulation of the protonation state of the OH^-/H_2O ligand by the active site Gln. This model provides a chemical basis for the proposals that the preservation of an active site Gln, but in a different position, could be related to metal ion specificity.[187,189]

If strong hydrogen-bond donation to the OH^-/H_2O ligand depresses the $E°$, then replacing it with weak hydrogen-bond donation should allow the $E°$ to rise, and enforced hydrogen-bond acceptance by residue 69 should cause the $E°$ to rise much more. Histidine is a conservative replacement for glutamine, but the crystal structure showed that the former lacks the hydrogen bonds with Trp122 and Asn72 that enforce the orientation of Gln69, with the result that His69 is able to orient itself to either donate or accept a hydrogen bond[74b] and thus minimize the energetic costs of changes in the protonation state of the OH^-/H_2O ligand.[182b,190] Indeed, the His69 was shown to accept a hydrogen bond from the ligand H_2O instead of donating one in E. coli $Q69H$-Fe^{2+}SOD,[150] and the $E°$ rose by 0.25 V, an amount large enough to mitigate the different intrinsic $E°$'s of Fe versus Mn (Figure 17).
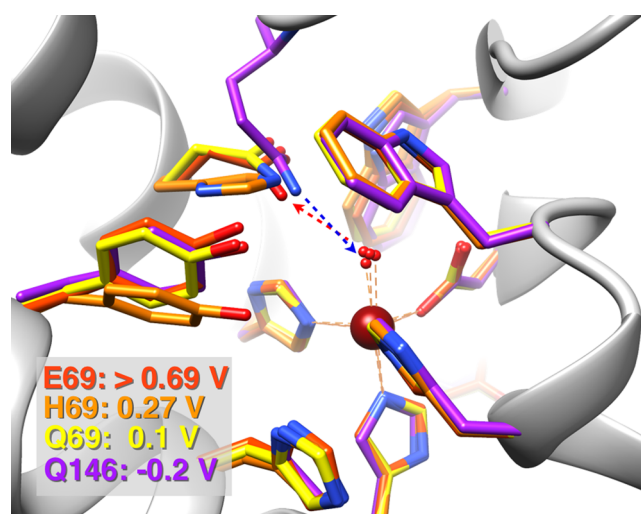
Figure 17. Retention of overall structure by the active sites of four FeSODs and MnSOD variants that have $E°$'s spanning >0.9 V. Magenta, E. coli Fe(Mn)SOD (PDB code: 1VEW);[184] yellow, E. coli WT Fe^{3+}SOD (PDB code: 1ISB);[126a] orange, E. coli Q69HFeSOD (PDB code: 1ZA5);[74b] red, E. coli Q69E-FeSOD (PDB code: 2NYB).[191] Dashed lines indicate hydrogen-bond donation from Gln146 to the OH^- ligand of MnSOD in blue and hydrogen-bond acceptance by the Glu69 of Q69E-FeSOD from the H_2O ligand in red.

Mutation of Gln69 to Glu increased the $E°$ of E. coli FeSOD by >0.66 V.[74b] Glu acts as an obligatory hydrogen-bond acceptor when deprotonated and stabilizes the reduced state's H_2O ligand with a strong hydrogen bond, in contrast with Gln, which donates a weak hydrogen bond favoring coordinated OH^- (Figure 17).[182a,191] In addition, oxidized $Q69E$-Fe^{3+}SOD coordinates OH^- as a sixth ligand at neutral pH, indicating that nearby Glu69 is protonated even at neutral pH, imposing an energetic cost on the oxidized state.[191] Finally, it was determined that the Glu69 of E. coli Q69E-FeSOD could serve as a built-in source of the proton taken up by the OH^- ligand upon reduction of Fe. This would constitute a considerably lower energetic cost than obtaining a proton from water as in WT-FeSOD and further favor reduction of the Fe.[191] Thus, the effects of mutating Gln69 of E. coli FeSOD demonstrate that this residue exerts a strong influence on the $E°$ of the metal ion, and the observed effects are consistent with a model in which the protein modulates the degree to which the OH^-/H_2O ligand is protonated, and protonation of this ligand is required for reduction of the metal ion.
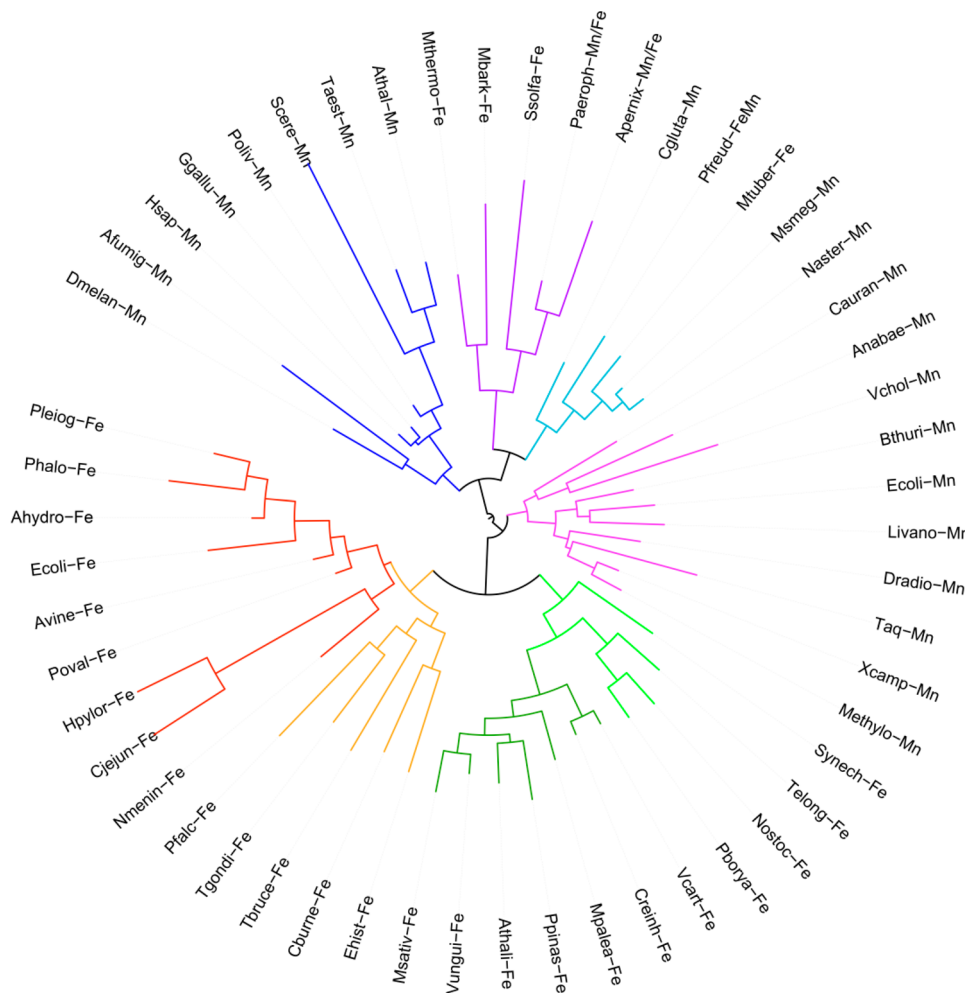
Figure 18. Unrooted dendogram of 53 members of the FeSOD and MnSOD family wherein branches are colored as follows (clockwise from top left): blue for mitochondrial MnSODs, magenta for archaeal SODs, teal for actinobacterial SODs, pink for bacterial MnSODs, light green for cyanobacterial FeSODs, dark green for FeSODs of plants and green algae, red for FeSODs of protists, and orange for FeSODs of bacteria. Sequences were chosen to represent diverse groups of organisms and different metal specificities.[188c] BLAST searches of the nonredundant database of the National Center for Biotechnology and Information (NCBI) were used to identify additional SOD sequences from weakly represented groups, and, in those cases in which sequences were very similar, only one exemplar was retained, the one for which the best information on metal ion use was available. Where possible, for bacterial and archaeal SODs especially, the identity of an SOD as Fe-dependent versus Mn-dependent was sought in primary literature, and the means by which its metal ion identity was determined is listed as "Anal" for direct analysis via atomic absorption or another spectroscopic method, or "H_2O_2" when it was inferred on the basis of the SOD's sensitivity or resistance to inactivation by H_2O_2 and a reference is provided. Some Fe/MnSODs are included, but given that the motivation of this exercise was to identify residues that correlate differentially with Fe or Mn use, others are described via Table 4 instead. The tree was displayed and colored using the interactive tree of life server hosted by the European Molecular Biology Laboratory.[400] The multiple sequence alignment upon which it is based was generated using MUSCLE[401] (in the "full" most stringent mode) for up to 16 interactions, as accessed via Phylogeny.fr hosted by the Centre National de la Recherche Scientifique.[402] The alignment was curated using Gblocks[403] at the most stringent setting (not allowing many contiguous nonconserved positions), and the results were inspected visually via the Phylogeny.fr interface. The phylogenetic tree was constructed by PhyML using the approximate likelihood-ratio test[404] and using the substitution model of Jones, Taylor, and Thornton with default parameters, and gaps were removed from the alignment. The tree topology was confirmed with COBALT via the National Center for Biotechnology Information server.[405] The sequences are identified in the figure using the following abbreviations corresponding to the following accession numbers: Afumig-Mn, *Aspergillus fumigatus* MnSOD (Eukaryota-mito) GI:18158811; Ahydro-Fe, *Aeromonas hydrophila* FeSOD (Gammaproteobacteria-Fe) GI:75530508; Anabae-Mn, *Anabaena* MnSOD (Cyanobacteria) GI:23200075 H_2O_2;[406] Apernix-Mn/Fe, *Aeropyrum pernix* Mn/FeSOD (Crenarchaeota) GI:321159640;[119] Athali-Fe, *Arabidopsis thaliana* FeSOD (Viridiplantae) GI:332659609; Athal-Mn, *Arabidopsis thaliana* MnSOD (Viridiplantae-mito) GI:15228407; Avine-Fe, *Azotobacter vinelandii* FeSOD (Gammaproteobacteria-Fe) GI:226720755 Anal.;[407] Bthuri-Mn, *Bacillus thuringiensis* MnSOD (Firmicutes) GI:228830333; Cauran-Mn, *Chloroflexus aurantiacus* MnSOD (Chloroflexii) GI:31074373 Anal.;[408] Cburne-Fe, *Coxiella burnetii* FeSOD (Gammaproteobacteria-Fe) GI:145002 H_2O_2;[409] Cgluta-Mn, *Corynebacterium glutamicum* MnSOD (Actinobacteria) GI:81783000; Cjejun-Fe, *Campylobacter jejuni* FeSOD (Epsilonproteobacteria) GI:218561849 H_2O_2;[410] Creinh-Fe, *Chlamydomonas reinhard* FeSOD (Viridiplantae) GI:158280091; Dmelan-Mn, *Drosophila melanogaster* MnSOD (Eukaryota-mito) GI:7302882; Dradio-Mn, *Deinococcus radiodurans* MnSOD (Bacteria-Deinococc) GI:32363428; Ecoli-Fe, *E. coli* FeSOD (Gammaproteobacteria-Fe) GI:84028734 Anal;[75a] Ecoli-Mn, *E. coli* MnSOD (Gammaproteobacteria-Mn) GI:134659 Anal;[74a,114c] Ehist-Fe, *Entamoeba histolytica* FeSOD (protozoan-Eukaryota) GI:464774 H_2O_2;[411] Ggallu-Mn, *Gallus gallus* MnSOD (Eukaryota-mito) GI:15419940; Hpylor-Fe, *Helicobacter pylori* FeSOD (Epsilonproteobacteria) GI:190016324;[412] Hsap-Mn, *Homo sapiens* MnSOD (Eukaryota-mito) GI:24987871; Livano-Mn, *Listeria ivanovii* MnSOD (Firmicutes) GI:134666; Mbark-Fe, *Methanosarcina barkeri* FeSOD (Euryarchaeota) GI:499627762 Anal.;[196d] Methylo-Mn, *Methylomonas* MnSOD (Gammaproteobacteria-Mn)

Figure 18. continued

GI:95281 Anal;[121] Mpalea-Fe, *Marchantia paleacea* FeSOD (Viridiplantae) GI:75243372; Msativ-Fe, *Medicago sativa* FeSOD (Viridiplantae) GI:75248782; Msmeg-Mn, *Mycobacterium smegmatis* MnSOD (Actinobacteria) GI:21264517 Anal;[120] Mthermo-Fe, *Methanobacterium thermoauto* FeSOD (Euryarchaeota) GI:23200500; Mtuber-Fe, *Mycobacterium tuberculosis* FeSOD (Actinobacteria) GI:809164 H_2O_2;[413] Nmenin-Fe, *Neisseria meningitidis* FeSOD (Betaproteobacteria) GI:7226122; Naster-Mn, *Nocardia asteroides* MnSOD (Actinobacteria) GI:1711453; Nostoc-Fe, *Nostoc* PCC7120 FeSOD (Cyanobacteria) GI:17132032; Paeroph-Mn/Fe, *Pyrobaculum aerophilum* Mn/FeSOD (Crenarchaeota) GI:14917043;[118] Pborya-Fe,: *Plectonema boryanum* FeSOD (Cyanobacteria) GI:1711435 Anal;[156b] Pfalc-Fe, *Plasmodium falciparum* FeSOD (protozoan-Eukaryota) GI:74946757;[414] Pfreud-FeMn, *Propionibacterium freudenreichii* (*shermanii*) Fe/MnSOD (Actinobacteria) GI:5542134 Anal.;[113b] Phalo-Fe, *Pseudoalteromonas haloplanktis* FeSOD (Gammaproteobacteria-Fe) GI:306440524; Pleiog-Fe, *Photobacterium leiognathi* FeSOD (Gammaproteobacteria-Fe) GI:134643 Anal;[139] Poliv-Mn, *Paralichthys olivaceus* MnSOD (Eukaryota-mito) GI:134676; Poval-Fe, *Pseudomonas ovalis* FeSOD (Gammaproteobacteria-Fe) GI:12084342 Anal;[114d] Ppinas-Fe, *Pinus pinaster* FeSOD (Viridiplantae) GI:75223482; Scere-Mn, *Saccharomyces cerevisiae* MnSOD (Eukaryota-mito) GI:217035334; Ssolfa-Fe, *Sulfolobus solfataricus* FeSOD (Crenarchaeota) GI:14286093 Anal.;[115,208] Synech-Fe, *Synechocystis* 6803 FeSOD (Cyanobacteria) GI:1653111; Taest-Mn, *Triticum aestivum* MnSOD (Viridiplantae-mito) GI:62131095; Taq-Mn, *Thermus aquaticus* MnSOD (Bacteria-Deinococ) GI:1711455; Tbruce-Fe, *Trypanosoma brucei* B2 FeSOD (protozoan-Eukaryota) GI:70834946 H_2O_2;[415] Telong-Fe, *Thermosynechococcus elongatus* FeSOD (Cyanobacteria) GI:34810955; Tgondi-Fe, *Toxoplasma gondii* FeSOD (protozoan-Eukaryota) GI:122066229; Vcart-Fe, *Volvox carteri* FeSOD (Viridiplantae) GI:121077704; Vchol-Mn, *Vibrio cholerae* MnSOD (Gammaproteobacteria-Mn) GI:14039308 upregulation in absence of Fe;[416] Vungui-Fe, *Vigna unguiculata* FeSOD (Viridiplantae) GI:56554197 H_2O_2;[417] Xcamp-Mn, *Xanthomonas campestris* MnSOD (Gammaproteobacteria-Mn) GI:76364224.

These studies have shown that proteins can exert a very large influence on the $E°$s of bound metal ions by modulating energies associated with proton uptake that is coupled to metal ion reduction. The >0.66 V change in $E°$ resulting from mutation of a single second-sphere residue is remarkable in that it was accompanied by only minor effects on the structure of the protein and active site despite its large effect on Fe reactivity. Thus, FeSOD provides us with an unusually striking example of a little-appreciated mechanism of redox tuning that bridges the gap between proteins and metal centers. Side chains such as those of Gln, Asn, Glu, Asp, and His can simultaneously hydrogen bond with several different residues and propagate tension in any one hydrogen bond to other hydrogen-bonding partners, leading to changes in the $E°$ of FeSOD by hundreds of millivolts in response to substitutions that are normally considered conservative (Gln → His) or are isosteric and isoelectronic but change the intrinsic pK_a of the residue (Gln → Glu). Even changes to third-sphere residues that surround the Gln produce significant changes in the $E°$ by modifying the position or polarization of Gln69.[180] The structure of FeSOD and MnSOD separates metal binding by conserved first-sphere residues that also provide a baseline for the value of $E°$, from strong differential redox tuning delivered by the second sphere by virtue of an exceptionally tunable ligand: OH^-/H_2O. This combination of robust metal binding with malleable redox tuning has allowed this family of SODs to evolve to support redox activity with either of two different metal ions,[192] a feat shared by only a few other redox-active enzymes.[193]

4.5. Evolution of FeSODs and MnSODs

4.5.1. Overview.
The sections that follow describe how amino acid sequence similarities among Fe- and/or MnSODs are remarkably consistent with what is known about the evolution of eukaryotic cells as well as the major branches of the tree of life. Mitochondrial MnSOD can be traced back to the archaeal origin of eukaryotic cells, chloroplast FeSOD to cyanobacterial origin and protist FeSOD to bacterial origin (of possibly more than one type, and possibly via lateral gene transfer). The conservation of SODs across the domains of life indicates that FeSODs and MnSODs existed as distinct types evolving independently before the emergence of eukaryotes, because these two clusters separately (Figure 18). Distinct FeSODs and MnSODs appear to have arisen even before divergence of major branches of bacteria, or moved among

branches by lateral gene transfer.[188a,194] However, FeSODs remain the most widely dispersed, consistent with a very early origin.[195]

4.5.2. Evolution of Bacterial FeSODs and MnSODs.
FeSOD is considered to be the most ancient of the SODs on the basis of its presence in all domains of life, including bacteria believed to be exceedingly primitive.[113b,114a,195,196] The use of Fe was natural given the early bioavailability of Fe and that Fe's intrinsic $E°$ is within the range required for disproportionation of $O_2^{•-}$. However, rising O_2 abundance increased the costs of Fe acquisition and toxicity, allowing other versions of SOD to be favored. The resulting bacterial MnSODs are more closely related to each other than they are to the FeSODs, which many bacteria retain in addition to a MnSOD (Figure 18).[197] Thus, the evidence indicates that most characterized bacterial MnSODs descend from a single ancient divergence. Early genes for MnSOD could have dispersed by lateral gene transfer,[194,198] which has affected one-third of bacterial genes by one estimate,[199] especially genes for proteins (such as MnSOD) that are not part of multiprotein assemblies.

4.5.3. Mitochondrial MnSODs.
MnSODs are best known as the SODs of mitochondria, and, based on their amino acid sequences, these form a phylogenetic group separate from the MnSODs of most bacteria (Figure 18). Intriguingly, MnSODs from members of the phylum of actinobacteria are distinct from MnSODs of other bacteria and instead group with mitochondrial MnSODs and archaeal MnSODs.[188a,200] While the SOD-centric view of evolution presented here might therefore suggest that mitochondria descend from an actinobacterial endosymbiont, other evidence indicates that mitochondria descend from an α-proteobacterial ancestor instead.[201] However, the host cell progenitor of eukaryotic cells is thought to have been archaeal,[201a,202] and mitochondrial MnSOD amino acid sequences resemble the MnSOD sequences of modern archaea more than those of α-proteobacteria. Mitochondrial MnSOD remains encoded in the nucleus but is localized to the mitochondrion by an N-terminal transit peptide. Thus, it is possible that mitochondrial MnSODs are derived from the archaeal ancestor of the host cell and not from the bacterial ancestor of mitochondria.

The clustering together of actinobacterial, archaeal, and mitochondrial SODs could reflect the fact that they are tetrameric in solution, in contrast to the dimeric nature of most bacterial SODs. Although the dimers of all three types of

tetrameric SODs overlay well with one another and with the dimer of dimeric MnSODs, the tetramers of archaeal and actinobacterial SODs overlay well with one another but not with mitochondrial SOD tetramers, which display a distinct dimer–dimer interaction.[203] Thus, the Fe- and/or MnSODs of actinobacteria are more similar to archaeal Fe- and/or MnSODs than they are to mitochondrial MnSODs, and may derive from a gene acquired via lateral gene transfer from an archaeal source. Both archaea and pathogenic bacteria are reported to have relatively high propensities for lateral gene transfer.[204]

4.5.4. Origins of Eukaryotic FeSODs. The FeSODs of very diverse bacterial species nonetheless cluster together, consistent with dispersal of a primordial FeSOD gene very early on.[197] Similarly, the FeSODs from the three kingdoms of protists represented in our comparison appear to share as much similarity with bacterial FeSODs as with one another (chromalveolates *Toxoplasma* and *Plasmodium*, amoebozoum *Entamoeba*, and excavate *Trypanosome*). More detailed reviews focusing on protist FeSODs have been published recently.[47,205] The SODs of modern α-proteobacteria (e.g., *Neisseria*) display greater homology to the FeSODs of modern protists than to the MnSODs of mitochondria, suggesting that the SOD of the α-protobacterial proto-mitochondrion may have been the predecessor of protist FeSODs (or that protist FeSOD gene(s) were acquired by lateral gene transfer).[197]

Plants and green algae also have one or more FeSODs found in plastids in general but chloroplasts in particular, as well as in the cytoplasm in certain cases.[109b,197] The gene(s) have been incorporated into the nuclear genome, but the resulting proteins are targeted to plastids by N-terminal plastid transit peptides.[109b] Chloroplast FeSODs cluster separately from the FeSODs of most bacteria, but resemble the FeSODs of cyanobacteria (Figure 18).[197] Thus, it is likely that chloroplast FeSOD originates from the genome of the cyanobacterial endosymbiont that gave rise to chloroplasts.[197,206]

A larger set of SOD sequences and comparisons at the level of nucleotide sequences instead of amino acid sequences would surely permit a more detailed analysis, but even our modest set of representative sequences suggests that our modern Fe- and/or MnSODs can all be traced to bacterial and archaeal origins in a way that is consistent with what we know about the evolution of modern organisms themselves.

4.6. A Possible Path from Fe to Mn?

4.6.1. Requirements for Evolution of MnSOD. It is impossible not to wonder how we acquired our legacy of distinct lineages of FeSODs and MnSODs. Whatever barriers arose between them have been too high for frequent crossing in the recent past, possibly because O_2 is more abundant now and the cost of compromised SOD activity is correspondingly higher. However, early in evolution this would have been less so,[207] and it is apparent that there have continued to exist some populations that experience only weak oxidative stress and that these could maintain a higher diversity of SOD gene sequences. Indeed, Fe/MnSODs tend to be found in anaerobes or facultative aerobes, and they tend to be less active than the metal-specific SODs (Table 4).[107] The simplest proposal is that optimization of MnSOD activity occurred on the basis of an ancient SOD that functioned with Fe but also had sufficient Mn-based activity to be optimized by natural selection and that was present in an organism that provided conditions for binding Mn.

The archaeal and actinobacterial SODs meet the first two criteria as they tend to be less metal ion specific than SODs of most bacteria. The archaeal Fe- and/or MnSODs that persist today include exemplars active with Fe,[110a,196d,208] active with Mn,[209] or active with either.[118,119] Similarly among actinobacterial Fe- and/or MnSODs, at least one is described as an FeSOD,[203a] another as a MnSOD,[200] and another as an Fe/MnSOD.[120] The metal ion promiscuity of the archaeal SODs is consistent with the tendency of archaea to inhabit anaerobic or microaerobic habitats at extreme temperatures or in solution conditions where selective pressure to optimize SOD activity may have been eclipsed by the demands of protein stability. In contrast, the MnSODs of modern aerobic bacteria likely represent the outcome of more intense selection for SOD activity.[196c,210] In this model, initial evolution leading to optimal SOD activity in eubacteria would have involved optimization of SOD for Fe use in organisms with sufficient means of Fe acquisition, and later recruitment and optimization for Mn use of a surviving gene for an Fe/MnSOD in organisms that provided sufficient Mn.

Existing evidence indicates that SOD binds either Fe or Mn depending largely on their availability;[113a,162] MnSOD must have evolved either after Mn was more bioavailable than Fe or in an organism such as *Lactobacillus* or *Neisseria* that achieves high internal Mn concentrations. Accumulation of hundred micromolar to millimolar $MnHPO_4$ and $MnHCO_3^+$ provides protection against oxidative stress in several organisms[211] and could have complemented a relatively unspecialized SOD, allowing variations that were not optimal for Fe use to persist or accumulate in the population. Such a SOD in such an environment would then have had a relatively high probability of acquiring Mn, thus creating the possibility of selection on the basis of Mn-supported SOD activity.

Despite clear overall separation of the sequences of MnSODs from those of FeSODs, there is considerable diversity within each group, and biochemical studies have identified some bacterial FeSODs and non-actinobacterial/non-archaeal MnSODs as cambialistic (Table 4). It is likely that cambialism is considerably more widespread than suggested by current nomenclature because most SODs listed in common databases have been classified on the basis of their amino acid sequences, whereas measurement of their Fe-supported activity and Mn-supported activity is much more laborious. Moreover, the term "cambialistic" has been applied to SODs representing a continuum from low but conditionally significant activity with the less competent metal to equal activity with either metal ion (Table 4). The existence of an entire spectrum of degrees of metal ion specificity is not surprising, but it suggests that there are accessible routes over the barriers between Fe- and Mn-specificity, and from specificity to cambialism. The latter supports the feasibility of the reverse: optimization of specificity from cambialism. As more reports of the Fe-based and Mn-based activities of individual SODs are published, we will no doubt learn how multiple features of the protein can fine-tune the ability of a SOD to use Mn versus Fe over the range allowed by the primary tuning mechanisms that appear to distinguish MnSODs from FeSODs.[188a,212]

The foregoing proposals build on new understanding of the diverse defenses in use against ROS, metal ion homeostasis, and bacterial evolution.[211d,213] They call for evolution of FeSODs and then MnSODs from relatively nonspecific ancestors, refinement of a bacterial gene for MnSOD, and dispersal of the descendants of that gene by lateral gene transfer among the

```
2er Structure                      aaaaaaaaaaaaaaaaaaaaaaaaa
PltCya-Fe   ----XXXXXXXXXPfXXXXXEXXlXXXTlXfHfXKHHXXYVXNXnXXXXXaXlXXXXlEXX  56
ProtistFe   ----MXlXlPXLXfXXnXLXXXISXEXlXfHhXKHHXXYVXKLNXXXnXXXXXnXlXn-  55
Bact-Fe     ----XXXXLXXLPfXXnalXXXlSXXalXfHhXKHHnTYlXnLNXLlXXTXlXXXXLX--  54
Bact-Mn     ----XXXXXPXLXYXYXALEXXlDXXTMXXHhXnHHXXYXnXXXAlXXXXXXXXXXXX  56
ArchActino  XXXXXXYXLPXLXfXXXXLXPhIXXnXXXlHhXXHHXXYVXXXXNXXlXXlXXXXXXXX-  55
Mito-Mn     ----XXXaLPXLXfXfXALnPXlXXnIXXlHhXKHHXaYVXXXNXaXnXXXXXXXXXnX-  51

2er Structure              aaaaaaaaaaaaaaaaaaaa          aaaaaaaaaa  aaa
PltCya-Fe   l---XXXXXXXXXXXXFNNAXQXWNHXFfWnXlKXXGGX--XPXGXXXXXlXXXFXaXnX  111
ProtistFe   ------llkXXXXXXIfNXAAQXfNHXFYfXXMXXXXX---XPXXXlXXXlXXXFXXXXn  106
Bact-Fe     ------XIIlXXSXGGlFNNAAQXfNHXFYfXXlXXXXXX--XXXXXlXXAlXXXfGSlXX  106
Bact-Mn     lXXXlXXlPXXXXXXlRNXXGGhXNHXXfWXXlXaXX----XXGXlXXXIXXXlGXXXX  112
ArchActino  --------XXXXXXXkXlaFXXXGhXXHXXfWXnlXPXXXXXXXPXXXlXXXIXXXfGXFXX  113
Mito-Mn     ------XXXlXlXXXlkFXGGGXXNHXllWXNLXPXXXXX--XXXLXXAIXXXfXSlXX  107

2er Structure   aaaaaaaaaaa    bbbbbbbb    bbbbbbb              bbbbbbb   aa
PltCya-Fe   lXXXFXXAXXTQFGaGWAWLXXXX-X-XLXlXKsXNAXXPlX------XXXXXlLXlDVWEH  165
ProtistFe   FKXXFaXXXXXHFGSGWXWLXXXX-X-KlXlXXTXnAXXPlX------nXXXPllXCDlWEH  160
Bact-Fe     FnXXlXXXaXXXFGSXWXWXXXXXX-X1XlXXTXXAXXPlT------XXXXPlLXXDlWEH  161
Bact-Mn     lKXXlXXXXXXFGSGfXWLXXXX-X-XlXlXSTXNQDXPlXXXXXXXXXXXXllXXDVWEH  172
ArchActino  lkXXFXXXAXXXXGXGWXXLXfXXXXXXLXXXXXXXHXXXX------XXXXXllXlDXfEH  169
Mito-Mn     lXXXXXaXXXXlQGSGWXflXXnXXXXnLXlXXXXnQD-----XlXXXXXXXXPlXXlDXWEH  164

2er Structure   a aaaa     aaaaaaaaa     aaaaaaaaaaa
PltCya-Fe   AYYlDXnNXRPXflXXXflXXLlXWnXXXXXXXXXXXXXX----  204
ProtistFe   AYYlDXkNnRXXYlnXfW-nlVNWXXXXnnl-----------  190
Bact-Fe     AYYlDXkNXRPXYlXXFfX-XlNWXXXXXXXXX---------  193
Bact-Mn     AYYlXfQXkRXXYlXXXfN-VlnWXXXXXXXXXXX-------  206
ArchActino  AfYlnYkNXkXXfXXXXWN-lXnWXXXXXXXXXXXXXXXXXXX  211
Mito-Mn     AYYLQYXNXkXXYXXXlXX-lXNXXXXXXXXXXXXX------  199
```

Figure 19. Alignment of consensus amino acid sequences from the different groups of SOD in Figure 18. Bold green letters indicate amino acids conserved in all 53 individual sequences, letters in blue indicate residues that are similar in all 53 sequences, letters in red indicate residues that distinguish FeSODs from others, letters in purple indicate residues that distinguish MnSODs from others. For each group of SODs the individual sequences were aligned, the conserved amino acid identities are presented as capital letters and positions where similarity is preserved within the group are shown as lower case letters. 'X' is used to mark the positions at which diverse amino acids are found. These consensus sequences for the different groups are then presented together in their global alignment. The different groups are PltCya: FeSODs from plants and cyanobacteria (11 sequences, numbering of *A. thaliana*), ProtistFe: FeSODs from protists (5 sequences, numbering of *Entamoeba histolica*), Bact-Fe: FeSODs from bacteria (9 sequences, numbering of *E. coli*), Bact-Mn: MnSODs from non-actinobacterial bacteria (10 sequences, numbering of *E. coli*), ArchActino: Fe-, Mn- and Fe/MnSODs from actinobacteria and archaea (10 sequences, numbering of *P. aerophilum*) and Mito-Mn: MnSODs from mitochondria (8 sequences, numbering of *H. sapiens*). Consensus sequences were generated using Clustal-Omega[418] multiple sequence alignments of the sequences listed in the caption of Figure 19 using up to 5 iterations, up to 3 guide-tree iterations and up to three HMM iterations without mBed clustering and allowing dealignment, via the EMBL-EBI server. For each group of sequences residues that were different or only weakly similar within the group were replaced by 'X'. Strongly similar residues were replaced by a lower-case letter indicating the category of residue present at the site with 'f' representing an aromatic side chain, 'l' representing a hydrophobe, 'a' representing A,S or T, 'n' representing a polar/charged side chain (D,E,Q,N,K,R), 'h' representing H or Y, and 'k' representing K or R. Residues that were identical in all sequences in the group were retained as capital letters. These consensus sequences were then aligned using Clustal-Omega to produce the result shown. All alignments were confirmed with COBALT via the NCBI server.[405] Numbering of *E. coli* SODs omits the N-terminal M, to produce agreement with amino acid numbering used in crystal structures. Stretches of amino acids participating in α-helices are indicated by 'a's and stretches participating in β-sheet strands by 'b's above each row.

different branches of bacteria that possess nonactinobacterial MnSOD now.

4.6.2. Signatures of Specificity for Fe or Mn. In studying present-day SODs, we are restricted to observing the tips of the branches of the evolutionary tree. The MnSODs of archaea and their relatives the actinobacterial MnSODs have been argued to have diverged less from ancestral Fe- and/or MnSODs. Therefore, to identify the results of optimization of Fe-based or Mn-based activity, we focus on the other five groups of SODs identified by our analysis: mitochondrial and bacterial MnSODs (nonactinobacterial), and bacterial, protist, and cyanobacterial-and-plant FeSODs (see Figure 18).

Many residues were identified with Fe-specificity or Mn-specificity based on early crystal structures.[187b] Since then, the explosion in amino acid sequences available has lowered the likelihood of fortuitous conservation. Accordingly, detailed study of larger collections of Fe- and/or MnSOD sequences has produced refined signatures of Fe specificity or Mn

specificity,[188c] and an effort focusing on protist FeSODs has also been published.[205] To develop hypotheses as to which residues are related to specific metal ion use, rather than shared as a result of other common properties or ancestry, it is useful to identify residues conserved within a group of related SODs, and then ask which of those residues are also conserved in different groups of SODs that share the same metal ion requirement. This will identify amino acid sequence signatures specific to all of the FeSODs or MnSODs in the set but can also distinguish them from residues correlated with other factors. Thus, Figure 19 compares the consensus sequences of each of the five major groups of FeSODs or MnSODs that emerged from the phylogenetic analysis in Figure 18. (The consensus sequence for archaeal and actinobacterial SODs is also included for comparison, but these SODs are not regarded as metal ion specific, as a group; see above.) The SODs all have roughly 200 residues, and some 40−60 are conserved within each group. However, only 11 residues are conserved over all our set of

SODs. We identify 7 residues as being conserved (or similar) among all of the FeSODs but conserved differently or not conserved among MnSODs, which we assign as signatures of Fe specificity. We identify 4 residues as signatures of Mn specificity by the same criterion in reverse. Because two Fe-signature residues occur at positions occupied by Mn-signature residues, our sequences reveal 9 positions where the amino acid identity appears related to metal ion activity (Figure 20). Hence, almost as many residues could be conserved signatures of metal ion specificity as are essential to SOD activity.

Res # (E. coli FeSOD)	Fe-act/ Mn-act	64	68	69	71	75	141	142
Fe		f		Q	f	F	A	
E. coli FeSOD	>100	f	a	Q	f	F	A	g
B. frag	2	f	G	Q	l	l	g	s
P. freud	1.0	a	a	g	v	v	h	q
P. ging	0.6	f	G	Q	l	l	A	g
M. smeg	0.07	a	G	g	i	i	Q	q
Methyl-J	0.04	r	G	g	a	l	Q	D
R. cap	0.02	f	s	Q	w	q	g	v
E. coli MnSOD	<0.01	r	G	g	a	l	Q	D
Mn		k	G				Q	D

Figure 20. Comparison of the residues at seven proposed specificity signature positions among 6 Fe/MnSODs with different metal ion dependencies for activity. Fe/Mn SODs from *B. fragilis*, *P. freudenrichii*, *P. gingivalis*, *M. smegmatis*, *Mehylomonas J*, and *R. capsulatus* (gray rows) are compared to the FeSOD and MnSOD from *E. coli* (white rows). Residues conserved among FeSODs but not among MnSODs are considered signatures of Fe specificity and are colored in orange (proposed Fe specificity signature residues 52 and 165 are omitted from this figure because they are more distant from the active site and could act via indirect or different means). Residues conserved among MnSODs but not among FeSODs are considered signatures of Mn specificity and are colored in purple. For each SOD, the ratio of its Fe-supported activity divided by its Mn-supported activity under the same conditions is reported (see also Table 5). Use of upper case and lower case letters follows the convention used for Figure 19.

Many of the 9 residues identified by our survey as signatures of metal ion specificity were also in the sets identified by a recent large analysis,[188c] and crucially the 9 residues include the Gln69 that exerts a strong influence on the metal ion $E°$ and its analogue to MnSOD Gln141 (residues are numbered according to *E. coli* FeSOD in this section, with *E. coli* MnSOD numbers supplied in parentheses, here 146).

We tested the possibility that these signature residues make additive contributions using a series of Fe/MnSODs for which the ratio of Fe-supported activity divided by Mn-supported activity varies from 2 to 0.02. Figure 20 shows that the Fe/MnSODs most active with Fe contain more of the Fe-specificity signature residues (orange squares) and those most active with Mn contain more Mn-specificity signature residues (purple squares), with one exception (below). The overall correlation thus supports our identification of these residues as related to metal ion specificity. Importantly, Fe/MnSODs with com-

parable Fe-supported and Mn-supported activities lack some or all of the signature residues for Fe-specificity and/or Mn-specificity. The continuum observed therefore suggests that cambialism can result from having some of the signatures for either of the metal ions and that the individual signature residues each contribute to the overall activity with each of the metal ions. Comparing two Fe/MnSODs from within one group (actinobacterial SODs), the SOD of *P. freudenreichii* has a 14-fold higher ratio of Fe-supported to Mn-supported activity than that of *M. smegmatis* SOD, and lacks the Mn-specificity signatures present in *M. smegmatis* SOD. This further supports the identification of these signatures as codeterminants of metal ion specificity. However, the SOD of *Rhodobacter capsulatus* has been found to function primarily with Mn and barely with Fe,[122] yet its amino acid sequence displays several of the hallmarks of an FeSOD and none of the signatures of MnSODs,[214] demonstrating that additional factors are not identified by this simple analysis and providing a strong cautionary lesson against using amino acid sequence information alone to infer the identity of the metal ion supporting function.

4.6.3. Structural Perspective and Ties to a Redox Basis for Metal Ion Specificity. To understand why certain residues may be conserved in the manner they are, it is helpful to view them in the context of the structure (Figure 21). Residues identical in all of our SODs (colored green in Figures 19 and 21) are strongly concentrated in the active site, as expected on the basis of evolutionary selection for activity. Residues are also conserved in the dimer interface, indicating that this too is critical.[188c] Seventeen more positions are occupied by residues of similar nature in our SOD collection (blue in Figures 19 and 21). These also feature prominently in the interface between monomers; however, they additionally make up two hydrophobic cores, one in each domain of the SOD monomer (Figure 21B) consistent with modular folding of the monomer,[126a] and possibly modular ancestry. Indeed, thermophilic SODs have been overexpressed as folded apo-proteins in mesophilic hosts,[118,215] and metal ion incorporation into apoprotein is gated by pre-exiting structure.[216] Folding of the N-terminal domain would bring together the ligand residues His26 and His73, whereas metal binding pins together the two domains, as each contributes two ligands.

The residues identified as signatures of Fe- or Mn specificity are colored orange-red and purple, respectively, in Figures 21 and 22. All FeSODs and MnSODs retain a second-sphere residue that hydrogen bonds to the OH^-/H_2O ligand as well as to other residues. However, in FeSODs, this residue is Gln69 from the N-terminal domain in an α-helix, whereas in mitochondrial MnSODs and non-actinobacterial bacterial MnSODs it is Gln141 (146) from the C-terminal domain in a loop between β-strands.[217] (The archaeal or actinobacterial SODs employ a His.) Figure 22 shows how the two different structures nonetheless place this Gln's side chain in position to hydrogen bond to the OH^-/H_2O ligand, and use the same hydrogen-bonding partners (Tyr34, Asn72, and Trp122).[187] Yet the different backbone positions of the Gln side chain in addition to neighbors that are differently conserved in MnSODs versus FeSODs can produce distinct orientations and different proximity to the OH^-/H_2O ligand.[218]

Gln69 (FeSOD) and Gln141/146 (MnSOD) as well as their adjacent residues account for most of the signatures of metal ion specificity we identified above on the basis of amino acid sequences (exceptions are positions 52 and 165, shown in
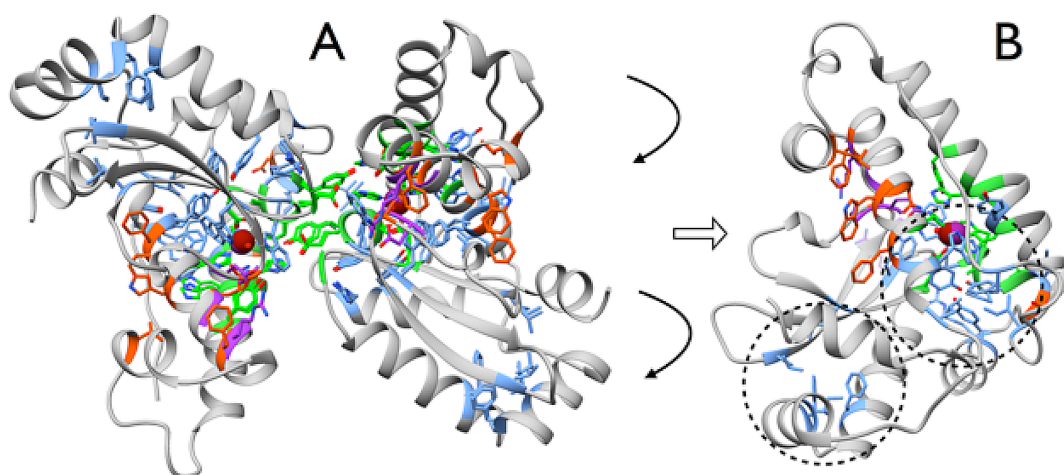
Figure 21. (A) Ribbon structure of E.coli FeSOD with residues conserved among all our Fe- and/or MnSODs in green, residues similar in all in blue, residues proposed to be signatures of Fe-specificity in orange-red and residues proposed to be signatures of Mn-specificity in purple from the structure of *E. coli* MnSOD overlaid on the structure of FeSOD but not shown; (B) right-hand monomer, rotated to bring its right-side to face the viewer and indicating with dashed circles clusters of residues similar in all Fe- and/or MnSODs that form hydrophobic cores of the N and C terminal domains. Figure is based on the coordinate sets 1ISB[126a] and 1D5N.[252a] Residues specific to FeSODs are based on 25 sequences, residues specific to the non-actinobacterial, non-archaeal MnSODs are based on 18 sequences. Conserved residues are four ligands of the metal ion (His26, His73, His160, Asp156), two participants in the active site H-bond network (His30, Tyr34), two that may aid in defining the conformation of the ligand side chains (His31, Ala161), and two that bridge the interface between monomers (Glu159 and Tyr163). Gly119 is also conserved, occurring before the beginning of the β-sheet where it appears to facilitate a sharp bend in the peptide backbone.
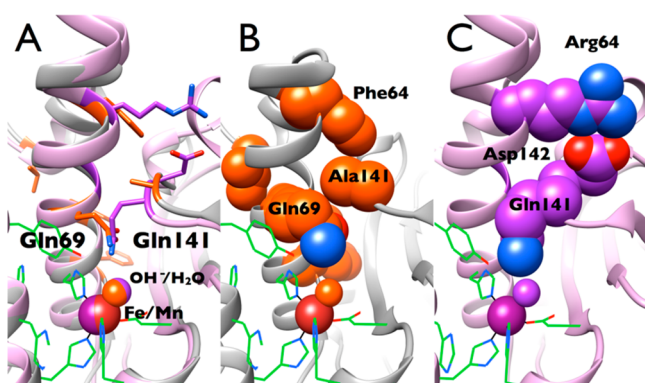

Figure 22. Residues constituting conserved differences between FeSODs and MnSODs, near the active site based on the coordinate sets 1ISB[126a] and 1D5N[252a] from *E. coli* proteins (A) superposition of FeSOD (grey ribbon) and MnSOD (orchid ribbon). Green residues are conserved in all SODs, orange-red are specific to FeSODs (in our set of sequences), purple are specific to MnSODs (in our sequences and excluding actinobacterial and archaeal SODs). (B) FeSOD only with space-filling depiction of Fe-specific Gln69 and residues that buttress it (Ala141 and Phe64) or contribute bulk to the back-side of the helix (Phe71 and Phe75). (C) MnSOD only with space-filling depiction of Mn-specific residues (Gln141, and Arg64 and Asp142 in FeSOD numbering; Gln146, Arg72 and Asp147 in MnSOD numbering) that are conserved among Mn-specific SODs and may help to hold together two domains with a salt bridge.

Figure 19). In FeSODs, Gln69 is held in place in part by Ala141 and the aromatic residue 64, which form a stack of sterically interacting residues (Figure 22B). Meanwhile, Phe75 and aromatic residue 71 are on the opposite side of the helix bearing Gln69 and Phe64, so their bulk could play a role in positioning the helix, pushing it toward the active site. Among non-actinobacterial and non-archaeal MnSODs, the foregoing residues are conserved differently or not conserved. In MnSOD, Asp142 (147 in MnSOD) immediately following Gln141 hydrogen bonds with an Arg or Lys from position 64

(72 in MnSOD). This salt bridge ties the loop containing Gln141 to the helix that bears Gln69 of FeSOD, thus holding together the two domains around the active site (Figure 22C). Push-back from the N-terminal domain is diminished by conservation of a Gly in position 68 in these SODs (76 of MnSOD). Together these changes constrain Gln141 to be close to the OH^-/H_2O ligand. Thus, conserved signatures in the sequences of groups of FeSODs and MnSODs suggest that a few residues may play particularly important roles in determining which metal ion is active, and observed correlations offer predictions that can be tested by mutagenesis. The identities and locations of these residues are consistent with the notion that metal ion activity and redox tuning are modulated by the positioning and polarization of the OH^-/H_2O ligand via constraints on the position, orientation, packing, and polarization of the active site Gln.

A complementary interaction targets the other axial ligand, His26, in many FeSODs and MnSODs and could modulate interactions between Mn and the OH^-/H_2O ligand via the *trans* effect.[212a] Many mitochondrial MnSODs, many of the actinobacterial MnSODs, and all the other bacterial MnSODs in our set have a residue (Met23) whose side chain can hydrogen bond with the ligand His26, whereas an aliphatic group is present in all of the FeSODs in our sequence set (Figure 19).

Archaeal and actinobacterial SODs were excluded from the above analysis because that group includes SODs with a spectrum of metal ion use, so residues conserved in this group are not signatures of specificity. Thus, a Gly at position 69 does not commit a SOD to use of Mn despite its conservation in MnSODs. Interestingly, archaeal and actinobacterial SODs conserve a His at position 141, which appears important to their ability to support activity with either Fe or Mn (Figure 19). His141 H-bonds to the ligand OH^-/H_2O (analogous to Gln69 or 141) and is expected to produce redox tuning intermediate between those of Gln69 and Gln141 because Gln141 produces an $E°$ that is ∼0.3 V lower than when the Gln

derives from position 69,[74a] but replacing Gln69 with His results in ∼0.25 V elevation of the $E°$.[74b] Experiments are underway to test the proposal that conversion of a His to a Gln as the hydrogen-bond donor to the OH^-/H_2O ligand (from position 141) could lower $E°$ and both commit and optimize the site for Mn use.[135b,219]

It is noteworthy that many of the Fe/MnSODs identified so far are the only Fe- and/or MnSOD family member possessed by the organism.[113b,c,214] That many of them derive from bacteria that are pathogens may reflect the greater amount of study devoted to pathogenic bacteria than to nonpathogens; however, many pathogens normally occupy anaerobic environments but face occasional extreme exposure to superoxide produced as part of the host immune response. They can also face Fe-deprivation due to sequestration of Fe by the host. Because SODs are important contributors to bacterial virulence, the abilities of these SODs to function with either Fe or Mn may have significance to disease and its possible prevention/treatment.

Many eukaryotic host cells defend themselves by producing ROS, with coordinated expression of MnSOD,[220] apparently inherited from an archaeal past. MnSOD's insensitivity to inactivation by peroxide may have been an important factor in its selection and evolution in mitochondria of higher organisms, and in turn higher organisms' ability to use ROS for self-defense.

5. MANGANESE SUPEROXIDE DISMUTASE

5.1. History and Properties

Shortly after the identification of the copper-containing protein erythrocuprein as a superoxide dismutase in 1969,[221] a dimeric manganese-containing enzyme was found in *E. coli* that carried out the same chemistry and was thus called manganese superoxide dismutase[222] or MnSOD. Since that time, dimeric and tetrameric MnSODs have been identified in a very diverse set of organisms; the reader is referred to section 4.6 for a discussion of the ubiquity of MnSOD. Prokaryotic MnSOD is located in the cytosol. Some eukaryotic cells, such as human cells, have MnSOD exclusively in the mitochondrial matrix, but in other cases it is found in the mitochondrial matrix and the cytosol, and, in the case of plants, in chloroplasts.

MnSOD naming is complex and not very consistent. Historically, SOD2 is mitochondrial MnSOD, but *sod2* and *sod3* have been used for two mitochondrial MnSODs in *Caenorhabditis elegans*,[223] and two MnSODs from *C. albicans*, one mitochondrial and one cytosolic, have been termed MnSOD2 and MnSOD3, respectively.[49] A system was proposed recently to distinguish the MnSODs by location as well as biological origin.[65a] Here, we will refer to MnSOD when mitochondrial MnSOD is discussed and MnSODc for a cytosolic MnSOD.

The importance of MnSOD in mammalian cells was underscored by studies of mice from which the MnSOD gene was deleted. In a landmark study, the authors showed that the MnSOD knockout mouse was able to develop embryonically but that the postnatal lifespan was only a few days.[224] Even in the heterozygous mouse model, severe deficiencies and sensitivity to aerobic environment were observed.[225] This is in contrast to the murine CuZnSOD, which is not crucial to survival.[226] The phenotypes resulting from MnSOD knockouts and CuZnSOD knockouts are quite variable across species with the former generally producing a more severely compromised phenotype in eukaryotes.[225b,227]

Human MnSOD is encoded in the nucleus, and the gene is found on chromosome 6 in the 6q21 region. In human cells, the encoded protein is a homotetramer with a monomeric unit of ca. 22 000 Da.[66] The apoprotein is localized to the mitochondrial matrix by an N-terminal leader sequence that is cleaved after transport. Protein and metal transport are discussed in detail in section 5.2.3. The most prevalent single nucleotide polymorphism (SNP) for human MnSOD leads to the replacement of valine at position 16 in the human enzyme to alanine. This mutation is in the leader sequence that controls transport of the enzyme into the mitochondrial matrix, and Ala16 is thought to facilitate enzyme transport and lead to a more active enzyme. Association of the Val16Ala mutant MnSOD with a particular disease process is complex and has been extensively reviewed.[228] The other well-characterized SNPs are the Ile58Thr and Leu60Phe. Again, these are not specifically associated with any disease process. Nevertheless, the Ile58Thr mutant leads to packing defects in the two four-helix bundles at the tetrameric interface, and the mutant enzyme is found predominantly as a dimer.[229] A consequence of this mutation is that the mutant enzyme is less stable thermally in vitro.[229] The reader is directed to some comprehensive surveys[220b,230] of the studies so far that point to some possible implications of this mutation in a variety of diseases (e.g., cancer, cardiovascular disease).

5.2. Structure

5.2.1. Tetramer versus Dimer. The very first crystal structure determined of a MnSOD[60] was that of the enzyme from the thermophilic bacterium *Thermus thermophilus* and revealed a tetrameric enzyme with a mononuclear trigonal bipyramidal active site. Since then, MnSOD has been shown to occur both as a tetramer and as a dimer, and the structures of the reduced and oxidized enzyme, as well as a number of specifically mutated enzymes, can be found in the Protein Database. Thus far, the MnSODs that are found in bacteria and most prokaryotes are dimeric, while the MnSODs found in eukaryotes (e.g., human, *C. elegans*, *Drosophila melanogaster*) are generally tetrameric. The monomeric structure has been shown to consist of two domains, a predominantly α-helical domain at the N-terminus and a domain composed of a small β sheet and α helices at the C-terminus.[60,63,231] The difference between dimeric and tetrameric MnSODs lies in the N-terminal region. In tetrameric MnSODs, this region consists of long α helices forming a hairpin structure, while in dimeric MnSODs, the α helices are much shorter (Figure 23). As noted earlier, there is a naturally occurring human mutant Ile58Thr MnSOD that is a dimer in solution instead of a tetramer, and it shows a loss of thermal stability.[229] The importance of the teramic structure has been elucidated recently through studies of the MnSOD from *C. albicans*, which, as noted above, crystallizes as a tetramer but is a dimer or "loose tetramer" in solution.[65a]

Two yeast MnSODs, a tetrameric enzyme from *S. cerevisiae* mitochondria (*Sc*MnSOD) and a dimeric enzyme from *C. albicans* cytosol (*Ca*MnSODc) were recently characterized and compared.[65b] The tetrameric structure was found to have no effect on the enzyme reactivity at neutral pH and room temperature.[65b] However, tetrameric *Sc*MnSOD is much more thermostable and resistant to pH, heat, and denaturant-induced unfolding relative to dimeric *Ca*MnSODc.[65b] Therefore,
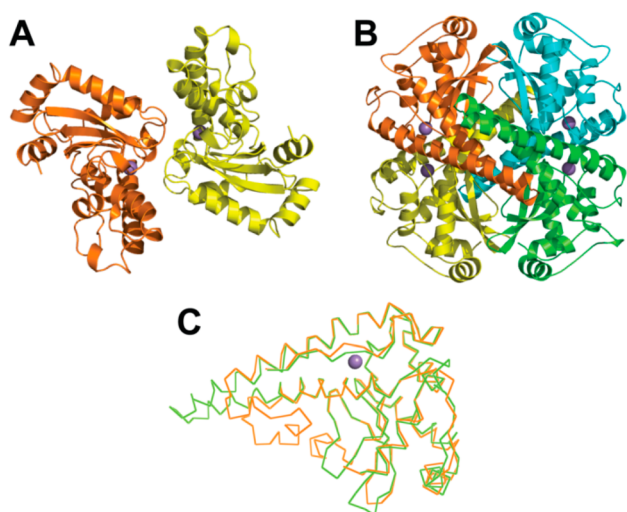
Figure 23. The structure of the dimeric (A) and tetrameric (B) MnSODs, showing the ribbon diagrams of *E. coli* (PDB code: 1VEW) and *S. cerevisiae* (PDB code: 3LSU) MnSOD. Comparison of the monomer structure between *E. coli* (orange) and *S. cerevisiae* (green) MnSOD is shown in panel C. The diagrams were generated using the PyMOL Molecular Graphics System.[396]

tetramerization does seem to lend significant stability to the MnSOD enzyme.

5.2.2. Active Site Structure. The solvent-exposed residues of MnSOD cluster such that the enzyme has patches of positive charge and patches of negative charge. This was first suggested in an early study from Fridovich and co-workers,[77] wherein residues were chemically modified and catalytic activity was measured and subsequently confirmed by an early crystal structure of the dimeric MnSOD from *Bacillus stearothermophilus* MnSOD.[232] Theoretical studies[233] using Brownian dynamics calculated that the protein provides significant electrostatic guidance to draw superoxide into the active site channel.

The active site structure of MnSOD is similar to that of FeSOD[66] (see section 4). The metal-binding ligands consist of three histidines, an aspartate, and a water or hydroxide molecule. Two of these histidines are from the N-terminal domain, and the remaining histidine and the aspartate come from the C-terminal domain. In the resting state of the native human and the bacterial enzymes, the enzymes are generally oxidized (Mn^{3+}SOD), and a water molecule is bound to the metal as the deprotonated hydroxide (Figure 24). The ligands around the metal form a distorted trigonal bipyramidal structure with little change in the active site geometry when the enzyme is oxidized or reduced. These five metal-binding ligands are invariant throughout all MnSODs characterized to date; the majority are isolated in the Mn^{3+}SOD form, while the fungal MnSODs of *S. cerevisiae* and *C. albicans* are isolated predominantly as the reduced (Mn^{2+}SOD) form.[65a]

The manganese is occluded from solvent and surrounded by a very important constellation of highly conserved second-sphere residues that form a hydrogen-bonding network.[66] This network starts at the metal-bound water, which hydrogen bonds with the glutamine 143 equivalent to Gln 141 in *E. coli* MnSOD. The carboxamide NH_2 of Gln143 can form a hydrogen bond with the nearby tyrosine 34 hydroxyl. The tyrosine 34 hydroxyl, nearby water, and the side chain of histidine 30 form a hydrogen-bond network that ends with
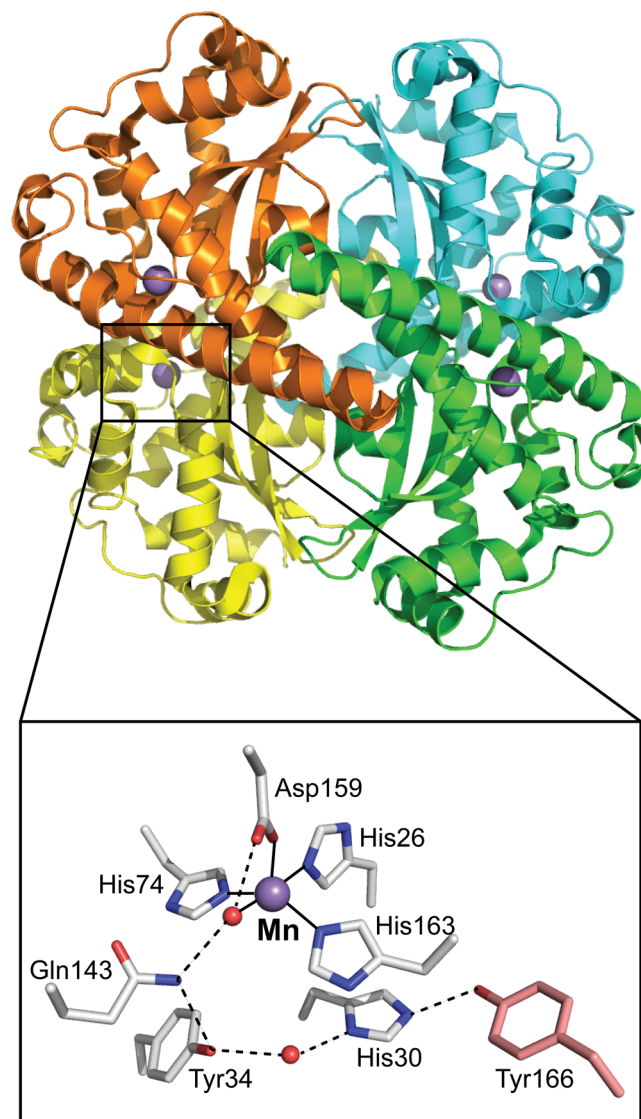
Figure 24. The tetrameric assembly (top) and active site structure (bottom) of human MnSOD (PDB code: 1LUV). The metal-binding ligands are His26, His74, His163, and Asp159. The hydrogen-bonding network is defined from the bound water to Gln143, Tyr34, the water between Tyr34 and His30, His30, and finally Tyr166 from the adjacent subunit (pink). The diagrams were generated using the PyMOL Molecular Graphics System.[396]

tyrosine 166 (using the human MnSOD numbering system). It is these residues that have received the most attention in the effort to decipher the contributions of the protein to the one electron-two proton transfers that convert superoxide into hydrogen peroxide.

The three mutant forms of MnSOD that are discussed in detail below are the Tyr34Phe mutant (human and *E. coli*),[94,234] the His30Asn human mutant,[235] and the Gln143Asn human/Gln146X (X = Leu, His, Ala) *E. coli* mutants[236] (Figure 25). All of these alterations to the residues belonging to the hydrogen-bonding network produce striking mechanistic consequences. The initial mutation to the hydrogen-bonding network was Tyr34Phe as this modification removes a hydroxyl group that is part of the hydrogen-bonding network and replaces it with hydrogen but leaves the remainder of the network unperturbed. The actual structural change at or near the active site is modest, and the change in overall $O_2^{\bullet-}$
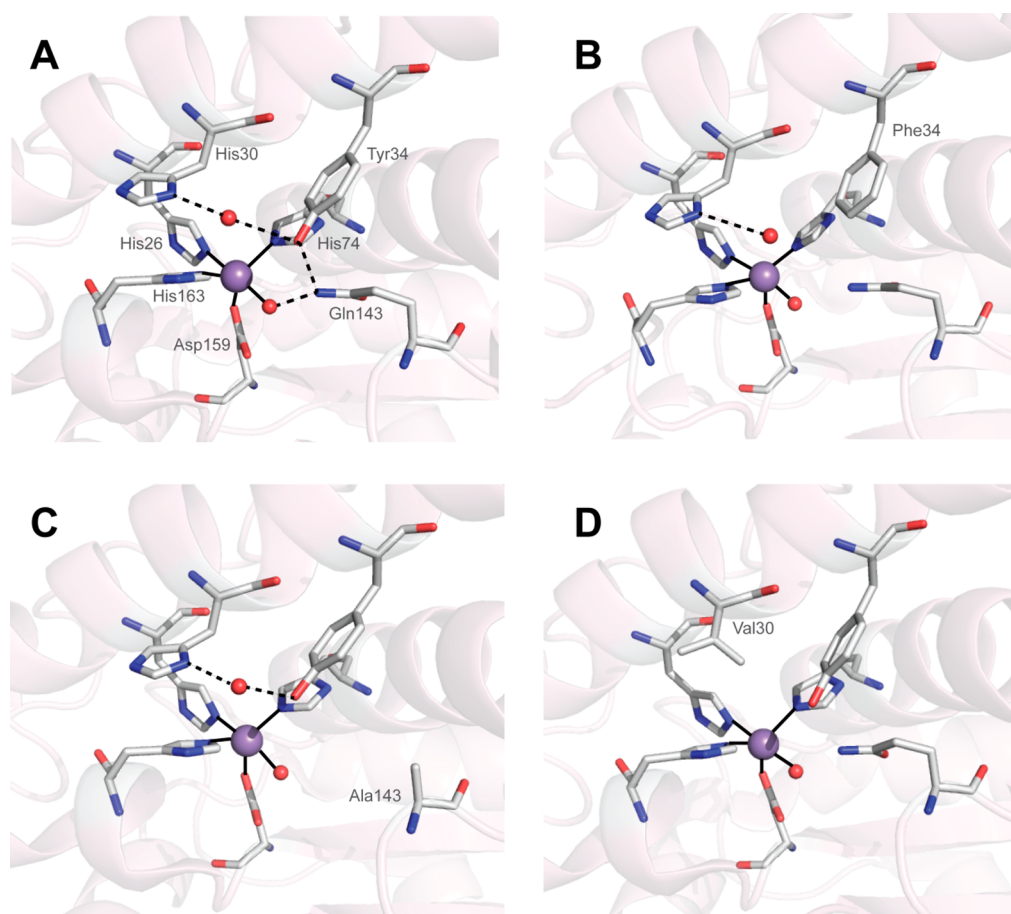
Figure 25. The active site structure of the human WT MnSOD (PDB code: 1LUV) and three mutants of the hydrogen-bonding network, Y34F (PDB code: 1AP5), Q143A (PDB code: 1EM1), and H30V (PDB code: 1N0N). Metal ions and solvent molecules are shown as spheres, and coordination and hydrogen bonds are shown as solid and dashed lines, respectively. The diagrams were generated using the PyMOL Molecular Graphics System.[396]

disproportionation at very low substrate/enzyme concentrations is also modest in both the bacterial and the human MnSODs;[94,234] see section 5.3.1. This is in accord with the overall structure of the enzyme wherein the electrostatic attraction of the superoxide to the positively charged region at the active site channel entrance is unperturbed and plays a seminal role in the rate constant. The same observation applies to the His30Asn or His30Gln mutants,[235a] where there is a subtle mechanistic change in response to a fairly small structural change. Mutation of this histidine does lead to a significant effect, however, observed in the in vivo experiments (see section 5.3).[235b] The most dramatic mutation is that of Gln143/Gln146 of human/*E. coli* MnSOD, respectively. If this residue is perturbed, there is a dramatic loss of activity, and both the *E. coli* and the human enzymes are isolated in the reduced state.[236] The structural change upon mutation of the Gln146 in *E. coli* MnSOD leads to a shift in the positioning of Tyr34 and Trp126 and disrupts the hydrogen-bonding network.

5.2.3. Manganese Acquisition by the Protein. As described in section 4, it is well-known that most MnSODs and FeSODs are extremely metal specific with respect to activity, despite the striking similarity in the protein and the active site structure,[93] and that there is a small subset of SODs that are called cambialistic that function with either iron or manganese. However, the cambialistic SODs are not as active as the metal-specific MnSODs and FeSODs. There has been much attention to the fact that MnSOD is able to acquire manganese in the presence of the generally higher concentration of iron in cells. However, the path by which MnSOD acquires the metal within the cell is not as clear. In addition, the metalation of the MnSOD apoenzyme is a complex process, requiring specific conditions.

5.2.3.1. In Vivo Metalation of the Protein. MnSOD is found in the mitochondria of eukaryotic cells, so the manganese must cross the cell membrane and then the mitochondrial membrane to become part of the intact metalated enzyme. The in vivo metalation of MnSOD from *S. cerevisiae* has been studied extensively by Culotta and co-workers.[213,237] Thus far, no specific chaperone has been discovered that serves to incorporate manganese directly into the protein, akin to the role of the copper chaperone for SOD1 (CCS) in CuZnSOD (see section 6). There are a series of more general manganese transporters, Smf1p and Smf2p, that can act on many divalent metals. Smf1p is a high-affinity manganese transporter that carries the metal across the cell membrane from the extracellular space into the cytosol. A similar manganese transporter, Smf2p, was found to be essential to manganese accumulation in yeast cells even though it does not locate at the cell membrane. Rather, it seems to be located at the surfaces of small vesicles within the cell that have been postulated to serve as storage for manganese. There may, in addition, be simple
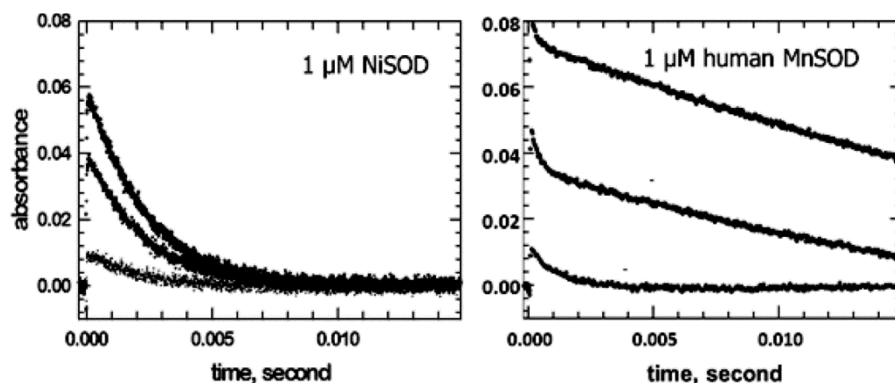
3884

dx.doi.org/10.1021/cr4005296 | *Chem. Rev.* 2014, 114, 3854−3918

Figure 26. Disappearance of different amounts of $O_2^{\bullet-}$ in the presence of either 1 μM NiSOD or 1 μM MnSOD.

phosphate transporters that can also deliver manganese across the cell membrane from the extracellular space into the cytosol because deletion of Smf1p still leaves the cell replete in manganese.

A gene was identified in *S. cerevisiae* that codes for a manganese transporter that brings manganese into the mitochondrial matrix, abbreviated Mtm1, for manganese trafficking factor for mitochondrial MnSOD.[238] This gene is essential for MnSOD activity, but, when deleted, manganese was still found in the mitochondrial matrix. Mtm1 is clearly not just a manganese transporter but also aids in insertion of manganese into the protein. This leads to the as-of-yet unsolved quandary as to why MnSOD is generally metalated properly in vivo even though there is substantially more iron than manganese in most cells and the apoprotein will bind iron equally well as manganese. It was suggested that the iron–sulfur centers that are found in many proteins compete for the iron and contribute to the described metal specificity.[239] Interestingly, the Lyme disease pathogen *Borrelia burgdorferi* is known to contain high levels of manganese and has no requirement for iron. In this case, most SOD is produced as the native Mn-containing form, which is an essential virulence factor, accompanied by a small amount of the apoprotein. However, expression of the MnSOD gene by *S. cerevisiae* in a high-iron medium results in an inactive enzyme.[240]

5.2.3.2. Metalation of the apo-Protein. The most complete studies of in vitro metalation of MnSOD have come from Whittaker and co-workers[241] and have involved studies of the MnSODs from *E. coli* and *T. thermophilus*. One of the earliest in vitro metalation studies[242] showed that the tetrameric apoenzyme from *T. thermophilus* could be metalated only at elevated temperature, comparable to that at which the bacterium normally lives. Later it was shown that temperature-mediated destabilization of protein structure was necessary for metalation of a series of bacteria-derived MnSODs, although the necessary temperature was lower for the mesophilic *E. coli* MnSOD than for any thermophilic enzymes. Metalation was found to be nonspecific with regard to metal ion identity, but activity was specific to manganese. A subsequent study[243] showed that the temperature dependence is not specific for the enzymes from thermophiles and that there is a thermally activated process that is first-order in metal ion and pH dependent and occurs in general for tetrameric apo-enzymes. In contrast, metalation of the apoenzyme from *E. coli*, a dimeric enzyme, showed somewhat different characteristics. Once again, metalation is dependent upon temperature,[168] but here the kinetic process seems to dominate.

Manganese acquisition is zero-order in metal, implying that the mechanism involves a protein conformational change from a closed to open configuration and that the temperature dependence is associated with the fast phase.[216a] A mechanism was suggested for the thermal activation that involves a more closed structure at lower temperature and pH. Upon temperature elevation, a salt bridge breaks and the enzyme twists slightly to form a more open structure capable of manganese binding, culminating in reversion to the closed structure. Surprisingly, the dimer interface is maintained throughout; there is no transient monomeric structure involved in the thermal metalation process.[216b]

A recently published crystal structure of the apo *E. coli* MnSOD shows that, in the crystal form, this protein has the same structure as the metalated enzyme, implying that MnSOD structure is a consequence of the protein folding and not, as is observed in CuZnSOD, somehow "locked down" by incorporation of the metal. In addition, it was suggested that dimer dissociation allows metal incorporation at low protein concentrations.[244]

Finally, in an effort to relate some of the observations regarding in vitro metalation to manganese trafficking in vivo, the human MnSOD was expressed in *S. cerevisiae*,[245] in which manganese trafficking research has been carried out extensively, as described in a previous section. Manganese acquisition was found to be thermally gated in vivo in the same fashion as observed in vitro. It should be noted that the yeast studies are generally carried out at room temperature, whereas in vivo temperature for human cells is substantially higher (ca. 37 °C).

5.3. Catalytic Mechanism

5.3.1. Catalysis. Manganese superoxide dismutase (MnSOD) may be viewed as the most mechanistically complex in the pantheon of superoxide dismutases. In contrast to the other SODs, MnSODs have distinctly different cellular activities at high and low concentrations of superoxide ($O_2^{\bullet-}$), a result of a phenomenon that has become known as "gating".[93,246] Furthermore, the extent of the gating varies among species. The mechanism of superoxide dismutation carried out by MnSOD has been elucidated via an array of stopped-flow and pulse radiolysis experiments.

The first pulse radiolysis studies showed two distinct phenomena. At relatively low ratios of $O_2^{\bullet-}$ to MnSOD ($[O_2^{\bullet-}]$:$[MnSOD] < 5$), simple oxidation and reduction of the enzyme[246a–c] was observed analogous to what was seen with CuZnSOD and FeSOD. However, when catalysis was studied under conditions where the concentration of $O_2^{\bullet-}$ was much higher than that of the enzyme, an unusual feature was

observed. Superoxide was found to disappear in a biphasic process with an initial fast step and a subsequent slower step, corresponding to a first-order "burst" phase and a "zero-order" phase, respectively (Figure 26). A mechanism that can explain the kinetics involves a branched pathway for reaction of the reduced MnSOD with $O_2^{\bullet-}$. Either the $O_2^{\bullet-}$ was rapidly converted to H_2O_2 or the $O_2^{\bullet-}$ was first bound to the manganese site, forming a metal−superoxyl or metal−peroxyl complex ($Mn^{2+}SOD-O_2^{\bullet-}$ or $Mn^{3+}SOD-O_2^{2-}$, here called very generally $MnO_2^+(H_2O)$), and then the peroxo moiety was protonated and released (see Scheme 4). This "gating" process

Scheme 4. Proposed Mechanisms for MnSOD

Mechanism 1

$$Mn^{3+}(OH^-) + O_2^{\bullet} (+H^+) \xrightarrow{k_1} Mn^{2+}(H_2O) + O_2 \tag{18}$$

$$Mn^{2+}(H_2O) + O_2^{\bullet} (+H^+) \xrightarrow{k_2} Mn^{3+}(OH^-) + H_2O_2 \tag{19}$$

$$Mn^{2+}(H_2O) + O_2^{\bullet} \xrightarrow{k_3} MnO_2^+(H_2O) \tag{20}$$

$$MnO_2^+(H_2O)(+H^+) \xrightarrow{k_4} Mn^{3+}(OH^-) + H_2O_2 \tag{21}$$

Mechanism 2

$$Mn^{3+}(OH^-) + O_2^{\bullet} (+H^+) \underset{k_{-1}}{\overset{k_1}{\rightleftarrows}} MnO_2^{2+}(H_2O) \underset{k_{-2}}{\overset{k_2}{\rightleftarrows}} Mn^{2+}(H_2O) + O_2 \tag{22}$$

$$Mn^{2+}(H_2O) + O_2^{\bullet} \underset{k_{-3}}{\overset{k_3}{\rightleftarrows}} MnO_2^+(H_2O)(+H^+) \underset{k_{-4}}{\overset{k_4}{\rightleftarrows}} Mn^{3+}(OH^-) + H_2O_2 \tag{23}$$

$$MnO_2^+(H_2O)(+H^+) \underset{k_{-5}}{\overset{k_5}{\rightleftarrows}} [MnO_2^+(H_2O)] \tag{24}$$
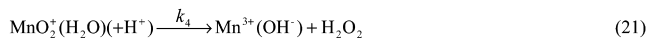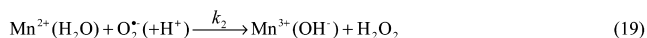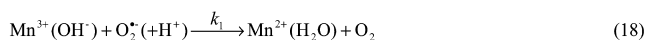
was attributed in those studies to a conformational change. It is interesting to note that, even though the two studies were carried out on MnSODs of different origins, *E. coli* and *Bacillus stearothermophilus*, respectively,[246a−c] th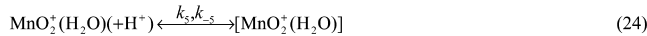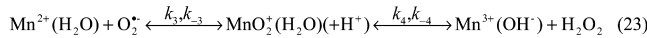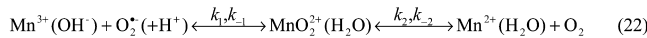e gating ratio between the fluxes in the two branches was invariant (Scheme 4, mechanism 1). This initial mechanism was then expanded to another one accounting for reversibility and protons in the different steps (Scheme 4, mechanism 2).[246d] In all cases, the formation of a complex between $Mn^{2+}SOD$ and $O_2^{\bullet-}$, generally called the "inhibited complex" or the "dead-end" complex, is required to explain the data. In the more generalized mechanism, a reversible isomerization, rather than a conformational change, was proposed; specifically, the authors proposed that a bound peroxy moiety isomerizes from a side-on to an end-on configuration.[246d] As can be seen in Scheme 4, mechanism 2 is a generalized version and mechanism 1 is the special case where the equilibria heavily favor forward reactions and the only kinetically relevant intermediate is that described above. The details of the "gating" phenomenon were clarified upon investigation of the human MnSOD[247] and will be discussed in the following section.

5.3.2. Gating and Protonation. In a simple ping-pong mechanism, where the manganese oscillates between oxidized (Mn^{3+}) and reduced (Mn^{2+}) ions, experiments where the oxidized enzyme is exposed to a substoichiometric burst of superoxide should result in stoichiometric loss of the absorption in the visible region. Accordingly, studies where the fully reduced MnSOD is exposed to a substoichiometric burst of superoxide should result in production of the oxidized enzyme with an absorbance band in the visible region at $\lambda_{max} = 480$ nm for $Mn^{3+}SOD$ (Figure 27A).[246a−c] In the example of Figure 27A, the *Deinococus radiodurans* (Drad) $Mn^{2+}SOD$ reacted with 5-fold less $O_2^{\bullet-}$ to form equimolar amounts of the $Mn^{3+}SOD$.[248] The rate constants were similar to that measured under catalytic conditions, 1.2×10^9 M^{-1} s^{-1} per metal site. A very illuminating analogous study was carried out using human
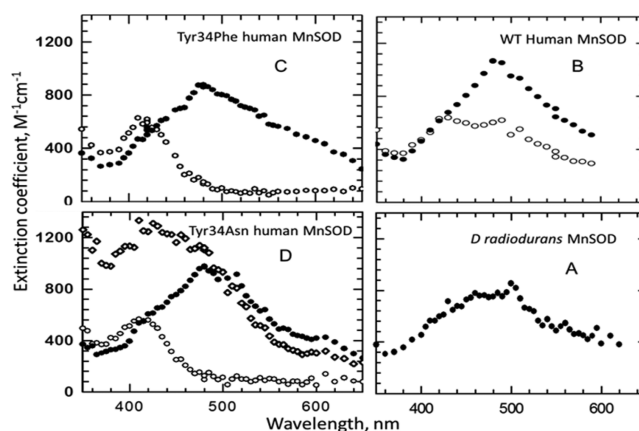

Figure 27. Absorption bands formed upon exposing $Mn^{2+}SOD$ to a burst of $O_2^{\bullet-}$. (○) Initial $Mn^{3+}SOD$ species formed immediately after the pulse; (●) final $Mn^{3+}SOD$ species formed after the pulse; and (◇) second transient formed after the pulse. $O_2^{\bullet-}$ is substoichiometric to MnSOD ([$O_2^{\bullet-}$]:[MnSOD] < 0.12).

$Mn^{2+}SOD$ ($hMn^{2+}SOD$).[93] In this case, an initial absorbance was formed rapidly, followed by a slower increase in the absorbance corresponding to $Mn^{3+}SOD$ (Figure 27B). The initial absorbance was attributed to $MnO_2^+(H_2O)$ ($\lambda_{max} = 420$ nm) and $Mn^{3+}SOD$, which were formed in roughly equal amounts. That corroborates the catalytic studies where the proportion of "burst" phase and "zero-order" phase is very different from that seen in the bacterial systems (Figure 26).

A crucial part of the proton-delivery process was elucidated in some studies from Miller and co-workers[130c,133b] where the proton count upon reduction of $Mn^{3+}SOD$ to $Mn^{2+}SOD$ was measured. The resting $Mn^{3+}SOD$ has a metal-bound hydroxide, and, as the manganese is reduced by $O_2^{\bullet-}$, there is a concomitant protonation of the bound OH^- to a bound H_2O (eq 18, mechanism 1, Scheme 4). That allows for the first H^+ to be locally available for donation to the second $O_2^{\bullet-}$ molecule (eq 19, mechanism 1, Scheme 4) such that only one additional H^+ is required to convert $O_2^{\bullet-}$ to H_2O_2. Theoretical studies of the reduction of $Mn^{3+}SOD$ by $O_2^{\bullet-}$ have shown that the Tyr34 in the proton transfer pathway described above (Figure 24) is responsible for maintaining the thermodynamic barrier to protonation of the hydroxide, and, when $O_2^{\bullet-}$ coordinates to $Mn^{3+}SOD$, there is a transfer of the proton through $O_2^{\bullet-}$ to the hydroxide, leading to a proton transfer concomitant with the electron transfer.[249]

The great interest in the mechanism described in Scheme 4 is focused on the protonation of the bound peroxy moiety and subsequent loss of H_2O_2 (eq 21, mechanism 1, Scheme 4). To clarify this aspect of the mechanism, many mutations were made of residues in the hydrogen-bonding network described above. In particular, the hydroxyl group of Tyr34, a residue that is conserved in MnSODs from all species thus far characterized, was of interest as the hydroxyl group is thought to be paramount in proton transfer to the peroxo moiety (eqs 19 and 21, mechanism 1, Scheme 4) and not just to form a thermodynamic barrier to protonation of the hydroxide (eq 18, mechanism 1, Scheme 4). The most obvious mutant is the Tyr34Phe, where the tyrosine is mutated to a phenylalanine, an amino acid identical to tyrosine except without the hydroxyl group.[234,250] The Tyr34Phe mutation yields an enzyme where the fast catalysis is eliminated (eqs 18 and 19, mechanism 1, Scheme 4), although protonation via the slow pathway is

relatively unchanged in comparison with the wild-type hMnSOD, as evidenced by the formation of the intermediate but no concomitant fast formation of $Mn^{3+}SOD$ (Figure 27C). Upon mutation of Tyr34 to the amino acid asparagine, an additional intermediate was observed (Figure 27D).[234b] In contrast, when a similar replacement of Tyr34 to Phe was made in two bacterial MnSODs, those of *Drad* and *E. coli*, the effect was much less dramatic. Tyr34Phe *Drad* MnSOD had the same gating between the fast pathway (eqs 18 and 19, mechanism 1, Scheme 4) and the slow pathway (eqs 18, 20, and 21, mechanism 1, Scheme 4) as the wild-type hMnSOD. The effect of the Tyr34Phe substitution on *E. coli* MnSOD was to lower the catalytic rate constant slightly.[234a] In this case, catalysis was measured via steady-state kinetics, and the effect of a change in protonation of bound peroxide or the gating ratio could not be measured. Given the dramatic effect upon gating observed in the Tyr34Phe hMnSOD mutant, a series of other mutations at position 34 in the human MnSOD were produced. Upon mutation of the tyrosine to alanine, asparagine, glutamine, and valine, gating remained the same with no discernible fast catalytic pathway (eqs 18 and 19, mechanism 1, Scheme 4); however, large variations were measured in the rate of protonation off of the bound peroxide (k_4).[234b] As noted above, a second intermediate was formed in the majority of these cases.

A recent series of studies[65a,251] involving the yeast MnSODs, *S. cerevisiae* mitochondrial enzyme (*Sc*MnSOD) and *C. albicans* cytoplasmic enzyme (*Ca*MnSODc), showed that they were isolated predominantly in the reduced form, unlike the majority of other wild-type MnSODs but similar to the Gln143 hMnSOD mutant enzymes (vide infra). These are the most efficient MnSODs isolated thus far, primarily because the gating favors fast catalysis (eqs 18 and 19, mechanism 1, Scheme 4). Upon oxidation, there is evidence for a small amount of a Mn^{3+} species distinct from the well-characterized five-coordinate Mn^{3+}.[65a] This species has an optical absorption around 400 nm and parallel-mode EPR resonances forming a sextet due to nuclear hyperfine interactions with interpeak spacings of approximately 4.5–5.0 mT, consistent with several previously observed six-coordinate Mn^{3+} complexes.[65a] Hydroxide was proposed as the sixth ligand.[65a] A sixth ligand was observed earlier by X-ray crystallography for the *E. coli* MnSOD under cryogenic conditions or at high pH.[252] A mechanism involving a transient 6-coordinate $Mn^{3+}SOD$ that is the catalytically active partner with $O_2^{\bullet-}$ was proposed and is described in section 5.3.3.[251b]

Another residue involved in the hydrogen-bonding network that is both at the dimer interface and at the entrance of the active site channel is His30. Upon mutation of His30 to Ala in *E. coli* MnSOD, reduction in activity to ca. 30% of the wild-type activity was observed.[253] A study was carried out in the hMnSOD where the His30 was mutated to Asn, Gln, and Val. The Val mutation led to an extremely inactive enzyme, likely a result of serious steric hindrance by the valine in the active site channel.[235a] In contrast, the His30Asn mutation led to no change in the gating ratio and to significantly slower catalysis, but the rate of protonation and release of the bound peroxy moiety, k_4, was increased by a factor of 4.[254] These minor changes resulted in faster disappearance of $O_2^{\bullet-}$ when $[O_2^{\bullet-}] >$ [MnSOD]. As will be discussed later, this had relevant biological consequences.

The final residue in the hydrogen-bonding network is Gln143 (Gln146 in *E. coli* MnSOD). As noted earlier, this glutamine forms a hydrogen bond with Tyr34 and the water ligand.[236] This residue also plays an important role in metal specificity as mutation of Gln146 to either Leu or His in *E. coli* MnSOD led to impaired metalation and an inactive enzyme.[236b] Replacement of the Glu143 in hMnSOD with smaller residues simply allows solvent water to maintain the hydrogen-bonding network such that protonation and release of the bound peroxy moiety occurs at the wild-type rate (k_4).[236a] However, in all cases, including a recent study of Gln143His rat MnSOD,[236d] thermal stability is sacrificed by altering this glutamine. Mutation of Gln143 also leads to isolation of the reduced enzyme.[236b]

Many other single point mutations were made to understand the factors controlling gating and protonation of the bound peroxy moiety in hMnSOD.[255] Of these, the only mutation that alters the gating ratio such as to make hMnSOD more "bacterial-like" is the replacement of Phe66 with Leu in hMnSOD.[255d] This residue lies on the dimer interface, suggesting that it is this interface that warrants further exploration. It is noteworthy that the gating ratio may favor the fast catalytic removal of $O_2^{\bullet-}$ but protonation has slowed. Indeed, protonation and release of the bound peroxide seems to be slower in most of the prokaryotic enzymes, suggesting a very subtle tuning of these rate constants.

5.3.3. Fast Catalysis through Six-Coordinate Mn(III) Species.

The protonation and release of H_2O_2 from the inhibited complex (see section 5.3.4) were believed to lead exclusively to the five-coordinate $Mn^{3+}SOD$ binding a hydroxide ligand (mechanisms 1 and 2, Scheme 4). Nevertheless, a recent study of a mutant yeast enzyme, Tyr34Phe *Sc*MnSOD, revealed a novel mechanism involving a six-coordinate Mn^{3+} species that is able to efficiently oxidize $O_2^{\bullet-}$ into O_2.[251b] Tyr34Phe *Sc*MnSOD resembles the Tyr34Phe hMnSOD mutants in that the fast pathway was almost completely lost, but an additional transient (Int_2), analogous to that discussed above (Figure 27D), was generated from the protonation of product-inhibited complex (Int_1) (Scheme 5).[251b] On the basis of its optical absorption, this

Scheme 5. Proposed Mechanisms for Y34F *Sc*MnSOD[251b]
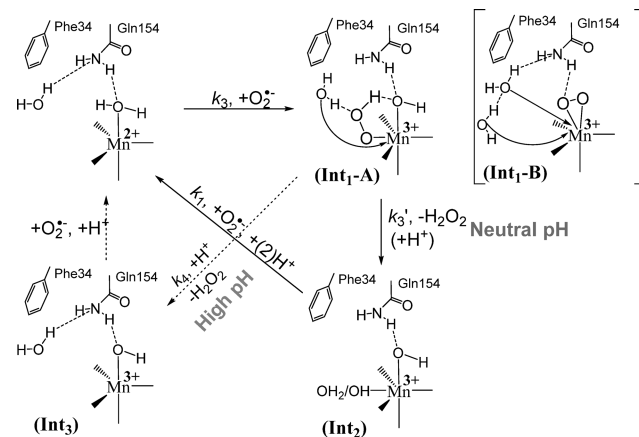
additional transient (Int_2) was proposed to contain a six-coordinate Mn^{3+} center.[251b] Because the rate constant for formation of Int_2, k_3', was reported to be independent of ionic strength, it was concluded that the electrostatic charge had not changed when Int_2 was generated and that the sixth ligand in

Int$_2$ could thus be a water molecule,[234b] although the possibility that it is instead OH$^-$ or OOH$^-$ could not be ruled out.

Surprisingly, although Tyr34Phe *Sc*MnSOD is gated considerably more toward the inhibited pathway relative to WT hMnSOD, the former was found to have higher catalytic efficiency than the latter under inhibiting conditions (Figure 28A). Further analysis of the kinetic data suggested that the
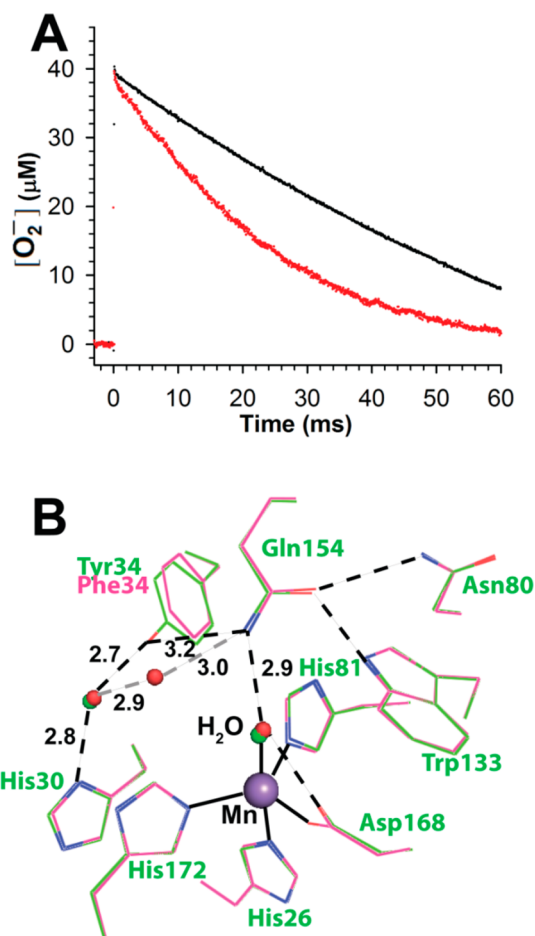

Figure 28. Catalysis and active-site structure of Y34F *S. cerevisiae* MnSOD (*Sc*MnSOD). (A) Decay of 41 μM O$_2^{\bullet-}$ catalyzed by 1 μM human WT MnSOD (black) and Y34F *Sc*MnSOD (red) in pH 7 phosphate buffer. (B) Superimposition of the active site of Y34F *Sc*MnSOD (chain A, red) onto that of WT *Sc*MnSOD (chain A, green) (adapted from ref 251b). Coordination bonds are indicated as solid lines, and hydrogen bonds are shown as dashed lines in WT (black) and Y34F (gray) *Sc*MnSOD, respectively.

putative six-coordinate Mn^{3+} intermediate, Int$_2$, rather than the five-coordinate Mn^{3+}SOD oxidizes O$_2^{\bullet-}$ in the catalytic cycle of Tyr34Phe *Sc*MnSOD (Scheme 5).[251b] The protonation of the inhibited complex in Tyr34Phe *Sc*MnSOD, which leads to formation of the six-coordinate Int$_2$, is much faster (k_3' = 310 s^{-1}) than in other systems, which leads to formation of the five-coordinate Mn^{3+}SOD (k_4 = 20–120 s^{-1}). Therefore, fast catalysis can be achieved via a six-coordinate Mn^{3+} species, bypassing the slow steps leading to five-coordinate Mn^{3+}SOD.

The observation of the putative six-coordinate intermediate correlates with the presence of an additional second-sphere water molecule that maintains the hydrogen-bonding network extending from the solvent ligand (Figure 28B). The additional second-sphere water molecule was therefore assigned a role as a

proton donor to the bound (hydro)peroxyl group, and this proton transfer could facilitate the rapid protonation of the inhibited complex and the subsequent departure of H$_2$O$_2$. However, the rapid proton transfer was pH-dependent. At increased pH, it was gradually replaced by a slower proton transfer pathway, which leads to the five-coordinate Mn^{3+} species (Scheme 5) as in WT hMnSOD. This study has significantly enhanced our understanding of MnSOD catalytic mechanism and may elucidate the reason for the low degree of product inhibition in the yeast enzymes.

5.3.4. The Inhibited Complex. Thus far in this Review, the bound peroxy moiety or "inhibited complex" has been left undefined. A very early suggestion was made that it represented a side-on peroxy moiety bound to the oxidized metal and that isomerization to an end-on structure was necessary to allow its protonation and release.[246d] The end-on conformation of a bound peroxy ligand is supported by several theoretical calculations showing that it is more stable than the side-on one.[249,256] Additional theoretical work[154] and then a recent cryotrapping experiment showed formation of a side-on peroxo complex.[252b] This species observed in the X-ray structure of H$_2$O$_2$-soaked crystals, however, does not necessarily represent the intermediates present under catalytic conditions. As long as the side-on peroxy moiety gets a proton from the water ligand, which is proposed to occur instantaneously upon formation of the inhibited complex,[257] the side-on peroxy must switch to an end-on conformation. Moreover, the side-on Mn–peroxo complexes are generally stable, and bound peroxyl would not be easily protonated or released.

The location of the bound peroxyl/hydroperoxyl group is also under debate. It could bind to the sixth ligand site in proximity of Tyr34 in the plane of His26, His74, and Asp159, as azide and fluoride both bind to this site.[258] Indeed, an end-on peroxyl group can be docked into the sixth ligand site without unfavorable steric interactions with the active-site residues.[251b] Moreover, the most probable inhibited complex has been calculated to be an end-on Mn^{3+}–hydroperoxo species with HOO$^-$ binding to the sixth ligand site and pointing toward the solvent ligand.[256] The peroxyl/hydroperoxyl group has also been proposed to bind at the axial position by replacing the solvent ligand. Such species were once observed in the structure of H$_2$O$_2$-soaked *Ec*MnSOD,[252b] suggesting they have a long lifetime.

5.3.5. Kinetic Variation among Species. The other unique feature that differentiates MnSOD from other SODs is the kinetic variation among species. This variation seems to be wholly explained by the gating ratio (k_2/k_3). The manifestation of this in the half-life of O$_2^{\bullet-}$ at a similar concentration of enzyme and superoxide can be seen in Figure 29. The interesting features here are that (i) protonation and release of the bound peroxide remains fairly constant in all species with k_4 ≈ 60–140 s^{-1}, (ii) hMnSOD is unquestionably the least efficient of all enzymes shown here, and (iii) the gating ratio varies from 1:1 to 15:1 in favor of fast catalysis. At a gating ratio of 15:1, the superoxide concentration must be significantly greater than 15 times that of the enzyme for any change in the rate of O$_2^{\bullet-}$ disappearance. This does not seem to be very realistic except perhaps in a superoxide "burst", supporting an observation that whereas the gating phenomenon may be interesting mechanistically, it has little physiological effect in most organisms.[93] It is for hMnSOD, with a gating ratio of 1:1, that a physiological effect might be expected.
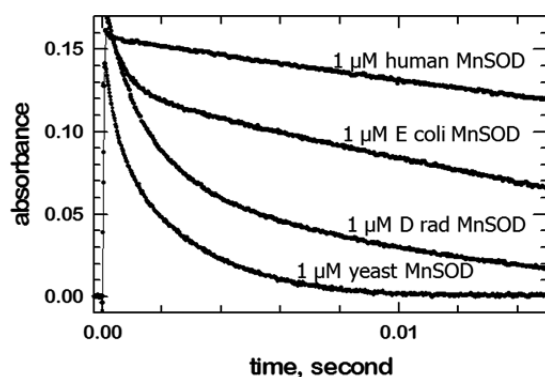
Figure 29. Disappearance of a burst of $O_2^{\bullet-}$ ($41\mu M$) in the presence of 1 μM of MnSOD from different organisms under the same conditions.

Human mitochondria were recently found to generate large bursts of $O_2^{\bullet-}$, termed "superoxide flashes", in tiny elliptical areas.[259] The observation of those flashes in human mitochondria suggests the inability of hMnSOD to remove efficiently high concentrations of $O_2^{\bullet-}$ in these tiny spaces in mitochondria, likely as a result of severe product inhibition. The inhibition of hMnSOD is proposed to be associated with the role of H_2O_2 as a signaling agent in mammalian cells.[65a,251a] H_2O_2 is found to participate in various cellular processes, including several important mitochondrial signaling pathways, such as tumor necrosis factor (TNF)-α-induced apoptosis and c-Jun NH_2-terminal kinase (JNK)-induced apoptosis.[65a] The decreased efficiency of hMnSOD under superoxide flashes prevents production of bursts of H_2O_2, which would result in aberrant oxidant-driven signaling.

A body of work[260] is accumulating in which overexpression of hMnSOD in human cells has been shown to be closely associated with tumor suppression. In addition, as discussed earlier, when the H30N hMnSOD was cloned into human tumor cells and then into mice with tumors, the result was enhanced cell death or tumoricidal behavior. The in vitro behavior of this enzyme is that at low $[O_2^{\bullet-}]$:[MnSOD] it is less efficient but at high ratios it is much more efficient at removing $O_2^{\bullet-}$, as compared to WT hMnSOD. The variation in catalytic efficiencies among species suggests that MnSOD acts like a true SOD in many species, but, within human cells, it can serve the dual purpose as a signaling agent as well. MnSOD, with this more complex mechanism described above, seems uniquely poised to execute these different roles.

6. COPPER−ZINC SUPEROXIDE DISMUTASE

6.1. History and Properties

The history of the SOD enzymes begins in 1969 with the landmark paper by McCord and Fridovich showing that bovine erythrocuprein, a copper-containing protein of unknown function, is in fact a superoxide dismutase.[104] Shortly thereafter, the presence of zinc in the enzyme, in addition to copper, was reported,[261] and the enzyme was subsequently termed copper−zinc superoxide dismutase, CuZnSOD, or SOD1. In 1982, the complete three-dimensional crystal structure of bovine CuZnSOD was solved.[262] Intracellular CuZnSODs, similar to bovine CuZnSOD, are now known to exist as homodimers in almost all eukaryotic organisms, where they play an important role in antioxidant defense. An extracellular form of SOD (EC-SOD), homologous to CuZnSOD, was identified in humans in

1987,[263] and it is now known that EC-SOD is tetrameric and exists in most mammals[55] and in many plants.[51]

Initial characterization of CuZnSODs focused primarily on the bovine and human intracellular enzymes, which were found to be remarkably stable. The first fungal CuZnSOD to be isolated was from the budding yeast *S. cerevisiae* by Goscin and Fridovich in 1972,[264] and its gene was cloned and sequenced in 1988.[265] Characterization of *S. cerevisiae* CuZnSOD demonstrated that it was also dimeric and similar to the mammalian enzymes in many respects, but that it was less stable and showed somewhat altered metal-binding properties.[265b,266] The cloning of the SOD1 gene in yeast enabled construction of sod1-delete yeast strains, which have proven to be a valuable model system for studies of oxidative stress and metal metabolism.[267]

CuZnSOD was considered an exclusively eukaryotic enzyme until its isolation from the bacterium *Photobacterium leiognathi*, in 1974.[268] It was subsequently found in the periplasm of many other gram-negative bacteria.[52,269] Although eukaryotic intracellular CuZnSODs are almost exclusively homodimeric (reviewed in refs 53,270), bacterial periplasmic CuZnSOD may be either monomeric or dimeric.[66] Interestingly, although the subunit fold is conserved in eukaryotic and prokaryotic CuZnSODs, the dimeric interfaces are distinctly different in the prokaryotic versus the eukaryotic dimeric proteins.[66,68a]

In 1993, mutations in the human CuZnSOD gene, which is located on chromosome 21 in the 21q22.11 region, were found to associate with some cases of familial amyotrophic lateral sclerosis (FALS),[271] a neurodegenerative disease characterized by motor neuron death in the brainstem and spinal cord. As reviewed below (section 6.6), these findings have focused much attention in the field of CuZnSOD on the linkage between mutations in human CuZnSOD and FALS.

6.2. Structure

Intracellular eukaryotic SOD1 is a 32-kDa homodimeric enzyme with each subunit holding one copper- and one zinc-binding site in close proximity and an intramolecular disulfide bond between Cys57 and Cys146 (according to the human SOD1 numbering, which is used throughout this Review). Each subunit folds as an eight-stranded, Greek-key β-barrel with seven connecting loops, of which loops IV (residues 49−83) and VII (residues 121−142), termed as the zinc and electrostatic loops, respectively, are functionally important. The zinc loop contains all four Zn-binding residues and a disulfide cysteine, Cys57. The electrostatic loop contains most of the second-sphere active site residues, including the catalytically important Arg143, and acts as an active-site lid, limiting access of solvent to the metal-binding sites.

The structure of the binuclear metal-binding site is dependent upon the oxidation state of copper. When the copper ion is reduced (Cu^+), it is ligated by His46, His48, and His120 in a nearly trigonal planar geometry (Figure 30). The zinc ion is coordinated nearby in a nearly tetrahedral geometry by three histidyl imidazoles (His63, His71, His80) and an aspartyl residue (Asp83) (Figure 30). Upon oxidation, the imidazolate side chain of His63 bridges the oxidized (Cu^{2+}) copper and zinc ions. In addition to His63, the copper ion also binds a water molecule and becomes five-coordinate in a distorted square pyramidal geometry, while the zinc ion retains the tetrahedral coordination geometry as in the reduced form of the enzyme. A second-sphere residue, Asp124, links the two metal-binding sites by forming hydrogen bonds with both
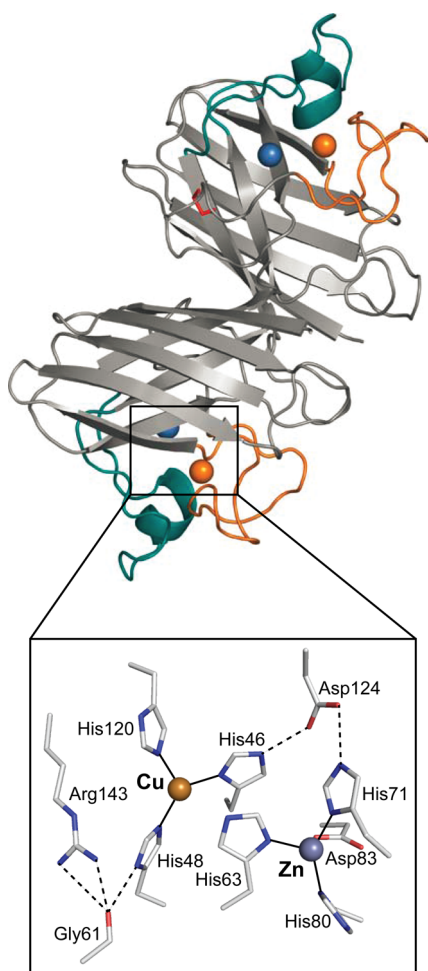
Figure 30. Stereo ribbon diagram of dimeric human SOD1 (top) (reproduced from ref 53) with the active site highlighted (PDB code: 1PU0) (bottom). Copper and zinc ions are shown as blue and orange spheres, respectively. The zinc loop is shown in orange and the electrostatic loop in teal. The intrasubunit disulfide bond is shown in red. The reduced metal-binding (Cu$^+$) site is shown. The diagrams were generated using the PyMOL Molecular Graphics System.[396]

His46 and His71 (Figure 30). Arg143 is a catalytically important second-sphere residue and is linked to copper ligand His48 through hydrogen bonds to Gly61 (Figure 30). It also forms a hydrogen bond with a disulfide cysteine, Cys57.

The monomer−dimer equilibrium of eukaryotic intracellular CuZnSOD is strongly influenced by the state of metalation and also by the status of the intrasubunit disulfide bonds. These are represented below as X,Y-SOD1$^{S-S/2SH}$, where X and Y stand for the metal ion in copper and zinc site, respectively (E means an empty site), and S−S and 2SH stand for oxidized and reduced disulfide bond, respectively. In the case of human CuZnSOD, the fully metalated protein, with the Cys57−Cys146 disulfide bonds intact (Cu,Zn-SOD1^{S-S}), is dimeric, as is the metal ion-free apoprotein (E,E-SOD1^{S-S}), so long as the disulfide bond is present. Analytical ultracentrifugation studies[272] of the monomer−dimer equilibrium showed that E,E-SOD1^{S-S} and Cu,Zn-SOD1^{S-S} are stable dimers even at very low concentrations (2 μM).[272a] Monomerization of the mature form of fully metalated bovine or human Cu,Zn-SOD1^{S-S} can occur in vitro in the presence of chaotropic agents, including urea,[265b,273] guanidinium hydrochloride (GuHCl),[274] and sodium dodecyl sulfate (SDS)[275] (reviewed

in ref 54). Monomerization of many of the dimeric ALS mutant human Cu,Zn-SOD1^{S-S} occurred at lower urea concentrations than that required to monomerize wild-type human Cu,Zn-SOD1^{S-S}, suggesting that the ALS mutations cause a lowering of the subunit affinities (see section 6.6).[276] These affinities are believed to be substantially weaker in *S. cerevisiae* Cu,Zn-SOD1^{S-S} than in bovine Cu,Zn-SOD1^{S-S}, based on the observation that the yeast enzyme readily exchanged subunits under ambient conditions,[265b,277] whereas exchange of subunits in bovine required the presence of 8 M urea.[265b,273b]

Stable disulfide bonds in intracellular proteins are usually rare, due to the overall reducing nature of the intracellular environment. When and how the disulfide bond of SOD1 is formed is thus intriguing. Given the fact that the cytosol favors reduced thiols, the formation of stable oxidized disulfide bonds in cytoplasmic proteins usually satisfies one of the two following conditions: (1) The disulfide bond has an abnormally low reduction potential and thus displays a high oxidation propensity; and (2) the protein is restricted to certain cellular compartments, such as the endoplasmic reticulum (ER) and the plasma membrane in eukaryotic cells, where the internal environment is relatively more oxidizing as compared to the cytoplasm.[278] In addition, the intracellular disulfide bond formation usually involves a cascade of disulfide bond transfers between a series of proteins.[278]

In the case of SOD1, CCS is able to promote disulfide bond formation in addition to delivery of copper into SOD1 (see section 6.4), although the dependence on CCS varies from species to species. The order of the dependence of SOD1 disulfide formation on CCS scales as yeast > human > *C. elegans*, with yeast SOD1 the most dependent and *C. elegans* SOD1 completely independent.[279]

The disulfide bond reduction potential was determined by incubating SOD1 with various ratios of oxidized or reduced glutathione or dithiothreitol (DTT) under anaerobic conditions, followed by alkylation of the free cysteine thiols.[279,280] The disulfide reduction potential of SOD1 was found to vary from species to species[279] but to remain constant whether or not metal ions are present in the native copper and zinc sites.[280] The apoproteins of yeast, human, and *C. elegans* SOD1 have a measured reduction potential of −234, −248, and −270 mV, respectively.[279] SOD1 with a high disulfide reduction potential, such as yeast SOD1, has a low oxidation propensity, which correlates with the protein's dependence on CCS (see section 6.4). Because the intracellular reduction potential maintained by the GSH/GSSG redox pair is −290 mV, the disulfide cysteines of these three SOD1s would be predominantly reduced in the cytosol.[279] This further explains the requirement for CCS in disulfide oxidation (see section 6.4). It has been proposed that the disulfide oxidation of CCS-independent SOD1s is facilitated by post-translational modifications (see section 6.4).[279]

Fully functional human Cu,Zn-SOD1^{S-S} is extraordinarily stable, melting at 92 °C and remaining folded in 8 M urea or 1% SDS (reviewed in ref 53). Removal of the metal ions (E,E-SOD1^{S-S}) decreases the melting temperature to 54 °C,[272b] and reduction of the disulfide bond results in the least stable form (E,E-SOD1^{2SH}), which melts at 42 °C.[53] Similarly stable as human SOD1, metalated and apo bovine SOD1 melt at temperatures of 96 and >50 °C, respectively.[281] Metalated yeast Cu,Zn-SOD1^{S-S} melts at a much lower temperature, 82 °C,[281] and is thus less thermostable than human and bovine Cu,Zn-SOD1^{S-S}.

3890

dx.doi.org/10.1021/cr4005296 | *Chem. Rev.* 2014, 114, 3854−3918

Human and bovine SOD1 each possess two free cysteines, Cys6 and Cys111 (numbering in human SOD1), in addition to Cys57 and Cys146, which are linked in the intrasubunit disulfide bond. Replacement of Cys6 and Cys111 with unreactive side chains elevates the thermostability of human and bovine SOD1, due to removal of the reactive thiol groups and inhibition of the formation of disulfide-cross-linked aggregates (see section 6.6).[265b,270e] *S. cerevisiae* SOD1 contains only the two cysteines that form the disulfide bond and no free cysteines.

The initial binding of one-zinc per dimer in apo hWT SOD1 has a more profound effect on thermal stability than binding of subsequent metal ions.[272b] The zinc-bound subunit stabilizes the metal-free subunit through dimerization and increases the melting temperature of the apo subunits from 54 to 61 °C,[272b] with the latter requiring dimer dissociation prior to melting. The zinc-bound subunits then self-associate to form a two-zinc dimer, which melts at a much higher temperature (76 °C). Addition of a second equivalent of Zn^{2+} increased the magnitude of the transition attributed to a two-zinc dimer, while the transition attributed to apo subunits was diminished.[272b] The observation of the endotherm of apoprotein in the differential scanning calorimetry (DSC) profile of two-zinc hWT suggests that zinc may dissociate from its binding site during the heating period.[282]
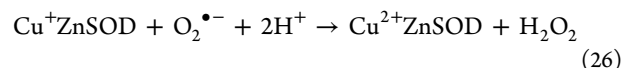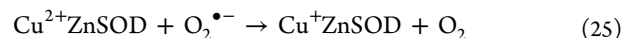
Although SOD1 from different species are structural homologues, they display different metal-binding behavior in vitro. Co^{2+} is commonly used as a substitute for Zn^{2+} in metal-binding studies because the latter is spectroscopically silent, while Co^{2+}, when bound to human SOD1, gives three intense bands in the optical spectrum.[283] Titration of Co^{2+} into human and bovine apo-SOD1 at pH 5.5 resulted in a two-cobalt derivative with Co^{2+} occupying the zinc site in each subunit.[283] In contrast, *S. cerevisiae* apo-SOD1 bound 2 equiv of Co^{2+} only if the pH was raised to 7 or higher, and in this case, the two Co^{2+} ions occupied both the copper and the zinc sites of the same subunit, leaving out a metal-free subunit.[283] The metal-free subunit was thus termed the "phantom subunit".

The "phantom subunit" phenomenon may be explained by the theory of internal stress proposed by Das et al.[284] Internal stress is proposed as a prerequisite for high metal-binding affinity of SOD1.[284] It therefore seems likely that apo *S. cerevisiae* SOD1 has less internal stress than apo hSOD1, leading to lower metal-binding affinity. Moreover, binding of one metal ion per dimer significantly stabilizes the dimeric form of WT hSOD1.[272b] Thus, when the apo form of *S. cerevisiae* SOD1 binds one metal ion, the metalated and the apo subunits will both be stabilized, which would further reduce the metal-binding affinity of the apo subunit so that it does not bind any metal ions.

The in vivo metalation of WT and FALS mutant hSOD1 in the cytoplasm of *E. coli* and human cells has been monitored directly by in-cell NMR in elegant studies by Banci and co-workers.[285] Addition of zinc ions to cell media led to the Zn-bound form (E,Zn-SOD1^{2SH}).[285a,c] When cell media were supplemented with copper, the recombinant hSOD1 expressed in *E. coli* cells bound copper stoichiometrically and formed the fully metalated protein, while only ∼25% of hSOD1 expressed in human cells was incorporated with copper.[285a] Indirect measurement of the in vivo metalation state by ^{64}Cu autoradiography[286] has identified the presence of copper-free SOD1 in human lymphoblasts[286b] and mouse fibroblasts.[286c]

6.3. Catalytic Mechanism

6.3.1. SOD Reaction. One molecule of $O_2^{\bullet-}$ reduces the Cu^{2+} center and forms O_2 (eq 25), and a second molecule of $O_2^{\bullet-}$ oxidizes the Cu^+ ion and forms H_2O_2 (eq 26). The rates of the two half reactions are both nearly diffusion-controlled at physiological pH.[53] The reactivity of the holoenzyme is nearly independent of pH over the range of 5.0−9.5 (reviewed in ref 53).

$$Cu^{2+}ZnSOD + O_2^{\bullet-} \rightarrow Cu^+ZnSOD + O_2 \qquad (25)$$

$$Cu^+ZnSOD + O_2^{\bullet-} + 2H^+ \rightarrow Cu^{2+}ZnSOD + H_2O_2 \qquad (26)$$

The mechanism described above is deceptive in its simplicity. As noted earlier, there is a two-proton requirement for the disproportionation process, and the structural change (shift of the imidazole) upon reduction of Cu^{2+} to Cu^+ demonstrates delivery of the first proton to the active site in this process. The "gating" observed in MnSOD and the redox control and k_{cat}/K_m phenomena found in FeSOD are not detectable in SOD1. However, the proton requirement becomes important when the bond between the bridging imidazole and the zinc is broken. The pH-independent region (pH 6−10) for diffusion-controlled catalysis has been shown to be pH-dependent when the zinc is absent (Cu,E-SOD1).[287] The pH-independence was restored when a non-native divalent metal ion such as Cu^{2+} or Co^{2+} was bound to the zinc site.

In fast kinetic studies using substoichiometric amounts of superoxide, it is possible to measure the rate constants for eqs 25 and 26 individually. Equation 25 was shown to be pH-independent regardless of the presence or absence of a metal ion in the zinc site. However, eq 26 was shown to be very pH-dependent, with an abrupt drop in activity at pH > 6 in the absence of a metal in the zinc site. This drop in activity has a 2-fold origin. It occurs in part because, upon reduction of Cu^{2+} to Cu^+, the imidazole dissociates from copper and protonates and, in the absence of zinc or another metal ion in the zinc site, the copper becomes fluxional. In the absence of a copper chelator, some portion of the "fluxional" copper can bind in the zinc site, where it provides no SOD activity. The resulting Cu,Cu-SOD1 enzyme is robust, albeit with reduced SOD activity because the amount of Cu in the native copper site has been reduced. In the presence of a copper chelator, the enzyme loses activity dramatically with increasing pH as a result of copper loss from the native copper site.

The other significant feature in the SOD1 mechanism is that of the electrostatic guidance of the $O_2^{\bullet-}$ into the active site. In this class of enzymes, the electrostatic guidance can be attributed almost completely to the arginine 143 that sits on the active site lid.[288] Upon neutralization of the positive charge of Arg143 (Arg143Ile), the rate constant drops by an order of magnitude.[270e,288c] Charge reversal by conversion of the positive charge to a negative charge (Arg143Asp or Arg143Glu) leads to a drop in the rate constant by another order of magnitude.[270e,288c] Furthermore, the carboxylate moiety of the substituted glutamate and aspartate can be protonated and deprotonated reversibly with a pK_a for both of those amino acids of ca. 6.2. Upon protonation (and charge neutralization) of the glutamate/aspartate mutant enzyme, the rate of catalysis becomes similar to that of the charge neutralized isoleucine mutant (Arg143Ile SOD1).

6.3.2. Peroxidative Reaction. SOD1 is known to exhibit peroxidative activity in addition to its dismutase activity.[53] The
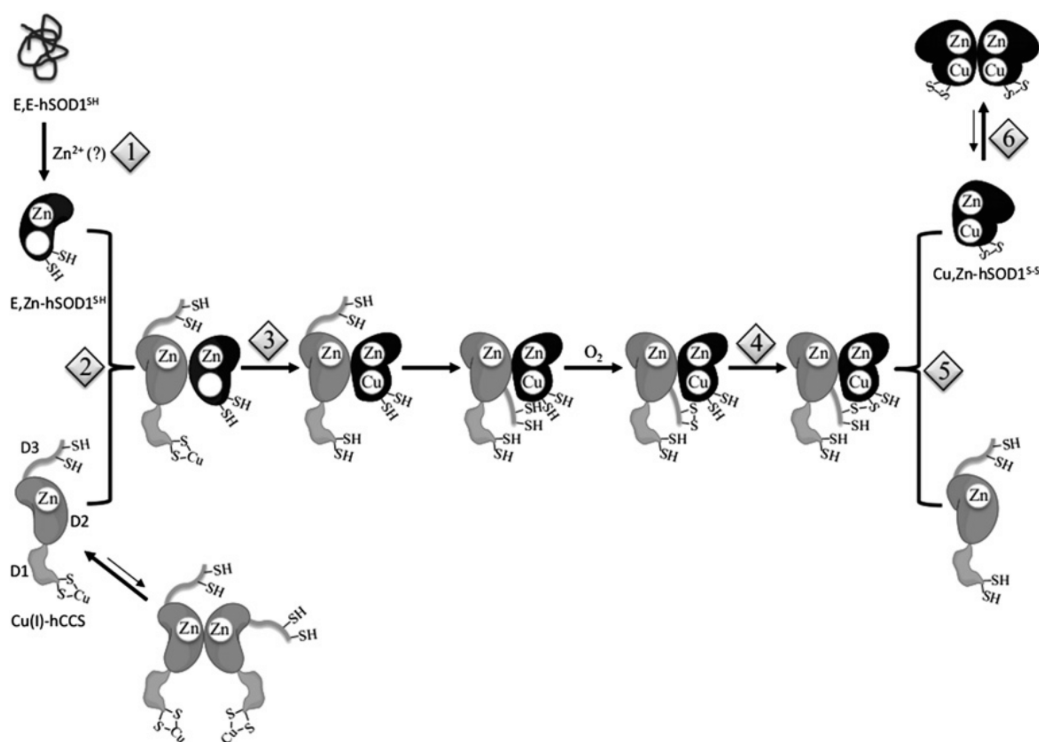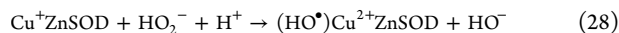
Figure 31. Schematic mechanism of CCS-dependent hSOD1 maturation in vitro (reproduced from ref 297). (1) Nascent hSOD1 (E,E-hSOD1^{SH}) acquires zinc from an unknown source, producing E,Zn-hSOD1^{SH}. (2) The hSOD1^{SH} monomer forms a heterodimer with a monomer Cu(I)-hCCS. The current study suggests that copper transfer (3) occurs before formation of the intermolecular (4), and then hSOD1 intramolecular (5), disulfide bond, resulting in the mature monomer (6) that dimerizes to the active state.
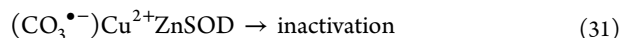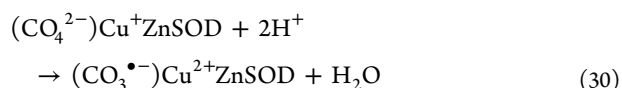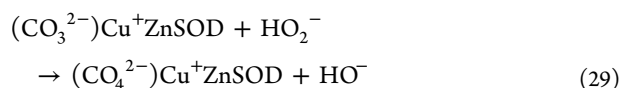
reaction of Cu^{2+}-SOD1 with a molecule of H$_2$O$_2$ leads to the reduction of the copper ion and the production of superoxide (eq 27). Cu$^+$-SOD1 reacts with a second molecule of H$_2$O$_2$, producing a hydroxyl radical at the active site and a hydroxide ion (eq 28). The highly reactive hydroxyl radical at the active site is able to oxidize the histidyl imidazole ligands,[53] ultimately leading to loss of the copper ion and inactivation of the enzyme.

$$\text{Cu}^{2+}\text{ZnSOD} + \text{HO}_2^- \rightarrow \text{Cu}^+\text{ZnSOD} + \text{O}_2^{\bullet-} + \text{H}^+ \qquad (27)$$

$$\text{Cu}^+\text{ZnSOD} + \text{HO}_2^- + \text{H}^+ \rightarrow (\text{HO}^\bullet)\text{Cu}^{2+}\text{ZnSOD} + \text{HO}^- \qquad (28)$$

Equation 28 has been shown to involve HO$_2^-$ itself, and, because the pK_a of HO$_2^-$, H$^+$/H$_2$O$_2$ is 11.9, the reaction rate increases an order of magnitude for every unit increase in pH from pH 7−11. At low pH (pH < 7), there is some indication that H$_2$O$_2$ becomes competitive as evidenced by a relatively pH invariant region around pH 5−6. Clearly, HO$_2^-$ has the same charge as O$_2^{\bullet-}$, and it has been shown to be subject to the same ionic strength constraints as O$_2^{\bullet-}$ (see section 2).[289]

Bicarbonate is known to accelerate the inactivation of SOD1 by H$_2$O$_2$ in the absence of phosphate.[53] Elam et al.[290] proposed a mechanism of bicarbonate-mediated peroxidation by SOD1. In this mechanism, the oxidation of Cu$^+$-SOD1 in the presence of bicarbonate occurs through peroxycarbonate (CO$_4^{2-}$), which can be formed from HO$_2^-$ reacting with the enzyme-bound CO$_3^{2-}$ (eqs 29 and 30). Peroxycarbonate is subsequently reduced to an enzyme-bound carbonate radical, CO$_3^{\bullet-}$, which leads to fast modifications of active-site residues and inactivation of the enzyme. A recent kinetic study provided evidence in support of this proposed mechanism by showing that the oxidation of Cu$^+$-SOD1 by peroxycarbonate is more

than 100-fold faster than the oxidation of Cu$^+$-SOD1 by H$_2$O$_2$.[291]

$$(\text{CO}_3^{2-})\text{Cu}^+\text{ZnSOD} + \text{HO}_2^-$$
$$\rightarrow (\text{CO}_4^{2-})\text{Cu}^+\text{ZnSOD} + \text{HO}^- \qquad (29)$$

$$(\text{CO}_4^{2-})\text{Cu}^+\text{ZnSOD} + 2\text{H}^+$$
$$\rightarrow (\text{CO}_3^{\bullet-})\text{Cu}^{2+}\text{ZnSOD} + \text{H}_2\text{O} \qquad (30)$$

$$(\text{CO}_3^{\bullet-})\text{Cu}^{2+}\text{ZnSOD} \rightarrow \text{inactivation} \qquad (31)$$

Direct structural evidence showing the capture of a (bi)carbonate ion at the active site of human SOD1 has recently been found.[292] In Cu$^+$-SOD1, it acts as an inner-sphere ligand by directly coordinating to the copper, and the Cu$^+$ becomes four-coordinate.[292] In contrast, in Cu^{2+}-SOD1, (bi)carbonate sits ~5 Å away from the copper.[292] The inner-sphere binding of (bi)carbonate in Cu$^+$-SOD1 confirms the presence of a bicarbonate-bound Cu$^+$ species as proposed by Elam et al.,[290] while the outer-sphere binding of (bi)carbonate in Cu^{2+}-SOD1 suggests a diffusible rather than enzyme-bound carbonate radical CO$_3^{\bullet-}$ in eq 30.

Liochev and Fridovich have proposed an alternative mechanism for the bicarbonate-mediated inactivation of SOD1, arguing that Cu$^+$-SOD1 is oxidized by H$_2$O$_2$ to Cu^{2+}-SOD1 bound with a hydroxyl radical (HO$^\bullet$) (eq 28), and that CO$_2$ reacts with HO$^\bullet$ to produce the carbonate radical (CO$_3^{\bullet-}$) that ultimately results in the enzyme inactivation.[293] They provided convincing evidence that CO$_2$ rather than bicarbonate facilitates the peroxidation reaction of SOD1 in the presence of H$_2$O$_2$.[293a] Hence, the mechanism of the bicarbonate-mediated peroxidation by SOD1 remains controversial.

6.4. Maturation Reactions

Activation of SOD1 involves several post-translational modifications, including acetylation of the N-terminus, insertion of copper and zinc ions, intramolecular disulfide formation between Cys57 and Cys146, and dimerization. These different steps are collectively called maturation reactions.

Several studies have shown that uptake of zinc occurs without the need of a chaperone,[266,285a] while the pathway of copper uptake varies from species to species. The incorporation of copper into SOD1 is known to occur via CCS in many organisms, including human and yeast,[270d] presumably through formation of an SOD1–CCS heterodimeric complex.[294] CCS also facilitates the disulfide bond formation in an O_2-dependent manner.[266] In addition to maturation via CCS, human SOD1 acquires copper through a CCS-independent pathway, in which copper is delivered into SOD1 by Cu(I)−GSH complexes and disulfide is oxidized without O_2.[295] *Caenorhabditis elegans* does not express CCS, and its SOD1 is activated solely through the CCS-independent pathway.[279]

Although the activation of *Saccharomyces cerevisiae* SOD1 was originally believed to rely totally on CCS, with strict requirements for copper and O_2,[279,295] it has recently been found that 15−20% of the yeast SOD1, when overexpressed in the absence of CCS, was able to acquire copper in vivo and to rescue the lysine auxotrophy, even in media depleted of copper.[296] Moreover, 30−50% of the disulfide bond of the yeast SOD1 was oxidized without CCS under these conditions.[296]

The molecular mechanism of SOD1 activation in vitro by CCS has largely been revealed. The CCS monomer can be divided into three domains (Figure 31). The N-terminal Domain I has a copper chaperone ATX1-like structure (ATX1: antioxidant 1 copper chaperone) and harbors the MXCXXC copper-binding motif. Domain II is a homologue to SOD1 and is critical for CCS to interact with an SOD1 subunit.[270d] Only a disulfide-reduced SOD1 can interact and form a heterodimer with CCS.[270d] Domain III is a short polypeptide with a conserved CXC motif. In a recent study, the maturation of human SOD1 in vitro via full-length or truncated forms (with one or two domains) of human CCS was studied using NMR and mass spectrometry.[297] The findings confirmed that Domain I of CCS is responsible for copper transfer and that Domain II is critical for the SOD1-CCS interaction (Figure 31). Convincing evidence also exists that Domain III is required for the disulfide bond formation in SOD1 via disulfide transfer through the two conserved cysteines in the CXC motif (Figure 31).[297] Although Domain III is able to bind copper, it should be noted that its affinity for copper is more than 1 order of magnitude weaker than the affinity of Domain I[298] and that Domain III cannot donate copper to SOD1.[297] Earlier studies indicated that CCS is able to activate the disulfide-reduced, apo human SOD1 (E,E-SOD1^{2SH});[266,270d] however, a recent study showed that the Zn-bound form, E,Zn-SOD1^{2SH}, rather than E,E-SOD1^{2SH} rapidly acquired copper from CCS,[297] suggesting that zinc binding could be a necessary step prior to copper incorporation.

The formation of the disulfide bond in SOD1 was monitored in live *Escherichia coli* and human cells using in-cell NMR.[285a,c] Expression of hSOD1 in human HEK293T cells without zinc or copper supplements resulted in two forms of disulfide-reduced SOD1, the apo form (E,E-SOD1^{2SH}) and the Zn-bound form (E,Zn-SOD1^{2SH}).[285a] Zn^{2+} supplemented to growth media was taken up by hSOD1 expressed in *E. coli* and human cells,

leading to the disulfide-reduced, Zn-bound protein (E,Zn-SOD1^{2SH}).[285a,c] Coexpression of human CCS with human SOD1 in zinc-supplemented media resulted in Cu-deficient, Zn-bound SOD1 with ∼50% oxidized disulfide bond, and complete disulfide formation was observed after the cells were incubated with Cu(II).[285a] These findings suggest that the disulfide oxidation of SOD1 by CCS can occur independently of copper insertion.[285a]

6.5. Functional Studies

Studies of the in vivo functions of eukaryotic CuZnSODs have benefited greatly from the development of SOD1-deletion mutant strains particularly in yeast and in mice. Yeast strains lacking CuZnSOD (*sod1Δ*) were first created by deletion-replacement mutations in the *S. cerevisiae* CuZnSOD gene.[267a] Higher levels of oxidative damage to both cytosolic and mitochondrial proteins in the *sod1Δ* strain as compared to those in wild-type yeast provide evidence that CuZnSOD protects yeast from oxidative stress.[299]

Comparison of *sod1Δ* to wild-type strains has also revealed a number of O_2-dependent defects in *sod1Δ* yeast.[300] When grown aerobically, *sod1Δ* yeast is auxotrophic for lysine,[300a] methionine,[300a] and leucine.[300c] The lysine and leucine auxotrophies have been attributed to $O_2^{•−}$-induced inactivation of the iron−sulfur cluster enzymes involved in their biosynthetic pathways.[300c] The defect of methionine biosynthesis appears to be due to depletion of NADPH by oxidative stress, as NADPH is critical for the function of two enzymes in the methionine biosynthesis pathway.[300f] The *sod1Δ* phenotypes also include impaired growth in air or 100% O_2,[300d] increased intracellular iron,[300b,d] vacuolar fragmentation,[300d] poor stationary-phase survival,[300d,301] increased O_2 consumption and respiration,[300e,302] lack of growth on ethanol,[301] sensitivity to high levels of zinc,[300d] and sensitivity to high pH, salt, and temperature.[300d,303] Moreover, two recent studies demonstrated disrupted glucose repression in *sod1Δ* yeast.[300e,302]

The effects of CuZnSOD deficiency in invertebrates vary from species to species. CuZnSOD-null *Drosophila* show a severe phenotype, that is, infertility and 80% reduction in lifespan.[304] *C. elegans* shows a very different behavior when SOD genes are inactivated. In *C. elegans*, there are five distinct genes that encode SODs, in which *sod-1* and *sod-5* code for the cytosolic CuZnSOD. Inactivation of one or more of these genes results in enhanced evidence of oxidative stress, but lifespan was unaffected.[305] A recent study by van Raamsdonk and Hekimi showed that the deletion of all five SOD genes in *C. elegans* increased levels of oxidative damage but again had minimal effect on lifespan.[306] These results challenge the oxidative stress theory of aging, at least in the *C. elegans* model system.

Early studies of CuZnSOD-null mice showed that they had normal development and survival,[226] in sharp contrast to MnSOD-null mice, which have severely pathogenic phenotypes.[224,225] However, more recent studies found a ∼30% decrease in the lifespan of the *sod1−/−* mice but not in that of the *sod1+/−* mice.[307] The reduction in the lifespan of the *sod1−/−* mice has been ascribed to a higher incidence of hepatocellular carcinoma.[307b]

The deletion of CuZnSOD gene in mice leads to many different phenotypes resembling aging, and CuZnSOD-knockout mice are therefore often considered as accelerated-aging models. For example, female mice lacking CuZnSOD have defects in ovarian function, leading to infertility.[308] Although
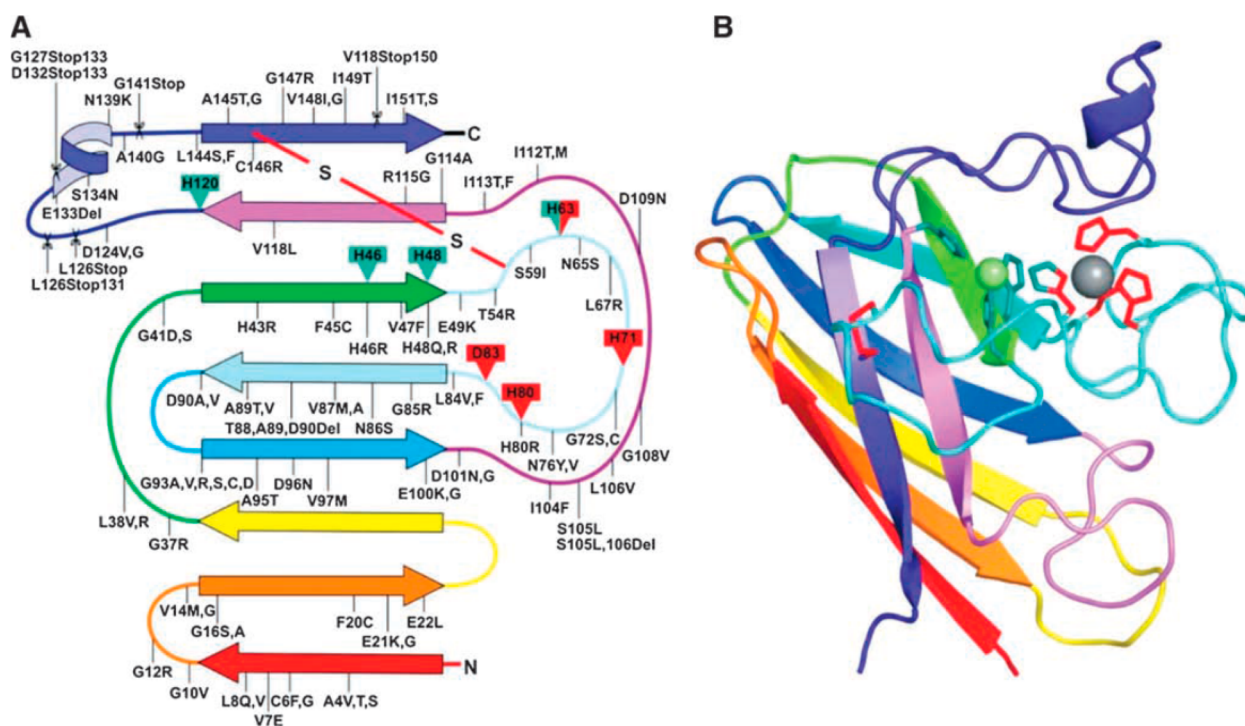
Figure 32. Secondary structure representation of SOD1 showing the locations of FALS-linked mutations (left) and a monomer of SOD1 (right) colored to match the drawing on the left (reproduced from ref 53). Copper ligands are shown in green and zinc ligands are shown in red. Copper and zinc ions are shown as green and gray spheres, respectively, and the intrasubunit disulfide bond is shown in red. Point mutation, deletions, and insertions are indicated with a line, whereas mutations that cause C-terminal truncations are shown as scissor cuts at the point of the stop codon.

CuZnSOD is not required for motor neuron development and function,[226] the motor neurons of the *sod1*−/− mice have been reported to display mitochondrial dysfunction and axonal degeneration, leading to accelerated age-related muscle atrophy.[309] CuZnSOD-null mice also develop hearing loss[310] and several eye diseases, such as age-related macular degeneration (AMD)[311] and cataract,[312] at earlier ages as compared to the wild-type mice.

In the case of bacteria, CuZnSOD is low in abundance relative to manganese- and iron-containing SODs, but it is induced under aerobic conditions.[52] It is therefore surprising that no phenotypes have been identified in CuZnSOD deletion mutants, even during aerobic growth.[313] The periplasmic localization of prokaryotic CuZnSOD suggests that this enzyme may play a role in defending bacteria against oxidative stress, and the enzyme has been proposed to protect pathogenic bacteria from the oxidative burst of mammalian macrophages by limiting the formation of a more destructive ROS, peroxynitrite, from superoxide and nitric oxide.[314] Early studies showed that CuZnSOD-deficient bacterial mutants were significantly more sensitive to extracellular superoxide generated by the xanthine/xanthine oxidase system.[313b,314,315] In another study, however, the presence of catalase, rather than purified CuZnSOD, was able to protect bacterial cells fully against the xanthine/xanthine oxidase system,[313a] suggesting that the detrimental effects come from hydrogen peroxide rather than superoxide. The CuZnSOD-deficient mutants were indeed more sensitive to higher levels of extracellular H_2O_2 as compared to the wild types,[313a] possibly suggesting that superoxide generated in the periplasm, if not removed by CuZnSOD, exacerbates oxidative damage caused by H_2O_2.

6.6. ALS Mutant Human CuZnSODs

6.6.1. Aggregation and SOD1-Linked ALS. ALS is a fatal neurodegenerative disease characterized by progressive death of motor neurons, leading to paralysis and eventually to patient death. The majority of ALS cases are sporadic (SALS), that is, of unknown cause, while a small subset of ALS cases is inherited or familial (FALS). Of all FALS cases, 10−15% are associated with mutation in the SOD1 gene. SOD1-linked FALS remains the most thoroughly studied form of inherited ALS.

As of 2013, more than 160 ALS-causing mutations, scattering throughout the 153-residue polypeptide, have been identified in the SOD1 gene (Figure 32). They are predominantly missense mutations with a few insertions, deletions, and C-terminus truncations.[53,316] The mutations are classified into two groups according to their locations, the metal-binding-region (MBR) mutations, and the wild-type-like (WTL) mutations.[317] MBR mutations locate at metal-binding residues or at the electrostatic loop. WTL mutations locate at positions remote from metal-binding sites.

FALS-linked SOD1 variants cause motor neuron loss by a gain of toxicity rather than a loss of SOD activity,[53,282,318] which has been supported by several lines of evidence. SOD1-deficient mice do not develop motor neuron degeneration;[226] in contrast, mice expressing FALS SOD1 variants develop ALS-like symptoms, even though they express normal levels of endogenous murine SOD1.[319] Moreover, many FALS variants possess normal enzymatic activity, and there is no correlation between levels of SOD activity and disease severity.[320]

Extracellular amyloid fibrils or intracellular inclusions with amyloid-like characteristics are found in many neurodegenerative diseases associated with peptide or protein aggregation.[321] Becuse SOD1-positive intracellular inclusions were found in

ALS patients and transgenic mice (Figure 33), aggregation of SOD1 protein is widely believed to underlie the disease
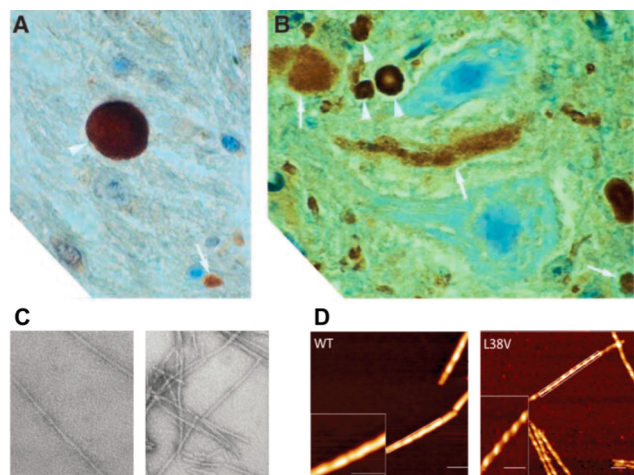

Figure 33. Aggregated forms of SOD1 found in vivo (A and B) and in vitro (C and D). (A) An SOD1-containing inclusion from the spinal cord of a FALS patient expressing a C-terminal truncated mutant SOD1, L126stop (reprinted with permission from ref 419). (B) SOD1-containing inclusions (arrowheads) from the spinal cord of transgenic mice expressing G85R hSOD1 (reprinted with permission from ref 419). The tissue was stained with an antibody recognizing both mouse and human SOD1. (C) Electron micrographs of SOD1 fibrils generated in the presence of 1 M GdHCl (left) and 5 mM DTT (right) (scale: 1 cm = 200 nm) (adapted from ref 328b). (D) AFM images of WT (left) and L38V (right) fibrils (scale: 1 cm = 100 nm) (adapted from ref 329). Insets show the magnified helical twist of the fibrils.

etiology.[53,270b,d,282,318,322] In addition, the results of several recent studies suggest that aggregated SOD1 is able to transmit from cell to cell in a fashion resembling prion proteins.[323] Misfolding and aggregation of SOD1 in ALS has been reviewed thoroughly elsewhere.[53,270b,c,282,318a,322c,324]

Unlike many other aggregative peptides and proteins (amyloid β, prion protein, α-synuclein, tau, and huntingtin protein) that are natively unfolded, mature, dimeric holo-SOD1 (Cu,Zn-SOD1^{S-S}) is very stable; therefore, the nascent, immature SOD1, lacking one or more of the post-translational modifications, is proposed to be responsible for aggregation of the protein in SOD1-linked FALS cases. Indeed, disulfide-reduced SOD1 was found to accumulate in transgenic mice expressing hWT and FALS mutant SOD1.[325] Spinal cords from ALS-transgenic mice and a SOD1-linked FALS patient were stained positively with antibodies that recognize exposed dimer interface.[326]

Upon removal of metal cofactors and/or of the intracellular disulfide, hWT SOD1 and FALS mutants aggregate in vitro either without[327] or with[328] mechanical agitation, with time courses similar to those determined for other amyloid peptides and proteins. The formation of amyloid fibrils of WT and FALS mutant SOD1s in vitro was confirmed using electron microscopy (EM) and atomic force microscopy (AFM) (Figure 33). AFM images of SOD1 amyloid fibrils showed the "bead-like" morphology due to periodic twists on the fibrils. The twist distance differs substantially between hWT and some FALS mutant fibrils.[329] The protease resistant pellets recovered from partial proteolytic digestion of WT and FALS mutant SOD1 fibrils contained predominantly the N-terminal region (1−63)

of SOD1, suggesting that the mechanisms of fibril formation were similar for WT and mutant SOD1 proteins and resulted in burial of the N-terminal regions of the SOD1 protein in the core of the amyloid fibril.[329]

6.6.2. Structure. Structures of WTL ALS mutant SOD1 proteins tend to resemble that of the WT enzyme except for local structural differences at the sites of mutation, while MBR SOD1 structures show a wider range of structural variations. Atomic-resolution structures have been determined for the WTL variants, Ala4Val,[276b,330] Gly37Arg,[331] His43Arg,[332] Thr54Arg,[333] Gly93Ala,[330] and Ile113Thr.[276b,333] In the MBR class, structures have been published for His46Arg,[334] Gly85Arg,[335] His80Arg,[336] Asp124Val,[336] Asp125His,[290] Ser146Asn,[334] and His46Arg/His48Gln (a combination of two MBR mutations).[337]

The zinc and electrostatic loops are frequently observed to be disordered in FALS SOD1 variants, as suggested by the breaks in the loop elements in their electron density maps.[330,334,337,338] As a result of the disorder in the loop elements, the edges of β-strands 5 and 6 become deprotected, leading to nonnative hydrogen-bonding and apolar interactions between SOD1 dimers, and self-assembly of β-barrels into high-order filamentous arrays.[334] Three different filamentous arrays have been observed (Figure 34): (1) linear amyloid-like filaments, (2) zigzag filaments, and (3) water-filled nanotubes. Both linear amyloid-like and zigzag filaments arise through the stacking of SOD1 β-barrels along a direction perpendicular to the dimer interface, while water-filled nanotubes are helical filaments consisting of four SOD1 dimers per turn and an inner water-filled cavity.[334] The crystallographic observation of high-order filamentous structures of ALS mutant SOD1 proteins may be related to the mechanism of formation of abnormal protein aggregates in ALS patients and disease models.[319,339]

FALS variants of SOD1 are generally more prone to unfolding than hWT. In global hydrogen−deuterium exchange (HDX) analysis, hWT apo-SOD1 (E,E-SOD1^{S-S}) became fully deuterated only when its melting temperature (52 °C) was reached, while the fully exchanged forms of Ala4Val and His48Gln apoproteins appeared at much lower temperatures, 36 and 42 °C, respectively.[340] Moreover, the third and fourth β strands, $\beta3$ and $\beta4$, of Ala4Val and Gly93Arg apoproteins are considerably less protected from HDX (Figure 35).[340,341] Because SOD1 amyloid fibrils have extensive β-sheet structure in a parallel arrangement (Figure 35B),[321] the results of the simulation and HDX analysis described above suggest the possibility of the unfolding and displacement of some β-strands initiating amyloidogenesis and subsequent aggregation of SOD1.

The holo enzymes of Gly93Ala[342] and Ser134Asn[343] variants exhibit a different mobility in solution relative to hWT, as revealed by NMR analysis. In contrast to hWT monomers, which are mostly folded at neutral pH and 37 °C,[344] many FALS mutations lead to substantial increases in the fraction of unfolded monomers,[276a,344] due to the destabilization of the monomer structure or the dimer interface or both.[276a] SOD1 apoproteins undergo a conformational change between the folded state and a short-lived excited state, the latter characterized by transient structural distortion revealed by nuclear spin relaxation dispersion experiments.[345] As compared to hWT SOD1, the population of the excited state is increased in three WTL-variants, Ala4Val, Asp90Ala, Gly93Ala, and one MBR-variant Gly85Arg.[345] Relative to hWT SOD1, the unfolding of FALS mutants (Ala4Val, Gly37Arg, Gly85Arg,
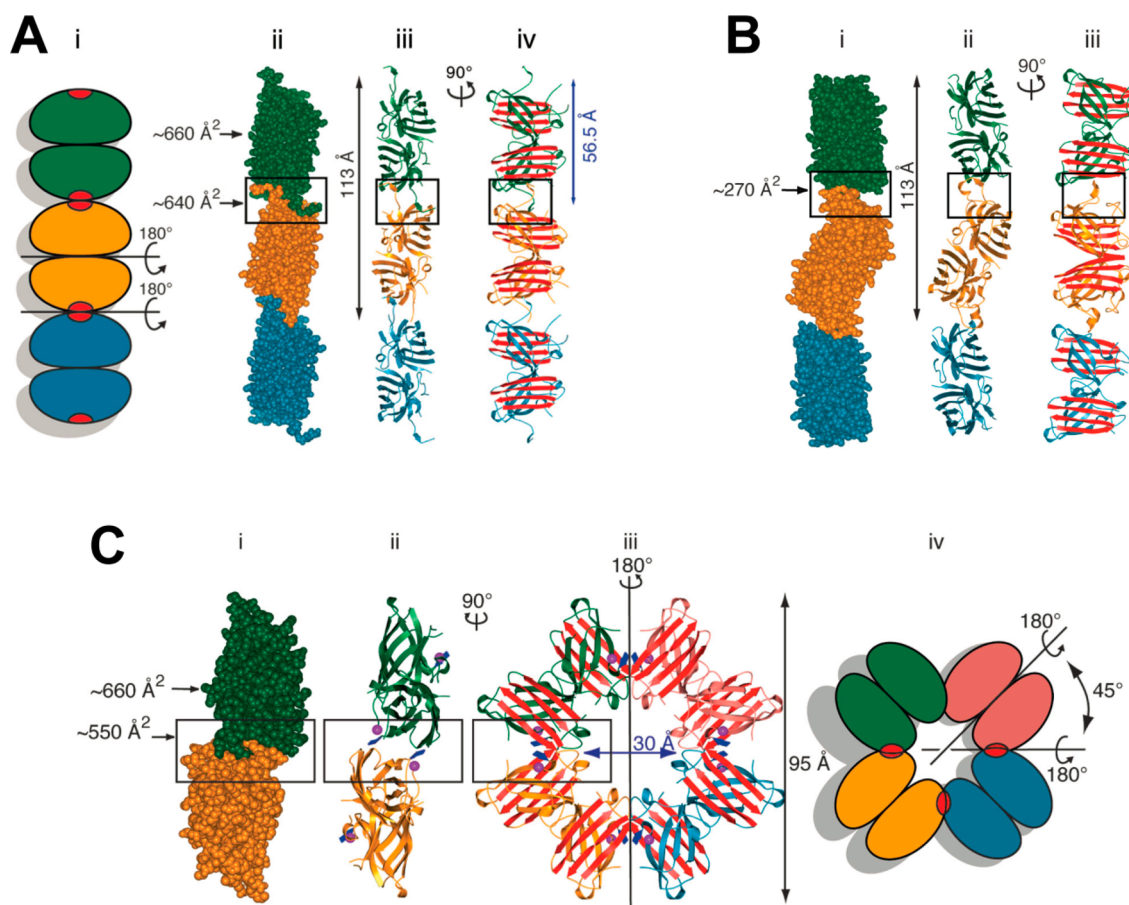
Figure 34. High-order filamentous assemblies formed by SOD1 mutant proteins (reprinted with permission from ref 334; this figure was modified from Figures 2–4 in the original paper). (A) Orthogonal views of the linear, amyloid-like filaments formed by S134N and apo H46R, represented by three dimers shown from top to bottom in green, gold, and blue, respectively. A schematic diagram of the tubular filament is shown in (i). Image (iv) is related to (ii) and (iii) by a rotation of 90°. (B) Orthogonal views of the zigzag filaments formed by apo H46R, represented by three SOD1 dimers in the same orientation as in (A). Image (iii) is related to (i) and (ii) by a rotation of 90°. (C) Orthogonal views of the water-filled helical filaments formed by Zn-H46R. One-half of the helical Zn-H46R filament, shown in (i) and (ii), is represented by the two dimers shown from top to bottom in green and gold. Image (ii) is related to the left half of (iii) by a rotation of 90°.

Gly93Ala, and Ile113Thr) in GuHCl undergoes a different pathway, populating higher fractions of Zn-loaded, Cu-deficient intermediates.[346] The higher propensity of FALS mutants to unfolding as well as the different unfolding pathway may be involved in aggregation and pathogenesis of these mutants in ALS.

Many FALS mutations are known to shift the monomer–dimer equilibrium of SOD1 toward monomer either by disrupting the dimer interface or by diminishing the protein's ability to bind metals and contain a disulfide bond. Lindberg et al.[276a] determined the monomer–dimer equilibrium of 15 FALS variants by size-exclusion chromatography and thermodynamic analysis. Most WTL variants tested in this study were found to possess a weakened dimer interface as compared to hWT.[276a]

FALS mutations have been known to increase the susceptibility of SOD1 to disulfide reduction. Several WTL variants were found to be more prone to disulfide breakage under reducing conditions than hWT, albeit containing similar amounts of copper and zinc as hWT protein.[347] MBR and metal-deficient WTL variants were found to contain a more labile disulfide bond than hWT,[347] due to the lack of stabilizing effects from metal binding.

A study by Bouldin et al.[280] explored the kinetics of disulfide reduction and found that Ala4Val and Gly93Ala were reduced at a faster rate than hWT, suggesting that the disulfide bond is kinetically more susceptible to reduction in FALS mutants than in hWT. Nevertheless, FALS mutations do not necessarily thermodynamically destabilize the disulfide bond. The disulfide reduction potential determined for the apo forms of hWT, Ala4Val, and Gly93Ala hSOD1 is −301, −282, and −315 mV, respectively,[280] suggesting the order of disulfide stability scales as Gly93Ala > hWT > Ala4Val.

Contrary to an early study showing that the destabilization of the apo state is a common feature to all FALS variants,[348] a later study by Rodriguez et al.[349] showed that the apoproteins of several MBR variants have equal or higher thermal stability than apo hWT. Although most apo WTL variants are destabilized relative to apo hWT,[349] the DSC profiles of three apo WTL variants, Asp101Asn, Glu100Lys, and Asn139Lys, are nearly identical to that of apo hWT. While the E,E-SOD1^{S-S} form of all FALS mutants melts above 37 °C,[349] the E,E-SOD1^{2SH} form of many mutants melts at or below 37 °C.[349,350] Furthermore, the destabilization caused by FALS mutations is more significant in the E,E-SOD1^{2SH} state; for example, the melting temperature of E,E-SOD1^{S-S} Gly37Arg is shifted lower by 10 °C relative to hWT, while in
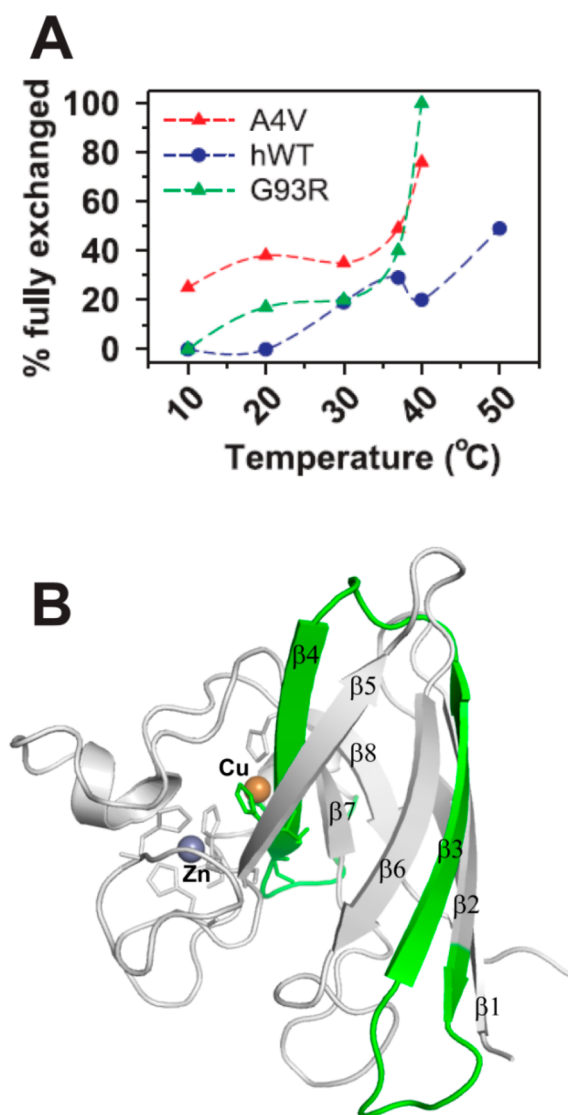
Figure 35. $\beta 3$ and $\beta 4$ strands (belonging to peptide 21−53) of apo mutant SOD1s are substantially more unfolded at physiological temperatures than those of apo hWT. (A) Profiles of the fractions of fully exchanged peptide 21−53 are shown as a function of temperature for the hWT, A4V, and G93R SOD1 proteins (reprinted with permission from ref 340). In this plot, the percentages of fully exchanged peptides are determined by the fractional area under the deconvoluted m/z curves in the mass spectra. (B) Structure of a monomer of hWT SOD1 (PDB code: 1PU0) with peptide 21−53 highlighted in green. This figure was generated using the PyMOL Molecular Graphics System.[396]

the E,E-SOD1^{2SH} state it is lowered by 15 °C.[350a] The reduced thermal stability may be related to the increased misfolding/aggregation propensity of E,E-SOD1^{2SH} FALS mutants.

6.6.3. Does WT SOD1 Play a Role in Sporadic ALS? Because similar histopathology and symptoms are observed in patients with either familial or sporadic ALS, it is reasonable to speculate that hWT SOD1 might play an analogous role in causing SALS. In support of this hypothesis, misfolded hWT SOD1 has been detected in SALS spinal cord tissues using several conformational antibodies raised against FALS mutants.[318a,351] In addition, hWT SOD1 isolated from spinal cords of SALS patients inhibited fast axonal transport (FAT) in squid axoplasm in a manner similar to FALS mutants,[352] and

knockdown of hWT SOD1 in astrocytes isolated from SALS patients ameliorated their toxicity to cultured motor neurons.[353] hWT SOD1, as a vaccine, was as effective as Gly93Ala SOD1 in rescuing neurodegeneration of low-copy Gly93Ala transgenic mice.[354] A particularly important result in support of this hypothesis is the discovery by Marklund and co-workers that mice expressing hWT SOD1 at a level close to that of high-copy Gly93Ala mice developed ALS-like symptoms and histopathology.[355]

In cell-free systems, hWT SOD1 has been observed to form amyloid fibrils as readily as FALS mutants,[328b] and the fibrils generated from hWT and mutant proteins share the same protease-protected region.[329] In a recent study, Ivanova et al. identified two segments, [101]DSVISLS[107] and [147]GVIGIAQ[153], from hWT SOD1 that have a high propensity for amyloid fibril formation.[356] Furthermore, uptake of aggregated hWT SOD1 induced the aggregation of endogenous SOD1 in neuronal cells.[351]

Misfolded hWT SOD1 generated from oxidation has been implicated in SALS. When oxidized in vitro, hWT SOD1 became aggregative like FALS mutants[352,357] and was recognized by conformational antibodies raised against FALS variants,[351] suggesting that oxidized hWT acquires an aberrant conformational epitope like the mutants. Higher levels of oxidized SOD1 were recently found in the lymphoblast cells derived from a subset of SALS patients as compared to those derived from FALS patients and healthy controls, and this oxidized SOD1 was able to form intracellular inclusions.[358] Furthermore, oxidized SOD1 exerts mutant-like toxic effects to cells through aberrant interactions with Hsc70,[357a] Bcl-2,[357a,358] and chromagranin B[357a,359] (reviewed in ref 351). However, the existing data cannot exclude the possibility that oxidation of SOD1 is a consequence rather than a cause of neurodegeneration in ALS.[351,360]

Although each of the studies described above supports the existence of a common SOD1-linked pathway in FALS and SALS, the hypothesis that hWT SOD1 plays a role in SALS remains controversial, and further study will be required to answer this question.

7. SUPEROXIDE REDUCTASES

7.1. History and Properties

Superoxide reductases are the most recently discovered of the enzymes known to detoxify $O_2^{\bullet-}$. As the name indicates, and in contrast with the SODs, which catalyze both the reduction and the oxidation of the superoxide anion, the reductases essentially catalyze only the reductive process (eq 32):

$$O_2^{\bullet-} + 2H^+ + SORred^X \rightarrow SORox^{X+1} + H_2O_2 \qquad (32)$$
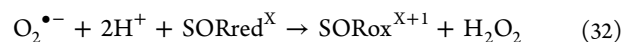
with the concomitant formation of one H_2O_2 molecule per $O_2^{\bullet-}$ consumed. This reaction is suicidal, in the sense that the enzyme has to be reactivated by rereduction, forcing the existence of at least one physiological partner, its reductant. Again, this is in contrast with the SODs, which act to stand alone, oscillating between two redox states by reacting sequentially with two molecules of substrate (Figure 36).

The first examples of these enzymes were isolated from sulfate reducing bacteria of the *Desulfovibrio* (*D.*) genus: desulfoferrodoxin (Dfx) from *D. vulgaris* Hildenborough and from *D. desulfuricans* ATCC 27774, in 1990,[361] and later neelaredoxin (Nlr) from *D. gigas*, in 1994.[362] These trivial names were given in the absence of a known function at the

- Superoxide dismutase

$O_2^{\bullet-}$ / O_2 → SOD → $O_2^{\bullet-}$ / H_2O_2 Metal = (Mn, Fe, Cu-Zn, Ni)

- Superoxide reductase
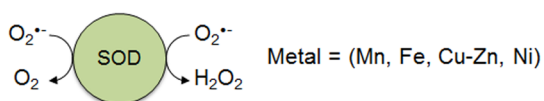
NADH / NAD$^+$ → SOR electron donor → SOR → $O_2^{\bullet-}$ / H_2O_2 Metal = Fe

Figure 36. Comparison of enzymatic activities of SODs and SORs.

time of their isolation. EPR, visible, resonance Raman, and Mössbauer spectroscopies revealed that as-isolated desulfoferrodoxin contained a desulforedoxin-like center (named center I) in the oxidized form and an Fe^{2+} ion bound mainly to nonsulfur ligands (named center II). Therefore, its name originated from the contraction of "desulforedoxin" and "ferrous" plus the suffix "redoxin" (from redox active proteins).[363] Desulforedoxin is a small protein of 3 kDa, having an Fe ion in a tetrahedrally distorted geometry, similar to those of rubredoxins.[364] The trivial name for neelaredoxin derived from the Sanskrit word for its color; that is, it is a blue protein in the oxidized form, having a single Fe ion (it is the only known blue iron protein).[362] Because of the spectroscopic and amino acid sequence data available by the time of their discovery, it was recognized ear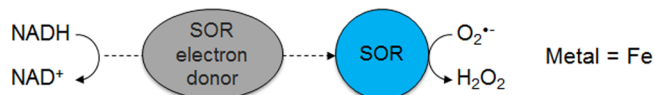ly that the two proteins were related to each other and to the gene product of the *rbo* gene previously sequenced from *D. vulgaris* Hildenborough; *rbo* stands for rubredoxin:oxidoreductase, another label given at that time due to the fact that *rbo* is part of a dicistronic unit encoding also for a rubredoxin, the simple Fe protein having an FeCys$_4$ center.[365] It is now known that rubredoxins are indeed the electrons donors for some SORs, but the genomic organizations may be quite diverse. The multitude of trivial names for these enzymes led to a large number of misannotations in the public databases.

In 1996, the group of D. Touati[366] attempted to find genes encoding SODs in the anaerobic sulfate-reducing bacterium *Desulfoarculus baarsii* by complementation studies of an *E. coli* strain in which the genes for the Fe- and Mn-SODs were deleted. At that time, it was still controversial if the absence of SODs would be a distinctive marker for anaerobic organisms. These experiments led to the finding of a gene whose product (a desulfoferrodoxin) rescued the phenotype of this *E. coli* deletion strain. This was a landmark discovery in the field of the SOR proteins, associating them for the first time to ROS detoxification. Later, other SORs were also shown to complement the same *E. coli* deletion strain.[367] Moreover, the expression of only the N-terminal domain, containing the desulforedoxin center, did not complement the *E. coli* sod⁻ mutant, providing the first hint that center II would be responsible for the catalytic activity. However, the same authors reported that Dfx from *D. baarsii* had no SOD activity, while it was subsequently reported that the proteins from *D. gigas*, *D. desulfuricans*, and also neelaredoxin from *Archaeoglobus fulgidus* indeed had SOD activity,[368] but orders of magnitude lower than those of SODs. Liochev and Fridovich proposed for the first time that these proteins could act as SORs, leading to elimination of $O_2^{\bullet-}$ and formation of H_2O_2.[369] This was finally shown to be the case by the experiments with the neelaredoxin

from *Pyrococcus (P.) furiosus* and desulfoferrodoxin from *D. baarsii*[370] and, subsequently, using pulse radiolysis measurements, for the *A. fulgidus* and *D. vulgaris* enzymes.[368c,371] Thereafter, pulse radiolysis has been of paramount importance in disentangling the molecular mechanism of SORs.[367b,372]

In part due to the difficult genetic manipulation of many Archaea and many anaerobes, few in vivo studies are available. A *D. vulgaris* mutant strain with increased resistance to O_2 was found to have *dfx* transcriptional levels higher than those of the wild-type strain;[373] in agreement with those results, a *D. vulgaris* *dfx* deletion mutant had a higher sensitivity to oxygen.[373] Up-regulation of the transcriptional level of SORs encoding genes was also observed in *Clostridium acetobutylicum*,[374] in *Thermotoga maritima*,[375] and in *Treponema denticola*[376] upon O_2 stress. In contrast, these levels apparently do not change in *D. vulgaris* and *P. furiosus*, under oxidative stress, which may indicate a constitutive expression of the SOR genes in several organisms.[377]

The SORs are examples of what has been called a "novel paradigm" for ROS detoxification: the reductive pathways mentioned in section 2.2.[378] In fact, the proteins of the rubrerythrin family are proposed to detoxify H_2O_2 by directly reducing it to water (substituting for catalases),[367c,378b,379] while the flavodiiron enzymes detoxify O_2 by directly reducing it to water.[36] Both of these families of enzymes have diiron centers of the histidine/carboxylate types, but in totally different protein scaffolds. Another recurrent theme in these $O_2^{\bullet-}$ and ROS-detoxifying proteins is the presence of additional electron-transfer domains, apart from the catalytic modules, which in some cases are thought to act as the electron entry point of the enzymes, rubredoxin-, desulforedoxin-, flavodoxin-, and flavin reductase-like domains, among others.

7.2. Occurrence, Amino Acid Sequences, and Classification

SORs were initially isolated from anaerobic Bacteria and Archaea, but it is now clear that these enzymes are present in all three domains of life, that is, also in Eukarya, and in anaerobes as well as in aerobes. While some organisms lack any of the SODs and thus appear to rely solely on SORs to defend themselves against superoxide, others contain in their genomes genes coding for enzymes of the two families, with one or more types of SORs and SODs. This apparent redundancy adds to an increased robustness of the organisms when dealing with $O_2^{\bullet-}$, paralleling what results from the multiplicity of SODs in a single organism, and has been observed in many other instances of different biological processes (e.g., with regards to O_2, the simultaneous presence of multiple respiratory oxygen reductases, of the heme-copper or cytochrome *bd* types in many Bacteria and Archaea).

It is difficult at present to have a comprehensive picture of the evolution of SORs. Studies performed recently have shown that the amino acid sequences of SORs cluster mainly according to the type of SOR, and not according to organism phylogeny, suggesting that multiple events of lateral gene transfer must have occurred throughout evolution.[58b,380] It is also impossible to predict which SOR protein could have been the common ancestor and whether they existed prior to the Great Oxidation Event (see section 2). SORs are examples of evolutionary diversity in nature, rather than being a specific type of enzyme designed for protection of particular anaerobes.

7.2.1. SOR Classifications. SORs are small enzymes, with about 110−180 amino acids in their sequences. SORs have been classified in several different ways. The major distinctive
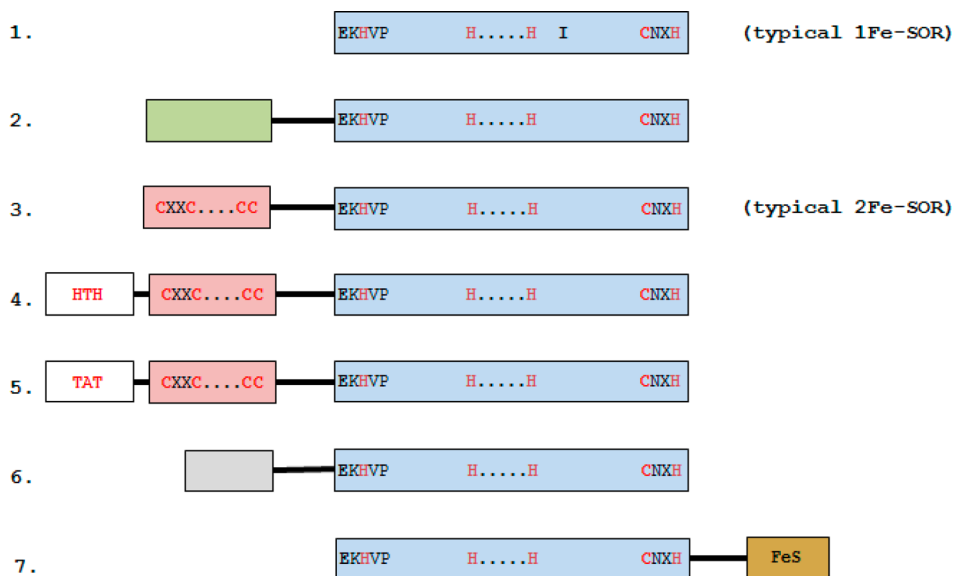
Figure 37. Different domain structures found for proteins containing a SOR catalytic domain (as in SORGOdb). These proteins are variations of the typical 1Fe- and 2Fe-SORs, and should not be viewed as individual catalytic classes. The domains and residues are colored as: blue, catalytic domain; pink, desulforedoxin-like domain; green, Dx like-domain, lacking the Fe center; brown, FeS domain in methanoferrodoxins; light gray, variable domain (HTH, helix−turn−helix domain; TAT, putative twin arginine signal peptide); red, metal ligands; black, highly conserved residues.

feature of these enzymes was, until quite recently, the presence of only one (in neelaredoxins) or of two (in desulfoferrodoxins) Fe atoms per polypeptide chain. Therefore, the simplest classification, and the most relevant in terms of mechanism, is to group them as 1Fe-SORs (the neelaredoxins) and 2Fe-SORs (the desulfoferrodoxins).[378b,380] This classification is adopted in this Review. The amino acid sequence of the 1Fe-SORs is homologous to the second domain of the 2Fe-SORs and constitutes the catalytic domain; the N-terminal domain of the 2Fe-SORs (see section 7.2.2) is homologous to desulforedoxins. The recent discovery of a SOR from some methanogens, named methanoferrodoxin, which has a domain harboring a $[4Fe-4S]^{2+/1+}$ cluster, may lead to an extension of this classification in the near future.[381] (It should be noted that this name is misleading because the suffix ferrodoxin was first used for the 2Fe-SORs (desulfoferrodoxins).)

A second classification took into consideration the primary and tertiary structures of SORs;[382] some enzymes contain only one Fe ion, but have a longer N-terminus with amino acid sequence and structural similarities with those of the respective domain of desulfoferrodoxins, but lacking the cysteine ligands to the desulforedoxin-like center. According to the authors, SORs would fall into three classes: Classes I (Dfxs), II (neelaredoxins), and III (neelaredoxins structurally homologous to desulfoferrodoxins, with only one Fe center). In dendograms constructed from available amino acid sequences, Class III enzymes cluster within the Class I enzymes; it is plausible that Class III SORs evolved from Class I proteins by loss of the cysteine residues binding the desulforedoxin-like center, an event that may have occurred more than once because the Dfxs are not monophyletic. Again, this classification misses the new family of methanoferrodoxins.

A much more detailed classification was proposed by Lucchetti-Miganeh and co-workers,[58b] based on the variability of N-terminal domains, and a carefully annotated SOR database was created and called SORGOdb (http://sorgo.genouest.org/) (Figure 37). The authors of this study classified SORs into seven classes. Class I or Dx-SOR includes the 2Fe-SORs, where

the N-terminal is a desulforedoxin-like (Dx) domain. Class II includes the 1Fe-SORs that have no extra N-terminal domain. Class III SORs are analogous to Dx-SORs but lacking some or all of the Fe cysteine ligands (FeCys$_4$) for the desulforedoxin-like Fe center and therefore lacking the FeCy$_4$ site (previously designated by others as Class III, where the *T. pallidum* SOR is the enzyme representing this class). Class IV includes SORs with an extra C-terminal domain containing an iron−sulfur center, as in the methanoferrodoxin from *Methanosarcina mazei*. The fifth class, termed HTH-Dx-SOR, includes Dx-SORs (2Fe-SOR) with an extended N-terminal helix−turn−helix (HTH) domain present in transcription regulators. The sixth class, termed TAT-SOR, includes SORs from only a few organisms, such as *Desulfuromonas acetoxidans* DSM 684 and *Geobacter sulfurreducens*, and the sequences are preceded by a putative twin-arginine signal peptide that suggests their periplasmic localization. This is in contrast to what is generally believed for the remaining SORs, on the basis of the lack of recognizable translocation signals. The seventh class, termed "atypical" SORs, includes SORs with a variety of N-terminal domains that range from a metallo-β-lactamase-like (as in the flavodiiron oxygen/NO reductases) to a NAD(P)H-FMN reductase-like domain. None of these has so far been isolated, and their existence awaits experimental validation.

The large majority of known SORs are those from Classes I and II, that is, the canonical 2Fe- or 1Fe-SORs (about 30% each), while the remaining classes together represent about a third of the so far identified SORs. With the exception of the Class IV (methanoferrodoxins) and the "atypical SORs", they all appear to contain one or two iron centers (the catalytic center plus the Dx/Rb-like center). This exhaustive analysis opens new perspectives on these ROS-detoxifying enzymes, the possibility of having a single multidomain enzyme that carries out multiple functions, for example, reduction of superoxide by the SOR domain and reduction of O$_2$ by the metallo-β lactamase-like domain.

All SORs so far isolated contain only Fe ions; however, to have an Fe-loaded recombinant enzyme, extra Fe must be

Table 6. SORs Catalytic Center Ligands and "Key" Amino Acid Residues

	"key residues"		catalytic Fe ligands − center II					
	Glu	Lys	His	His	His	Cys	His	site-directed mutants
1Fe-SOR								
P. furiosus	E14	K15	H16	H41	H47	C111	H114	
P. horikoshi	E23	K24	H25	H50	H56	C111	H114	
D. gigas	E15	K16	H17	H45	H51	C115	H118	
A. fulgidus	E12	K13	H14	H40	H46	C110	H113	Glu12Val, Glu12Gln[372b]
T. maritima	E15	K16	H17	H45	H51	C115	H118	
T. pallidum	E48	K40	H50	H70	H76	C119	H122	Glu48Ala[372i]
N. equitans		K9	H10	H35	H41	C97	H100	
I. hospitalis	E23		H25	H50	H56	C109	H112	Glu23Ala, Thr24Lys[383]
2Fe-SOR								
D. vulgaris	E47	K48	H49	H69	H74	C115	H118	Glu47Ala, Glu48Ala[372c]
D. desulfuricans	E47	K48	H49	H69	H74	C115	H118	
D. baarsii	E47	K48	H49	H69	H74	C115	H118	Glu47Ala, Lys48Ile[372d,g]
A. fulgidus	E47	K48	H49	H69	H74	C115	H118	

Table 7. Available SORs X-ray Crystallographic Structures

type	organism	protein	PDB	resolution (Å)	oligomerization	center oxidation State	ref
1Fe-SOR	*Pyrococcus furiosus* (Archaea)	WT	1DO6	2.0	tetrameric	1/2 oxidized, 1/2 reduced	71b
			1DQI	1.7		oxidized	
				2.0		reduced	
	Pyrococcus horikoshii Ot3 (Archaea)	WT	2HVB	2.5	tetrameric	oxidized	structural genomics
	Thermotoga maritima (Bacteria)	WT	2AMU	2.0	tetrameric	reduced[a]	structural genomics
			3QZB	1.1	tetrameric		
	Treponema pallidum (Bacteria)	WT	1Y07	1.55	dimeric	reduced[b]	71c
2Fe-SOR	*Desulfovibrio desulfuricans* (Bacteria)	WT	1DFX	1.9	dimeric	reduced[c]	71a
	Desulfoarculus baarsii (Bacteria)	Glu47Ala	1VZI	1.15	dimeric	reduced	390
		Glu46Ala	1VZG	1.69		oxidized, ferrocyanide-bound	
		Glu46Ala	1VZH	1.69		oxidized, ferrocyanide-bound	
		WT	2JI1	1.7	dimeric	reduced[c]	370c
		Glu114Ala	2JI2	1.7		reduced, NO₃-bound	
		Glu114Ala	2JI3	1.95		oxidized, (hydro)peroxo-bound	

[a]The center has the glutamate-residue unbound and thus is considered to be in the reduced form. [b]Some of the residues in the loop containing the motif -EKHVP were not modeled. [c]Assuming reduced state from [Fe(His)$_4$Cys] conformation.

supplied to the common *E. coli* growth media, otherwise the proteins become loaded with Zn^{2+} and are inactive. To date, however, we have no knowledge of the metalation process for the SORs or of their relative affinities for Fe and Zn. This lack of knowledge about in vivo metalation pathways is not unique to these enzymes and is, in fact, quite common for other mononuclear Fe enzymes, as well as for diiron-containing proteins.

For the purpose of this Review, and in the absence of enough data for the less usual SORs, we focus only on the 1Fe- and 2Fe-SORs, a quite convenient classification to highlight the properties known for these enzymes.

7.2.2. Amino Acid Sequences: Metal Ligands. Analysis of the amino acid sequences retrieved from the public databases, from both complete and incomplete genomes, shows the striking characteristic that very few amino acid residues are strictly conserved (Figure 37, Table 6).[380] These are (i) the ligands to the metal centers, four histidines, and a cysteine for the catalytic site, all in the catalytic domain; (ii) the four cysteines in the 2Fe-SORs, at the N-terminal segment; and (iii) a proline at the characteristic motif −(E)(K)HxP−, where the histidine is a ligand to the Fe, and the glutamate, when

present, a ligand to the Fe^{3+} ion. Other residues that were previously considered strictly conserved and catalytically important have turned out not to be conserved, such as the above-mentioned glutamate residue (which throughout this Review will be named simply glutamate) bound to center II in several oxidized SORs, or the lysine residue, also at the −(E)(K)HxP− motif, and located close to the catalytic site. Interestingly, the glutamate and the lysine residues are conserved in all 2Fe-SORs so far known, with variability found in the 1Fe-SORs. This very low overall amino acid conservation, common in the prokaryote world, establishes the minimal requisites for the catalytic mechanism.

The comparative analysis of the amino acid sequences, together with structural data, has been the basis for the construction of site-directed mutants (of the glutamate and lysine residues), and for the study of the enzymes naturally lacking these amino acids (see Table 6).

Thus far, only a few SORs were studied with some details: six are from Bacteria, the 2Fe-SORs from anaerobic sulfate reducing bacteria (*D. vulgaris*,[367b,372c,384] *D. baarsii*,[370b,372d,g,385] and *D. desulfuricans* ATCC 27774[363,368b]), the 1Fe-SORs from the microaerophilic bacteria *Treponema pallidum*[372a,i,385b,386]
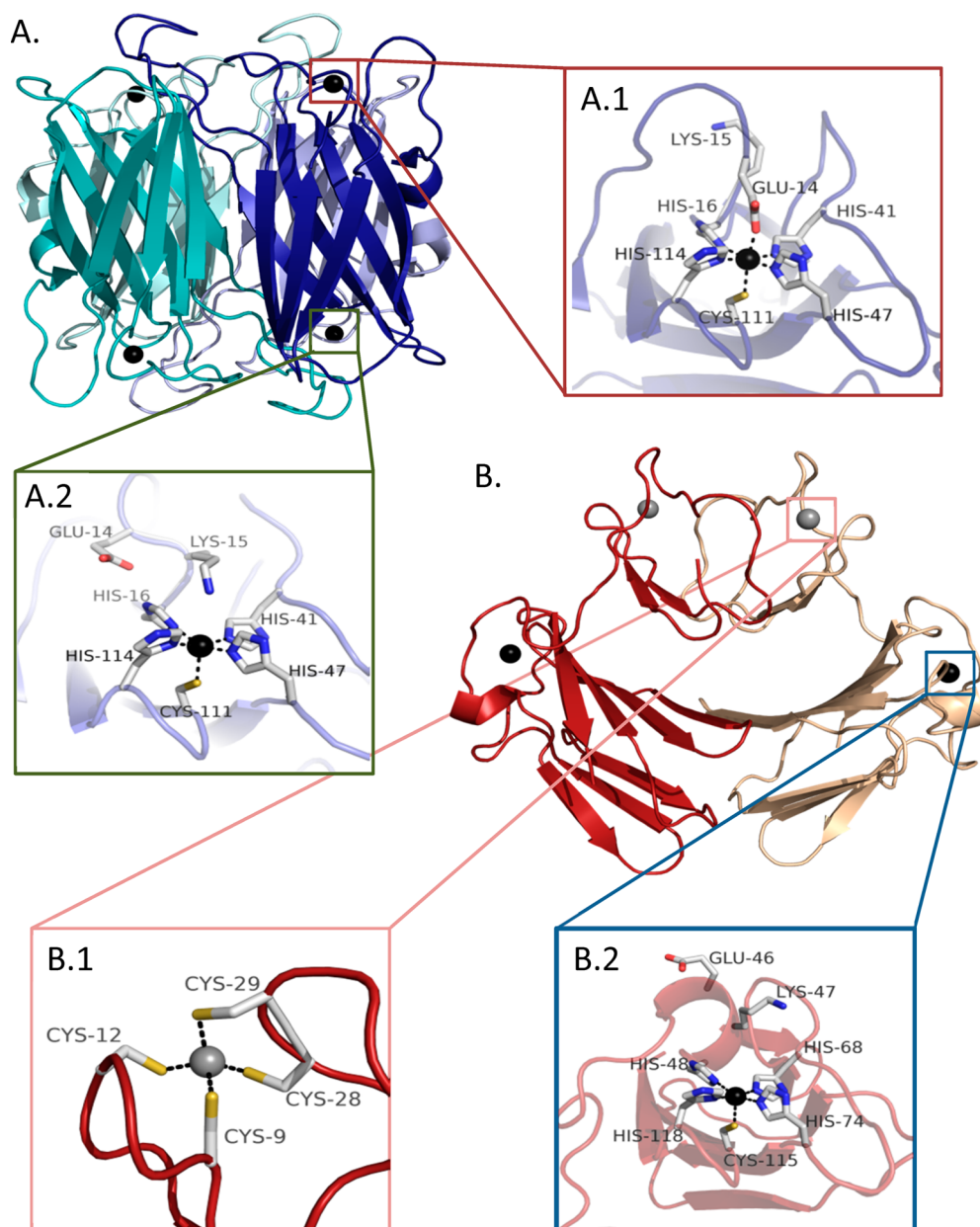
Figure 38. Crystallographic structures of 1Fe- and 2Fe-SORs. (A) Structure of *P. furiosus* 1Fe-SOR tetramer (PDB code: 1DO6), showing the SOR active sites in the oxidized (A.1) and reduced (A.2) forms. (B) Structure of the *D. desulfuricans* 2Fe-SOR dimer with details of center I (DX-like center) and SOR active site (presumably in the reduced form) shown in B.1 and B.2, respectively. The figures were generated using the PyMOL Molecular Graphics System.[396]

and *denticola*,[387] and the sulfate-reducing bacterium *D. gigas*.[362,367a] Within Archaea, they are from the hyperthermophiles (1Fe and 2Fe-SORs from *A. fulgidus*,[368c,372b,e,f,388] 1Fe-SORs from *Pyrococcus furiosus*,[370a,389] *Ignicoccus hospitalis*,[383] and *Nanoarchaeum equitans*[372h]). Thus far, only one SOR from a eukaryote, the anaerobic protozoan *Giardia intestinalis*, was studied (also a 1Fe-SOR).[57] Although several other organisms have also been studied, the interspecies differences are found to be minimal. Therefore, the organism is specifically mentioned here only when necessary.

7.3. Structure

7.3.1. Overall Structure. Several SOR structures have been determined by X-ray crystallography (Table 7). Among these, the structures of the *D. desulfuricans* 2Fe-SOR and the *Pyrococcus (P.) furiosus* 1Fe-SOR were the first to be published (Figure 38).[71a,b]

Whereas the 1Fe-SORs are tetramers, forming a cube with the active centers diagonally oriented at opposite positions (Figure 38, panel A), 2Fe-SORs are dimers (Figure 38, panel B); these quaternary structures are observed both in the crystals and in solution. The SOR catalytic center is localized in a domain that adopts a 3 + 4 stranded β-barrel in an immunoglobulin-like fold (SOR domain, Figure 39, panel A). It contains an Fe ion coordinated in a square-pyramidal geometry by four histidine imidazole nitrogens (three N_ε and one N_δ) distributed in an equatorial plane and by a sulfur from a fifth axial cysteine-ligand ([Fe(His)$_4$Cys]). The metal ligands are located in the loops connecting the β strands. The 2Fe-SORs have a second domain at the N-terminus, connected to
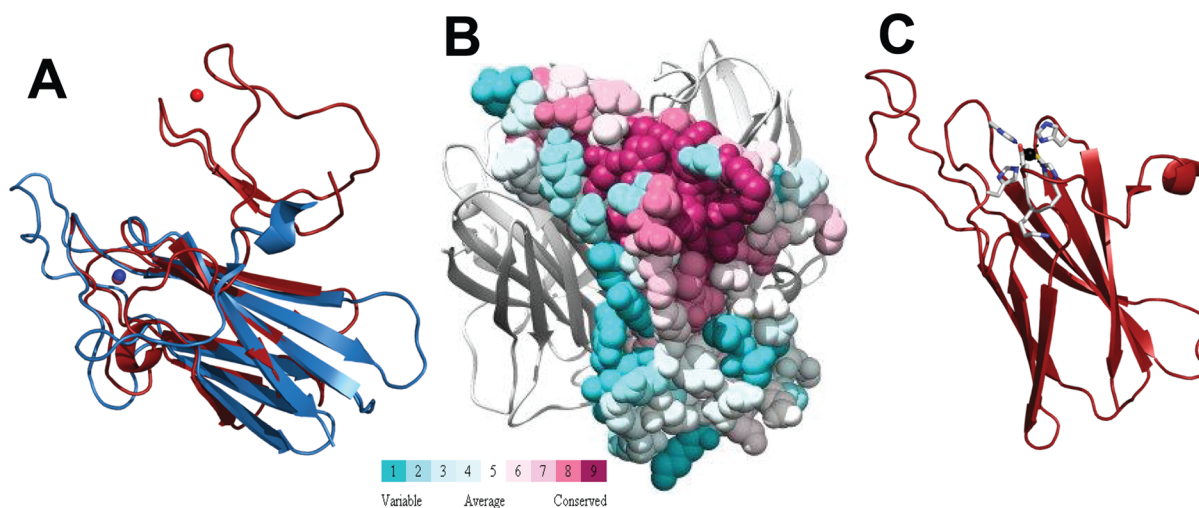
Figure 39. Structural conservation in SORs. (A) Superimposition of 1Fe-SOR (blue) and 2Fe-SOR (red) monomers (PDB codes: 1DO6 and 1DFX); (B) structural conservation of amino acid residues in the monomer of 1Fe-SOR, mapped over *P. furiosus* structure and made using ConSurf;[398,420] and (C) ribbon diagram of the same monomer in B (PDB code: 1DO6). Panels A and C were generated using the PyMOL Molecular Graphics System.[396]

the immunoglobulin-like catalytic domain by a short stretch of ca. 15 residues, having a short 3_{10} helix. This domain contains a slightly distorted tetrahedral $[Fe(Cys)_4]$ site that has a high homology to *D. gigas* desulforedoxin (Dx).[364b] This site, which is often referred to as "center I", was initially proposed to mediate intradomain electron transfer between a 2Fe-SOR redox partner and its SOR active center, but no evidence supporting this claim has been produced so far. In fact, the Fe—Fe distance is about 25 Å, too large to allow catalytically significant intramolecular electron transfer. Instead, Emerson et al. have shown that the disruption of center I has no effect on the in vitro or in vivo activity of the *D. vulgaris* 2Fe-SOR.[367b] Additionally, the *T. pallidum* 1Fe-SOR, which can be viewed as a "naturally mutated" 2Fe-SOR that lost center I, retains its efficient in vitro and in vivo SOR activity.[386b] The ~15 residues loop connecting the two domains in the 2Fe-SORs or between the short 3_{10} helix and the catalytic domain contains the mostly conserved (E)(K)HxP-motif. In both SOR types, the active centers are very solvent exposed, and this is determinant for the SOR catalytic features. As expected, the amino acid residues near the catalytic center are rather conserved, while those far from it are quite variable (Figure 39B).

The unprecedented structural features of the SOR active center $[Fe(His)_4Cys]$ can only be compared to the active site of cytochrome P450 monooxygenase enzymes (P450). In P450, the Fe is also coordinated by four nitrogens from a porphyrin ring and by an axial cysteine ligand. Despite these similarities, the chemistries of the SOR and P450 centers are quite different. While the SOR reduces superoxide to hydrogen peroxide, P450 binds O_2 and catalyzes its two-electron reduction and double protonation to cleave the O—O bond, yielding 1 equiv of water and an enzyme intermediate known as Compound I (see section 7.5).

7.3.2. Redox-Linked Structural Changes in the SOR Active Center. When in its Fe^{3+} state, the SOR $[Fe(His)_4Cys]$ center can adopt an octahedral geometry, with an extra glutamate ligand binding to the Fe in the position opposite to the axial cysteine $[Fe(His)_4CysGlu]$ (Figure 38A.1). This conformation was only unambiguously shown in the crystallographic structures of the 1Fe-SORs from *P. furiosus* and *P.*

horikoshii (PDB codes: 1DO6, 1DQI,[71b] and 2HVB). The structure of the reduced center was determined after incubation of *P. furiosus* SOR crystals with sodium dithionite, showing the typical $[Fe(His)_4Cys]$ configuration (PDB code: 1DDK[71b]), albeit with low Fe occupancy at two of its subunits (~20%). Thus, the change in the Fe redox-state in 1Fe-SORs is accompanied by a change in the Fe coordination, and this occurs together with a significant movement of two loop regions (Gly9-Lys15 and Gly36-Pro40, *P. furiosus* SOR numbering). These structural changes are expected to occur during catalysis, but their importance for the actual catalytic mechanism is still not fully understood (see section 7.5). The change in conformation upon oxidation/reduction is expected to also occur in 2Fe-SORs, and indeed Fourier transform infrared (FTIR) studies suggest that the glutamate binds the Fe^{3+} center in the SORs from *D. baarsii* and *T. pallidum* and that this process is coupled to the change in the Fe redox state.[385b] Unfortunately, no crystallographic data have so far supported the binding of the glutamate ligand to the center in 2Fe-SORs, probably due to the difficulty of maintaining these enzymes in the Fe^{3+} state, in part due to X-ray-induced photoreduction of the protein during structural data collection.[71b,389a,390]

7.3.3. Crystallographic Structures of Reaction Intermediates. Upon superoxide reduction, an Fe^{3+}—(hydro)-peroxo species is formed (see catalytic mechanism below). Such an intermediate has been trapped in *D. baarsii* 2Fe-SOR crystals after incubation with H_2O_2, and the structure shows the (hydro)peroxo group bound in an end-on geometry to the Fe ion (Figure 40).[370c] In this elegant experiment, the presence of the (hydro)peroxo ligand was determined by resonance Raman measurements on the crystal. The position of the (hydro)-peroxo in the center appears to be stabilized by the lysine residue (Lys48 in *D. baarsii*) that is part of the conserved (E)(K)HxP-motif and by hydrogen bonding to the (hydro)-peroxo either directly or through water molecules. This lysine residue appears also to contribute to a positively charged antenna to attract anions into the Fe^{2+} center.[390]
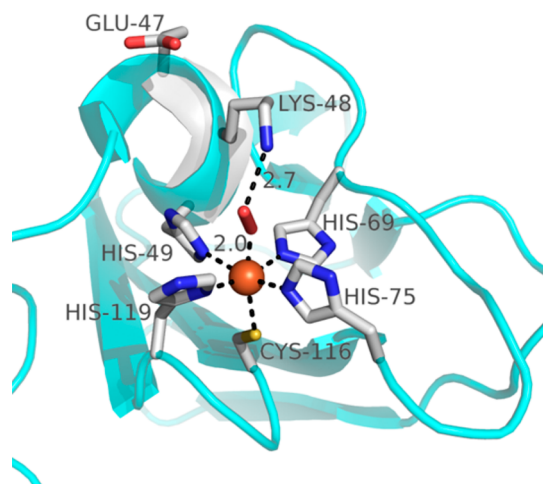
Figure 40. Structure of the (hydro)peroxo intermediate in 2Fe-SOR from *D. baarsii* (subunit C in PDB 2JI3). This figure was generated using the PyMOL Molecular Graphics System.[396]

7.4. Metal Centers

Superoxide reductases have been explored using a wide range of spectroscopic tools, UV−visible, resonance Raman, EPR, Mössbauer, variable temperature MCD, EXAFS, and FTIR, and these studies have shed light on the electronic properties of the sites and on their reactivity with the substrate, the $O_2^{\bullet-}$ anion, and other small ligands.

7.4.1. Spectroscopic Properties. Both Fe sites (centers I and II, or the Dx-like center and the catalytic one) are in a high-spin state in the oxidized Fe^{3+} ($S = 5/2$) and reduced Fe^{2+} ($S = 2$) forms, as evidenced by EPR and Mössbauer spectroscopies.[361−363,368b,c,372e,381,384b,387,389,390] Both centers exhibit EPR resonances at low magnetic field in the Fe^{3+} state, with variable rhombicities ($E/D \sim 0.1$ to ~ 0.3), resulting from several of the spin Kramer doublets according to the respective transition probabilities and thermal populations; the energy separations between the doublets are small, with a zero field splitting $|D|$ of less than 0.5 cm^{-1}. These resonances, broad due to significant E/D strain and local heterogeneities, change according to pH and to the state of the enzymes.[362,389a,391] At high pH, all center II forms convert to a quasi-isotropic system, with g-values around 4.3 due to the $|S = \pm 3/2\rangle$ middle Kramer doublet of the $S = 5/2$ spin manifold, and a minor intensity resonance at $g \approx 9.2$ due to the $|S = \pm 1/2\rangle$ doublet. The cyanide anion is an inhibitor of SODs and a classical ligand for metal centers. SORs

in the Fe^{3+} state bind cyanide at center II, yielding a low-spin $S = 1/2$ species, with an axial EPR spectrum at g-values of 2.27 and 1.96.[362,368b,384d,385a] Other anionic small ligands, like the fluoride or azide anions, bind also to the catalytic center, but do not induce a spin state change due to their weak field character. MCD spectroscopy showed that cyanide remains bound to the metal center in the Fe^{2+} state.

Electronic absorption spectroscopy allows a much clearer distinction between the two sites in oxidized SORs. Center I has the features of an oxidized desulforedoxin FeCys$_4$ site, with maxima at 375 and 495 nm and a broad shoulder at 560 nm, due to ligand (cysteine sulfur) to metal charge transfer transitions. Center II has in general broad absorption bands at ~560 or ~660 nm, depending on the absence or the presence of the glutamate ligand, respectively, and a shoulder at 330 nm. This 660 nm absorbance in the visible region accounts for the unusual colors of 1Fe-SORs (blue) and the oxidized 2Fe-SORs (gray, a mixture of blue with pink from the Dx site). In glutamate-lacking enzymes (wild-type or site-directed mutants), the 660 nm is blue-shifted to higher energies, ca. 560 nm.

MCD showed that the 560/660 nm bands result from a sulfur-to-iron charge transfer transition,[389a] involving the Fe-cysteine ligand. In the fully reduced state, both types of SORs are colorless, while the half-reduced 2Fe-SORs (center I oxidized, center II reduced) are pink. These features have been essential to investigate the catalytic mechanism of SORs, by combining absorption spectroscopy with fast kinetics techniques (pulse radiolysis and stopped-flow).

7.4.2. pH Equilibria. Since the isolation of the first 1Fe-SOR from *D. gigas*,[362] there has been increasing evidence for pH-dependent equilibria at or near the catalytic site, some of which are of mechanistic relevance. In fact, the reduction reaction involves the consumption of two protons, because at physiological pH the superoxide anion is in the basic, deprotonated form (p$K_a \approx 4.8$), while the product is fully protonated.

The SORs in the oxidized state are prone to pH-induced changes, reflected in alterations of the electronic properties of the catalytic center. In enzymes with a glutamate-bound Fe, there is a drastic change in the electronic spectra at pH > 9, with the absorption band maxima shifting to ~590 nm (Figure 41). This transition has an apparent pK_a of ~9.5. The chemical identity of the basic form was established by resonance Raman and MCD spectroscopies. A vibrational band was detected at 466−471 cm^{-1}, characteristic of a high-spin Fe^{3+}−OH
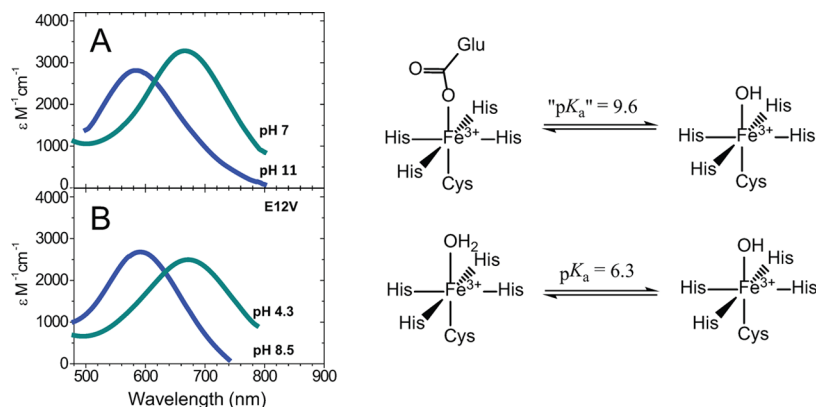

Figure 41. pH equilibria in SORs. Left panels: visible spectra of wild-type (A) and E12V (B) *A. fulgidus* SORs.

stretching mode vibration, in the wild type and E47A and K48I mutants of the *D. baarsii* 2Fe-SOR. This band disappeared at lower pH values, and had a clear isotopic shift when the samples were prepared in $H_2^{18}O$ or D_2O, suggesting that in the basic form, a hydroxide substitutes for the glutamate as a ligand to the Fe^{3+}.[385c] The same observation was subsequently reported for the 1Fe-SORs from *A. fulgidus* and *N. equitans*[388] and corroborated the earlier evidence from MCD that at high pH the cysteine and histidine ligands remain bound.

This pH-induced transition corresponds to a ligand exchange where the glutamate side chain is substituted by a hydroxide anion:

$$His_4Fe-Glu_p + OH^- \rightarrow His_4Fe-OH + Glu_p^- \qquad (33)$$

where subscript P means that the glutamate is a residue of the protein. It is assumed that the unbound glutamate, which is quite solvent exposed, will remain in the deprotonated, anionic form at the pH values used for the experiments (pH > 5). The value of the apparent pK_a gives an indication of the relative affinities of the Fe ion for each ligand (hydroxide or glutamate); that is, the pK_a is not a proton ionization constant for the glutamate-bound enzymes. This ligand exchange has been monitored in a similar way by EPR spectroscopy[362,372d,389a] and by FTIR.[385b] In the EPR spectrum, a species with E/D of 0.25–0.3 appears at high pH.[362,372d,389a] In site-directed glutamate mutants and the *N. equitans* enzyme (an enzyme naturally lacking the glutamate), a pH-dependent equilibrium was also detected, but with an apparent pK_a ca. 3 units lower (Figure 41 and Table 8).[372e,h] Again, resonance Raman data have shown

Table 8. Experimental pK_a Values for SORs

	organism	wild-type pK_a	glutamate-mutation pK_a	ref
1Fe-SOR	*A. fulgidus*	9.6	6.3	372b
	G. intestinalis	8.7		57
	N. equitans	6.5		372h
	I. hospitalis	10.5	6.5	383
2Fe-SOR	*D. baarsii*	9	7.6	372d,g,385e
	A. fulgidus	8.5		372f

that the basic form corresponds to a hydroxide-bound Fe. However, in these cases, the pH dependence may be plausibly attributed to a true protonic equilibrium due to the protonation of the hydroxide ligand at acidic pH values, leading presumably to a water-bound state. These processes are essential to understand the reactivity of SORs with $O_2^{\bullet-}$.

The protonation states of the His and Cys ligands are not known. On the basis of the hydrogen-bonding patterns deduced from SOR crystal structures and of what is generally known for metal centers, the cysteine sulfur is most probably in the anionic, sulfide form (thus contributing to the lowering of the reduction potential of the $Fe^{3+/2+}$ pair), while the histidines are most probably in the neutral form. This does not preclude that at least one of the histidines may be in the fully deprotonated state.

As mentioned above, small anions like fluoride, cyanide, azide, and chloride bind at or very close to the catalytic site, leading to slight shifts in the absorbance maxima.

7.4.3. Redox Thermodynamics. The two Fe centers of 2Fe-SORs are redox active and have quite distinct reduction potentials. At neutral pH values, center I has a potential close to 0 mV, similar to that for the isolated desulforedoxin from *D.*

gigas, while center II has a reduction potential between 190 and 365 mV, depending on the enzyme.[362,363,372b,d,h,383,386a] It is this large difference in potentials that permitted detailed studies of the events at catalytic center II, without interference from center I, in 2Fe-SORs. Because of the redox-linked dissociation of the glutamate, in enzymes having this amino acid, their reduction potential corresponds to two processes, the ionization of the Fe ion and the dissociation/binding of a ligand; that is, under these conditions it does not correspond to a simple redox equilibrium (a situation reminiscent of that for Fe and CuZn SODs).

The reduction potential of center I for the *D. baarsii* 2Fe-SOR steadily decreases as pH increases, by about −70 mV per pH unit, suggesting the involvement of a single protonatable group with a pK_a^{ox} lower than 5.5, the minimum pH value tested. The reduction potentials for center II of the SORs from *D. baarsii* and *I. hospitalis* are constant at pH 5–9 (at higher pH values, most SORs are unstable). However, for the glutamate mutants of both enzymes (*I. hospitalis* E23A and *D. barsii* E47A), the potential at pH 5.5 shows a huge increase to 520–550 mV, as compared to the wild-type enzymes, and decreases at higher pH values by ∼ −60 mV per pH unit, with a pK_a^{ox} of about 6.5. As the glutamate-lacking enzymes have the Fe^{3+} bound to a water molecule or to a hydroxide anion, above the pK_a^{ox}, the large difference in potential for the acidic forms may result from the substitution of an anionic ligand, that is, the glutamate, which would preferentially stabilize the Fe^{3+} form, by a neutral water molecule. The decrease in potential as the pH increases would be due to ionization of the bound water molecule.

It is particularly relevant to analyze the redox thermodynamics involved in the reduction of $O_2^{\bullet-}$ with that of the SOR catalytic center and to compare it with those of the SODs (Figure 4). The potentials for the SOR catalytic center are similar to those reported for the SODs and are therefore not only perfectly adequate for superoxide reduction (E'_0 ($O_2^{\bullet-}$/H_2O_2) = 0.91 V, vs NHE, at pH 7) but also have a similar driving force. The same would be true for the oxidation of the superoxide anion (E'_0 (O_2/$O_2^{\bullet-}$) = −0.18 V, at pH 7), which means that the reason that the SORs fail to carry out the oxidative part of the dismutation reaction is not thermodynamic.

7.5. Catalytic Mechanism

The mechanism of $O_2^{\bullet-}$ reduction has been scrutinized mainly using pulse radiolysis[367b,372] and, at a slower time scale, by stopped flow spectroscopy,[57,372e,384c] both coupled to visible absorption spectroscopy. The identification of some reaction intermediates has been achieved by preparing possible intermediate state analogues chemically (e.g., by incubation of the enzyme with hydrogen peroxide, which, however, has the caveat of the partial instability of the enzyme under those conditions). The pulse radiolysis approach allows the production of defined amounts of the superoxide anion in a very fast time scale and is indeed essential to delineate the oxidative part of the catalytic mechanism of these enzymes (reduction of superoxide to hydrogen peroxide and concomitant oxidation of the Fe^{2+} enzyme to the Fe^{3+}, resting state).

For the pulse radiolysis experiment, the Fe^{3+} enzyme is first reduced to the Fe^{2+} state using either a cobalt-60 source or sodium ascorbate. The reduced enzyme, which is colorless as there is no electronic absorption in the visible region, is then pulsed with an electron beam in the presence of O_2, which

generates calibrated amounts of superoxide that are substoichiometric with respect to the enzyme concentration. The reaction is monitored optically, and the spectrum of each enzyme species is measured over a sufficiently long period (up to seconds). It should nevertheless be stressed that intermediates will only be detected if they have long enough lifetimes and sufficiently detectable absorbances. The absence of an observable intermediate species may just be due to an unfortunate combination of those factors; these limitations have posed significant challenges in defining the SOR reductive mechanism.

7.5.1. First Intermediate. The catalytic process occurs through an inner-sphere mechanism. The first step of the reaction is common to all SORs studied thus far (Figure 42).
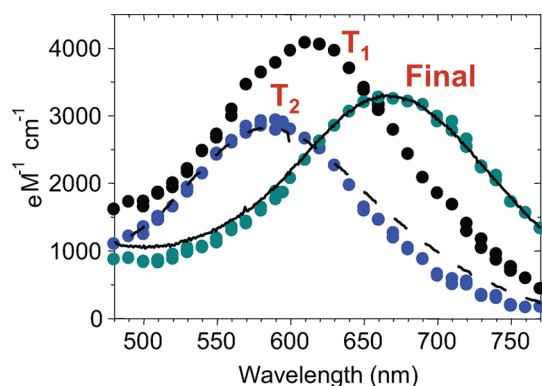

Figure 42. Reconstituted spectra of reaction intermediates (T_1 and T_2) upon pulsing *A. fulgidus* 1Fe-SOR with $O_2^{\bullet-}$.

After the superoxide pulse, the first observed intermediate, T1, has an absorption maximum at about 620 nm. This process occurs with a second-order rate constant of $\sim 10^9$ M^{-1} s^{-1} (first order in superoxide and enzyme), that is, at a diffusion-limited rate analogous to those for all SODs. This rate is, within experimental error, pH independent over the range of enzyme stability.

The nature of the T1 intermediate is at present controversial. One hypothesis is that it corresponds to an $Fe^{3+}-$(hydro)-peroxo species,[371,372e,378b] while another posits that it is an undetected, short-lived $Fe^{2+}-O_2^{\bullet-}$ form that decays into an Fe—hydroperoxo en route to the next intermediate.[385e] Both mechanisms have received support from theoretical calculations.[378a,385e,392] In either case, reduction of the $O_2^{\bullet-}$ is accompanied (in a sequential or simultaneous, proton-coupled process) by a concomitant protonation at the distal oxygen. The source of this proton is currently unknown, but it may well come from the water molecules surrounding the solvent-exposed metal site. Both experimental data with metal complexes and theoretical calculations have suggested that superoxide reduction is thermodynamically favored if proton assisted (see sections on SOD catalytic mechanisms).[392a,c,393]

Whatever the nature of the observable first intermediate (in the following we will label as T1 the $Fe^{3+}-$hydroperoxo form, whether it has or has not been experimentally observed), the next detectable species may be either the final, resting form (Fe^{3+} bound to the glutamate or a water/hydroxide anion, depending on the pH and on the presence or absence of the glutamate ligand), or a second intermediate.

7.5.2. Second Intermediate. For some enzymes, the Fe—hydroperoxide species decays in a pseudo first-order process to another intermediate T2 (Figure 42). This intermediate has an electronic spectrum strikingly identical to that of the Fe^{3+} hydroxide bound form (absorbance maximum at ca. 580 nm), revealed by the pH studies of the Fe^{3+} enzymes (see section 7.4.2). This means that at this stage the product, H_2O_2, was already released to the bulk. The rate of decay (k_2) of T1 to T2 is pH-dependent involving a rate-limiting protonation step, decreasing as the pH is increased from ~ 5 to 8.5; at pH > 8.5,
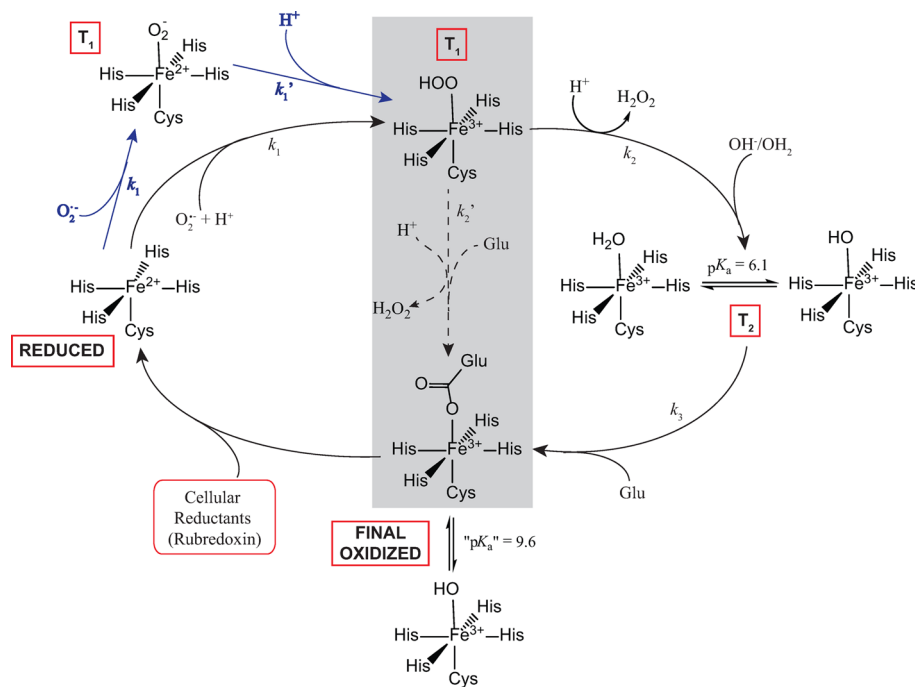

Figure 43. Catalytic mechanism for SOR $O_2^{\bullet-}$ reduction, contemplating the two possible structures for T_1 and the two mechanisms involving one or two macroscopically observed intermediates.

the process is pH-independent or even increases slightly with increasing pH. The dependence at low pH was described as resulting from the sum of a second-order process (proton-dependent) and a first-order one (pH-independent):

$$k_{2,\text{obs}} = k_2''[\text{H}^+] + k_2' \tag{34}$$

with a value for k_2'' of $\sim 10^9$ M^{-1} s^{-1}, that is, a diffusion-limited protonation step. In accordance with this interpretation, k_2 shows a clear deuterium isotopic effect.[372c]

The formation of the (hydro)peroxo form and its dissociation as H_2O_2 means that heterolytic cleavage of the peroxo bound moiety does not occur and that high-valent Fe-oxygen species are not formed. This contrasts with what happens in cytochrome P450s, where an oxo-ferryl cation radical is formed. The proposed explanation for this difference is that in P450s the second proton attacks the distal oxygen, favoring the scission of the oxygen O−O bond, while in SORs the proton binds to the proximal oxygen, which is directly bound to the Fe atom, leading to the release of the symmetric H_2O_2 molecule. Recent DFT calculations show that the protonation of proximal versus distal oxygen can in part be explained by the different charge distributions in the Fe^{III}−OOH intermediates and different positioning of the active centers in the two enzymes (P450 active center is embedded in the protein).[392c]

Upon dissociation of the product, at least for some of the enzymes thus far studied, a hydroxide ion is bound to the Fe center and is subsequently protonated (depending on pH) or substituted by the glutamate ligand (final step). Thus, there may be a concerted addition of an acidified water molecule (by forming a hydrogen bond with a nearby amino acid, see below), which transfers one of its protons to the proximal oxygen and binds to the Fe ion, maintaining the total charge of the site. Upon detailed analysis of the reaction profile of the *A. fulgidus* enzyme, a question was raised whether the hydroxide−bound species would be formed upon a simple chemical oxidation of the enzyme, in the absence of the substrate.[372e] The experiment was performed using stopped flow kinetics, starting with the reduced enzyme and oxidizing it chemically. Although the rate constant of the first reaction could not be determined, due to its high value as compared to the instrument dead time, it was nevertheless possible to show the formation of the Fe−hydroxide species upon oxidation, which subsequently decayed to the final resting species.

7.5.3. Final Resting Fe^{3+} State. In some enzymes, the hydroxide-bound intermediate is not detected, but as discussed above, this may be a consequence of the relative rate constants. In those instances, the final species is identical to the oxidized enzyme (with the glutamate bound or, in its absence, with a water or hydroxide bound, depending on pH). For the enzymes with a detectable hydroxide intermediate, this intermediate dissociates in a first-order process into the resting species (again the exact nature of the final form will depend upon the pH).

A global catalytic scheme is shown (Figure 43), highlighting the several proposals and macroscopic mechanisms so far put forward.

7.5.4. Role of Specific Amino Acid Residues. The role of two quasi-conserved amino acids has been analyzed in terms of their influence on the catalytic mechanism and assessed by the construction of site-directed mutants or by studying the few examples of naturally occurring enzymes lacking these residues: the glutamate ligand (E12 in *A. fulgidus* 1Fe-SOR, E47 in *D.*

vulgaris 2Fe-SOR), and the lysine of the motif −(E)(K)HVxP− (K13 in *A. fulgidus* 1Fe-SOR).[372b,c,e,g,h,383,385e]

Initially, the glutamate was proposed to assist the release of the product from the catalytic site or to be involved in some proton transfer events. However, all available data revealed that its substitution (natural or artificial) did not lead to any measurable difference in the rate constants. It was also proposed that the glutamate would function to "cover" or protect the active site of the Fe^{3+} enzyme, against binding of exogenous anions. This is a point that must await further investigation.

The other kinetically important amino acid is the lysine located at the amino acid stretch −(E)(K)HxP−. Initially it was thought that the lysine contributed to the positive surface charge near the active site and thus was responsible for the high, diffusion-limited rate constant for binding of the anionic substrate. However, except for the *D. baarsii* SOR lysine mutant, which showed an approximately 10-fold decrease of the rate for formation of the first intermediate in the absence of the lysine, essentially no change was observed for the other enzymes with the lysine absent. These differences may reflect the presence in some SORs of sufficient residues to compensate for the absence of the lysine.[372c,g,383]

A more interesting hypothesis is that the lysine, upon detachment of the glutamate, would acquire a position that allows it to stabilize the hydroperoxide ligand, either directly or through water molecules, and would also facilitate the protonation of the hydroperoxo (by acidifying the water molecule). As just mentioned, the distinct results found for different enzymes are inconclusive in this respect, or, as it so often occurs, the enzymes are particularly robust for those single amino acid changes.

7.6. Physiological Electron Donors − Reductive Path

It was initially assumed, due to the genomic organization, that rubredoxins would be the ultimate electron donors to the superoxide reductases.[394] In fact, in several cases, and irrespective of the gene's organizations, rubredoxins (or even desulforedoxin) were shown to donate electrons efficiently to SORs (with second-order rate constants in the order of 10^6−10^7 M^{-1} s^{-1}, or higher).[372f,384a,395] However, it is now known that many organisms having SORs do not contain in their genomes, at least as much as it has been explored, genes coding for rubredoxins/desulforedoxins, indicating that other types of electron donors must exist in those organisms. Furthermore, those electron donors have, in turn, to be reduced by other enzymes, and it is generally thought that this may occur at the expense of NAD(P)H oxidoreductases.

7.7. SORs versus SODs

SODs are found in all types of living organisms, from simple microbes to humans; this conservation by itself reflects its fundamental role in our present day oxygen-rich world. SORs, by contrast, have so far only been found in prokaryotes, Bacteria and Archaea, and recently in unicellular eukaryotes. Can we say from this for sure that SORs constitute crude, ancient systems for superoxide detoxification? Or are they just examples of natural variability? At this point, an answer to this question would be purely speculative.

The major physiological differences stem from the fact that SODs are stand-alone enzymes, using two successive reactions with the substrate for cycling the enzyme back and forth, while SORs have to rely on one or (possibly) two accessory proteins to be fed with electrons from NAD(P)H. Although SODs

consume two superoxide anions per reaction cycle, and SORs only one anion molecule, in SORs there is a simultaneous consumption of NAD(P)H, therefore diminishing the overall negative redox status of the cell, which will, ultimately, also reduce the intracellular superoxide production. Moreover, the SODs produce potentially toxic O_2 as a product, while the SORs do not.

Thermodynamically, SORs and SODs have the adequate reduction potentials to oxidize and reduce the superoxide anion. Why then do SORs have SOD activities about three orders of magnitude lower than those of SODs? This remains an intriguing question, because even the enzymes (wild type, like the one from *N. equitans*, or the several glutamate mutants studied) that lack the glutamate ligand to the Fe^{3+} form have an activity not much higher than those having it.

Much has been learned already about these fascinating fast enzymes, but several relevant questions remain to be addressed, such as the transcriptional regulation of these "novel" enzymes and the in vivo metalation processes. Finally, will other ROS scavenging systems, in addition to SODs and SORs, be discovered in the future, through the increasing genome sequencing and biochemical progress, as a result of the tremendous diversity of life?

8. CONCLUSIONS

The historic discovery by McCord and Fridovich in 1969 of the first SOD enzyme marks the beginning of our appreciation of the significance of ROS in biological oxidative stress and signaling and of the importance of diverse antioxidant systems to modern aerobic life. The fact that four evolutionarily unrelated metalloenzymes arose to protect organisms against O_2^- toxicity, that is, NiSOD, Fe/MnSODs, CuZnSOD, and SORs, provides excellent examples both of convergent evolution and of nature's ingenuity (in a Darwinian and a non teleological sense). These efficient and robust systems allowed life to continue developing after the Great Oxidation Event occurred on early Earth, by combating the products of noncontrolled and incomplete O_2 reduction.

Interestingly, there are some striking similarities in these four very different enzymes, which are certainly a consequence of the reactions catalyzed. Their reduction potentials all fall between the potentials for one-electron reduction of O_2 and one-electron reduction of $O_2^{\bullet-}$. Binding of $O_2^{\bullet-}$ by the enzymes occurs by either inner- or outer-sphere mechanisms (this, in some cases, is still a matter of dispute), and the rate constants are extremely high, close to the diffusion limit. They all reduce $O_2^{\bullet-}$ to H_2O_2 selectively through the redox chemistry of the metal ion at each active site. Reactions of SOD and SOR enzymes also involve redox coupled structural changes, including ligand dissociation (SORs, Ni- and CuZnSODs), and proton-coupled electron transfer. It also appears that two similar strategies developed to "attract" the substrate: a positively lined channel in CuZn- and Fe/MnSODs, and a positive surface charge around the solvent exposed active sites of SORs. Although the NiSOD active site is also solvent exposed, the surface surrounding it does not show significant positively charged areas.[89] All sites are also accessible to protons, either by channels or from water molecules close to the metal sites.

The rise of O_2 on Earth is one of the better-understood examples of the intimate two-way relationship between life and its chemical context. A remarkable amount of O_2-sensitive biochemistry survived and remains central to metabolism in

aerobes in part because of the evolution of enzymes able to consume ROS with efficiencies that rank among the highest of enzymes. The diversity of the enzymes that arose to metabolize superoxide speaks to the urgency of the problems of biological oxidative stress and of the versatility of life. We look forward with great interest to future surprises as this fascinating story of O_2 on Earth continues to unfold.

AUTHOR INFORMATION
Corresponding Authors
*E-mail: abreu@itqb.unl.pt.
*E-mail: cabelli@bnl.gov.
*E-mail: mmaroney@chem.umass.edu.
*E-mail: afm@uky.edu.
*E-mail: miguel@itqb.unl.pt.
*E-mail: jsv@chem.ucla.edu.
Notes
The authors declare no competing financial interest.

Biographies

Yuewei Sheng is currently a Postdoctoral Researcher at the University of California, Los Angeles (UCLA). She received her Bachelor's Degree in Chemistry from Nanjing University in China in 2007 and her Ph.D. Degree in Chemistry from UCLA in 2012, under the supervision of Professor Joan Selverstone Valentine. As a graduate student, she was rewarded Dissertation Year Fellowship, John M. Jordan Memorial Award, and Chinese Government Award for Outstanding Self-Financed Students Abroad. She conducts research in biochemistry and bioinorganic chemistry, investigating the structure–function relationships of metalloenzymes, metals and oxidative stress, and biophysical inquiry into protein aggregation in neurodegenerative diseases.

Isabel A. Abreu graduated in Biochemistry from Universidade de Lisboa in 1996 and received her Ph.D. in Biochemistry from the Instituto de Tecnologia Química e Biológica António Xavier-Universidade Nova de Lisboa (ITQB-UNL) in 2002, studying the mechanism of superoxide reductases, under the supervision of Miguel Teixeira. She was a Research Associate at Brookhaven National Laboratory (NY), where she worked with Diane Cabelli, specializing in the mechanistic aspects of MnSOD catalysis, and a Postdoctoral Fellow at Rockefeller University (NY) with Nam-Hai Chua. She was awarded a Ciência2008 staff position at Instituto de Biologia Molecular e Celular (Porto, Portugal) from 2009 to 2012, and, during that time, she was a visiting researcher at Margarida Oliveira's Genomics of Plant Stress laboratory (GPlantS), ITQB, Oeiras. She is presently at GPlantS as a researcher from Instituto de Biologia Experimental e Tecnológica, Oeiras, Portugal. Her main focus is the regulation of the proteome by post-translational modifications, during the response of plants to abiotic stress.

Diane E. Cabelli was born in 1953 in Columbia, Missouri. She received an A.B. in Chemistry in 1973 from Bryn Mawr College and a Ph.D. in Chemistry in 1979 from the University of Texas (Austin) with Michael J. S. Dewar and Alan H. Cowley. This was followed by a nontraditional year, courtesy of a National Museum Act Fellowship, spent studying pigments in medieval Armenian Gospel books in collaboration with Thomas Mathews at New York University Institute of Fine Arts. In 1981, she joined Brookhaven National Laboratory as a Postdoctoral Research Associate, where she remains and is currently a Scientist. Her research involves Radiation Chemistry, using an accelerator to probe reaction mechanisms in water with a focus on redox reactions involving metals.

Michael J. Maroney was born in 1954 in Ames, IA. He received his B.S. in Chemistry from Iowa State University in 1976, and his Ph.D. in Chemistry from the University of Washington (Seattle) in 1981. Following a stint at Chevron Research Co., he was a postdoctoral

associate at Northwestern University (with Dr. William Trogler) and at the University of Minnesota (with Lawrence Que, Jr.). He joined the Chemistry Department at the University of Massachusetts-Amherst in 1985, where he has been Professor of Chemistry since 1995. He pursues research in biological inorganic chemistry with an emphasis on the biological roles of nickel.

Anne-Frances Miller is Professor of Chemistry, Professor of Molecular and Cellular Biochemistry, and member of the Markey Cancer Center at the University of Kentucky. Her research seeks to understand enzymatic redox catalysis with the objective of retuning redox enzymes and electron carriers to deploy them in bioremediation, semisynthesis, and solar energy. She earned her Ph.D. in biophysical chemistry at Yale University and undertook postdoctoral training in bioinorganic chemistry at the Massachusetts Institute of Technology and in NMR spectroscopy at Brandeis University. She was assistant and associate professor of chemistry at the Johns Hopkins University, moving to Kentucky for family. She was awarded the Biophysical Society Young Investigator award in 2006, was visiting scientist at the Massachusetts Institute of Technology in 2007−08, ran the Boston marathon in 2010, and was cochair of the Enzymes, Coenzymes, and Metabolic Pathways Gordon Research Conference in 2011. She has authored 80 publications and given 50 public lectures.

Miguel Teixeira was born in Lisbon in 1957. He graduated in Chemistry from the Universidade Técnica de Lisboa, 1981. Still as an undergraduate student, he joined António V. Xavier's Molecular Biophysics Group, where he performed his Ph.D. work on bacterial hydrogenases under the supervision of J. J. G. Moura. After being awarded his Ph.D. in Chemistry, by the Universidade Nova de Lisboa (UNL), in 1986, he spent one and a half years as a research associate and Fullbright Fellow at the Physics Department, Emory University, Atlanta, with B. H. Huynh. After returning to Portugal, and until 1997, he was Assistant Professor at Faculdade de Ciências e Tecnologia, UNL, and started his own group at the new Instituto de Tecnologia

Química e Biológica António Xavier (ITQB-UNL); in 1997, he moved definitively to ITQB as Associate Professor and finally as Full Professor of Biological Chemistry. Since 1990 he is the leader of the ITQB MetalloEnzymes and Molecular Bioenergetics Laboratory, devoted to the understanding of molecular mechanisms of microbial redox enzymes, mainly catalyzing the reduction of small molecules, such as O_2, NO, H_2O_2, or $O_2^{\bullet-}$.

Joan Selverstone Valentine graduated from Smith College in Northampton, MA, in 1967 with an A.B. in Chemistry. Four years later, she was the first woman to receive a Ph.D. in Chemistry from Princeton University. After a year as an Instructor at Princeton, she was appointed Assistant Professor of Chemistry at Rutgers University in New Brunswick in 1972. In 1980, she moved to UCLA, where she is now Distinguished Research Professor of Chemistry and Biochemistry. She also holds the position of Distinguished Professor at Ewha Womans University in Seoul, Korea. Her lifelong research interests include all aspects of metals and dioxygen in biology. Outside of research, her most important interests are her husband, Andy; her children, David, Elizabeth, and Benjamin; and her four wonderful grandchildren, Brynn, Evan, Maleeha, and Rhys.

ACKNOWLEDGMENTS

ABBREVIATIONS

SOD	superoxide dismutase
SOR	superoxide reductase
ROS	reactive oxygen species
NAD(P)H	nicotinamide adenine dinucleotide (phosphate) hydrogen
EPR	electron paramagnetic resonance
CD	circular dichroism
PDB	protein data bank
ESI—MS	electrospray ionization—mass spectrometry
SOMO	single occupied molecular orbital
ENDOR	electron nuclear double resonance
MCD	magnetic circular dichroism
HOMO	highest occupied molecular orbital
XAS	X-ray absorption spectroscopy
LMCT	ligand to metal charge transfer
DFT	density function theory
EXAFS	extended X-ray absorption fine structure
ABTS	2,2′-azinobis-(3ethylbenzthiazoline-6-sulfonate)
NMR	nuclear magnetic resonance
NCBI	National Center for Biotechnology and Information
IMS	intermembrane space
SNP	single nucleotide polymorphism
Drad	Deinococus radiodurans
CCS	copper chaperone for SOD1
TNF	tumor necrosis factor
JNK	c-Jun NH_2-terminal kinase
ALS	amyotrophic lateral sclerosis
HDX	hydrogen—deuterium exchange
SDS	sodium dodecyl sulfate
GuHCl	guanidinium hydrochloride
DTT	dithiothreitol
GSH/GSSG	reduced/oxidized gluthathione
HEK	human embryonic kidney
EM	electron microscopy
AFM	atomic force microscopy
DSC	differential scanning calorimetry
Bcl-2	B-cell lymphoma 2
FAT	fast axonal transport
Hsp	heat shock protein
Dfx	desulfoferrodoxin
Nlr	neelaredoxin
Dx	desulforedoxin-like
FMN	flavin mononucleotide
HTH	helix—turn—helix
FTIR	Fourier transform infrared spectroscopy
TAT	putative twin arginine signal peptide

REFERENCES

(1) Sessions, A. L.; Doughty, D. M.; Welander, P. V.; Summons, R. E.; Newman, D. K. *Curr. Biol.* **2009**, *19*, R567.

(2) Raymond, J.; Segrè, D. *Science* **2006**, *311*, 1764.

(3) Koppenol, W. H.; Stanbury, D. M.; Bounds, P. L. *Free Radical Biol. Med.* **2010**, *49*, 317.

(4) (a) Narayana, P. A.; Suryanarayana, D.; Kevan, L. *J. Am. Chem. Soc.* **1982**, *104*, 3552. (b) Martins-Costa, M. T. C.; Anglada, J. M.; Francisco, J. S.; Ruiz-Lopez, M. F. *Angew. Chem., Int. Ed.* **2012**, *51*, 5413.

(5) Bielski, B. H.; Cabelli, D. E.; Arudi, R. L.; Ross, A. B. *J. Phys. Chem. Ref. Data* **1985**, *14*, 1041.

(6) Bielski, B. H.; Richter, H. W. *J. Am. Chem. Soc.* **1977**, *99*, 3019.

(7) Rao, P. S.; Hayon, E. *Biochem. Biophys. Res. Commun.* **1973**, *51*, 468.

(8) (a) Valentine, J. S.; Quinn, A. E. *Inorg. Chem.* **1976**, *15*, 1997. (b) McClune, G. J.; Fee, J. A.; McCluskey, G. A.; Groves, J. T. *J. Am. Chem. Soc.* **1977**, *99*, 5220.

(9) (a) Gargaud, M.; Martin, H.; López-García, P.; Montmerle, T.; Pascal, R. *Young Sun, Early Earth and the Origins of Life. Lessons for Astrobiology*; Springer: New York, 2012. (b) Miriyala, S.; Spasojevic, I.; Tovmasyan, A.; Salvemini, D.; Vujaskovic, Z.; St Clair, D.; Batinic-Haberele, I. *Biochim. Biophys. Acta* **2012**, *1822*, 794. (c) Canfield, D. E. *Oxygen: A Four Billion Year History*; Princeton University Press: Princeton, NJ, 2014.

(10) (a) Catling, D. C.; Claire, M. W. *Earth Planet. Sci. Lett.* **2005**, *237*, 1. (b) Holland, H. D. *Philos. Trans. R. Soc., B* **2006**, *361*, 903.

(11) Canfield, D. E.; Rosing, M. T.; Bjerrum, C. *Phil. Trans. R. Soc., B* **2006**, *361*, 1819.

(12) (a) Anbar, A. D.; Duan, Y.; Lyons, T. W.; Arnold, G. L.; Kendall, B.; Creaser, R. A.; Kaufman, A. J.; Gordon, G. W.; Scott, C.; Garvin, J.; Buick, R. *Science* **2007**, *317*, 1903. (b) Kendall, B.; Reinhard, C. T.; Lyons, T. W.; Kaufman, A. J.; Poulton, S. W.; Anbar, A. D. *Nat. Geosci.* **2010**, *3*, 647.

(13) Sousa, F. L.; Thiergart, T.; Landan, G.; Nelson-Sathi, S.; Pereira, I. A. C.; Allen, J. F.; Lane, N.; Martin, W. F. *Phil. Trans. R. Soc., B* **2013**, *368*, 20130088.

(14) Widdel, F.; Schnell, S.; Heising, S.; Ehrenreich, A.; Assmus, B.; Schink, B. *Nature* **1993**, *362*, 834.

(15) Kim, J. D.; Yee, N.; Nanda, V.; Falkowski, P. G. *Proc. Natl. Acad. Sci. U.S.A.* **2013**, *110*, 1073.

(16) Fischer, W. W.; Knoll, A. H. *Geol. Soc. Am. Bull.* **2006**, *121*, 222.

(17) Haqq-Misra, J.; Kasting, J. F.; Lee, S. *Astrobiology* **2011**, *11*, 293.

(18) (a) Frey, M. M.; Stewart, R. W.; McConnell, J. R.; Bales, R. C. *J. Geophys. Res.* **2005**, *110*, D23301. (b) Kirschvink, J. L.; Kopp, R. E. *Phil. Trans. R. Soc., B* **2008**, *363*, 2755.

(19) Kim, K. M.; Qin, T.; Jiang, Y.-Y.; Chen, L.-L.; Xiong, M.; Caetano-Anollés, D.; Zhang, H.-Y.; Caetano-Anollés, G. *Structure* **2012**, *20*, 67.

(20) (a) Castresana, J.; Lübben, M.; Saraste, M.; Higgins, D. G. *EMBO J.* **1994**, *13*, 2516. (b) Gribaldo, S.; Talla, E.; Brochier-Armanet, C. *Trends Biochem. Sci.* **2009**, *34*, 375.

(21) (a) Brioukhanov, A. L.; Netrusov, A. I. *Appl. Biochem. Microbiol.* **2007**, *43*, 567. (b) Imlay, J. A. *Mol. Microbiol.* **2008**, *68*, 801.

(22) Buckel, W.; Golding, B. T. *Annu. Rev. Microbiol.* **2006**, *60*, 27.

(23) Jang, S.; Imlay, J. A. *Mol. Microbiol.* **2010**, *78*, 1448.

(24) (a) Pan, N.; Imlay, J. A. *Mol. Microbiol.* **2001**, *39*, 1562. (b) Lessner, F. H.; Jennings, M. E.; Hirata, A.; Duin, E. C.; Lessner, D. J. *J. Biol. Chem.* **2012**, *287*, 18510. (c) Major, T. A.; Burd, H.; Whitman, W. B. *FEMS Microbiol. Lett.* **2004**, *239*, 117.

(25) Subczynski, W. K.; Widomska, J.; Feix, J. B. *Free Radical Biol. Med.* **2009**, *46*, 707.

(26) Valentine, J. S.; Wertz, D. L.; Lyons, T. J.; Liou, L.-L.; Goto, J. J.; Gralla, E. B. *Curr. Opin. Chem. Biol.* **1998**, *2*, 253.

(27) Imlay, J. A. *Adv. Microb. Physiol.* **2002**, *46*, 111.

(28) (a) Sawyer, D. T.; Valentine, J. S. *Acc. Chem. Res.* **1981**, *14*, 393. (b) Fridovich, I. *Acc. Chem. Res.* **1982**. (c) Sawyer, D. T.; Valentine, J. S. *Acc. Chem. Res.* **1982**, *15*, 200.

(29) Carlioz, A.; Touati, D. *EMBO J.* **1986**, *5*, 623.

(30) Boehm, D. E.; Vincent, K.; Brown, O. R. *Nature* **1976**, *262*, 418.

(31) Imlay, J. A. *Mol. Microbiol.* **2006**, *59*, 1073.

(32) (a) Vargas, M.; Kashefi, K.; Blunt-Harris, E. L.; Lovley, D. R. *Nature* **1998**, *395*, 65. (b) Weber, K. A.; Achenbach, L. A.; Coates, J. D. *Nat. Rev. Microbiol.* **2006**, *4*, 752.

(33) Bedard, K.; Lardy, B.; Krause, K. H. *Biochimie* **2007**, *89*, 1107.

(34) Diaz, J. M.; Hansel, C. M.; Voelker, B. M.; Mendes, C. M.; Andeer, P. F.; Zhang, T. *Science* **2013**, *340*, 1223.

(35) (a) Kurtz, D. M., Jr. *Acc. Chem. Res.* **2004**, *37*, 902. (b) Kurtz, D. M., Jr. *J. Inorg. Biochem.* **2006**, *100*, 679. (c) Pinto, A. F.; Rodrigues, J. V.; Teixeira, M. *Biochim. Biophys. Acta, Proteins Proteomics* **2010**, *1804*, 285.

(36) (a) Frazão, C.; Silva, G.; Gomes, C. M.; Matias, P.; Coelho, R.; Sieker, L.; Macedo, S.; Liu, M. Y.; Oliveira, S.; Teixeira, M.; Xavier, A. V.; Rodrigues-Pousada, C.; Carrondo, M. A.; Le Gall, J. *Nat. Struct.*

Biol. **2000**, *7*, 1041. (b) Vicente, J. B.; Carrondo, M. A.; Teixeira, M.; Frazão, C. In *Handbook of Metalloproteins*; Messerschmidt, A., Ed.; John Wiley & Sons, Ltd.: Chichester, 2011; Vols. *4 and 5*.

(37) Gonçalves, V. L., Vicente, J. B., Saraiva, L. M., Teixeira, M. *Flavodiiron Proteins and Their Role in Cyanobacteria*. Obinger, C., Peschek, G. A., Eds.; Springer: New York, 2011.

(38) (a) Dupont, C. L.; Butcher, A.; Valas, R. E.; Bourne, P. E.; Caetano-Anollés, G. *Proc. Natl. Acad. Sci. U.S.A.* **2010**, *107*, 10567. (b) Merchant, S. S.; Helmann, J. D. *Adv. Microb. Physiol.* **2012**, *60*, 91.

(39) (a) Fraústo, J. J. R.; da Silva, J.; Williams, R. J. P. *The Biological Chemistry of the Elements: The Inorganic Chemistry of Life*; Oxford University Press: Oxford, 1991. (b) Saito, M. A.; Sigman, D. M.; Morel, F. M. M. *Inorg. Chim. Acta* **2003**, *356*, 308.

(40) Crichton, R. R.; Pierre, J.-L. *BioMetals* **2001**, *14*, 99.

(41) (a) Barnese, K.; Gralla, E. B.; Valentine, J. S.; Cabelli, D. E. *Proc. Natl. Acad. Sci. U.S.A.* **2012**, *109*, 6892. (b) Stadtman, E. R.; Berlett, B. S.; Chock, P. B. *Proc. Natl. Acad. Sci. U.S.A.* **1990**, *87*, 384.

(42) Barondeau, D. P.; Kassmann, C. J.; Bruns, C. K.; Tainer, J. A.; Getzoff, E. D. *Biochemistry* **2004**, *43*, 8038.

(43) (a) Dupont, C. L.; Neupane, K.; Shearer, J.; Palenik, B. *Environ. Microbiol.* **2008**, *10*, 1831. (b) Wolfe-Simon, F.; Grzebyk, D.; Schofield, O.; Falkowski, P. G. *J. Phycol.* **2005**, *41*, 453.

(44) Fridovich, I. *Annu. Rev. Biochem.* **1975**, *44*, 147.

(45) (a) Brioukhanov, A.; Netrusov, A.; Sordel, M.; Thauer, R. K.; Shima, S. *Arch. Microbiol.* **2000**, *174*, 213. (b) Kardinahl, S.; Schmidt, C. L.; Petersen, A.; Schafer, G. *FEMS Microbiol. Lett.* **1996**, *138*, 65.

(46) (a) Page, M. D.; Allen, M. D.; Kropat, J.; Urzica, E. I.; Karpowicz, S. J.; Hsieh, S. I.; Loo, J. A.; Merchant, S. S. *Plant Cell* **2012**, *24*, 2649. (b) Bowler, C.; Vanmontagu, M.; Inzé, D. *Annu. Rev. Plant Phys.* **1992**, *43*, 83.

(47) Dufernez, F.; Yernaux, C.; Gerbod, D.; Noël, C.; Chauvenet, M.; Wintjens, R.; Edgcomb, V. P.; Capron, M.; Opperdoes, F. R.; Viscogliosi, E. *Free Radical Biol. Med.* **2006**, *40*, 210.

(48) (a) May, B. P.; Dennis, P. P. *J. Bacteriol.* **1987**, *169*, 1417. (b) Knapp, S.; Kardinahl, S.; Hellgren, N.; Tibbelin, G.; Schäfer, G.; Ladenstein, R. *J. Mol. Biol.* **1999**, *285*, 689.

(49) Lamarre, C.; LeMay, J.-D.; Deslauriers, N.; Bourbonnais, Y. *J. Biol. Chem.* **2001**, *276*, 43784.

(50) (a) Cheng, W.; Tung, Y. H.; Liu, C. H.; Chen, J. C. *Fish Shellfish Immunol.* **2006**, *20*, 438. (b) Gómez-Anduro, G. A.; Barillas-Mury, C. V.; Peregrino-Uriarte, A. B.; Gupta, L.; Gollas-Galván, T.; Hernández-López, J.; Yepiz-Plascencia, G. *Dev. Comp. Immunol.* **2006**, *30*, 893.

(51) Alscher, R. G.; Erturk, N.; Heath, L. S. *J. Exp. Bot.* **2002**, *53*, 1331.

(52) Benov, L. T.; Fridovich, I. *J. Biol. Chem.* **1994**, *269*, 25310.

(53) Valentine, J. S.; Doucette, P. A.; Potter, S. Z. *Annu. Rev. Biochem.* **2005**, *74*, 563.

(54) Lyons, T. J.; Gralla, E. B.; Valentine, J. S. *Met. Ions Biol. Syst.* **1999**, *36*, 125.

(55) Oury, T. D.; Crapo, J. D.; Valnickova, Z.; Enghild, J. J. *Biochem. J.* **1996**, *317*, 51.

(56) Nivière, V.; Fontecave, M. *J. Biol. Inorg. Chem.* **2004**, *9*, 119.

(57) Testa, F.; Mastronicola, D.; Cabelli, D. E.; Bordi, E.; Pucillo, L. P.; Sarti, P.; Saraiva, L. M.; Giuffrè, A.; Teixeira, M. *Free Radical Biol. Med.* **2011**, *51*, 1567.

(58) (a) Pinto, A. F.; Rodrigues, J. V.; Teixeira, M. *Biochim. Biophys. Acta* **2010**, *1804*, 285. (b) Lucchetti-Miganeh, C.; Goudenège, D.; Thybert, D.; Salbert, G.; Barloy-Hubler, F. *BMC Microbiol.* **2011**, *11*, 105.

(59) Herbst, R. W.; Guce, A.; Bryngelson, P. A.; Higgins, K. A.; Ryan, K. C.; Cabelli, D. E.; Garman, S. C.; Maroney, M. J. *Biochemistry* **2009**, *48*, 3354.

(60) Stallings, W. C.; Pattridge, K. A.; Strong, R. K.; Ludwig, M. L. *J. Biol. Chem.* **1985**, *260*, 16424.

(61) Ursby, T.; Adinolfi, B. S.; Al-Karadaghi, S.; De Vendittis, E.; Bocchini, V. *J. Mol. Biol.* **1999**, *286*, 189.

(62) Barra, D.; Schinina, M. E.; Bossa, F.; Puget, K.; Durosay, P.; Guissani, A.; Michelson, A. M. *J. Biol. Chem.* **1990**, *265*, 17680.

(63) Borgstahl, G. E. O.; Parge, H. E.; Hickey, M. J.; Beyer, W. F., Jr.; Hallewell, R. A.; Tainer, J. A. *Cell* **1992**, *71*, 107.

(64) Palma, J. M.; López-Huertas, E.; Corpas, F. J.; Sandalio, L. M.; Gómez, M.; del Río, L. A. *Physiol. Plant.* **1998**, *104*, 720.

(65) (a) Sheng, Y.; Stich, T. A.; Barnese, K.; Gralla, E. B.; Cascio, D.; Britt, R. D.; Cabelli, D. E.; Valentine, J. S. *J. Am. Chem. Soc.* **2011**, *133*, 20878. (b) Sheng, Y.; Durazo, A.; Schumacher, M.; Gralla, E. B.; Cascio, D.; Cabelli, D. E.; Valentine, J. S. *PloS One* **2013**, *8*, e62446.

(66) Perry, J. J.; Shin, D. S.; Getzoff, E. D.; Tainer, J. A. *Biochim. Biophys. Acta* **2010**, *1804*, 245.

(67) (a) Battistoni, A.; Rotilio, G. *FEBS Lett.* **1995**, *374*, 199. (b) Pesce, A.; Capasso, C.; Battistoni, A.; Folcarelli, S.; Rotilio, G.; Desideri, A.; Bolognesi, M. *J. Mol. Biol.* **1997**, *274*, 408.

(68) (a) Bourne, Y.; Redford, S. M.; Steinman, H. M.; Lepock, J. R.; Tainer, J. A.; Getzoff, E. D. *Proc. Natl. Acad. Sci. U.S.A.* **1996**, *93*, 12774. (b) Bordo, D.; Matak, D.; Djinovic-Carugo, K.; Rosano, C.; Pesce, A.; Bolognesi, M.; Stroppolo, M. E.; Falconi, M.; Battistoni, A.; Desideri, A. *J. Mol. Biol.* **1999**, *285*, 283.

(69) Forest, K. T.; Langford, P. R.; Kroll, J. S.; Getzoff, E. D. *J. Mol. Biol.* **2000**, *296*, 145.

(70) Pesce, A.; Battistoni, A.; Stroppolo, M. E.; Polizio, F.; Nardini, M.; Kroll, J. S.; Langford, P. R.; O'Neill, P.; Sette, M.; Desideri, A.; Bolognesi, M. *J. Mol. Biol.* **2000**, *302*, 465.

(71) (a) Coelho, A. V.; Matias, P.; Fülöp, V.; Thompson, A.; Gonzalez, A.; Carrondo, M. A. *J. Biol. Inorg. Chem.* **1997**, *2*, 680. (b) Yeh, A. P.; Hu, Y.; Jenney, F. E., Jr.; Adams, M. W.; Rees, D. C. *Biochemistry* **2000**, *39*, 2499. (c) Santos-Silva, T.; Trincão, J.; Carvalho, A. L.; Bonifácio, C.; Auchère, F.; Raleiras, P.; Moura, I.; Moura, J. J.; Romão, M. J. *J. Biol. Inorg. Chem.* **2006**, *11*, 548.

(72) Imlay, J. A.; Fridovich, I. *J. Biol. Chem.* **1991**, *266*, 6957.

(73) Barrette, W. C.; Sawyer, D. T.; Fee, J. A.; Asada, K. *Biochemistry* **1983**, *22*, 624.

(74) (a) Vance, C. K.; Miller, A.-F. *J. Am. Chem. Soc.* **1998**, *120*, 461. (b) Yikilmaz, E.; Rodgers, D. W.; Miller, A.-F. *Biochemistry* **2006**, *45*, 1151.

(75) (a) Vance, C. K.; Miller, A.-F. *Biochemistry* **2001**, *40*, 13079. (b) Lévêque, V. J.-P.; Vance, C. K.; Nick, H. S.; Silverman, D. N. *Biochemistry* **2001**, *40*, 10586.

(76) Azab, H. A.; Banci, L.; Borsari, M.; Luchinat, C.; Sola, M.; Viezzoli, M. S. *Inorg. Chem.* **1992**, *31*, 4649.

(77) Benovic, J.; Tillman, T.; Cudd, A.; Fridovich, I. *Arch. Biochem. Biophys.* **1983**, *221*, 329.

(78) Gabbianelli, R.; D'Orazio, M.; Pacello, F.; O'Neill, P.; Nicolini, L.; Rotilio, G.; Battistoni, A. *Biol. Chem.* **2004**, *385*, 749.

(79) Cabelli, D. E.; Riley, D.; Rodriguez, J. A.; Valentine, J. S.; Zhu, H. In *Biomimetic Oxidations Catalyzed by Transition Metal Complexes*; Meunier, B., Ed.; World Scientific: River Edge, NJ, 1998.

(80) Zilbermann, I.; Maimon, E.; Cohen, H.; Meyerstein, D. *Chem. Rev.* **2005**, *105*, 2609.

(81) Bryngelson, P. A.; Maroney, M. J. *Met. Ions Life Sci.* **2007**, *2*, 417.

(82) (a) Youn, H.-D.; Kim, E.-J.; Roe, J.-H.; Hah, Y. C.; Kang, S.-O. *Biochem. J.* **1996**, *318*, 889. (b) Youn, H.-D.; Youn, H.; Lee, J.-W.; Yim, Y.-I.; Lee, J. K.; Hah, Y. C.; Kang, S.-O. *Arch. Biochem. Biophys.* **1996**, *334*, 341.

(83) Maroney, M. J. *Curr. Opin. Chem. Biol.* **1999**, *3*, 188.

(84) Lubitz, W.; Ogata, H.; Rüdiger, O.; Reijerse, E. *Chem. Rev.* **2014**, DOI: 10.1021/cr4005814.

(85) (a) Mirza, S. A.; Pressler, M. A.; Kumar, M.; Day, R. O.; Maroney, M. J. *Inorg. Chem.* **1993**, *32*, 977. (b) Adzamli, I. K.; Deutsch, E. *Inorg. Chem.* **1980**, *19*, 1366. (c) Grapperhaus, C. A.; Darensbourg, M. Y. *Acc. Chem. Res.* **1998**, *31*, 451.

(86) Choudhury, S. B.; Lee, J.-W.; Davidson, G.; Yim, Y.-I.; Bose, K.; Sharma, M. L.; kang, S.-O.; Cabelli, D. E.; Maroney, M. J. *Biochemistry* **1999**, *38*, 3744.

(87) Bryngelson, P. A.; Arobo, S. E.; Pinkham, J. L.; Cabelli, D. E.; Maroney, M. J. *J. Am. Chem. Soc.* **2004**, *126*, 460.

(88) (a) Barondeau, D. P.; Kassmann, C. J.; Bruns, C. K.; Tainer, J. A.; Getzoff, E. D. *Biochemistry* **2004**, *43*, 8038. (b) Fiedler, A. T.;

Bryngelson, P. A.; Maroney, M. J.; Brunold, T. C. *J. Am. Chem. Soc.* **2005**, *127*, 5449.

(89) Wuerges, J.; Lee, J.-W.; Yim, Y.-I.; Yim, H.-S.; Kang, S.-O.; Carugo, K. D. *Proc. Natl. Acad. Sci. U.S.A.* **2004**, *101*, 8569.

(90) Ryan, K. C.; Johnson, O. E.; Cabelli, D. E.; Brunold, T. C.; Maroney, M. J. *J. Biol. Inorg. Chem.* **2010**, *15*, 795.

(91) Murphy, L. M.; Strange, R. W.; Hasnain, S. S. *Structure* **1997**, *5*, 371.

(92) Lee, H.-I.; Lee, J.-W.; Yang, T.-C.; Kang, S.-O.; Hoffman, B. M. *J. Biol. Inorg. Chem.* **2010**, *15*, 175.

(93) Abreu, I. A.; Cabelli, D. E. *Biochim. Biophys. Acta* **2010**, *1804*, 263.

(94) Guan, Y.; Hickey, M. J.; Borgstahl, G. E. O.; Hallewell, R. A.; Lepock, J. R.; O'Connor, D.; Hsieh, Y.; Nick, H. S.; Silverman, D. N.; Tainer, J. A. *Biochemistry* **1998**, *37*, 4722.

(95) (a) Hunter, T.; Ikebukuro, K.; Bannister, W. H.; Bannister, J. V.; Hunter, G. J. *Biochemistry* **1997**, *36*, 4925. (b) Miller, A.-F.; Sorkin, D. L.; Padmakumar, K. *Biochemistry* **2005**, *44*, 5969.

(96) Johnson, O. E.; Ryan, K. C.; Maroney, M. J.; Brunold, T. C. *J. Biol. Inorg. Chem.* **2010**, *15*, 777.

(97) Ryan, K. C.; Maroney, M. J. "Nickel Superoxide Dismutase," in *Encyclopedia of Metalloproteins*, Kretsinger, R. H.; Uversky, V. N.; Permyakov, A., Eds.; Springer: New York, 20131505−1515.

(98) Szilagyi, R. K.; Bryngelson, P. A.; Maroney, M. J.; Hedman, B.; Hodgson, K. O.; Solomon, E. I. *J. Am. Chem. Soc.* **2004**, *126*, 3018.

(99) (a) Pelmenschikov, V.; Siegbahn, P. E. M. *J. Am. Chem. Soc.* **2006**, *128*, 7466. (b) Prabhakar, R.; Morokuma, K.; Musaev, D. G. *J. Comput. Chem.* **2006**, *27*, 1438.

(100) Pelmenschikov, V.; Siegbahn, P. E. M. *Inorg. Chem.* **2005**, *44*, 3311.

(101) Eitinger, T. *J. Bacteriol.* **2004**, *186*, 7821.

(102) (a) Kim, E. J.; Chung, H. J.; Suh, B. S.; Hah, Y. C.; Roe, J. H. *Mol. Microbiol.* **1998**, *27*, 187. (b) Ahn, B.-E.; Cha, J.; Lee, E.-J.; Han, A.-R.; Thompson, C. J.; Roe, J.-H. *Mol. Microbiol.* **2006**, *59*, 1848.

(103) Yost, F. J., Jr.; Fridovich, I. *J. Biol. Chem.* **1973**, *248*, 4905.

(104) McCord, J. M.; Fridovich, I. *J. Biol. Chem.* **1969**, *244*, 6049.

(105) Keele, B. B., Jr.; McCord, J. M.; Fridovich, I. *J. Biol. Chem.* **1970**, *245*, 6176.

(106) Hatchikian, E. C.; Henry, Y. A. *Biochimie* **1977**, *59*, 153.

(107) Hassan, H. M. *Adv. Genet.* **1989**, *26*, 65.

(108) Opperdoes, F. R.; Borst, P.; Spits, H. *Eur. J. Biochem.* **1977**, *76*, 21.

(109) (a) Salin, M. L.; Bridges, S. M. *Arch. Biochem. Biophys.* **1980**, *201*, 369. (b) Pilon, M.; Ravet, K.; Tapken, W. *Biochim. Biophys. Acta* **2011**, *1807*, 989.

(110) (a) Kirby, T. W.; Lancaster, J. R., Jr.; Fridovich, I. *Arch. Biochem. Biophys.* **1981**, *210*, 140. (b) Joshi, P.; Dennis, P. P. *J. Bacteriol.* **1993**, *175*, 1572.

(111) Steinman, H. M.; Hill, R. L. *Proc. Natl. Acad. Sci. U.S.A.* **1973**, *70*, 3725.

(112) Stallings, W. C.; Pattridge, K. A.; Strong, R. K.; Ludwig, M. L. *J. Biol. Chem.* **1984**, *259*, 10695.

(113) (a) Gregory, E. M. *Arch. Biochem. Biophys.* **1985**, *238*, 83. (b) Meier, B.; Barra, D.; Bossa, F.; Calabrese, L.; Rotilio, G. *J. Biol. Chem.* **1982**, *257*, 13977. (c) Pennington, C. D.; Gregory, E. M. *J. Bacteriol.* **1986**, *166*, 528.

(114) (a) Gregory, E. M.; Dapper, C. H. *Arch. Biochem. Biophys.* **1983**, *220*, 293. (b) Brock, C. J.; Harris, J. I. *Biochem. Soc. Trans.* **1977**, *5*, 1537. (c) Ose, D. E.; Fridovich, I. *Arch. Biochem. Biophys.* **1979**, *194*, 360. (d) Yamakura, F. *J. Biochem.* **1978**, *83*, 849.

(115) Yamano, S.; Maruyama, T. *J. Biochem.* **1999**, *125*, 186.

(116) Meier, B.; Gabbianelli, R. *J. Inorg. Biochem.* **1998**, *70*, 57.

(117) Hiraoka, B. Y.; Yamakura, F.; Sugio, S.; Nakayama, K. *Biochem. J.* **2000**, *345*, 345.

(118) Whittaker, M. M.; Whittaker, J. W. *J. Biol. Inorg. Chem.* **2000**, *5*, 402.

(119) Yamano, S.; Sako, Y.; Nomura, N.; Maruyama, T. *J. Biochem.* **1999**, *126*, 218.

(120) Yamakura, F.; Kobayashi, K.; Tagawa, S.; Morita, A.; Imai, T.; Ohmori, D.; Matsumoto, T. *Biochem. Mol. Biol. Int.* **1995**, *36*, 233.

(121) Matsumoto, T.; Terauchi, K.; Isobe, T.; Matsuoka, K.; Yamakura, F. *Biochemistry* **1991**, *30*, 3210.

(122) Tabares, L. C.; Bittel, C.; Carrillo, N.; Bortolotti, A.; Cortez, N. *J. Bacteriol.* **2003**, *185*, 3223.

(123) Martin, M. E.; Byers, B. R.; Olson, M. O. J.; Salin, M. L.; Aruneaux, J. E. L.; Tolbert, C. *J. Biol. Chem.* **1986**, *261*, 9361.

(124) Ose, D. E.; Fridovich, I. *J. Biol. Chem.* **1976**, *251*, 1217.

(125) (a) Ringe, D.; Petsko, G. A.; Yamakura, F.; Suzuki, K.; Ohmori, D. *Proc. Natl. Acad. Sci. U.S.A.* **1983**, *80*, 3879. (b) Stallings, W. C.; Powers, T. B.; Pattridge, K. A.; Fee, J. A.; Ludwig, M. L. *Proc. Natl. Acad. Sci. U.S.A.* **1983**, *80*, 3884.

(126) (a) Lah, M. S.; Dixon, M. M.; Pattridge, K. A.; Stallings, W. C.; Fee, J. A.; Ludwig, M. L. *Biochemistry* **1995**, *34*, 1646. (b) Schmidt, M.; Scherk, C.; Iakovleva, O.; Nolting, H. F.; Meier, B.; Parak, F. *Inorg. Chim. Acta* **1998**, *276*, 65.

(127) Dooley, D. M.; Jones, T. F.; Karas, J. L.; McGuirl, M. A.; Brown, R. D., III; Koenig, S. H. *J. Am. Chem. Soc.* **1987**, *109*, 721.

(128) Edwards, R. A.; Baker, H. M.; Whittaker, M. M.; Whittaker, J. W.; Jameson, G. B.; Baker, E. N. *J. Biol. Inorg. Chem.* **1998**, *3*, 161.

(129) (a) Koehntop, K. D.; Emerson, J. P.; Que, L., Jr. *J. Biol. Inorg. Chem.* **2005**, *10*, 87. (b) Kovaleva, E. G.; Lipscomb, J. D. *Science* **2007**, *316*, 453.

(130) (a) Stallings, W. C.; Metzger, A. L.; Pattridge, K. A.; Fee, J. A.; Ludwig, M. L. *Free Radical Res. Commun.* **1991**, *12–13*, 259. (b) Li, J.; Fisher, C. L.; Chen, J. L.; Bashford, D.; Noodleman, L. *Inorg. Chem.* **1996**, *35*, 4694. (c) Miller, A.-F.; Padmakumar, K.; Sorkin, D. L.; Karapetian, A.; Vance, C. K. *J. Inorg. Biochem.* **2003**, *93*, 71. (d) Han, W.-G.; Lovell, T.; Noodleman, L. *Inorg. Chem.* **2002**, *41*, 205.

(131) Bull, C.; Fee, J. A. *J. Am. Chem. Soc.* **1985**, *107*, 3295.

(132) (a) Sawyer, D. T.; Gibian, M. J.; Morrison, M. M.; Seo, E. T. *J. Am. Chem. Soc.* **1978**, *100*, 627. (b) Miller, A.-F. In *Handbook of Metalloproteins*; Wieghardt, K., Huber, R., Poulos, T. L., Messerschmidt, A., Eds.; Wiley and Sons: Chichester, 2001; Vol. *1*.

(133) (a) Miller, A.-F. *Curr. Opin. Chem. Biol.* **2004**, *8*, 162. (b) Maliekal, J.; Karapetian, A.; Vance, C.; Yikilmaz, E.; Wu, Q.; Jackson, T.; Brunold, T. C.; Spiro, T. G.; Miller, A.-F. *J. Am. Chem. Soc.* **2002**, *124*, 15064. (c) Abreu, I. A.; Rodriguez, J. A.; Cabelli, D. E. *J. Phys. Chem. B* **2005**, *109*, 24502.

(134) (a) de Grotthuss, C. J. T. *Ann. Chim.* **1806**, *58*, 54. (b) Cukierman, S. *Biochim. Biophys. Acta* **2006**, *1757*, 876.

(135) (a) Whittaker, M. M.; Whittaker, J. W. *Biochemistry* **1997**, *36*, 8923. (b) Edwards, R. A.; Whittaker, M. M.; Whittaker, J. W.; Baker, E. N.; Jameson, G. B. *Biochemistry* **2001**, *40*, 15. (c) Lévêque, V. J.-P.; Stroupe, M. E.; Lepock, J. R.; Cabelli, D. E.; Tainer, J. A.; Nick, H. S.; Silverman, D. N. *Biochemistry* **2000**, *39*, 7131. (d) Ramilo, C. A.; Lévêque, V.; Guan, Y.; Lepock, J. R.; Tainer, J. A.; Nick, H. S.; Silverman, D. N. *J. Biol. Chem.* **1999**, *274*, 27711.

(136) Greenleaf, W. B.; Silverman, D. N. *J. Biol. Chem.* **2002**, *277*, 49282.

(137) (a) Slykhouse, T. O.; Fee, J. A. *J. Biol. Chem.* **1976**, *251*, 5472. (b) Fee, J. A.; McClune, G. J.; Lees, A. C.; Zidovetzki, R.; Pecht, I. *Isr. J. Chem.* **1981**, *21*, 54. (c) Tierney, D. L.; Fee, J. A.; Ludwig, M. L.; Penner-Hahn, J. E. *Biochemistry* **1995**, *34*, 1661.

(138) Fee, J. A.; McClune, G. J.; O'Neill, P.; Fielden, E. M. *Biochem. Biophys. Res. Commun.* **1981**, *100*, 377.

(139) Lavelle, F.; McAdam, M. E.; Fielden, E. M.; Roberts, P. B.; Puget, K.; Michelson, A. M. *Biochem. J.* **1977**, *161*, 3.

(140) Benovic, J.; Tillman, T.; Cudd, A.; Fridovich, I. *Arch. Biochem. Biophys.* **1983**, *221*, 329.

(141) Jackson, T. A.; Yikilmaz, E.; Miller, A.-F.; Brunold, T. C. *J. Am. Chem. Soc.* **2003**, *125*, 8348.

(142) Grove, L. E.; Xie, J.; Yikilmaz, E.; Karapetian, A.; Miller, A.-F.; Brunold, T. C. *Inorg. Chem.* **2008**, *47*, 3993.

(143) Sorkin, D. L.; Duong, D. K.; Miller, A.-F. *Biochemistry* **1997**, *36*, 8202.

(144) (a) Vaillancourt, F. H.; Bolin, J. T.; Eltis, L. D. *Crit. Rev. Biochem. Mol. Biol.* **2006**, *41*, 241. (b) Bruijnincx, P. C. A.; van Koten, G.; Klein Gebbink, R. J. M. *Chem. Soc. Rev.* **2008**, *37*, 2716.

(145) (a) Whittaker, J. W.; Solomon, E. I. *J. Am. Chem. Soc.* **1988**, *110*, 5329. (b) Niederhoffer, E. C.; Fee, J. A.; Papaefthymiou, V.; Münck, E. *Isotope and Nuclear Chemistry Division, Annual Report*; Los Alamos National Laboratory: Los Alamos, NM, 1987.

(146) (a) Aruoma, O. I.; Halliwell, B. *Biochem. J.* **1987**, *241*, 273. (b) Prousek, J. *Pure Appl. Chem.* **2007**, *79*, 2325.

(147) (a) Yamakura, F. *Biochem. Biophys. Res. Commun.* **1984**, *122*, 635. (b) Beyer, W. F., Jr.; Fridovich, I. *Biochemistry* **1987**, *26*, 1251. (c) Dooley, D. M.; Koras, J. F.; Jones, T. F.; Coti, C. E.; Smith, S. B. *Inorg. Chem.* **1986**, *25*, 4761.

(148) Vathyam, S.; Byrd, R. A.; Miller, A.-F. *Magn. Reson. Chem.* **2000**, *38*, 536.

(149) Sorkin, D. L.; Miller, A.-F. *Biochemistry* **1997**, *36*, 4916.

(150) Miller, A.-F.; Yikilmaz, E.; Vathyam, S. *Biochim. Biophys. Acta* **2010**, *1804*, 275.

(151) Jackson, T. A.; Xie, J.; Yikilmaz, E.; Miller, A.-F.; Brunold, T. C. *J. Am. Chem. Soc.* **2002**, *124*, 10833.

(152) (a) Fee, J. A.; DiCorleto, P. E. *Biochemistry* **1973**, *12*, 4893. (b) Bertini, L.; Luchinat, C.; Monnanni, R. *J. Am. Chem. Soc.* **1985**, *107*, 2178.

(153) Baes, C. F., Jr.; Mesmer, R. E. *The Hydrolysis of Cations*; John Wiley & Sons: New York, 1976.

(154) Jackson, T. A.; Karapetian, A.; Miller, A.-F.; Brunold, T. C. *Biochemistry* **2005**, *44*, 1504.

(155) Perrin, D. D. *Dissociation Constants of Inorganic Acids and Bases in Aqueous Solution*; Pergamon: Oxford, 1982.

(156) (a) Yamakura, F.; Rardin, R. L.; Petsko, G. A.; Ringe, D.; Hiraoka, B. Y.; Nakayama, K.; Fujimura, T.; Taka, H.; Murayama, K. *Eur. J. Biochem.* **1998**, *253*, 49. (b) Asada, K.; Yoshikawa, K.; Takahashi, M.; Maeda, Y.; Enmanji, K. *J. Biol. Chem.* **1975**, *250*, 2801.

(157) (a) Bannister, J. V.; Bannister, W. H.; Rotilio, G. *CRC Crit. Rev. Biochem.* **1987**, *22*, 111. (b) Steinman, H. M. In *Superoxide Dismutase*; Oberley, L. W., Ed.; CRC Press: Boca Raton, FL, 1982; Vol. *I*.

(158) (a) Takao, M.; Yasui, A.; Oikawa, A. *J. Biol. Chem.* **1991**, *266*, 14151. (b) Meier, B.; Sehn, A. P.; Michel, C.; Saran, M. *Arch. Biochem. Biophys.* **1994**, *313*, 296. (c) Yamakura, F.; Suzuki, K. *Biochim. Biophys. Acta* **1986**, *874*, 23.

(159) Barra, D.; Schininà, M. E.; Bossa, F.; Puget, K.; Durosay, P.; Guissani, A.; Michelson, A. M. *J. Biol. Chem.* **1990**, *265*, 17680.

(160) Seyedsayamdost, M. R.; Xie, J.; Chan, C. T. Y.; Schultz, P. G.; Stubbe, J. *J. Am. Chem. Soc.* **2007**, *129*, 15060.

(161) Yim, M. B.; Chock, P. B.; Stadtman, E. R. *J. Biol. Chem.* **1993**, *268*, 4099.

(162) Beyer, W. F., Jr.; Fridovich, I. *J. Biol. Chem.* **1991**, *266*, 303.

(163) (a) Yang, M.; Cobine, P. A.; Molik, S.; Naranuntarat, A.; Lill, R.; Winge, D. R.; Culotta, V. C. *EMBO J.* **2006**, *25*, 1775. (b) Luk, E.; Carroll, M.; Baker, M.; Culotta, V. C. *Proc. Natl. Acad. Sci. U.S.A.* **2003**, *100*, 10353. (c) Culotta, V. C.; Yang, M.; O'Halloran, T. V. *Biochim. Biophys. Acta* **2006**, *1763*, 747.

(164) Cavadini, P.; Biasiotto, G.; Poli, M.; Levi, S.; Verardi, R.; Zanella, I.; Derosas, M.; Ingrassia, R.; Corrado, M.; Arosio, P. *Blood* **2007**, *109*, 3552.

(165) Mancuso, M.; Davidzon, G.; Kurlan, R. M.; Tawil, R.; Bonilla, E.; Mauro, S. D.; Powers, J. M. *J. Neuropathol. Exp. Neurol.* **2005**, *64*, 280.

(166) Yamakura, F.; Kobayashi, Y.; Furukawa, S.; Suzuki, Y. *Free Radical Biol. Med.* **2007**, *43*, 423.

(167) Niederhoffer, E. C.; Naranjo, C. M.; Bradley, K. L.; Fee, J. A. *J. Bacteriol.* **1990**, *172*, 1930.

(168) Mizuno, K.; Whittaker, M. M.; Bächinger, H. P.; Whittaker, J. W. *J. Biol. Chem.* **2004**, *279*, 27339.

(169) Cotruvo, J. A., Jr.; Stubbe, J. *Metallomics* **2012**, *4*, 1020.

(170) Outten, C. E.; O'Halloran, T. V. *Science* **2001**, *292*, 2488.

(171) Dean, J. A., Ed. *Lange's Handbook of Chemistry*, 13th ed.; McGraw-Hill: New York, 1985.

(172) Stein, J.; Fackler, J. P.; McClune, G. J.; Fee, J. A.; Chan, L. T. *Inorg. Chem.* **1979**, *18*, 3511.

(173) Liu, G.-F.; Filipović, M.; Heinemann, F. W.; Ivanović-Burmazović, I. *Inorg. Chem.* **2007**, *46*, 8825.

(174) Gupta, R.; Borovik, A. S. *J. Am. Chem. Soc.* **2003**, *125*, 13234.

(175) Verhagen, M. F. J. M.; Meussen, E. T. M.; Hagen, W. R. *Biochim. Biophys. Acta* **1995**, *1244*, 99.

(176) Yamakura, F.; Suzuki, K. *J. Biochem. (Tokyo)* **1980**, *88*, 191.

(177) Miller, A.-F.; Sorkin, D. L. *Comments Mol. Cell. Biophys.* **1997**, *9*, 1.

(178) Barrette, W. C., Jr.; Sawyer, D. T.; Fee, J. A.; Asada, K. *Biochemistry* **1983**, *22*, 624.

(179) Miller, A.-F. *Acc. Chem. Res.* **2008**, *41*, 501.

(180) Yamakura, F.; Sugio, S.; Hiraoka, B. Y.; Ohmori, D.; Yokota, T. *Biochemistry* **2003**, *42*, 10790.

(181) Vance, C. K.; Miller, A.-F. *Biochemistry* **1998**, *37*, 5518.

(182) (a) Grove, L. E.; Xie, J.; Yikilmaz, E.; Miller, A.-F.; Brunold, T. C. *Inorg. Chem.* **2008**, *47*, 3978. (b) Jackson, T. A.; Brunold, T. C. *Acc. Chem. Res.* **2004**, *37*, 461.

(183) Jackson, T. A.; Gutman, C. T.; Maliekal, J.; Miller, A.-F.; Brunold, T. C. *Inorg. Chem.* **2013**, *52*, 3356.

(184) Edwards, R. A.; Whittaker, M. M.; Whittaker, J. W.; Jameson, G. B.; Baker, E. N. *J. Am. Chem. Soc.* **1998**, *120*, 9684.

(185) Yamakura, F.; Kobayashi, K.; Ue, H.; Konno, M. *Eur. J. Biochem.* **1995**, *227*, 700.

(186) Hsieh, H.; Guan, Y.; Tu, C.; Bratt, P. J.; Angerhofer, A.; Lepock, J. R.; Hickey, M. J.; Tainer, J. A.; Nick, H. S.; Silverman, D. N. *Biochemistry* **1998**, *37*, 4731.

(187) (a) Carlioz, A.; Ludwig, M. L.; Stallings, W. C.; Fee, J. A.; Steinman, H. M.; Touati, D. *J. Biol. Chem.* **1988**, *263*, 1555. (b) Parker, M. W.; Blake, C. C. F. *FEBS Lett.* **1988**, *229*, 377.

(188) (a) Smith, M. W.; Doolittle, R. F. *J. Mol. Evol.* **1992**, *34*, 175. (b) Wintjens, R.; Noël, C.; May, A. C. W.; Gerbod, D.; Dufernez, F.; Capron, M.; Viscogliosi, E.; Rooman, M. *J. Biol. Chem.* **2004**, *279*, 9248. (c) Wintjens, R.; Gilis, D.; Rooman, M. *Proteins: Struct., Funct., Bioinf.* **2008**, *70*, 1564.

(189) Stoddard, B. L.; Howell, P. L.; Ringe, D.; Petsko, G. A. *Biochemistry* **1990**, *29*, 8885.

(190) Yikilmaz, E.; Xie, J.; Miller, A.-F.; Brunold, T. C. *J. Am. Chem. Soc.* **2002**, *124*, 3482.

(191) Yikilmaz, E.; Porta, J.; Grove, L. E.; Vahedi-Faridi, A.; Bronshteyn, Y.; Brunold, T. C.; Borgstahl, G. E. O.; Miller, A.-F. *J. Am. Chem. Soc.* **2007**, *129*, 9927.

(192) Miller, A.-F. *FEBS Lett.* **2012**, *586*, 585.

(193) (a) Cotruvo, J. A.; Stubbe, J. *Biochem.* **2010**, *49*. (b) Emerson, J. P.; Kovaleva, E. G.; Farquhar, E. R.; Lipscomb, J. D.; Que, L., Jr. *Proc. Natl. Acad. Sci. U.S.A.* **2008**, *105*, 7347. (c) Fielding, A. J.; Kovaleva, E. G.; Farquhar, E. R.; Lipscomb, J. D.; Que, L., Jr. *J. Biol. Inorg. Chem.* **2011**, *16*, 341. (d) Abbouni, B.; Oehlmann, W.; Stolle, P.; Pierik, A. J.; Auling, G. *Free Radical Res.* **2009**, *43*, 943.

(194) Doolittle, W. F.; Bapteste, E. *Proc. Natl. Acad. Sci. U.S.A.* **2007**, *104*, 2043.

(195) Asada, K.; Kanematsu, S.; Okaka, S.; Hayakawa, T. In *Chemical and Biochemical Aspects of Superoxide and Superoxide Dismutase*; Bannister, J. V., Hill, H. A. O., Eds.; Elsevier: New York, 1980.

(196) (a) Hatchikian, E. C.; Henry, Y. A. *Biochimie* **1977**, *59*, 153. (b) Schwartz, R. M.; Dayhoff, M. O. *Science* **1978**, *199*, 395. (c) Sousa, F. L.; Thiergart, T.; Landan, G.; Nelson-Sathi, S.; Pereira, I. A. C.; Allen, J. F.; Lane, N.; Martin, W. F. *Philos. Trans. R. Soc., B* **2013**, *368*, 20130088. (d) Brioukhanov, A.; Netrusov, A.; Sordel, M.; Thauer, R. K.; Shima, S. *Arch. Microbiol.* **2000**, *174*, 213.

(197) Wolfe-Simon, F.; Grzebyk, D.; Schofield, O.; Flakowski, P. G. *J. Phycol.* **2005**, *41*, 453.

(198) Szöllősi, G. J.; Boussau, B.; Abby, S. S.; Tannier, E.; Daubin, V. *Proc. Natl. Acad. Sci. U.S.A.* **2012**, *109*, 17513.

(199) Chan, C. X.; Beiko, R. G.; Darling, A. E.; Ragan, M. A. *Genome Bio. Evol.* **2009**, *1*, 429.

(200) Thangaraj, H. S.; Lamb, F. I.; Davis, E. O.; Jenner, P. J.; Jeyakumar, L. H.; Colston, M. J. *Infect. Immun.* **1990**, *58*, 1937.

(201) (a) Gray, M. W.; Burger, G.; Lang, B. F. *Science* **1999**, *283*, 1476. (b) van der Giezen, M. *BioScience* **2011**, *61*, 594.

(202) Martin, W.; Hoffmeisster, M.; Rotte, C.; Henze, K. *Biol. Chem.* **2001**, *382*, 1521.

(203) (a) Cooper, J. B.; McIntyre, K.; Badasso, M. O.; Wood, S. P.; Zhang, Y.; Garbe, T. R.; Young, D. *J. Mol. Biol.* **1995**, *246*, 531. (b) Borgstahl, G. E. O.; Parge, H. E.; Hickey, M. J.; Beyer, W. F., Jr.; Hallewell, R. A.; Tainer, J. A. *Cell* **1992**, *71*, 107.

(204) (a) Abby, S. S.; Tannier, E.; Gouy, M.; Daubin, V. *Proc. Natl. Acad. Sci. U.S.A.* **2012**, *109*, 4962. (b) Marri, P. R.; Bannantine, J. P.; Paustian, M. L.; Golding, G. B. *Can. J. Microbiol.* **2006**, *52*, 560. (c) Deppenmeier, U.; Johann, A.; Hartsch, T.; Merkl, R.; Schmitz, R. A.; Martinez-Arias, R.; Henne, A.; Wiezer, A.; Bäumer, S.; Jacobi, C.; Brüggemann, H.; Lienard, T.; Christmann, A.; Bömeke, M.; Steckel, S.; Bhattacharyya, A.; Lykidis, A.; Overbeek, R.; Klenk, H. P.; Gunsalus, R. P.; Fritz, H. J.; Gottschalk, G. *J. Mol. Microb. Biotechnol.* **2002**, *4*, 453.

(205) Bachega, J. F. R.; Navarro, M. V. A. S.; Bleicher, L.; Bortoleto-Bugs, R. K.; Dive, D.; Hoffmann, P.; Viscogliosi, E.; Garratt, R. C. *Proteins: Struct., Funct., Bioinf.* **2009**, *77*, 26.

(206) (a) Bowler, C.; van Camp, W.; van Montagu, M.; Inze, D. *Crit. Rev. Plant Sci.* **1994**, *13*, 199. (b) Grace, S. C. *Life Sci.* **1990**, *47*, 1875. (c) Van Camp, W.; Bowler, C.; Villarroel, R.; Tsang, E. W. T.; Van Montagu, M.; Inze, D. *Proc. Natl. Acad. Sci. U.S.A.* **1990**, *87*, 9903.

(207) Parfey, L. W.; Lahr, D. J. G.; Knoll, A. H.; Katz, L. A. *Proc. Natl. Acad. Sci. U.S.A.* **2011**, *108*, 13624.

(208) Dello Russo, A.; Rullo, R.; Nitti, G.; Masullo, M.; Bocchini, V. *Biochim. Biophys. Acta* **1997**, *1343*, 23.

(209) (a) May, B. P.; Dennis, P. P. *J. Bacteriol.* **1987**, *169*, 1417. (b) May, B. P.; Tam, P.; Dennis, P. P. *Can. J. Microbiol.* **1989**, *35*, 171.

(210) Arndt, N. T.; Nisbet, E. G. *Annu. Rev. Earth Planet. Sci.* **2012**, *40*, 521.

(211) (a) Archibald, F. S.; Duong, M.-N. *J. Bacteriol.* **1984**, *158*, 1. (b) Barnese, K.; Gralla, E. B.; Valentine, J. S.; Cabelli, D. E. *Proc. Natl. Acad. Sci. U.S.A.* **2012**, *109*, 6892. (c) Tseng, H.-J.; Srikhanta, Y.; McEwan, A. G.; Jennings, M. P. *Mol. Microbiol.* **2001**, *40*, 1175. (d) McNaughton, R. L.; Reddi, A. R.; Clement, M. H. S.; Sharma, A.; Barnese, K.; Rosenfeld, L.; Gralla, E. B.; Valentine, J. S.; Culotta, V. C.; Hoffman, B. M. *Proc. Natl. Acad. Sci. U.S.A.* **2010**, *107*, 15335.

(212) (a) Jameson, G. B.; Adams, J. J.; Hempsteadaaa, P. D.; Anderson, B. F.; Morgenstern-Badarau, I.; Whittaker, J. W.; Baker, E. N. *J. Inorg. Biochem.* **2003**, *96*, 70. (b) Hiraoka, B. Y.; Yamakura, F.; Ohmori, D. *J. Inorg. Biochem.* **1999**, *74*, 343.

(213) Culotta, V. C.; Yang, M.; Hall, M. D. *Eukaryotic Cell* **2005**, *4*, 1159.

(214) Cortez, N.; Carrillo, N.; Pasternak, C.; Balzer, A.; Klug, G. *J. Bacteriol.* **1998**, *180*, 5413.

(215) Amo, T.; Atomi, H.; Imanaka, T. *J. Bacteriol.* **2003**, *185*, 6340.

(216) (a) Whittaker, M. M.; Mizuno, K.; Bächinger, H. P.; Whittaker, J. W. *Biophys. J.* **2006**, *90*, 598. (b) Whittaker, M. M.; Whittaker, J. W. *Biochemistry* **2008**, *47*, 11625. (c) Whittaker, M. M.; Lerch, T. F.; Kirillova, O.; Chapman, M. S.; Whittaker, J. W. *Arch. Biochem. Biophys.* **2011**, *505*, 213.

(217) Parker, M. W.; Blake, C. C. F.; Barra, D.; Bossa, F.; Schinina, M. E.; Bannister, W. H.; Bannister, J. V. *Protein Eng.* **1987**, *1*, 393.

(218) Schwartz, A. L.; Yikilmaz, E.; Vance, C. K.; Vathyam, S.; Koder, R. L., Jr.; Miller, A.-F. *J. Inorg. Biochem.* **2000**, *80*, 247.

(219) Bunting, K.; Cooper, J. B.; Badasso, M. O.; Tickle, I. J.; Newton, M.; Wood, S. P.; Zhang, Y.; Young, D. *Eur. J. Biochem.* **1998**, *251*, 795.

(220) (a) Visner, G. A.; Dougall, W. C.; Wilson, J. M.; Burr, I. A.; Nick, H. S. *J. Biol. Chem.* **1990**, *265*, 2856. (b) Dhar, S. K.; St Clair, D. K. *Free Radical Biol. Med.* **2012**, *52*, 2209.

(221) McCord, J. M.; Fridovich, I. *J. Biol. Chem.* **1969**, *244*, 6049.

(222) Keele, B. B., Jr.; McCord, J. M.; Fridovich, I. *J. Biol. Chem.* **1970**, *245*, 6176.

(223) Hunter, T.; Bannister, W. H.; Hunter, G. J. *J. Biol. Chem.* **1997**, *272*, 28652.

(224) Li, Y.; Huang, T. T.; Carlson, E. J.; Melov, S.; Ursell, P. C.; Olson, J. L.; Noble, L. J.; Yoshimura, M. P.; Berger, C.; Chan, P. H.; Wallace, D. C.; Epstein, C. J. *Nat. Genet.* **1995**, *11*, 376.

(225) (a) Lebovitz, R. M.; Zhang, H.; Vogel, H.; Cartwright, J., Jr.; Dionne, L.; Lu, N.; Huang, S.; Matzuk, M. M. *Proc. Natl. Acad. Sci. U.S.A.* **1996**, *93*, 9782. (b) Williams, M. D.; Van Remmen, H.; Conrad, C. C.; Huang, T. T.; Epstein, C. J.; Richardson, A. *J. Biol. Chem.* **1998**, *273*, 28510.

(226) Reaume, A. G.; Elliott, J. L.; Hoffman, E. K.; Kowall, N. W.; Ferrante, R. J.; Siwek, D. F.; Wilcox, H. M.; Flood, D. G.; Beal, M. F.; Brown, R. H., Jr.; Scott, R. W.; Snider, W. D. *Nat. Genet.* **1996**, *13*, 43.

(227) Landis, G. N.; Tower, J. *Mech. Ageing Dev.* **2005**, *126*, 365.

(228) Holley, A. K.; Bakthavatchalu, V.; Velez-Roman, J. M.; St Clair, D. K. *Int. J. Mol. Sci.* **2011**, *12*, 7114.

(229) Borgstahl, G. E. O.; Parge, H. E.; Hickey, M. J.; Johnson, M. J.; Boissinot, M.; Hallewell, R. A.; Lepock, J. R.; Cabelli, D. E.; Tainer, J. A. *Biochemistry* **1996**, *35*, 4287.

(230) Crawford, A.; Fassett, R. G.; Geraghty, D. P.; Kunde, D. A.; Ball, M. J.; Robertson, L. K.; Coombes, J. S. *Gene* **2012**, *501*, 89.

(231) Ludwig, M. L.; Metzger, A. L.; Pattridge, K. A.; Stallings, W. C. *J. Mol. Biol.* **1991**, *219*, 335.

(232) Parker, M. W.; Blake, C. C. F. *J. Mol. Biol.* **1988**, *199*, 649.

(233) Sines, J.; Allison, S.; Wierzbicki, A.; McCammon, J. A. *J. Phys. Chem.* **1990**, *94*, 959.

(234) (a) Whittaker, M. M.; Whittaker, J. W. *Biochemistry* **1997**, *36*, 8923. (b) Perry, J. J.; Hearn, A. S.; Cabelli, D. E.; Nick, H. S.; Tainer, J. A.; Silverman, D. N. *Biochemistry* **2009**, *48*, 3417.

(235) (a) Hearn, A. S.; Stroupe, M. E.; Cabelli, D. E.; Ramilo, C. A.; Luba, J. P.; Tainer, J. A.; Nick, H. S.; Silverman, D. N. *Biochemistry* **2003**, *42*, 2781. (b) Davis, C. A.; Hearn, A. S.; Fletcher, B.; Bickford, J.; Garcia, J. E.; Leveque, V.; Melendez, J. A.; Silverman, D. N.; Zucali, J.; Agarwal, A.; Nick, H. S. *J. Biol. Chem.* **2004**, *279*, 12769.

(236) (a) Leveque, V. J.; Stroupe, M. E.; Lepock, J. R.; Cabelli, D. E.; Tainer, J. A.; Nick, H. S.; Silverman, D. N. *Biochemistry* **2000**, *39*, 7131. (b) Edwards, R. A.; Whittaker, M. M.; Whittaker, J. W.; Baker, E. N.; Jameson, G. B. *Biochemistry* **2001**, *40*, 15. (c) Hunter, T.; Bannister, J. V.; Hunter, G. J. *Eur. J. Biochem.* **2002**, *269*, 5137. (d) Castellano, I.; Cecere, F.; De Vendittis, A.; Cotugno, R.; Chambery, A.; Di Maro, A.; Michniewicz, A.; Parlato, G.; Masullo, M.; Avvedimento, E. V.; De Vendittis, E.; Ruocco, M. R. *Biopolymers* **2009**, *91*, 1215.

(237) Culotta, V. C.; Yang, M.; O'Halloran, T. V. *Biochim. Biophys. Acta, Mol. Cell Res.* **2006**, *1763*, 747.

(238) (a) Luk, E.; Carroll, M.; Baker, M.; Culotta, V. C. *Proc. Natl. Acad. Sci. U.S.A.* **2003**, *100*, 10353. (b) Luk, E.; Yang, M.; Jensen, L. T.; Bourbonnais, Y.; Culotta, V. C. *J. Biol. Chem.* **2005**, *280*, 22715.

(239) Aguirre, J. D.; Culotta, V. C. *J. Biol. Chem.* **2012**, *287*, 13541.

(240) Aguirre, J. D.; Clark, H. M.; McIlvin, M.; Vazquez, C.; Palmere, S. L.; Grab, D. J.; Seshu, J.; Hart, P. J.; Saito, M.; Culotta, V. C. *J. Biol. Chem.* **2013**, *288*, 8468.

(241) Whittaker, J. W. *Biochim. Biophys. Acta* **2010**, *1804*, 298.

(242) Whittaker, M. M.; Whittaker, J. W. *J. Biol. Chem.* **1999**, *274*, 34751.

(243) Whittaker, M. M.; Whittaker, J. W. *Arch. Biochem. Biophys.* **2009**, *491*, 69.

(244) Whittaker, M. M.; Lerch, T. F.; Kirillova, O.; Chapman, M. S.; Whittaker, J. W. *Arch. Biochem. Biophys.* **2011**, *505*, 213.

(245) Whittaker, M. M.; Whittaker, J. W. *Arch. Biochem. Biophys.* **2012**, *523*, 191.

(246) (a) Pick, M.; Rabani, J.; Yost, F.; Fridovich, I. *J. Am. Chem. Soc.* **1974**, *96*, 7329. (b) McAdam, M. E.; Fox, R. A.; Lavelle, F.; Fielden, E. M. *Biochem. J.* **1977**, *165*, 71. (c) McAdam, M. E.; Levelle, F.; Fox, R. A.; Fielden, E. M. *Biochem. J.* **1977**, *165*, 81. (d) Bull, C.; Niederhoffer, E. C.; Yoshida, T.; Fee, J. A. *J. Am. Chem. Soc.* **1991**, *113*, 4069.

(247) Hsu, J.-L.; Hsieh, Y.; Tu, C.; O'Connor, D.; Nick, H. S.; Silverman, D. N. *J. Biol. Chem.* **1996**, *271*, 17687.

(248) Abreu, I. A.; Hearn, A.; An, H.; Nick, H. S.; Silverman, D. N.; Cabelli, D. E. *Biochemistry* **2008**, *47*, 2350.

(249) Abreu, I. A.; Rodriguez, J. A.; Cabelli, D. E. *J. Phys. Chem. B* **2005**, *109*, 24502.

(250) Hearn, A. S.; Tu, C.; Nick, H. S.; Silverman, D. N. *J. Biol. Chem.* **1999**, *274*, 24457.

(251) (a) Barnese, K.; Sheng, Y.; Stich, T. A.; Gralla, E. B.; Britt, R. D.; Cabelli, D. E.; Valentine, J. S. *J. Am. Chem. Soc.* **2010**, *132*, 12525. (b) Sheng, Y.; Gralla, E. B.; Schumacher, M.; Cascio, D.; Cabelli, D. E.; Valentine, J. S. *Proc. Natl. Acad. Sci. U.S.A.* **2012**, *109*, 14314.

(252) (a) Borgstahl, G. E. O.; Pokross, M.; Chehab, R.; Sekher, A.; Snell, E. H. *J. Mol. Biol.* **2000**, *296*, 951. (b) Porta, J.; Vahedi-Faridi, A.; Borgstahl, G. E. O. *J. Mol. Biol.* **2010**, *399*, 377. (c) Tabares, L. C.; Cortez, N.; Agalidis, I.; Un, S. *J. Am. Chem. Soc.* **2005**, *127*, 6039. (d) Campbell, K. A. University of California, Davis, 1999.

(253) Edwards, R. A.; Whittaker, M. M.; Whittaker, J. W.; Baker, E. N.; Jameson, G. B. *Biochemistry* **2001**, *40*, 4622.

(254) Hearn, A. S.; Fan, L.; Lepock, J. R.; Luba, J. P.; Greenleaf, W. B.; Cabelli, D. E.; Tainer, J. A.; Nick, H. S.; Silverman, D. N. *J. Biol. Chem.* **2004**, *279*, 5861.

(255) (a) Greenleaf, W. B.; Perry, J. J. P.; Hearn, A. S.; Cabelli, D. E.; Lepock, J. R.; Stroupe, M. E.; Tainer, J. A.; Nick, H. S.; Silverman, D. N. *Biochemistry* **2004**, *43*, 7038. (b) Cabelli, D. E.; Guan, Y.; Leveque, V.; Hearn, A. S.; Tainer, J. A.; Nick, H. S.; Silverman, D. N. *Biochemistry* **1999**, *38*, 11686. (c) Hearn, A. S.; Stroupe, M. E.; Cabelli, D. E.; Lepock, J. R.; Tainer, J. A.; Nick, H. S.; Silverman, D. N. *Biochemistry* **2001**, *40*, 12051. (d) Zheng, J.; Domsic, J. F.; Cabelli, D.; McKenna, R.; Silverman, D. N. *Biochemistry* **2007**, *46*, 14830.

(256) Carrasco, R.; Morgenstern-Badarau, I.; Cano, J. *Inorg. Chim. Acta* **2007**, *360*, 91.

(257) Rulisek, L.; Jensen, K. P.; Lundgren, K.; Ryde, U. *J. Comput. Chem.* **2006**, *27*, 1398.

(258) (a) Whittaker, M. M.; Whittaker, J. W. *Biochemistry* **1996**, *35*, 6762. (b) Tabares, L. C.; Cortez, N.; Hiraoka, B. Y.; Yamakura, F.; Un, S. *Biochemistry* **2006**, *45*, 1919.

(259) Wang, W.; Fang, H.; Groom, L.; Cheng, A.; Zhang, W.; Liu, J.; Wang, X.; Li, K.; Han, P.; Zheng, M.; Yin, J.; Mattson, M. P.; Kao, J. P. Y.; Lakatta, E. G.; Sheu, S.-S.; Ouyang, K.; Chen, J.; Dirksen, R. T.; Cheng, H. *Cell* **2008**, *134*, 279.

(260) (a) Oberley, L. W. *Antioxid. Redox Signaling* **2001**, *3*, 461. (b) Policastro, L.; Molinari, B.; Larcher, F.; Blanco, P.; Podhajcer, O. L.; Costa, C. S.; Rojas, P.; Durán, H. *Mol. Carcinog.* **2004**, *39*, 103. (c) Buettner, G. R.; Ng, C. F.; Wang, M.; Rodgers, V. G. J.; Schafer, F. Q. *Free Radical Biol. Med.* **2006**, *41*, 1338.

(261) Carrico, R. J.; Deutsch, H. F. *J. Biol. Chem.* **1970**, *245*, 723.

(262) Tainer, J. A.; Getzoff, E. D.; Beem, K. M.; Richardson, J. S.; Richardson, D. C. *J. Mol. Biol.* **1982**, *160*, 181.

(263) Hjalmarsson, K.; Marklund, S. L.; Engström, A.; Edlund, T. *Proc. Natl. Acad. Sci. U.S.A.* **1987**, *84*, 6340.

(264) Goscin, S. A.; Fridovich, I. *Biochim. Biophys. Acta* **1972**, *289*, 276.

(265) (a) Bermingham-McDonogh, O.; Gralla, E. B.; Valentine, J. S. *Proc. Natl. Acad. Sci. U.S.A.* **1988**, *85*, 4789. (b) Galiazzo, F.; Carrì, M. T.; Ciriolo, M. R.; Rotilio, G. In *Metal Ions in Fungi*; Winkelmann, G., Winge, D. R., Eds.; Marcel Dekker, Inc.: New York, 1994; Vol. *11* (c) Natvig, D. O.; Dvorachek, W. H., Jr.; Sylvester, K. In *Metal Ions in Fungi*; Winkelmann, G., Winge, D. R., Eds.; Marcel Dekker, Inc.: New York, 1994; Vol. *11*.

(266) Furukawa, Y.; Torres, A. S.; O'Halloran, T. V. *EMBO J.* **2004**, *23*, 2872.

(267) (a) Gralla, E. B.; Valentine, J. S. *J. Bacteriol.* **1991**, *173*, 5918. (b) Luk, E.; Jensen, L. T.; Culotta, V. C. *J. Biol. Inorg. Chem.* **2003**, *8*, 803. (c) Gonidakis, S.; Longo, V. D. In *Oxidative Stress in Aging*; Miwa, S., Beckman, K. B., Muller, F. L., Eds.; Humana Press: Totowa, NJ, 2008.

(268) Puget, K.; Michelson, A. M. *Biochem. Biophys. Res. Commun.* **1974**, *58*, 830.

(269) (a) Fridovich, I. *J. Biol. Chem.* **1997**, *272*, 18515. (b) Imlay, K. R.; Imlay, J. A. *J. Bacteriol.* **1996**, *178*, 2564.

(270) (a) Valentine, J. S.; Hart, P. J. *Proc. Natl. Acad. Sci. U.S.A.* **2003**, *100*, 3617. (b) Shaw, B. F.; Valentine, J. S. *Trends Biochem. Sci.* **2007**, *32*, 78. (c) Hart, P. J. *Curr. Opin. Chem. Biol.* **2006**, *10*, 131. (d) Furukawa, Y.; O'Halloran, T. V. *Antioxid. Redox Signaling* **2006**, *8*,

847. (e) Bertini, I.; Mangani, S.; Viezzoli, M. S. *Advances in Inorganic Chemistry*; Academic Press: New York, 1998; Vol. *45*.

(271) Rosen, D. R.; Siddique, T.; Patterson, D.; Figlewicz, D. A.; Sapp, P.; Hentati, A.; Donaldson, D.; Goto, J.; O'Regan, J. P.; Deng, H.-X.; et al. *Nature* **1993**, *362*, 59.

(272) (a) Doucette, P. A.; Whitson, L. J.; Cao, X.; Schirf, V.; Demeler, B.; Valentine, J. S.; Hansen, J. C.; Hart, P. J. *J. Biol. Chem.* **2004**, *279*, 54558. (b) Potter, S. Z.; Zhu, H.; Shaw, B. F.; Rodriguez, J. A.; Doucette, P. A.; Sohn, S. H.; Durazo, A.; Faull, K. F.; Gralla, E. B.; Nersissian, A. M.; Valentine, J. S. *J. Am. Chem. Soc.* **2007**, *129*, 4575.

(273) (a) Bannister, J. V.; Anastasi, A.; Bannister, W. H. *Biochem. Biophys. Res. Commun.* **1978**, *81*, 469. (b) Marmocchi, F.; Venardi, G.; Bossa, F.; Rigo, A.; Rotilio, G. *FEBS Lett.* **1978**, *94*, 109.

(274) (a) Mei, G.; Rosato, N.; Silva, N., Jr.; Rusch, R.; Gratton, E.; Savini, I.; Finazzi-Agro, A. *Biochemistry* **1992**, *31*, 7224. (b) Silva, N., Jr.; Gratton, E.; Mei, G.; Rosato, N.; Rusch, R.; Finazzi-Agro, A. *Biophys. Chem.* **1993**, *48*, 171.

(275) (a) Rigo, A.; Marmocchi, F.; Cocco, D.; Viglino, P.; Rotilio, G. *Biochemistry* **1978**, *17*, 534. (b) Marmocchi, F.; Venardi, G.; Caulini, G.; Rotilio, G. *FEBS Lett.* **1974**, *44*, 337.

(276) (a) Lindberg, M. J.; Byström, R.; Boknäs, N.; Andersen, P. M.; Oliveberg, M. *Proc. Natl. Acad. Sci. U.S.A.* **2005**, *102*, 9754. (b) Hough, M. A.; Grossmann, J. G.; Antonyuk, S. V.; Strange, R. W.; Doucette, P. A.; Rodriguez, J. A.; Whitson, L. J.; Hart, P. J.; Hayward, L. J.; Valentine, J. S.; Hasnain, S. S. *Proc. Natl. Acad. Sci. U.S.A.* **2004**, *101*, 5976.

(277) Arnold, L. D.; Lepock, J. R. *FEBS Lett.* **1982**, *146*, 302.

(278) Kadokura, H.; Katzen, F.; Beckwith, J. *Annu. Rev. Biochem.* **2003**, *72*, 111.

(279) Leitch, J. M.; Jensen, L. T.; Bouldin, S. D.; Outten, C. E.; Hart, P. J.; Culotta, V. C. *J. Biol. Chem.* **2009**, *284*, 21863.

(280) Bouldin, S. D.; Darch, M. A.; Hart, P. J.; Outten, C. E. *Biochem. J.* **2012**, *446*, 59.

(281) Roe, J. A.; Butler, A.; Scholler, D. M.; Valentine, J. S.; Marky, L.; Breslauer, K. J. *Biochemistry* **1988**, *27*, 950.

(282) Chattopadhyay, M.; Valentine, J. S. *Antioxid. Redox Signaling* **2009**, *11*, 1603.

(283) Lyons, T. J.; Nersissian, A.; Goto, J. J.; Zhu, H.; Gralla, E. B.; Valentine, J. S. *J. Biol. Inorg. Chem.* **1998**, *3*, 650.

(284) Das, A.; Plotkin, S. S. *Proc. Natl. Acad. Sci. U.S.A.* **2013**, *110*, 3871.

(285) (a) Banci, L.; Barbieri, L.; Bertini, I.; Luchinat, E.; Secci, E.; Zhao, Y.; Aricescu, A. R. *Nat. Chem. Biol.* **2013**, *9*, 297. (b) Banci, L.; Bertini, I.; Cantini, F.; D'Onofrio, M.; Viezzoli, M. S. *Protein Sci.* **2002**, *11*, 2479. (c) Banci, L.; Barbieri, L.; Bertini, I.; Cantini, F.; Luchinat, E. *PloS One* **2011**, *6*, e23561.

(286) (a) Wang, J.; Caruano-Yzermans, A.; Rodriguez, A.; Scheurmann, J. P.; Slunt, H. H.; Cao, X. H.; Gitlin, J.; Hart, P. J.; Borchelt, D. R. *J. Biol. Chem.* **2007**, *282*, 345. (b) Petrovic, N.; Comi, A.; Ettinger, M. J. *J. Biol. Chem.* **1996**, *271*, 28331. (c) Bartnikas, T. B.; Gitlin, J. D. *J. Biol. Chem.* **2003**, *278*, 33602.

(287) Ellerby, L. M.; Cabelli, D. E.; Graden, J. A.; Valentine, J. S. *J. Am. Chem. Soc.* **1996**, *118*, 6556.

(288) (a) Borders, C. L., Jr.; Johansen, J. T. *Biochem. Biophys. Res. Commun.* **1980**, *96*, 1071. (b) Cudd, A.; Fridovich, I. *J. Biol. Chem.* **1982**, *257*, 11443. (c) Fisher, C. L.; Cabelli, D. E.; Tainer, J. A.; Hallewell, R. A.; Getzoff, E. D. *Proteins* **1994**, *19*, 24.

(289) (a) Viglino, P.; Scarpa, M.; Rotilio, G.; Rigo, A. *Biochim. Biophys. Acta* **1988**, *952*, 77. (b) Cabelli, D. E.; Allen, D.; Bielski, B. H.; Holcman, J. *J. Biol. Chem.* **1989**, *264*, 9967.

(290) Elam, J. S.; Malek, K.; Rodriguez, J. A.; Doucette, P. A.; Taylor, A. B.; Hayward, L. J.; Cabelli, D. E.; Valentine, J. S.; Hart, P. J. *J. Biol. Chem.* **2003**, *278*, 21032.

(291) Ranguelova, K.; Ganini, D.; Bonini, M. G.; London, R. E.; Mason, R. P. *Free Radical Biol. Med.* **2012**, *53*, 589.

(292) Strange, R. W.; Hough, M. A.; Antonyuk, S. V.; Hasnain, S. S. *PloS One* **2012**, *7*, e44811.

(293) (a) Liochev, S. I.; Fridovich, I. *Proc. Natl. Acad. Sci. U.S.A.* **2004**, *101*, 743. (b) Liochev, S. I.; Fridovich, I. *Free Radical Biol. Med.* **2010**, *48*, 1565.

(294) Lamb, A. L.; Torres, A. S.; O'Halloran, T. V.; Rosenzweig, A. C. *Nat. Struct. Biol.* **2001**, *8*, 751.

(295) Carroll, M. C.; Girouard, J. B.; Ulloa, J. L.; Subramaniam, J. R.; Wong, P. C.; Valentine, J. S.; Culotta, V. C. *Proc. Natl. Acad. Sci. U.S.A.* **2004**, *101*, 5964.

(296) Sea, K. W.; Sheng, Y.; Lelie, H. L.; Kane Barnese, L.; Durazo, A.; Valentine, J. S.; Gralla, E. B. *J. Biol. Inorg. Chem.* **2013**, *18*, 985.

(297) Banci, L.; Bertini, I.; Cantini, F.; Kozyreva, T.; Massagni, C.; Palumaa, P.; Rubino, J. T.; Zovo, K. *Proc. Natl. Acad. Sci. U.S.A.* **2012**, *109*, 13555.

(298) Allen, S.; Badarau, A.; Dennison, C. *Biochemistry* **2012**, *51*, 1439.

(299) Sturtz, L. A.; Diekert, K.; Jensen, L. T.; Lill, R.; Culotta, V. C. *J. Biol. Chem.* **2001**, *276*, 38084.

(300) (a) Liu, X. F.; Elashvili, I.; Gralla, E. B.; Valentine, J. S.; Lapinskas, P.; Culotta, V. C. *J. Biol. Chem.* **1992**, *267*, 18298. (b) De Freitas, J. M.; Liba, A.; Meneghini, R.; Valentine, J. S.; Gralla, E. B. *J. Biol. Chem.* **2000**, *275*, 11645. (c) Wallace, M. A.; Liou, L. L.; Martins, J.; Clement, M. H.; Bailey, S.; Longo, V. D.; Valentine, J. S.; Gralla, E. B. *J. Biol. Chem.* **2004**, *279*, 32055. (d) Sanchez, R. J.; Srinivasan, C.; Munroe, W. H.; Wallace, M. A.; Martins, J.; Kao, T. Y.; Le, K.; Gralla, E. B.; Valentine, J. S. *J. Biol. Inorg. Chem.* **2005**, *10*, 913. (e) Sehati, S.; Clement, M. H.; Martins, J.; Xu, L.; Longo, V. D.; Valentine, J. S.; Gralla, E. B. *Free Radical Biol. Med.* **2011**, *50*, 1591. (f) Jensen, L. T.; Sanchez, R. J.; Srinivasan, C.; Valentine, J. S.; Culotta, V. C. *J. Biol. Chem.* **2004**, *279*, 29938.

(301) Longo, V. D.; Gralla, E. B.; Valentine, J. S. *J. Biol. Chem.* **1996**, *271*, 12275.

(302) Reddi, A. R.; Culotta, V. C. *Cell* **2013**, *152*, 224.

(303) Sanchez, R. University of California, Los Angeles, 2003.

(304) Phillips, J. P.; Campbell, S. D.; Michaud, D.; Charbonneau, M.; Hilliker, A. J. *Proc. Natl. Acad. Sci. U.S.A.* **1989**, *86*, 2761.

(305) Van Raamsdonk, J. M.; Hekimi, S. *Antioxid. Redox Signaling* **2010**, *13*, 1911.

(306) Van Raamsdonk, J. M.; Hekimi, S. *Proc. Natl. Acad. Sci. U.S.A.* **2012**, *109*, 5785.

(307) (a) Pérez, V. I.; Bokov, A.; Van Remmen, H.; Mele, J.; Ran, Q.; Ikeno, Y.; Richardson, A. *Biochim. Biophys. Acta* **2009**, *1790*, 1005. (b) Elchuri, S.; Oberley, T. D.; Qi, W.; Eisenstein, R. S.; Jackson Roberts, L.; Van Remmen, H.; Epstein, C. J.; Huang, T. T. *Oncogene* **2005**, *24*, 367.

(308) (a) Ho, Y.-S.; Gargano, M.; Cao, J.; Bronson, R. T.; Heimler, I.; Hutz, R. J. *J. Biol. Chem.* **1998**, *273*, 7765. (b) Matzuk, M. M.; Dionne, L.; Guo, Q.; Kumar, T. R.; Lebovitz, R. M. *Endocrinology* **1998**, *139*, 4008. (c) Noda, Y.; Ota, K.; Shirasawa, T.; Shimizu, T. *Biol. Reprod.* **2012**, *86*, 1.

(309) (a) Flood, D. G.; Reaume, A. G.; Gruner, J. A.; Hoffman, E. K.; Hirsch, J. D.; Lin, Y. G.; Dorfman, K. S.; Scott, R. W. *Am. J. Pathol.* **1999**, *155*, 663. (b) Muller, F. L.; Song, W.; Liu, Y.; Chaudhuri, A.; Pieke-Dahl, S.; Strong, R.; Huang, T. T.; Epstein, C. J.; Roberts, L. J., II; Csete, M.; Faulkner, J. A.; Van Remmen, H. *Free Radical Biol. Med.* **2006**, *40*, 1993. (c) Jang, Y. C.; Lustgarten, M. S.; Liu, Y.; Muller, F. L.; Bhattacharya, A.; Liang, H.; Salmon, A. B.; Brooks, S. V.; Larkin, L.; Hayworth, C. R.; Richardson, A.; Van Remmen, H. *FASEB J.* **2010**, *24*, 1376. (d) Fischer, L. R.; Igoudjil, A.; Magrane, J.; Li, Y.; Hansen, J. M.; Manfredi, G.; Glass, J. D. *Brain* **2011**, *134*, 196. (e) Fischer, L. R.; Li, Y.; Asress, S. A.; Jones, D. P.; Glass, J. D. *Exp. Neurol.* **2012**, *233*, 163.

(310) (a) Keithley, E. M.; Canto, C.; Zheng, Q. Y.; Wang, X.; Fischel-Ghodsian, N.; Johnson, K. R. *Hear Res.* **2005**, *209*, 76. (b) McFadden, S. L.; Ding, D. L.; Reaume, A. G.; Flood, D. G.; Salvi, R. J. *Neurobiol. Aging* **1999**, *20*, 1.

(311) (a) Imamura, Y.; Noda, S.; Hashizume, K.; Shinoda, K.; Yamaguchi, M.; Uchiyama, S.; Shimizu, T.; Mizushima, Y.; Shirasawa, T.; Tsubota, K. *Proc. Natl. Acad. Sci. U.S.A.* **2006**, *103*, 11282. (b) Hashizume, K.; Hirasawa, M.; Imamura, Y.; Noda, S.; Shimizu, T.;

3915

dx.doi.org/10.1021/cr4005296 | *Chem. Rev.* 2014, 114, 3854−3918

Shinoda, K.; Kurihara, T.; Noda, K.; Ozawa, Y.; Ishida, S.; Miyake, Y.; Shirasawa, T.; Tsubota, K. *Am. J. Pathol.* **2008**, *172*, 1325.

(312) Olofsson, E. M.; Marklund, S. L.; Behndig, A. *Clin. Exp. Ophthalmol.* **2012**, *40*, 813.

(313) (a) Gort, A. S.; Ferber, D. M.; Imlay, J. A. *Mol. Microbiol.* **1999**, *32*, 179. (b) Wilks, K. E.; Dunn, K. L.; Farrant, J. L.; Reddin, K. M.; Gorringe, A. R.; Langford, P. R.; Kroll, J. S. *Infect. Immun.* **1998**, *66*, 213.

(314) De Groote, M. A.; Ochsner, U. A.; Shiloh, M. U.; Nathan, C.; McCord, J. M.; Dinauer, M. C.; Libby, S. J.; Vazquez-Torres, A.; Xu, Y.; Fang, F. C. *Proc. Natl. Acad. Sci. U.S.A.* **1997**, *94*, 13997.

(315) Schnell, S.; Steinman, H. M. *J. Bacteriol.* **1995**, *177*, 5924.

(316) (a) Seetharaman, S. V.; Prudencio, M.; Karch, C.; Holloway, S. P.; Borchelt, D. R.; Hart, P. J. *Exp. Biol. Med. (Maywood)* **2009**, *234*, 1140. (b) Pasinelli, P.; Brown, R. H. *Nat. Rev. Neurosci.* **2006**, *7*, 710.

(317) (a) Hayward, L. J.; Rodriguez, J. A.; Kim, J. W.; Tiwari, A.; Goto, J. J.; Cabelli, D. E.; Valentine, J. S.; Brown, R. H., Jr. *J. Biol. Chem.* **2002**, *277*, 15923. (b) Rodriguez, J. A.; Valentine, J. S.; Eggers, D. K.; Roe, J. A.; Tiwari, A.; Brown, R. H., Jr.; Hayward, L. J. *J. Biol. Chem.* **2002**, *277*, 15932. (c) Potter, S. Z.; Valentine, J. S. *J. Biol. Inorg. Chem.* **2003**, *8*, 373.

(318) (a) Sheng, Y.; Chattopadhyay, M.; Whitelegge, J.; Valentine, J. S. *Curr. Top. Med. Chem.* **2012**, *12*, 2560. (b) Boillée, S.; Vande Velde, C.; Cleveland, D. W. *Neuron* **2006**, *52*, 39.

(319) Bruijn, L. I.; Becher, M. W.; Lee, M. K.; Anderson, K. L.; Jenkins, N. A.; Copeland, N. G.; Sisodia, S. S.; Rothstein, J. D.; Borchelt, D. R.; Price, D. L.; Cleveland, D. W. *Neuron* **1997**, *18*, 327.

(320) Borchelt, D. R.; Lee, M. K.; Slunt, H. S.; Guarnieri, M.; Xu, Z. S.; Wong, P. C.; Brown, R. H., Jr.; Price, D. L.; Sisodia, S. S.; Cleveland, D. W. *Proc. Natl. Acad. Sci. U.S.A.* **1994**, *91*, 8292.

(321) Chiti, F.; Dobson, C. M. *Annu. Rev. Biochem.* **2006**, *75*, 333.

(322) (a) Cleveland, D. W.; Rothstein, J. D. *Nat. Rev. Neurosci.* **2001**, *2*, 806. (b) Bruijn, L. I.; Miller, T. M.; Cleveland, D. W. *Annu. Rev. Neurosci.* **2004**, *27*, 723. (c) Rakhit, R.; Chakrabartty, A. *Biochim. Biophys. Acta* **2006**, *1762*, 1025. (d) Ross, C. A.; Poirier, M. A. *Nat. Med.* **2004**, *10*, S10.

(323) (a) Grad, L. I.; Guest, W. C.; Yanai, A.; Pokrishevsky, E.; O'Neill, M. A.; Gibbs, E.; Semenchenko, V.; Yousefi, M.; Wishart, D. S.; Plotkin, S. S.; Cashman, N. R. *Proc. Natl. Acad. Sci. U.S.A.* **2011**, *108*, 16398. (b) Münch, C.; O'Brien, J.; Bertolotti, A. *Proc. Natl. Acad. Sci. U.S.A.* **2011**, *108*, 3548. (c) Sundaramoorthy, V.; Walker, A. K.; Yerbury, J.; Soo, K. Y.; Farg, M. A.; Hoang, V.; Zeineddine, R.; Spencer, D.; Atkin, J. D. *Cell. Mol. Life Sci.* **2013**.

(324) (a) Polymenidou, M.; Cleveland, D. W. *Cell* **2011**, *147*, 498. (b) Wood, J. D.; Beaujeux, T. P.; Shaw, P. J. *Neuropathol. Appl. Neurobiol.* **2003**, *29*, 529. (c) Mulligan, V. K.; Chakrabartty, A. *Proteins* **2013**, *81*, 1285.

(325) (a) Jonsson, P. A.; Graffmo, K. S.; Andersen, P. M.; Brännström, T.; Lindberg, M.; Oliveberg, M.; Marklund, S. L. *Brain* **2006**, *129*, 451. (b) Zetterström, P.; Stewart, H. G.; Bergemalm, D.; Jonsson, P. A.; Graffmo, K. S.; Andersen, P. M.; Brännström, T.; Oliveberg, M.; Marklund, S. L. *Proc. Natl. Acad. Sci. U.S.A.* **2007**, *104*, 14157.

(326) Rakhit, R.; Robertson, J.; Vande Velde, C.; Horne, P.; Ruth, D. M.; Griffin, J.; Cleveland, D. W.; Cashman, N. R.; Chakrabartty, A. *Nat. Med.* **2007**, *13*, 754.

(327) Banci, L.; Bertini, I.; Durazo, A.; Girotto, S.; Gralla, E. B.; Martinelli, M.; Valentine, J. S.; Vieru, M.; Whitelegge, J. P. *Proc. Natl. Acad. Sci. U.S.A.* **2007**, *104*, 11263.

(328) (a) Furukawa, Y.; Kaneko, K.; Yamanaka, K.; O'Halloran, T. V.; Nukina, N. *J. Biol. Chem.* **2008**, *283*, 24167. (b) Chattopadhyay, M.; Durazo, A.; Sohn, S. H.; Strong, C. D.; Gralla, E. B.; Whitelegge, J. P.; Valentine, J. S. *Proc. Natl. Acad. Sci. U.S.A.* **2008**, *105*, 18663. (c) Oztug Durer, Z. A.; Cohlberg, J. A.; Dinh, P.; Padua, S.; Ehrenclou, K.; Downes, S.; Tan, J. K.; Nakano, Y.; Bowman, C. J.; Hoskins, J. L.; Kwon, C.; Mason, A. Z.; Rodriguez, J. A.; Doucette, P. A.; Shaw, B. F.; Silverstone Valentine, J. *PloS One* **2009**, *4*, e5004.

(329) Chan, P. K.; Chattopadhyay, M.; Sharma, S.; Souda, P.; Gralla, E. B.; Borchelt, D. R.; Whitelegge, J. P.; Valentine, J. S. *Proc. Natl. Acad. Sci. U.S.A.* **2013**, *110*, 10934.

(330) Galaleldeen, A.; Strange, R. W.; Whitson, L. J.; Antonyuk, S. V.; Narayana, N.; Taylor, A. B.; Schuermann, J. P.; Holloway, S. P.; Hasnain, S. S.; Hart, P. J. *Arch. Biochem. Biophys.* **2009**, *492*, 40.

(331) Hart, P. J.; Liu, H.; Pellegrini, M.; Nersissian, A. M.; Gralla, E. B.; Valentine, J. S.; Eisenberg, D. *Protein Sci.* **1998**, *7*, 545.

(332) DiDonato, M.; Craig, L.; Huff, M. E.; Thayer, M. M.; Cardoso, R. M.; Kassmann, C. J.; Lo, T. P.; Bruns, C. K.; Powers, E. T.; Kelly, J. W.; Getzoff, E. D.; Tainer, J. A. *J. Mol. Biol.* **2003**, *332*, 601.

(333) Banci, L.; Bertini, I.; Boca, M.; Calderone, V.; Cantini, F.; Girotto, S.; Vieru, M. *Proc. Natl. Acad. Sci. U.S.A.* **2009**, *106*, 6980.

(334) Elam, J. S.; Taylor, A. B.; Strange, R.; Antonyuk, S.; Doucette, P. A.; Rodriguez, J. A.; Hasnain, S. S.; Hayward, L. J.; Valentine, J. S.; Yeates, T. O.; Hart, P. J. *Nat. Struct. Biol.* **2003**, *10*, 461.

(335) Cao, X.; Antonyuk, S. V.; Seetharaman, S. V.; Whitson, L. J.; Taylor, A. B.; Holloway, S. P.; Strange, R. W.; Doucette, P. A.; Valentine, J. S.; Tiwari, A.; Hayward, L. J.; Padua, S.; Cohlberg, J. A.; Hasnain, S. S.; Hart, P. J. *J. Biol. Chem.* **2008**, *283*, 16169.

(336) Seetharaman, S. V.; Winkler, D. D.; Taylor, A. B.; Cao, X. H.; Whitson, L. J.; Doucette, P. A.; Valentine, J. S.; Schirf, V.; Demeler, B.; Carroll, M. C.; Culotta, V. C.; Hart, P. J. *Biochemistry* **2010**, *49*, 5714.

(337) Winkler, D. D.; Schuermann, J. P.; Cao, X.; Holloway, S. P.; Borchelt, D. R.; Carroll, M. C.; Proescher, J. B.; Culotta, V. C.; Hart, P. J. *Biochemistry* **2009**, *48*, 3436.

(338) (a) Antonyuk, S.; Elam, J. S.; Hough, M. A.; Strange, R. W.; Doucette, P. A.; Rodriguez, J. A.; Hayward, L. J.; Valentine, J. S.; Hart, P. J.; Hasnain, S. S. *Protein Sci.* **2005**, *14*, 1201. (b) Strange, R. W.; Antonyuk, S.; Hough, M. A.; Doucette, P. A.; Rodriguez, J. A.; Hart, P. J.; Hayward, L. J.; Valentine, J. S.; Hasnain, S. S. *J. Mol. Biol.* **2003**, *328*, 877.

(339) (a) Watanabe, M.; Dykes-Hoberg, M.; Culotta, V. C.; Price, D. L.; Wong, P. C.; Rothstein, J. D. *Neurobiol. Dis.* **2001**, *8*, 933. (b) Wang, J.; Xu, G.; Borchelt, D. R. *Neurobiol. Dis.* **2002**, *9*, 139.

(340) Durazo, A.; Shaw, B. F.; Chattopadhyay, M.; Faull, K. F.; Nersissian, A. M.; Valentine, J. S.; Whitelegge, J. P. *J. Biol. Chem.* **2009**, *284*, 34382.

(341) Shaw, B. F.; Durazo, A.; Nersissian, A. M.; Whitelegge, J. P.; Faull, K. F.; Valentine, J. S. *J. Biol. Chem.* **2006**, *281*, 18167.

(342) Shipp, E. L.; Cantini, F.; Bertini, I.; Valentine, J. S.; Banci, L. *Biochemistry* **2003**, *42*, 1890.

(343) Banci, L.; Bertini, I.; D'Amelio, N.; Gaggelli, E.; Libralesso, E.; Matecko, I.; Turano, P.; Valentine, J. S. *J. Biol. Chem.* **2005**, *280*, 35815.

(344) (a) Kayatekin, C.; Zitzewitz, J. A.; Matthews, C. R. *J. Mol. Biol.* **2010**, *398*, 320. (b) Svensson, A.-K.; Bilsel, O.; Kayatekin, C.; Adefusika, J. A.; Zitzewitz, J. A.; Matthews, C. R. *PloS One* **2010**, *5*, e10064.

(345) Teilum, K.; Smith, M. H.; Schulz, E.; Christensen, L. C.; Solomentsev, G.; Oliveberg, M.; Akke, M. *Proc. Natl. Acad. Sci. U.S.A.* **2009**, *106*, 18273.

(346) Ip, P.; Mulligan, V. K.; Chakrabartty, A. *J. Mol. Biol.* **2011**, *409*, 839.

(347) Tiwari, A.; Hayward, L. J. *J. Biol. Chem.* **2003**, *278*, 5984.

(348) Lindberg, M. J.; Tibell, L.; Oliveberg, M. *Proc. Natl. Acad. Sci. U.S.A.* **2002**, *99*, 16607.

(349) Rodriguez, J. A.; Shaw, B. F.; Durazo, A.; Sohn, S. H.; Doucette, P. A.; Nersissian, A. M.; Faull, K. F.; Eggers, D. K.; Tiwari, A.; Hayward, L. J.; Valentine, J. S. *Proc. Natl. Acad. Sci. U.S.A.* **2005**, *102*, 10516.

(350) (a) Vassall, K. A.; Stubbs, H. R.; Primmer, H. A.; Tong, M. S.; Sullivan, S. M.; Sobering, R.; Srinivasan, S.; Briere, L.-A.; Dunn, S. D.; Colón, W.; Meiering, E. M. *Proc. Natl. Acad. Sci. U.S.A.* **2011**, *108*, 2210. (b) Furukawa, Y.; O'Halloran, T. V. *J. Biol. Chem.* **2005**, *280*, 17266.

(351) Rotunno, M. S.; Bosco, D. A. *Front. Cell. Neurosci.* **2013**, *7*, 253.

(352) Bosco, D. A.; Morfini, G.; Karabacak, N. M.; Song, Y.; Gros-Louis, F.; Pasinelli, P.; Goolsby, H.; Fontaine, B. A.; Lemay, N.;

3916

dx.doi.org/10.1021/cr4005296 | *Chem. Rev.* 2014, 114, 3854–3918

McKenna-Yasek, D.; Frosch, M. P.; Agar, J. N.; Julien, J. P.; Brady, S. T.; Brown, R. H., Jr. *Nat. Neurosci.* **2010**, *13*, 1396.

(353) Haidet-Phillips, A. M.; Hester, M. E.; Miranda, C. J.; Meyer, K.; Braun, L.; Frakes, A.; Song, S.; Likhite, S.; Murtha, M. J.; Foust, K. D.; Rao, M.; Eagle, A.; Kammesheidt, A.; Christensen, A.; Mendell, J. R.; Burghes, A. H.; Kaspar, B. K. *Nat. Biotechnol.* **2011**, *29*, 824.

(354) Takeuchi, S.; Fujiwara, N.; Ido, A.; Oono, M.; Takeuchi, Y.; Tateno, M.; Suzuki, K.; Takahashi, R.; Tooyama, I.; Taniguchi, N.; Julien, J. P.; Urushitani, M. *J. Neuropathol. Exp. Neurol.* **2010**, *69*, 1044.

(355) Graffmo, K. S.; Forsberg, K.; Bergh, J.; Birve, A.; Zetterstrom, P.; Andersen, P. M.; Marklund, S. L.; Brännström, T. *Hum. Mol. Genet.* **2013**, *22*, 51.

(356) Ivanova, M. I.; Sievers, S. A.; Guenther, E. L.; Johnson, L. M.; Winkler, D. D.; Galaleldeen, A.; Sawaya, M. R.; Hart, P. J.; Eisenberg, D. S. *Proc. Natl. Acad. Sci. U.S.A.* **2014**, *111*, 197.

(357) (a) Ezzi, S. A.; Urushitani, M.; Julien, J. P. *J. Neurochem.* **2007**, *102*, 170. (b) Rakhit, R.; Cunningham, P.; Furtos-Matei, A.; Dahan, S.; Qi, X. F.; Crow, J. P.; Cashman, N. R.; Kondejewski, L. H.; Chakrabartty, A. *J. Biol. Chem.* **2002**, *277*, 47551.

(358) Guareschi, S.; Cova, E.; Cereda, C.; Ceroni, M.; Donetti, E.; Bosco, D. A.; Trotti, D.; Pasinelli, P. *Proc. Nat. Acad. Sci. U.S.A.* **2012**, *109*, 5074.

(359) Urushitani, M.; Sik, A.; Sakurai, T.; Nukina, N.; Takahashi, R.; Julien, J. P. *Nat. Neurosci.* **2006**, *9*, 108.

(360) Andersen, J. K. *Nat. Rev. Neurosci.* **2004**, *5*, S18.

(361) Moura, I.; Tavares, P.; Moura, J. J. G.; Ravi, N.; Huynh, B. H.; Liu, M. Y.; Legall, J. *J. Biol. Chem.* **1990**, *265*, 21596.

(362) Chen, L.; Sharma, P.; Le Gall, J.; Mariano, A. M.; Teixeira, M.; Xavier, A. V. *Eur. J. Biochem.* **1994**, *226*, 613.

(363) Tavares, P.; Ravi, N.; Moura, J. J. G.; LeGall, J.; Huang, Y.-H.; Crouse, B. R.; Johnson, M. K.; Huynh, B. H.; Moura, I. *J. Biol. Chem.* **1994**, *269*, 10504.

(364) (a) Moura, I.; Bruschi, M.; Le Gall, J.; Moura, J. J. G.; Xavier, A. V. *Biochem. Biophys. Res. Commun.* **1977**, *75*, 1037. (b) Archer, M.; Huber, R.; Tavares, P.; Moura, I.; Moura, J. J. G.; Carrondo, M. A.; Sieker, L. C.; LeGall, J.; Romao, M. J. *J. Mol. Biol.* **1995**, *251*, 690.

(365) Brumlik, M. J.; Voordouw, G. *J. Bacteriol.* **1989**, *171*, 4996.

(366) Pianzzola, M. J.; Soubes, M.; Touati, D. *J. Bacteriol.* **1996**, *178*, 6736.

(367) (a) Silva, G.; LeGall, J.; Xavier, A. V.; Teixeira, M.; Rodrigues-Pousada, C. *J. Bacteriol.* **2001**, *183*, 4413. (b) Emerson, J. P.; Cabelli, D. E.; Kurtz, D. M., Jr. *Proc. Natl. Acad. Sci. U.S.A.* **2003**, *100*, 3802. (c) Lumppio, H. L.; Shenvi, N. V.; Summers, A. O.; Voordouw, G.; Kurtz, D. M., Jr. *J. Bacteriol.* **2001**, *183*, 101.

(368) (a) Silva, G.; Oliveira, S.; Gomes, C. M.; Pacheco, I.; Liu, M. Y.; Xavier, A. V.; Teixeira, M.; LeGall, J.; Rodrigues-Pousada, C. *Eur. J. Biochem.* **1999**, *259*, 235. (b) Romão, C. V.; Liu, M. Y.; Le Gall, J.; Gomes, C. M.; Braga, V.; Pacheco, I.; Xavier, A. V.; Teixeira, M. *Eur. J. Biochem.* **1999**, *261*, 438. (c) Abreu, I. A.; Saraiva, L. M.; Carita, J.; Huber, H.; Stetter, K. O.; Cabelli, D.; Teixeira, M. *Mol. Microbiol.* **2000**, *38*, 322.

(369) Liochev, S. I.; Fridovich, I. *J. Biol. Chem.* **1997**, *272*, 25573.

(370) (a) Jenney, F. E., Jr.; Verhagen, M. F. J. M.; Cui, X.; Adams, M. W. W. *Science* **1999**, *286*, 306. (b) Lombard, M.; Fontecave, M.; Touati, D.; Nivière, V. *J. Biol. Chem.* **2000**, *275*, 115. (c) Katona, G.; Carpentier, P.; Nivière, V.; Amara, P.; Adam, V.; Ohana, J.; Tsanov, N.; Bourgeois, D. *Science* **2007**, *316*, 449.

(371) Coulter, E. D.; Emerson, J. P.; Kurtz, D. M.; Cabelli, D. E. *J. Am. Chem. Soc.* **2000**, *122*, 11555.

(372) (a) Nivière, V.; Lombard, M.; Fontecave, M.; Houée-Levin, C. *FEBS Lett.* **2001**, *497*, 171. (b) Abreu, I. A.; Saraiva, L. M.; Soares, C. M.; Teixeira, M.; Cabelli, D. E. *J. Biol. Chem.* **2001**, *276*, 38995. (c) Emerson, J. P.; Coulter, E. D.; Cabelli, D. E.; Phillips, R. S.; Kurtz, D. M., Jr. *Biochemistry* **2002**, *41*, 4348. (d) Nivière, V.; Asso, M.; Weill, C. O.; Lombard, M.; Guigliarelli, B.; Favaudon, V.; Houée-Levin, C. *Biochemistry* **2004**, *43*, 808. (e) Rodrigues, J. V.; Abreu, I. A.; Cabelli, D.; Teixeira, M. *Biochemistry* **2006**, *45*, 9266. (f) Rodrigues, J. V.; Saraiva, L. M.; Abreu, I. A.; Teixeira, M.; Cabelli, D. E. *J. Biol. Inorg. Chem.* **2007**, *12*, 248. (g) Lombard, M.; Houée-Levin, C.; Touati, D.;

Fontecave, M.; Nivière, V. *Biochemistry* **2001**, *40*, 5032. (h) Rodrigues, J. V.; Victor, B. L.; Huber, H.; Saraiva, L. M.; Soares, C. M.; Cabelli, D. E.; Teixeira, M. *J. Biol. Inorg. Chem.* **2008**, *13*, 219. (i) Mathé, C.; Nivière, V.; Houée-Levin, C.; Mattioli, T. A. *Biophys. Chem.* **2006**, *119*, 38.

(373) Voordouw, J. K.; Voordouw, G. *Appl. Environ. Microbiol.* **1998**, *64*, 2882.

(374) Kawasaki, S.; Watamura, Y.; Ono, M.; Watanabe, T.; Takeda, K.; Niimura, Y. *Appl. Environ. Microbiol.* **2005**, *71*, 8442.

(375) Le Fourn, C.; Fardeau, M.-L.; Ollivier, B.; Lojou, E.; Dolla, A. *Environ. Microbiol.* **2008**, *10*, 1877.

(376) McHardy, I.; Keegan, C.; Sim, J.-H.; Shi, W.; Lux, R. *PloS One* **2010**, *5*, e13655.

(377) (a) Williams, E.; Lowe, T. M.; Savas, J.; DiRuggiero, J. *Extremophiles* **2007**, *11*, 19. (b) Zhang, W.; Culley, D. E.; Hogan, M.; Vitiritti, L.; Brockman, F. J. *Antonie van Leeuwenhoek* **2006**, *90*, 41.

(378) (a) Kurtz, D. M., Jr. *Acc. Chem. Res.* **2004**, *37*, 902. (b) Kurtz, D. M., Jr. *J. Inorg. Biochem.* **2006**, *100*, 679.

(379) Coulter, E. D.; Kurtz, D. M. *Arch. Biochem. Biophys.* **2001**, *394*, 76.

(380) Pinto, A. F.; Rodrigues, J. V.; Teixeira, M. *Biochim. Biophys. Acta, Proteins Proteomics* **2010**, *1804*, 285.

(381) Krätzer, C.; Welte, C.; Dörner, K.; Friedrich, T.; Deppenmeier, U. *FEBS J.* **2011**, *278*, 442.

(382) Pereira, A. S.; Tavares, P.; Folgosa, F.; Almeida, R. M.; Moura, I.; Moura, J. J. G. *Eur. J. Inorg. Chem.* **2007**, 2569.

(383) Pinto, A. F. *Reductive Scavenging of Reactive Oxygen Species on Prokaryotes*; ITQB-UNL: Lisbon, 2012.

(384) (a) Emerson, J. P.; Coulter, E. D.; Phillips, R. S.; Kurtz, D. M., Jr. *J. Biol. Chem.* **2003**, *278*, 39662. (b) Clay, M. D.; Emerson, J. P.; Coulter, E. D.; Kurtz, D. M., Jr.; Johnson, M. K. *J. Biol. Inorg. Chem.* **2003**, *8*, 671. (c) Huang, V. W.; Emerson, J. P.; Kurtz, D. M., Jr. *Biochemistry* **2007**, *46*, 11342. (d) Yang, T.-C.; McNaughton, R. L.; Clay, M. D.; Jenney, F. E., Jr.; Krishnan, R.; Kurtz, D. M., Jr.; Adams, M. W. W.; Johnson, M. K.; Hoffman, B. M. *J. Am. Chem. Soc.* **2006**, *128*, 16566. (e) Clay, M. D.; Yang, T.-C.; Jenney, F. E., Jr.; Kung, I. Y.; Cosper, C. A.; Krishnan, R.; Kurtz, D. M., Jr.; Adams, M. W. W.; Hoffman, B. M.; Johnson, M. K. *Biochemistry* **2006**, *45*, 427.

(385) (a) Mathé, C.; Mattioli, T. A.; Horner, O.; Lombard, M.; Latour, J.-M.; Fontecave, M.; Nivière, V. *J. Am. Chem. Soc.* **2002**, *124*, 4966. (b) Berthomieu, C.; Dupeyrat, F.; Fontecave, M.; Verméglio, A.; Nivière, V. *Biochemistry* **2002**, *41*, 10360. (c) Mathé, C.; Nivière, V.; Mattioli, T. A. *J. Am. Chem. Soc.* **2005**, *127*, 16436. (d) Bonnot, F.; Houée-Levin, C.; Favaudon, V.; Nivière, V. *Biochim. Biophys. Acta* **2010**, *1804*, 762. (e) Bonnot, F.; Molle, T.; Ménage, S.; Moreau, Y.; Duval, S.; Favaudon, V.; Houée-Levin, C.; Nivière, V. *J. Am. Chem. Soc.* **2012**, *134*, 5120.

(386) (a) Jovanović, T.; Ascenso, C.; Hazlett, K. R. O.; Sikkink, R.; Krebs, C.; Litwiller, R.; Benson, L. M.; Moura, I.; Moura, J. J. G.; Radolf, J. D.; Huynh, B. H.; Naylor, S.; Rusnak, F. *J. Biol. Chem.* **2000**, *275*, 28439. (b) Lombard, M.; Touati, D.; Fontecave, M.; Nivière, V. *J. Biol. Chem.* **2000**, *275*, 27021.

(387) Caranto, J. D.; Gebhardt, L. L.; MacGowan, C. E.; Limberger, R. J.; Kurtz, D. M., Jr. *Biochemistry* **2012**, *51*, 5601.

(388) Todorovic, S.; Rodrigues, J. V.; Pinto, A. F.; Thomsen, C.; Hildebrandt, P.; Teixeira, M.; Murgida, D. H. *Phys. Chem. Chem. Phys.* **2009**, *11*, 1809.

(389) (a) Clay, M. D.; Jenney, F. E., Jr.; Hagedoorn, P. L.; George, G. N.; Adams, M. W. W.; Johnson, M. K. *J. Am. Chem. Soc.* **2002**, *124*, 788. (b) Clay, M. D.; Jenney, F. E., Jr.; Noh, H. J.; Hagedoorn, P. L.; Adams, M. W. W.; Johnson, M. K. *Biochemistry* **2002**, *41*, 9833.

(390) Adam, V.; Royant, A.; Nivière, V.; Molina-Heredia, F. P.; Bourgeois, D. *Structure* **2004**, *12*, 1729.

(391) Tavares, P.; Ravi, N.; Moura, J. J. G.; LeGall, J.; Huang, Y.-H.; Crouse, B. R.; Johnson, M. K.; Huynh, B. H.; Moura, I. *J. Biol. Chem.* **1994**, *269*, 10504.

(392) (a) Silaghi-Dumitrescu, R.; Silaghi-Dumitrescu, I.; Coulter, E. D.; Kurtz, D. M., Jr. *Inorg. Chem.* **2003**, *42*, 446. (b) Horner, O.; Mouesca, J.-M.; Oddou, J.-L.; Jeandey, C.; Nivière, V.; Mattioli, T. A.;

Mathé, C.; Fontecave, M.; Maldivi, P.; Bonville, P.; Halfen, J. A.; Latour, J.-M. *Biochemistry* **2004**, *43*, 8815. (c) Surawatanawong, P.; Tye, J. W.; Hall, M. B. *Inorg. Chem.* **2010**, *49*, 188. (d) Attia, A. A. A. A.; Cioloboc, D.; Lupan, A.; Silaghi-Dumitrescu, R. *J. Biol. Inorg. Chem.* **2013**, *18*, 95.

(393) (a) Theisen, R. M.; Kovacs, J. A. *Inorg. Chem.* **2005**, *44*, 1169. (b) Nam, E.; Alokolaro, P. E.; Swartz, R. D.; Gleaves, M. C.; Pikul, J.; Kovacs, J. A. *Inorg. Chem.* **2011**, *50*, 1592. (c) Kovacs, J. A.; Brines, L. M. *Acc. Chem. Res.* **2007**, *40*, 501.

(394) Rodrigues, J. V.; Abreu, I. A.; Saraiva, L. M.; Teixeira, M. *Biochem. Biophys. Res. Commun.* **2005**, *329*, 1300.

(395) Auchère, F.; Pauleta, S. R.; Tavares, P.; Moura, I.; Moura, J. J. G. *J. Biol. Inorg. Chem.* **2006**, *11*, 433.

(396) Schrodinger, LLC, 2010.

(397) Borgstahl, G. E. O.; Pokross, M.; Chehab, R.; Sekher, A.; Snell, E. H. *J. Mol. Biol.* **2000**, *296*, 951.

(398) Pettersen, E. F.; Goddard, T. D.; Huang, C. C.; Couch, G. S.; Greenblatt, D. M.; Meng, E. C.; Ferrin, T. E. *J. Comput. Chem.* **2004**, *25*, 1605.

(399) Guex, N. *Experientia* **1996**, *52*, A26.

(400) Letunic, I.; Bork, P. *Nucleic Acids Res.* **2011**, *39*, w475.

(401) Edgar, R. C. *BMC Bioinf.* **2004**, *5*, 113.

(402) Dereeper, A.; Guignon, V.; Blanc, G.; Audic, S.; Buffet, S.; Chevenet, F.; Dufayard, J.-F.; Guindon, S.; Lefort, V.; Lescot, M.; Claverie, J.-M.; Gascuel, O. *Nucleic Acids Res.* **2008**, *36*, W465.

(403) Castresana, J. *Mol. Biol. Evol.* **2000**, *17*, 540.

(404) Anisimova, M.; Gascuel, O. *Syst. Biol.* **2006**, *55*, 539.

(405) Papadopoulos, J. S.; Agarwala, R. *Bioinformatics* **2007**, *23*, 1073.

(406) Regelsberger, G.; Atzenhofer, W.; Rüker, F.; Peschek, G. A.; Jakopitsch, C.; Paumann, M.; Furtmüller, P. G.; Obinger, C. *J. Biol. Chem.* **2002**, *277*, 43615.

(407) Pagani, S.; Colnaghi, R.; Palagi, A.; Negri, A. *FEBS Lett.* **1995**, *357*, 79.

(408) Lancaster, V. L.; LoBrutto, R.; Selvaraj, F. M.; Blankenship, R. E. *J. Bacteriol.* **2004**, *186*, 3408.

(409) Heinzen, R. A.; Frazier, M. E.; Mallavia, L. P. *Infect. Immun.* **1992**, *60*, 3814.

(410) Pesci, E. C.; Cottle, D. L.; Pickett, C. L. *Infect. Immun.* **1994**, *62*, 2687.

(411) Tannich, E.; Bruchhaus, I.; Walter, R. D.; Horstmann, R. D. *Mol. Biochem. Parasitol.* **1991**, *49*, 61.

(412) Dunn, B. E.; Cohen, H.; Blaser, M. J. *Clin. Microbiol. Rev.* **1997**, *10*, 720.

(413) Kang, S.-K.; Jung, Y.-J.; Kim, C.-H.; Song, C.-Y. *Clin. Diagn. Lab. Immun.* **1998**, *5*, 784.

(414) Bécuwe, P.; Gratepanche, S.; Fourmaux, M.-N.; Van Beeumen, J.; Samyn, B.; Mercereau-Puijalon, O.; Touzel, J. P.; Slomianny, C.; Camus, D.; Dive, D. *Mol. Biochem. Parasitol.* **1996**, *76*, 125.

(415) (a) Le Trant, N.; Meshnick, S. R.; Kitchener, K.; Eaton, J. W.; Cerami, A. *J. Biol. Chem.* **1983**, *258*, 125. (b) Kabiri, M.; Steverding, D. *Biochem. J.* **2001**, *360*, 173.

(416) Mey, A. R.; Wyckoff, E. E.; Kanakurthy, V.; Fisher, C. R.; Payne, S. M. *Infect. Immun.* **2005**, *73*, 8167.

(417) Moran, J. F.; James, E. K.; Rubio, M. C.; Sarath, G.; Klucas, R. V.; Becana, M. *Plant. Physiol.* **2003**, *133*, 773.

(418) Sievers, F.; Wilm, A.; Dineen, D. G.; Gibson, T. J.; Karplus, K.; Li, W.; Lopez, R.; McWilliam, H.; Remmert, M.; Söding, J.; Thompson, J. D.; Higgins, D. G. *Mol. Syst. Biol.* **2011**, *7*, 539.

(419) Bruijn, L. I.; Houseweart, M. K.; Kato, S.; Anderson, K. L.; Anderson, S. D.; Ohama, E.; Reaume, A. G.; Scott, R. W.; Cleveland, D. W. *Science* **1998**, *281*, 1851.

(420) (a) Landau, M.; Mayrose, I.; Rosenberg, Y.; Glaser, F.; Martz, E.; Pupko, T.; Ben-Tal, N. *Nucleic Acids Res.* **2005**, *33*, W299. (b) Glaser, F.; Pupko, T.; Paz, I.; Bell, R. E.; Bechor-Shental, D.; Martz, E.; Ben-Tal, N. *Bioinformatics* **2003**, *19*, 163.